THE UNIVERSITY OF SYDNEY

Increasing Sustainability in Buildings Through Energy-Efficient Concrete

by

Peyman Zandifaez

A thesis submitted to fulfill requirements for the degree of
Doctor of Philosophy

Supervisor: Associate Professor Daniel Dias-da-Costa

School of Civil Engineering

Faculty of Engineering

The University of Sydney

November 2023

Statement of originality

I, Peyman Zandifaez, hereby declare that the thesis entitled “Increasing sustainability in buildings through energy-efficient concrete” and the work presented in body of this thesis is the result of my own investigations. I also confirm that this thesis has not been submitted for any degree and all the assistance received in preparation of this thesis and sources is acknowledged.

Peyman Zandifaez

Dedication

To my beautiful wife and best friend, Ida, I am grateful beyond words for your unwavering love and support throughout my doctoral research journey. Your kind words have lifted me up when I needed it most, and your patience and understanding have been a constant source of comfort.

To my parents and sister, Neda, for their inspiration, love, and support which have given me confidence to pursue my dreams and never give up on them. Your belief in me has been an anchor in my life. Thank you for everything you have done for me.

To all my friends in Sydney and Tehran, and to you who read this thesis.

Acknowledgements

The journey of completing a dissertation is an extraordinary and unforgettable experience that is filled with triumphs and setbacks. I am pleased to say that I was not alone on this journey, as I received invaluable support and guidance from many people along the way. I want to express my appreciation to all those who helped me during this journey. Without their encouragement and assistance, I would not have been able to make it this far.

To begin with, I would like to express my sincere gratitude to my supervisor, Professor Dias-da-Costa for his continuous support throughout my PhD research. He has been a constant source of inspiration, providing me with the encouragement, guidance, and motivation needed to stay on the course. His keen insight and consideration challenged me to think more critically and inspired me to be the best version of myself.

I would also like to sincerely thank Professor Nezhad, my primary supervisor at the University of Sydney, for his guidance and mentorship throughout my academic journey. Although he is no longer affiliated with the academic institution and had no official responsibilities for my research, Professor Nezhad remained a valuable source of support. He continued participating in my meetings and provided invaluable insights into my work. I am deeply grateful for his continued guidance and will always cherish his impact on my life.

I would like to express my sincerest appreciation to Professor Zhou at the University of Tennessee, Knoxville for his invaluable support during the experimental phase of my thesis. As a visiting scholar over the past two years, I had the pleasure of collaborating with Professor Zhou, who provided exceptional guidance and expertise, which was instrumental in the successful completion of my project. Professor Zhou made himself readily available to answer my questions and provide valuable insights into my work.

I firmly believe that successfully completing PhD studies requires more than just academic support, and I feel blessed to have had the unconditional support of friends like Bahman, Elyas, Aidin, Hooman and Alireza throughout my PhD journey.

Lastly, I would like to express my deepest regards to my wife and best friend, Ida, for always being there for me. She has been my rock, confidante, and constant source of inspiration. I cannot imagine having completed this journey without her by my side.

Abstract

The energy performance of buildings is influenced by a wide range of climatic and design-related variables, including but not limited to ambient temperature, heating and cooling systems, and thermal properties of building elements. Given the synergetic effects of these parameters, the widespread use of concrete in the building industry, and the significant amount of energy loss through this construction material used in building envelopes, this thesis explored the magnitude of the impact of the thermal properties of concrete compared to other influential factors and assessed their critical role in the energy performance of buildings. Increasing the energy efficiency of concrete has been of interest and holds significant promise in reducing the energy consumption of concrete structures. To this end, several approaches have been employed to improve the thermal performance of concrete, such as partial to full replacement of cement and natural aggregates with supplementary cementitious materials and recycled concrete aggregates, respectively, resulting in the production of lightweight concrete. However, incorporating recycled contents into concrete mixes beyond certain percentages can negatively impact the mechanical performance of concrete, which poses a challenge for engineers and designers balancing thermal, environmental, and mechanical performances. With the goal of spanning the mentioned requirements, this thesis proposed an AI-assisted framework integrating data-driven modelling techniques and multi-objective optimisation algorithms to optimise recycled aggregate concrete mixes targeting energy performance-related and economic objectives without compromising their mechanical strength. The effectiveness of the developed framework in minimising the thermal and environmental performance of concrete was examined through several case studies and comparisons with available experimental findings. Furthermore, the thesis investigated the connections between sustainable developments in the concrete industry and the emerging technology of additive manufacturing.

The additive manufacturing technology holds significant promise in the coming years, including improved sustainability indicators, labour safety, and architectural flexibility. Also, the increasing research focus on the application of additive manufacturing, particularly concrete 3D printing, and its potential for widespread integration in the construction sector highlight the critical need for a comprehensive exploration of 3DP concrete properties. Nevertheless, the unique characteristics of this method, diverging from conventional construction approaches, come with certain challenges. These challenges, however, can be effectively addressed by leveraging commonly used sustainable practices.

In this sense, incorporating recycled contents and air bubbles into concrete mixes was found to be an effective approach to address some hurdles associated with concrete 3D printing, which is a

promising technique for large-scale construction projects due to its speed and cost-efficiency. The results showed that increasing air voids allowed for replacing recycled content beyond commonly used percentages, resulting in lightweight and ultra-lightweight 3D printable cementitious composites with significant thermal conductivity improvements. The findings suggest the potential application of the proposed numerical and experimental approaches in energy-efficient buildings, as considerable improvements by up to 11% and 29% were shown in the thermal and environmental performances of concrete mixes, respectively. Further improvements in thermal properties, particularly in the thermal conductivity of 3D printable mixes were shown, by up to 89%, appealing to insulation and acoustic applications.

Table of Contents

List of Figures

List of Tables

Acronyms

ACDP	acidification potential
AGE-MOEA	adaptive geometry estimation based many-objective evolutionary algorithm
ANN	artificial neural network
C	ordinary portland cement
CS	compressive strength
Cagg	coarse aggregate
EE	embodied energy
EUI	energy use intensity
FA	fly ash
FAC	fly ash cenosphere
Fagg	fine aggregate
FC	foam concrete
FFDP	fossil fuel depletion potential
GBM	gradient boosting machine
GWP	global warming potential
KNN	k nearest Neighbours
MLR	multiple linear regression
MOO	multi-objective optimisation
NSGA-II	Non-dominated Sorting Genetic Algorithm II
OE	operating energy
R^2	r-square
RF	random Forest
RMSE	root mean squared error
LCA	life cycle assessment
LWC	lightweight concrete
LWA	lightweight aggregate
MAE	mean absolute error
NA	natural aggregate
PCM	phase change material
ULWC	ultra-lightweight concrete
RCA	recycled concrete aggregate
RAC	recycled aggregate concrete
SCMs	supplementary cementitious materials
SF	silica fume
SP	superplasticiser
TC	Thermal conductivity
Xgboost	extreme gradient boosting machine
W	water

Chapter 1 Introduction

1.1 Background of the research

The construction and building sector accounts for up to 40% of total energy use and carbon emissions worldwide (Barcelo et al., 2014). Therefore, identifying design and construction strategies to reduce the energy consumption and carbon footprint of buildings and infrastructure is a topic of growing interest in academia and industries. The choice of construction materials is among various design decisions affecting the energy and environmental implications associated with buildings. In this context, concrete is currently the most-used construction material globally and the second most-used after water (Shariq et al., 2010), with a significant impact on the overall embodied carbon and energy of buildings and infrastructures (Huntzinger & Eatmon, 2009). However, the impact of concrete on the energy use and environmental footprints of buildings is not limited to its embodied phase, which is associated mainly with energy consumed during the production of concrete. Concrete has also been found to considerably affect the operating energy (OE) needs of buildings- the energy consumed during the service life of buildings- partly through its ability to provide significant thermal mass, as well as its other unique thermal properties (Asadi et al., 2018a; Ramesh et al., 2010b). Accordingly, increasing energy performance in buildings through improving the energy efficiency of concrete, including decreasing the embodied energy (EE) of concrete and optimising its impact on the OE of buildings, has been of interest to decision-makers and building designers (Chua et al., 2013).

In this sense, improving the sustainability indicators of concrete is a pressing concern due to its potential to mitigate environmental footprints, save natural resources, and enhance the thermal performance of buildings. With the ever-growing demands for construction, the transition towards energy-efficient concrete is not only inevitable but crucial. This urgency is highlighted by the fact that the construction sector is responsible for about 40% of global energy consumption and carbon emissions using traditional approaches. The latter relies on the excessive use of Portland cement and natural resources, resulting in non-energy-efficient concrete considering both embodied and operating aspects. Using sustainable practices, however, the OE can be improved by enhancing thermal properties, including thermal mass and insulation capabilities, resulting in a reduction in heating and cooling loads during the service life of buildings. This is particularly effective in addressing the challenges of climate change and the need for net-zero buildings. Furthermore, formulating high-performance mix designs using SCMs and LWA can also significantly mitigate

the carbon footprint associated with concrete production, thereby improving its EE, which is aligned with global sustainability goals. Given the considerable impact of both EE and OE on each other, this study has targeted the energy performance of concrete, placing particular emphasis on operational energy due to its higher share throughout the lifecycle of concrete. Thus, in-depth investigations focused on energy-efficient concrete can pave the way toward a greener and more sustainable future.

Significant efforts have been made in academia and industry to minimise the embodied carbon of concrete. Such strategies mainly rely on reducing the cement content of concrete through its full or partial replacement with Supplementary Cementitious Materials (SCMs), including Ground Granulated Blast-Furnace slag (GGBFS) and Fly Ash (FA) (Ashish, 2019; Rahla et al., 2019). However, it has also been shown that variations in the mix design of concrete aimed at reducing its embodied carbon by varying SCM contents could significantly affect the thermal properties of concrete, thereby influencing the impact of concrete on the OE of buildings (Cseh et al., 2021; Sargam et al., 2020). It is, therefore, critical to consider the choice of concrete materials in buildings by taking into account both EE and OE implications in conjunction rather than in isolation, given the trade-off may exist between EE and OE (Shadram & Mukkavaara, 2018).

The relationship between the EE of concrete and its impact on its OE in buildings is complex and can be influenced by project specifications, including design geometry, other material choices, and environmental indices (Dixit et al., 2012). This is because apart from the properties of concrete, the OE of buildings is influenced by numerous other design-related variables, including but not limited to windows, lighting, and operating schedule (X. Cao et al., 2016; Omer, 2008), which adds complexity to modelling the impact of concrete mix design on the OE of buildings. For instance, the thermal properties of building envelopes, window-to-wall ratio, and operating schedule can impact the heating/cooling loads and lighting required (Kossecka & Kosny, 2002; Sassine et al., 2021) (Ordoñez et al., 2014). Therefore, a detailed life cycle assessment (LCA) is commonly required to model the overlapping impact of concrete design on the EE and OE of building materials (Khasreen et al., 2009). For this purpose, in-depth and comprehensive studies spanning the synergetic effects of design choices are required to assess the importance of influential factors. The relative share of OE and EE in the life cycle energy of buildings has been extensively investigated using LCA (Abbasi & Noorzai, 2021). The results indicate that OE typically, on average, accounts for 80 to 90% of the energy demand during the life cycle of buildings (Ibn-Mohammed et al., 2013; Najjar et al., 2019). Given the significant contribution of OE to lifecycle energy and, therefore,

lifecycle carbon in buildings, it is critical that design decisions with regard to the choice of material are made by considering not only the impact of the material on EE and carbon but also on its OE and carbon. However, this is rarely considered in current sustainable practices in the construction industry, where material-level decisions are mostly focused on embodied carbon reduction.

In this sense, a portion of OE is attributed to climate-dependent demands, such as heating/cooling, while the rest is attributed to climate-independent demands, e.g., plug loads (H. X. Zhao & Magoulès, 2012). In other words, energy demand in buildings is affected by both design-related and environmental parameters. The latter comprises several indices, including but not limited to ambient temperature, relative humidity, solar radiation, and wind speed (X. Cao et al., 2016). Among these indices, ambient temperature plays a central role in OE, mainly because it directly influences the level of impact and importance of design-related parameters (Pérez-Bella et al., 2015). For instance, in hot and Mediterranean climates, large windows are desirable for natural light and ventilation as they help reduce the need for artificial lighting and maintain thermal comfort. In contrast, cold climates prioritise insulation and minimising heat loss, requiring smaller windows or advanced insulation such as double or triple glazing. Therefore, a broad spectrum of parameters, including environmental and design-related influence the energy performance of buildings. However, these parameters are not easily available in the early stages of projects, necessitating simplified predictive models that require minimum data to estimate energy consumption in buildings.

In addition, the impacts of design-related factors on OE vary in light of a wide range of parameters, including the thermal performance of building elements, operating schedule, and construction quality (Robati et al., 2017). To enhance OE efficiency, a proper understanding of contributing factors, such as walls, roof, and windows, is necessary (Karimpour et al., 2014). The buildings exchange heat (energy) through building envelopes, such as exterior walls, roofs, glazing, and ground floor, as well as infiltration (air exchange) that takes place around openings since these elements are in direct exposure to the outdoor environment (L. Wang & Greenberg, 2015). Thus, the thermal properties of building envelopes significantly impact energy performance in buildings (Berardi et al., 2018), highlighting the use of materials with improved thermal properties can result in more energy saving. Previous studies have widely investigated the effects of the thermal properties of concrete as a widely used material in building envelopes (Asadi et al., 2018a; Real, Gomes et al., 2016). The thermal properties of concrete can be improved by reducing its density via several means, such as incorporating SCMs as partial replacement of cement, lightweight

aggregates (LWA) as partial to full replacement of Natural Aggregates (NA), introducing air into the mix, and adopting Phase Change Materials (PCMs) (Khedari et al., 2001; Q. Li et al., 2022; Zhu et al., 2015). The first three approaches reduce the weight of concrete, thus lowering its density and thermal conductivity, which results in lightweight concrete (LWC) production. In this context, SCMs and LWA exhibit lower thermal conductivity compared to cement, contributing to an overall improvement in thermal conductivity. Similarly, increasing air bubbles in concrete mixes can significantly enhance their thermal performance, primarily owing to the insulative properties of these air voids. PCMs, however, impact the thermal performance of concrete at different scales by providing an effective method to minimise the heating and cooling loads by reducing the temperature fluctuations. They encompass a wide range of materials, including paraffin-based, fatty acid, and salt hydrates. PCMs can store and release heat by changing their phase from solid to liquid or liquid to gas (V. V. Tyagi & Buddhi, 2007; Wei et al., 2018). However, their adoption in the construction industry is currently limited due to their relatively high costs (Adesina, 2019). The use of LWA and SCMs is, therefore, generally considered to be more viable options; and are commonly used strategies in the current practice partly due to their structural and economic benefits (Pacheco Torgal et al., 2012).

A majority of the common SCMs used in concrete are by-products of other industries. These include FA, Silica Fume (SF), and GGBFS, which are the by-products of coal combustion, silicon and ferrosilicon, and iron and steel industries, respectively (Siddique, 2010; Siddique & Bennacer, 2012; Siddique & Chahal, 2011). The partial replacement of cement content with SCMs can improve both the thermal and structural performance of concrete while at the same time leading to a significant reduction in concrete's embodied energy and carbon by reducing its cement content (Aprianti et al., 2015a). While replacing cement with common SCMs up to a certain limit (typically between 20% to 40%, depending on the type of SCM) has been demonstrated to enhance durability, the cost of production (Mo et al., 2017), and long-term mechanical performance (Saad et al., 1996), the excessive replacement of SCMs adversely impacts the early age properties of concrete including its early age strength development (Rivera et al., 2015). Considering the conflicting impacts of utilising SCMs on the thermal properties of concrete (and therefore its impact on OE), EE, structural performance and costs, this study aims to optimise concrete mixes containing SCMs to maximise the overall sustainability, performance and financial benefits.

LWC has also played a crucial role in modern construction by enhancing the structural, thermal and environmental properties of buildings (M. R. Ahmad et al., 2019). LWC has been proven to

reduce heating and cooling demands and minimise environmental implications (Dinelli et al., 1996). This is due to the lower thermal mass and improved insulation capacity of LWC compared to normal concrete (Cavalline et al., 2017). LWC typically incorporates lightweight fillers that increase insulation properties and reduce heat exchange through this type of concrete. In addition to its sustainability benefits, LWC also offers significant structural benefits, particularly in the construction of multi-story buildings, by providing flexibility and reduced self-weight loads, as well as improved durability, seismic response, and fire resistance (Ke et al., 2009).

Typically, LWC is designed by replacing ordinary constituents such as cement and NA with SCMs and LWA, respectively (Falliano et al., 2020; Sivakrishna et al., 2020). LWA constituent options could encompass a large spectrum of materials, including recycled construction and demolition waste (CDW) (Muñoz-Ruiperez et al., 2016), expanded shale (M. Zhao et al., 2018), expanded clay (Rashad, 2018), and expanded and crushed glass (Adhikary & Rudzionis, 2020). According to EN 206-1, the density of LWC ranges between 800 to 2000 kg/m3 (Burbano-Garcia et al., 2021). Due to the lower weight of LWA, incorporating them into concrete mixes can reduce the density and thermal conductivity of concrete, which can then be leveraged to improve the embodied energy efficiency of buildings (Vives et al., 2021). One of the most widely available types of LWA is recycled concrete aggregates (RCA) produced by crushing concrete waste generated during concrete production and after the demolition of concrete structures, making it a significant component of CDW. Utilising RCAs in concrete not only has a positive impact on OE but also serves as a vital pathway towards achieving circular economy objectives in the construction industry (Sonawane & Pimplikar, 2012; Y. Zhang et al., 2019). However, replacing NA with RCA, if not optimised, can negatively affect the mechanical performance of concrete due to RCA's higher water absorption and lower density, as well as the weaker interfacial transition zone between RCA and mortar in concrete compared to that of NA and mortar (L. Zheng et al., 2017a). Therefore, while RCA offers significant energy efficiency and other environmental benefits, it is critical to optimise mix designs to ensure maximum environmental benefits under mechanical constraints.

To further reduce the density of concrete, recent attention has been paid to the production of lightweight and ultra-lightweight concrete (LWC and ULWC). The density of ULWC is lower compared to ordinary concrete (OC) and LWC (Roberz et al., 2017). ULWC can be achieved by introducing air into mixtures to increase air voids using foaming agents, thus producing foam concrete (FC) with enhanced thermal properties (Shi et al., 2021). Incorporating foaming agents beyond a certain percentage can reduce the density of mixes to lower than 800kg/m3 (Falliano et

al., 2021). ULWC has demonstrated low thermal conductivity and limited structural applications due to its poor load-bearing properties. However, its high thermal resistance can make ULWC appealing to thermal and acoustic insulations (X. Zhang et al., 2020). One of the key areas of the application of ULWC in the construction industry is its use in 3D printing, enabling the production of lighter and more energy-efficient elements while offering architectural design flexibility. In concrete 3D-printed elements, a significant challenge lies in the structural capacity to support their own weight (Paul et al., 2018). This issue can be primarily attributed to the moldless nature of concrete 3D printing. Therefore, the printed elements should be capable of bearing their weights in the fresh state (Ding et al., 2020). To address this limitation, incorporating LWA, SCMs, and foaming agents into mixtures have been employed to produce lightweight and ultra-lightweight 3D printable concrete, resulting in enhanced thermal performance in printed elements (Falliano et al., 2020). However, considering the conflicting implications of SCMs, LWA and foaming agents on the mechanical properties and thermal properties of ULWCs, it is critical to optimise ULWC mixes to maximise energy efficiency benefits while meeting performance requirements for widespread practical use.

While the above strategies provide reliable pathways to reduce the EE and OE of buildings, the complex nature of the overlapping impact of each of these pathways on not only the thermal properties but also the mechanical performance of concrete complicates identifying the optimal mix design decision. In addition, the traditional concrete mix design methodologies are focused solely on optimising the mechanical properties of concrete and do not account for energy efficiency implications as mix design objectives (Abreu et al., 2018; Deng et al., 2020; H. Zhang et al., 2022). While significant progress has been made to develop computational methods that allow considering multiple objectives, there is currently limited research on mix optimisation methods tailored for concrete mixes with RCAs, SCMs and foaming agents to achieve the optimal energy performance (Demirboğa, 2007; H. Zhao et al., 2018a).

To address this challenge, this thesis will focus on filling the gaps in the design of such mixes by leveraging state-of-the-art mix optimisation methods. This is expected to remove one of the key barriers in leveraging RCAs, SCMs and foaming agents to improve the operating energy efficiency of buildings. To design concrete mixes containing high SCM and RCA content, the focus is placed on leveraging data-driven modelling techniques and metaheuristic optimisation algorithms. These methods, despite their potential advantages, have not yet been explored to meet operating energy efficiency-related objectives. The choice of this methodology is justified by the high accuracy of

data-driven modelling techniques in establishing complex relationships between several inputs and outputs compared to traditional modelling methods. On the contrary, to eliminate the barriers hindering the broader use of ULWC in practice and unlock its embodied energy efficiency benefits, this study will employ an experimental mix optimisation methodology for 3DP ULWC. Unlike data-driven optimisation, as selected for optimising concrete mixes containing RCA and SCM, the focus is on experimental optimisation. This is due to the lack of sufficient data about 3DP LWC and ULWC required by data-driven approaches. Extensive experimental testing will be leveraged to develop ULWC concrete mixes with high concentrations of foaming agents and RCA, offering significant potential for use in insulation applications. The emphasis is placed on ensuring the suitability of these mixes for use in 3D printing as a viable technological pathway for manufacturing LWC and ULWC for insulation applications.

1.2 Research Objectives

Considering the background presented above, the overarching objective of this research is to present novel numerical and experimental concrete mix design approaches to improve the operating energy efficiency of concrete in buildings. The latter is achieved by concentrating on the thermal performance of concrete mix designs throughout the operating phase of the building, which has not been adequately studied previously. In the former, the particular focus is placed on enabling the design of concrete mixes containing SCMs, LWAs and foaming agents, given the unique thermal properties they may offer. To achieve this, the specific objectives of this thesis include:

- To assess the relative significance of the thermal properties of concrete compared to other influential factors affecting energy use in buildings.
- To accurately measure the effect of concrete mix design decisions on energy consumption throughout the entire service life of buildings.
- To develop a reliable methodology to optimise concrete mixes containing RCA and SCMs using data-driven and metaheuristic optimisation approaches.
- To mitigate limitations on the use of recycled content and high concentration of foaming agents to design 3D printable mixes that allow widespread use of these mixes in insulation applications.

1.3 Research Questions

In light of the background provided, addressing the following questions can contribute to achieving the objectives outlined in this section:

- What are the key parameters influencing the energy performance of buildings?
- How does the impact of the thermal properties of concrete compare to other design-related and environmental factors in influencing the energy performance of buildings?
- What are the prevailing strategies and technologies employed to enhance the thermal performance of concrete?
- To what extent can common sustainable practices improve the energy performance of concrete?
- How can utilising the commonly employed strategies for improving the energy performance of concrete facilitate the integration of additive manufacturing in the construction sector?

1.4 Dissertation Organisation

This dissertation is divided into six chapters. The focus and scope of each chapter are as follows:

- Chapter 1 presents an overview of the challenges faced by the concrete industry in designing concrete mixes with improved energy efficiency benefits and the objectives of this thesis.
- Chapter 2 presents a comprehensive literature review of the findings of previous studies with regard to the impact of concrete mix design on the operating energy of buildings, potential pathways to optimise this impact, and state-of-the-art in concrete mix optimisation to meet energy efficiency objectives. The gaps in the literature are highlighted.
- Chapter 3 develops an OE predictive model and investigates the relative importance of various influential factors through a detailed sensitivity analysis. The findings provide compelling evidence on the significant impact that concrete mix designs can have on the operating energy efficiency of buildings.
- Chapter 4 proposes an AI-assisted RAC optimisation framework to design concrete mixes containing both RCAs and SCMs as partial replacements for NAs and cement. The optimisation framework is designed not only to meet the required mechanical performance objectives but also to provide improved thermal and environmental properties as required to improve the energy efficiency implications of concrete.
- Chapter 5 proposes an experimental mix design approach to 3D printable FC with low density and thermal conductivity for use in insulation applications to allow further reduction in the OE demand of concrete buildings.

- Chapter 6 concludes the research findings and presents the recommended future research directions.

1.5 Authorship attribution statement

Part of Chapter 4 of this thesis has been published in the Journal of *Construction and Building Materials* (Zandifaez et al., 2023). I was responsible for designing and executing the study, analysing the data and results, and drafting the manuscript.

The findings outlined in Chapter 2, Chapter 3, and Chapter 5 of this thesis are submitted as journal articles. I was responsible for designing and executing the publications, analysing the data and results, and drafting the manuscripts.

In addition to the statements above, in cases where I am not the corresponding author of a published item, permission to include the published material has been granted by the corresponding author.

Peyman Zandifaez, 14 November 2023

As the supervisor for the candidature upon which this thesis is based, I can confirm that the authorship attribution statements above are correct.

Daniel Dias-da-Costa, 14 November 2023

Chapter 2 A systematic review of the evidence on improving sustainability in buildings through increasing energy efficiency of concrete

2.1 Abstract

The environmental concerns attributed to the energy performance of buildings have become pressing in the past two decades. Therefore, improving the energy efficiency of building elements, particularly concrete as the most commonly used material in construction, has been of interest among scholars. The cumulative body of research surrounding energy-efficient concrete follows the conventional methods, in which the number of target publications is limited. The present study has conducted a systematic review of the literature (SRL) on increasing the energy efficiency of concrete considering embodied and operating phases through analysing the bibliometric records on the topic. Further, a comprehensive manual review on commonly adopted approaches obtained from the SRL is carried out. For this purpose, a set of keywords is defined, followed by a series of constraints, resulting in 283 records focusing on the topic from 2000 to 2022 using the database of Scopus. The VOSviewer software is also adopted for quantitative and meta-analysis, where statistical data, including the frequency and origin of documents, institution, source of publication, and keyword trends over time, are presented. Moreover, research hotspots are classified into four clusters, and a qualitative analysis of sustainable practices to improve the energy efficiency of concrete is presented. A growing research interest is noticed in the twofold studies focused on improving the energy performance of concrete concerning both embodied and operating phases. The results also highlight the increasing connection between automation technologies and sustainable developments in the construction sector. This study helps scholars and decision-makers understand the current state and trends regarding the energy efficiency of concrete. The identified gaps and potential future research directions are also presented.

2.2 Introduction

The construction sector is a significant energy consumer, with a 40% contribution to global energy use and CO2 emissions, resulting in global warming and natural resources depletion (X. Cao et al., 2016). Material choices in this sector, however, depend on a wide range of factors, including their performance and the cost of production (Mukherjee & Vesmawala, 2013). Thanks to the mechanical properties, cost-effectiveness, and durability of concrete, this substance has become the most commonly used material in the built environment (Meyer, 2006) With that being said,

increasing the energy efficiency of concrete throughout its life cycle (i.e., production and operation) can improve sustainability in buildings (Akande et al., 2015).

Annual production of over 6 billion tons of concrete highlights the significant role of its embodied energy within the life cycle of buildings (Mohamad et al., 2021), which refers to the environmental footprints associated with extracting, manufacturing, and transporting concrete to the construction site (Yeo & Gabbai, 2011). However, the energy performance of concrete is not merely limited to its embodied phase, as massive energy use is attributed to concrete structures during their operating phase, evidenced by previous studies (Ramesh et al., 2010). The importance of the energy performance of concrete in the operating phase is crucial due to its widespread use in building envelopes and its thermal properties (i.e. thermal mass and conductivity), which facilitate significant energy exchange between indoor and outdoor environments (B. Huang et al., 2022). Consequently, optimising the concrete choices used in building envelopes can reduce the energy consumption in buildings without compromising thermal comfort in the indoor zones (Loonen et al., 2013). Considering both embodied and operating phases, the energy efficiency of concrete within its life cycle has drawn research attention (Ding & Ying, 2019). Findings in the literature have pointed to a relative share between embodied energy (EE) and operating energy (OE), which complicates establishing a balance between these two (Shadram & Mukkavaara, 2019), meaning an increase in one leads to a decrease in the other and vice versa.

This trade-off between OE and EE depends on project-specific factors, necessitates considering their relative share in designing energy-efficient concrete (Humar et al., 2011). Nevertheless, most of the available studies have focused on reducing either EE or OE, which can negatively impact the other (Utama & Gheewala, 2009). The energy efficiency of concrete, however, encompasses a wide range of conflicting properties; thus, investigating sustainable practices to improve its energy efficiency should consider embodied and operating perspectives, as both serve as driving factors (Tam et al., 2018). In this sense, in-depth reviews of the body of research are necessary to shed light on methods, trends, findings, and gaps in the literature surrounding the energy efficiency of concrete. However, traditional approaches used in previous studies may not be effective in dealing with the large volumes of records. Therefore, leveraging systematic methods can help address this shortcoming and ensure a comprehensive dataset.

An SRL is a systematic review approach aiming to identify, assess, and synthesise as much possible relevant data to offer a thorough overview of the current state of knowledge on a specific topic

(Cioffi et al., 2020). The process typically involves searching the desired database, followed by defining a set of criteria to collect, appraise, and synthesise the obtained records (Hosseini et al., 2018). Review studies in the literature have provided valuable insights into the energy efficiency of concrete, although an SRL has not been carried out. For instance, several studies have investigated strategies to mitigate the environmental footprints of concrete (Bajpai et al., 2020; Hamad et al., 2021; Zeng & Chini, 2017), while some have sought effective approaches to increase the thermal performance of concrete throughout improving its insulation capacity (Cseh et al., 2021; Drissi et al., 2019; S. Wang et al., 2023). More evidence on the environmental implications and thermo-mechanical properties of cementitious composites is also found (Duchesne, 2021; Elshahawi et al., 2021). Using manual review approaches in these studies, however, limits the scope of the topic, thereby overlooking the correlation between key drivers, which may be addressed using systematic review methods. Table 2.1 summarises comprehensive review studies contributed to the topic.

Table 2.1 Summary of reviews

Number	**Targeted properties**				**Review type**	**Reference**	**Cited by**
	M	TC	TES	CE			
1				✓	Manual	(Hasanbeigi et al., 2012)	512
2	✓	✓	✓		Manual	(Asadi et al., 2022)	17
3				✓	Systematic	(Busch et al., 2022)	21
4	✓	✓		✓	Manual	(Collivignarelli et al., 2020)	51
5				✓	Systematic	(V. W. Y. Tam et al., 2018)	657
6	✓			✓	Manual	(Boobalan et al., 2022)	1
7				✓	Manual	(Mehta, 2010)	97
8		✓	✓		Manual	(Asadi et al., 2018c)	393
9	✓			✓	Manual	(Sivakrishna et al., 2020)	107
10	✓	✓			Manual	(N. P. Tran et al., 2022)	5
11				✓	Systematic	(Tinoco et al., 2022)	16
12		✓	✓		Manual	(Shafigh et al., 2018)	95
13				✓	Manual	(P. Wu et al., 2014)	124
14		✓	✓		Systematic	(Borri et al., 2021)	58
15	✓				Systematic	(Ahmed et al., 2021)	84
16	✓				Systematic	(X. Li et al., 2022)	43
17	✓	✓			Manual	(Fu et al., 2020)	74
18				✓	Manual	(Imbabi et al., 2012)	789
19	✓	✓			Manual	(Shah et al., 2021)	14
20	✓			✓	Systematic	(Yang et al., 2022)	42

*M: Mechanical; TC: Thermal conductivity; TES: Thermal energy storage; CE: Carbon emissions

To tackle this shortcoming, several studies have recently employed systematic analysis methods to provide comprehensive information, including trends, most contributed areas, potential gaps, and future research directions on the energy efficiency of concrete. From a thermal conduction view, López-Alonso et al. (2021) and Majumdar et al. (2022) have highlighted the effectiveness of industrial residuals and fibers on the thermal properties of concrete using systematic review methods. From a thermal energy storage perspective, using bibliometric analysis approaches, the historical achievements in the application of different types of phase change materials (PCMs) in concrete have been explored (Afgan & Bing, 2021; Boquera et al., 2021). At a different scale, Xu et al. (2016) have also systematically reviewed the use of concentrating solar power technologies to increase the insulation capacity of concrete. From an environmental view, the inclusion of a wide range of recycled contents and fibers in concrete has been explored through bibliometric analysis (Ahmad et al., 2021; Tam et al., 2018). Exploring the literature shows that systematic review studies on energy-efficient concrete considering its environmental, mechanical, and thermal performances are missing, as shown in Table 2.1. Therefore, the present study has conducted an SRL on increasing the energy efficiency of concrete considering its environmental footprints and thermo-mechanical properties during embodied and operating phases, followed by a qualitative analysis. This study evaluates the relevant documents from several viewpoints to provide a clear picture of research achievements, trends, and required developments.

2.3 Methodology

This section describes the method used to conduct the SRL on the energy efficiency of concrete. The current review study carries out both quantitative and qualitative analyses. Science mapping analysis is adopted to carry out the former as it has exhibited promising abilities in illustrating systematic patterns in a large collection of literature and bibliometrics databases (Cobo et al., 2011). The quantitative analysis encompasses four steps: selection of tools, keyword categorisation and data acquisition, quantitative bibliometric analysis and hotspot clustering, and material evaluation.

The present study has used the 2000-2022 core collection of Scopus as a widely used scientific search tool (Meho & Rogers, 2008) to gather the required dataset for quantitative analyses. Also, VOSviewer is utilised for mapping and visualising the obtained scholarly dataset considering 3 points of contributing authors, institutions, and keyword clustering, as it provides critical features required for analysing bibliometric networks (van Eck & Waltman, 2010).

In the data acquisition process, three categories of keywords are defined in the Scopus database, as listed in Table 2.2. The keywords are chosen to ensure gathering the maximum quantity of relevant documents within the defined scope of the study. The first category seeks documents related to the wide scope of sustainability of concrete in the construction sector and building industry. The second category includes a set of keywords that covers the embodied aspect of concrete by searching for documents concerning its environmental implications, while the third category limits the search by considering the indices that impact the thermal performance of concrete during its operating phase. Therefore, the design of the keywords aims to collect scholarly evidence on the energy efficiency of concrete considering both EE and OE in the construction sector.

Table 2.2 Selected keywords

Keyword categories		
1	**2**	**3**
Construct* AND Build* AND Sustain* AND Concrete	"Sustainability" or "Energy" or "Environment" or "Greenhouse gases" or "Global warming" or "Recycl*" or "Sustainable concrete" or "Embodied energy" or "Green building" or "Environmental footprints" or "Environmental impacts" or "Natural resources" or "Construction waste"	"Thermal properties" or "Thermal conductivity" or "thermal mass" or "Operating energy" or "Temperature" or "Porosity" or "Sustainable construction" or "Heat transfer" or "Air voids"

It should be noted that the defined categories of keywords are connected using the Boolean "and" operator, while the search is limited to the defined time frame of 22 years. To collect a wide range of publications, the keywords are explored within the title, abstract, and keywords of articles, resulting in 901 documents. Six constraints are also considered to refine the results and gather the maximum number of relevant records, listed in Table 2.3 The search has led to 283 documents after applying the defined exclusion constraints. Figure 2.1 shows the structure of the SRL used to collect the dataset.

Table 2.3 Exclusion

ID	**Exclusion constraints**
C1	Subject areas other than engineering, energy, and environmental science
C2	Document types other than article, conference paper, review, book chapter, conference review, and book
C3	Journals with document number less than 20
C4	Documents that only had abstracts available
C5	Documents written in any language other than English
C6	Documents not focusing on the energy efficiency of concrete in buildings

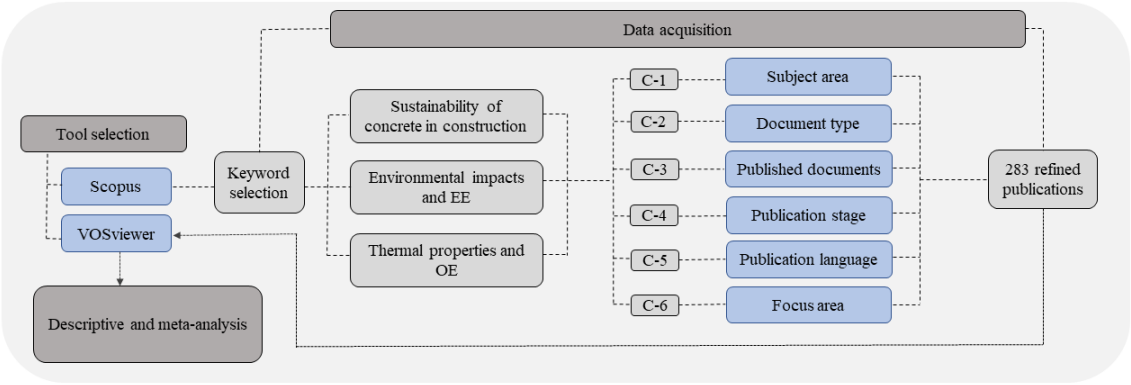

Figure 2.1 The structure of methodology

The quantitative and meta-analyses of 283 collected documents are carried out, and statistics about the frequency of documents, contributing countries, and scholarly venues are presented. Using the VOSviewer tool, informative maps about participating authors and institutions based on the bibliometric data of the refined dataset are generated. Furthermore, the use of VOSviewer allowed for identifying the hotspots and state-of-the-art sustainable practices to improve the energy efficiency of concrete as well as the groups of keywords that are mostly used together in a set of relevant documents (Oladinrin et al., 2022). Therefore, the visual categorisation of the most used keywords is presented based on their co-occurrence patterns within the dataset. The developed clusters provide insights into the desired subject and the results are utilised for the evaluation of materials. Moreover, a qualitative analysis on the SRL is carried out to discuss the developments, adopted approaches, and shortcomings of increasing energy efficiency in concrete.

2.4 Results and discussion

This section presents the results of the bibliometric analysis of the refined publications, including a set of quantitative and meta-analyses on the published year, institution, source, region, authors, and keyword clustering. Moreover, a qualitative review based on the findings of the SRL is proposed.

2.4.1 Quantitative bibliometric and meta-analysis

Our SRL on the refined 283 documents shows a growing trend in the research published within the scope of the current study. Figure 2.2 shows the frequency of published documents from 2000 to 2022.

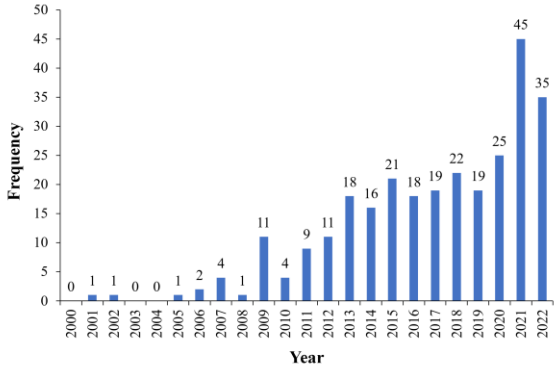

Figure 2.2 Articles published from 2000 to 2022

The results indicate that within the first eight years, from 2000 to 2007, only nine studies are published, while this number has significantly increased to 70 and 204 from 2008 to 2014 and 2015 to 2022, respectively. This growth shows the importance of the sustainability of concrete among researchers over time. This is also reflected in a sharp increase between 2020 and 2021, which implies the popularity of the topic in recent years. It is worth mentioning that the final seven years of the period account for about 72% of the published documents. As can be seen, in the first seven years, the energy efficiency of concrete has received less attention, with as much as a 3% contribution to 22 years of research. The reason might be the lack of attention to the general concept of sustainability in the construction sector, back in those days. This is also confirmed by Rwelamila et al. (2000), where the authors have attributed the lack of focus on sustainable construction to conventional approaches in construction projects. The authors have concluded that these approaches lack a relationship management system that cannot address sustainable-related concerns in buildings. Similarly, Bon and Hutchinson (2000) have stated that economic challenges are the main reason as to why sustainability is not a hotspot in the construction sector. Between 2008 to 2014, the rate at which studies are published has significantly elevated. This can be attributed to the awareness raised about climate change, carbon emissions, and their negative environmental impacts, in addition to observing the tangible effects of adopting sustainable practices in improving the energy efficiency of concrete (Habert & Roussel, 2009; Jaillon & Poon, 2008; Potbhare et al., 2009). Also, the increasing number of studies from 2015 to 2022 lies in the remarkable contribution of both developed and developing countries to energy saving in buildings through developing energy-efficient concrete (Giama & Papadopoulos, 2015; Kumanayake & Luo, 2018; Yaphary et al., 2017) and extensive achievements in the replacement of a wide range of recycled contents with the environmentally expensive constituents in concrete mixtures along with the inclusion of thermal storage materials (Mah et al., 2018; Tijani et al., 2022). This ascending trend in the publications can also be related to the commitments of decision-makers to the

sustainability regulations established by the Green Building Council (GBC) and the Intergovernmental Panel on Climate Change (IPCC) (Cordero et al., 2019).

Figure 2.3 (a) shows the top 15 countries with the most published documents on improving the energy efficiency of concrete in the construction sector. As the figure shows, this topic has been of interest among the pioneering developed countries, including the United States, Australia, and China with 14.4%, 13.3%, and 9% contributions, respectively, followed by Italy, Spain, and the United Kingdom. Conducting an SRL enables the identification of the leading journals that address the energy-related and sustainability concerns of concrete in buildings. Figure 2.3 (b) presents the top 15 journals in which the related research works have been published. Journal of Cleaner Production is the leading venue, accounting for 20.5% of the published research, followed by Construction and Building Materials and Energy and Buildings, with 18.6% and 8.7% contributions, respectively. These journals mainly publish studies focused on improving the energy efficiency of concrete in the construction sector (Farooq et al., 2021; Ho & Huynh, 2022; Lee et al., 2022).

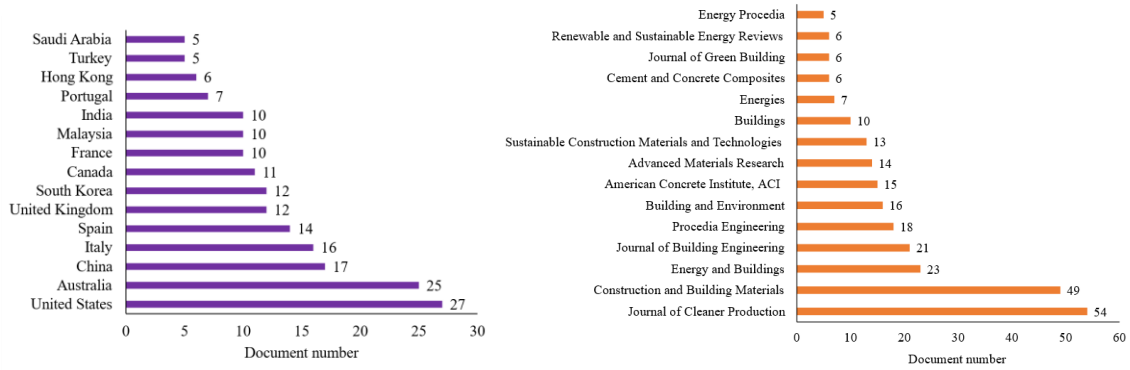

(a) (b)

Figure 2.3 The number of published documents based on region and source

Figure 2.4 presents the top contributing institutions with minimum documents and citations of 2 and 30, respectively. It is worth mentioning that in the maps obtained by VOSviewer, the size of circles is determined based on a quantitative relationship (i.e., contributing organisations or keywords) associated with an item in a network, while the lines denote the connection between items (Van Eck & Waltman, 2013). The results show that Griffith University, Yonsei University, and the University of Bologna are leading in the number of publications. However, in terms of citations, the Columbia University with 958 citations, is ranked first among 30 institutions, followed by the City University of Hong Kong and the Hong Kong Polytechnic University. Moreover, RMIT and the Technology University of Malaysia are among the top 10 universities

with the most citations. This indicates that the number of documents cannot ensure citations, as four documents from Colombia University and the City University of Hong Kong are cited nearly four times more than nine documents from Griffith and Yonsei universities.

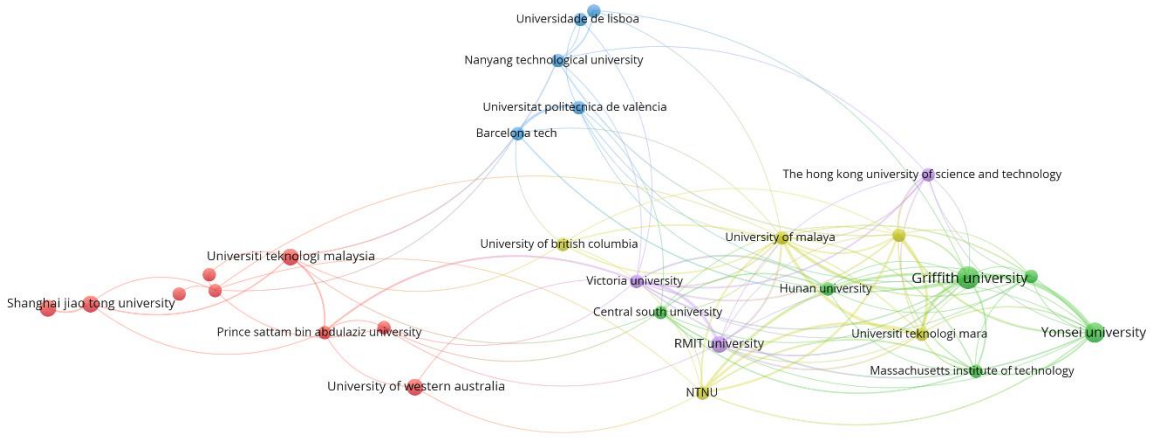

Figure 2.4 Publications based on institution

In addition to the affiliations, the present study has analysed the published studies considering the authors, as shown in Figure 2.5. The results indicate that 60 authors have published at least two publications with more than 40 total citations. As can be seen, collaboration among authors with the highest number of documents has increased with a focus on the environmental footprints of concrete (W. Lu et al., 2020; Oh et al., 2016; H. S. Park et al., 2013; Sandanayake et al., 2017), which is consistent with the research trends in last eight years of the defined time frame. This shows that the topic has received research attention among scholars over time. Our analysis indicates that authors with the highest number of documents and citations have more frequently collaborated, as the closeness of bigger nodes is shown in Figure 2.5. This calls for more effort to integrate the currently tiny contributors into linked research groups, indicating a point that needs more attention.

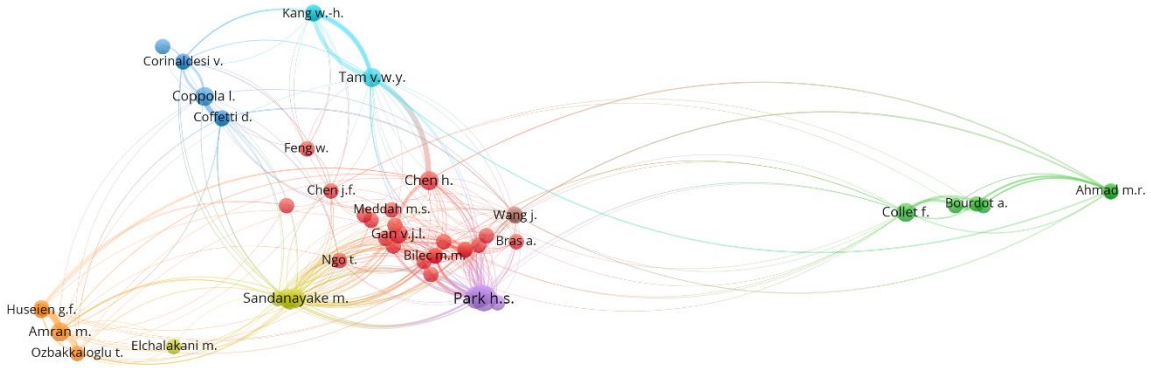

Figure 2.5 Publications based on author names

2.4.2 Keywords clustering and citation burst analysis

Numerous studies has been performed on the energy efficiency of concrete in the past decades. Thus, identifying and analysing all the trending keywords used may not be practical using traditional review methods. To address this, the current study leverages the systematic analysis capability of VOSviewer and explores trend keywords and topics, as shown in Figure 2.6. To generate the bibliometric maps, a multi-stage selection is undertaken within the software to refine the presented results. The results indicate that 110 keywords have been used over eight times in the collected publications.

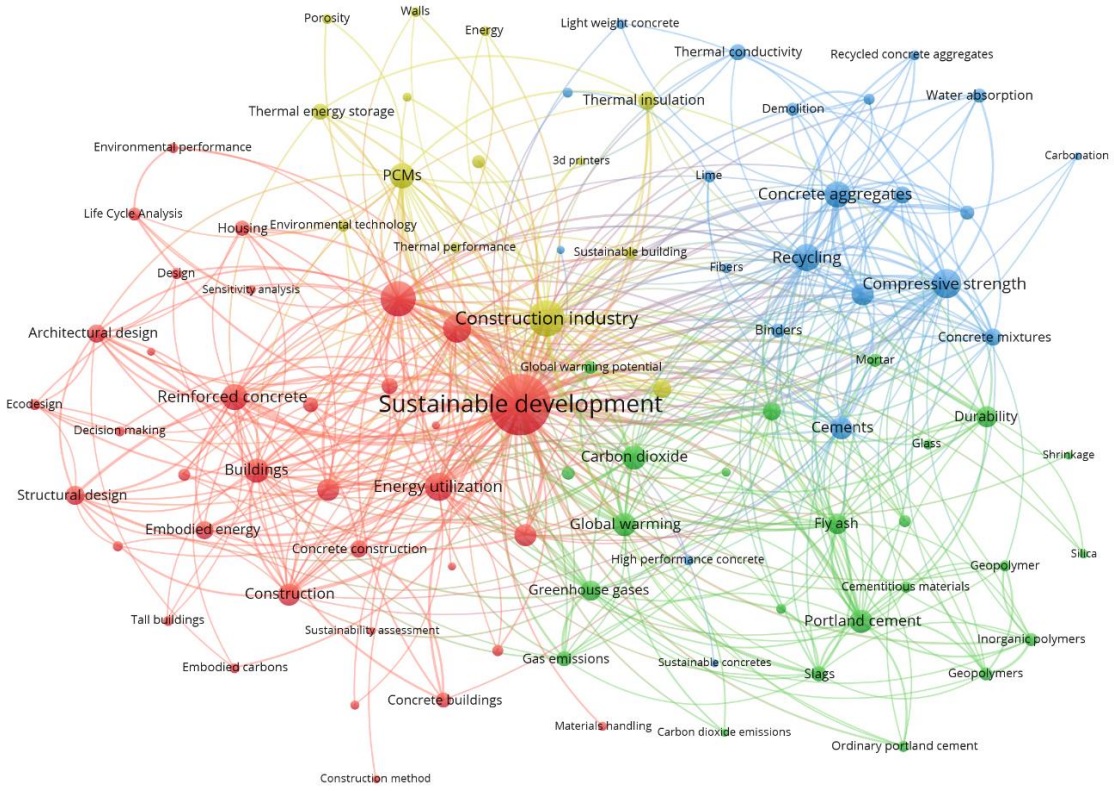

Figure 2.6 Keyword clustering

In Figure 2.6, four clusters of keywords are shown, while different hotspots are colour coded. In this figure the circles indicate keywords, the size of the circles denotes their frequency in the collected publications, and the lines show the connection among the keywords. However, all the used keywords and their connections are not reflected in Figure 2.6 due to the visualising limitations.

In the first cluster, shown in red, the most frequent keywords are sustainable development, building materials, and concrete construction. The main focus of this cluster is on the sustainability of

concrete and the energy consumption attributed to this building material. In this context, Meglin & Kytzia (2019) have studied the results of the life cycle analysis (LCA) of concrete and how production technology, socio-technical settings, and methodological choices impact the LCA results. Similarly, Dossche et al. (2015) have investigated factors contributing to the environmental footprints of high-strength concrete using LCA. The authors have concluded that the share of construction waste production and transportation is not negligible; however, they can be improved by up to 30%. The second cluster, coded green, considers the environmental implications of concrete, as its most frequent keywords are global warming, greenhouse gases, carbon dioxide emissions, and portland cement. Thus, this group seeks the environmental footprints of cementitious composites by including a wide range of lightweight fillers such as fly ash, slag, and geopolymers can be seen in this cluster. For instance, Elchalakani et al. (2017) and Sandanayake et al. (2018) have investigated the environmental implications (i.,e. carbon emission) of fly ash, slag, recycled aggregates, and geopolymer-based concretes. In another study, Patel et al. (2020) have shown a 20% improvement in several environmental indices of concrete at 20% replacement of cement with a specific type of glass powder. The third cluster, shown in blue, accounts for the effect of recycled contents on the mechanical performance of concrete, as strong connections can be found among compressive strength and a set of sustainable practices, including recycling, recycled aggregates, demolition, and fiber (Guo et al., 2018; Johra et al., 2021). Although all the used keywords are not reflected in Figure 2.6, our analysis shows that the thermal performance of recycled aggregate concrete (RAC) and supplementary cementitious materials (SCMs)-incorporated concrete are also investigated in this cluster, which is considerably less researched compared to mechanical performance. The last cluster, shown in yellow, however, contributes to the thermal performance of concrete during the operating phase, as the presence of thermal-related keywords such as thermal insulation, thermal performance, porosity, thermal storage, PCM, and building envelopes in this cluster indicates (Damdelen, 2019; Figueiredo et al., 2016; Tran Le et al., 2010). It is worth mentioning that direct links between 3d printers, sustainable development, and the construction industry can be seen in Figure 2.6 (S. A. Khan et al., 2021; Mahadevan et al., 2020).

An in-depth review of these 4 clusters and their focuses indicates that improving the energy efficiency of concrete has been investigated through a wide range of approaches, such as including SCMs and recycled contents, increasing the porosity of cementitious composites, and using thermal energy storage materials. Furthermore, the impacts of these approaches on the mechanical, environmental, and thermal performances of concrete have been sought. The results show that some

of the mentioned sustainable practices improve the energy efficiency of concrete in the operating phase (i.,e. PCMs and porous concrete), while some consider the energy efficiency in both embodied and operating phases (SCMs and recycled contents). However, the concentration of the studies is on embodied phase by minimising the environmental footprints of concrete. As a result, improving the energy efficiency of concrete by focusing on its operating phase is limited, despite the higher energy use attributed to this phase, as opposed to EE, throughout the life cycle of buildings. Meanwhile, research on energy-efficient concrete considering its operating phase is drawing attention.

2.4.3 Qualitive analysis

Our SRL shows that extensive efforts have been made to improve the energy efficiency of concrete, as the most commonly used material in this sector (Asadi et al., 2021; Becchio et al., 2009; Małek et al., 2021). Using systematic analysis, four most adopted strategies are identified, and qualitative analysis is conducted on them in the following:

2.4.3.1 Incorporating lightweight aggregates (LWA)

Operating phase: The energy performance of concrete is a function of a wide range of factors, including the type of aggregates and cementitious materials (Asadi et al., 2018). Aggregates (fine and coarse) encompass 60-75% of the concrete volume, thereby governing the thermal properties of concrete (Wang et al., 2021). The thermal properties of coarse aggregate vary based on its composition and degree of crystallisation (M.I. Khan, 2002). The findings indicate that an increase in the coarse aggregate content can increase the thermal conductivity of concrete (Kazmi et al., 2021). This lies in the less porous structure of coarse aggregates (Zhang et al., 2015). It has been reported that a 1% increase in the porosity of concrete can decrease its thermal conductivity by up to 0.6% (Real et al., 2021). Hence, replacing coarse and fine aggregates to a certain percentage with LWA, resulting in lightweight concrete (LWC) can be an effective approach to improve the thermal performance of concrete (L. H. Nguyen et al., 2014). The density of LWC ranges between 1350 to 1850 kg/m3, while the density of normal concrete (NC) varies between 2400 to 2500 kg/m3, which highlights the higher thermal conductivity of NC (Samson et al., 2017). The superior thermal properties of LWC can be attributed to the higher amount of air trapped in its porous structure compared to NC (Demirbog, 2003). According to Holm and Bremner (2000), the density of LWC is roughly 23% less than NC, while the thermal conductivity of LWC and NC vary between 0.5 to 0.86 w/mk and 1.4 to 2.9 w/mk.

It is stated that a 50 to 70% reduction in the thermal conductivity of concrete is achieved by reducing the density of NC from 2000–2600 kg/m3 to 1400 to 1800 kg/m3 (dos Santos & Matias, 2006). Real et al. (2016) have also reported a 40 to 53% reduction in the thermal conductivity of NC using LWA. To produce LWC, a wide range of LWA can be used, including expanded clays and shales, pumice perlite, and various wastes, such as blended waste, clay brick, rubber, plastic, oil palm shell, and agricultural and recycled concrete aggregates (RCA) (Bogas et al., 2014; Y. Zhao et al., 2018). The latter, however, is among the widely used LWA (Y. Liu et al., 2021), as it can also address the environmental implications associated with landfills and reduce embodied carbon, cost of production, and exploitation of the natural resources, thereby contributing to green construction (Bonoli et al., 2021). Zhu et al. (2015) have explored the thermal properties of three different RAC types using RCA. The authors have stated that the three samples have lower thermal conductivity than that in NC. They have also found a direct relationship between thermal conductivity and the density of RAC mixes. Reviewing the literature shows more evidence of the superior thermal performance of RAC than NC (Xiao et al., 2010). Among the developed countries, China and the United States are responsible for producing 2360 and 600 million tons of construction demolition and waste (CDW), which can be recycled into RCA (Mullett, 2022).

- ***Embodied phase:*** This approach has been used to increase the energy efficiency of concrete by reducing the embodied energy attributed to concrete production. Hossain et al. (2016) have reported respective 65% and 58% reductions in greenhouse gases and non-renewable energy consumption using RCA obtained from CDW recycling through an LCA. In another study, the environmental benefits of incorporating RCA in pavement application are investigated. The results have indicated that utilising RCA can alleviate environmental concerns, including energy and water consumption, carbon emissions, and construction waste generation, while it might cause the production of toxic gases, such as NOx, a dangerous gas for humans (Sereewatthanawut & Prasittisopin, 2020). Colangelo et al. (2018) have concluded that introducing RCA can reduce the environmental impacts associated with concrete, while it is required to quantify the energy consumption associated with RCA transportation. It has been reported that incorporating recycled aggregates as a replacement for natural aggregates can also reduce the cost of production up to 20% (L. Zheng et al., 2017b).

The findings in the literature have highlighted the effectiveness of RAC in alleviating heat exchange through concrete due to its improved thermal properties. Therefore, RAC can be used as an effective thermal insulation material, compared to NC. Moreover, using RAC can address environmental concerns associated with CDW landfills, natural resources depletion, and CO2 emissions. However, using recycled aggregates can reduce the mechanical properties of concrete due to its higher porosity, water absorption, and weaker bonds that it forms with new pastes, compared to CA (Debieb et al., 2010). This shortcoming can be addressed by incorporating materials that increase the mechanical performance of concrete, such as SCMs, which can compensate for the strength reduction (Qureshi et al., 2020).

2.4.3.2 Incorporating SCMs

- ***Operating phase***: SCMs are mostly the by-products of other industries and encompass a wide range of materials, including fly ash, silica fume, blast furnace slag, rice husk ash, and corn cob ash (Vejmelková et al., 2012). The partial replacement of cement content with SCMs is among the effective approaches to energy-efficient concrete (Sargam et al., 2020). Cseh et al. (2021) have studied the effect of SCMs on the heat transfer of concrete. The authors have reported a significant reduction in the thermal conductivity of concrete by partially replacing cement content with fly ash. Chen et al. (2016) have reported the effectiveness of replacing cement content by 8-20% with fly ash and 3-5% with slag in reducing the thermal conductivity and density of mixes. Adewoyin et al. (2022) have recently concluded that incorporating four types of SCMs (fly ash, slag, silica fume, and expanded glass) can reduce the thermal conductivity and density of mortar by 10.1% and 25.4%, respectively. By reviewing the literature, more evidence on the efficiency of SCMs in improving the thermal properties of concrete can be found (Demirboğa, 2007).

- ***Embodied phase***: Similar to LWA, SCMs are also mainly used to produce energy-efficient concrete considering its embodied phase. Vargas & Halog (2015) have shown a reduction in carbon dioxide emissions using a specific type of fly ash obtained from an ultra-fine grinding process. Samad & Shah (2017) have reviewed the impact of using a set of SCMs, including fly ash, slag, rice husk ash, and silica fume on the environmental implications of concrete. The authors have highlighted the effectiveness of SCMs in reducing the negative environmental footprints of concretes in their embodied phase. S. A. Miller (2018) has conducted a study to explore the environmental benefits stemming from adopting SCMs. The results have shown that using higher SCMs does not necessarily result in lower

environmental footprints. The author has concluded that structural design and transportation should be taken into consideration in the design process. The impact of SCMs on the environmental performance of cementitious composites is extensively explored in the literature (Jiang et al., 2022; Kurda et al., 2019; J. J. Wang et al., 2017).

The combined effects of utilising both SCMs and recycled aggregates on concrete have been extensively investigated, focusing on the mechanical properties and environmental footprints of concrete (Qureshi et al., 2020; W. Zhang et al., 2019). In contrast, the impact of using SCMs and RA on the thermal performance of concrete is rarely researched. The findings in the literature show that only a handful of researchers have explored the impact of both approaches on the thermal properties of concrete. Sargam et al. (2020) have investigated the impact of incorporating SCMs, in particular slag and fly ash, on the thermal properties of recycled aggregates-incorporated concrete. The results have shown a reduction in the thermal conductivity of mixes. Martinez et al. (2022) have explored the impact of replacing cement and coarse aggregate contents with ground recycled concrete as SCM and RCA on the thermal performance of concrete. The results have shown that the replacement of cement and natural aggregates by 10 to 25 wt% and 50% with the selected SCM and RCA can lower thermal conductivity by 7.9 to 11.8% and increase specific heat capacity by 6.0 to 9.1%. According to the existing literature, the effect of utilising SCMs and RA on the thermal properties of concrete is limited to the two mentioned documents. Therefore, more studies are required to further evaluate the effectiveness of the aforementioned approach in improving the thermal properties of concrete.

2.4.3.3 Increasing porous structure

The findings in the literature show that increasing the porous structure of concrete has promises to reduce the operating energy demand of concrete (Radhi, 2011; Shon et al., 2021). This can be achieved by injecting air into concrete mixtures using foaming agents or aluminium powder (Ramamurthy et al., 2009). A high concentration of air voids increases the porous structure while reducing the density and thermal conductivity of mixes. As a result, the aerated concrete becomes suitable for thermal insulation and acoustic applications (Raj et al., 2019). The density of foam concrete (FC) usually varies between 300 to 1600 kg/m3, and it can be used for thermal insulation, non-load bearing, and load-bearing applications depending on the obtained density (Jones & McCarthy, 2006). Despite a wide range of FC applications, the share of its use in construction projects is roughly 5.6% in North America and Australia (X. Zhao et al., 2015).

The thermal performance of FC has been extensively explored (Proshin et al., 2005; N H Zahari, 2009). Due to its cellular microstructure, using FC ensures the improved thermal properties of concrete. It has been concluded that thermal conductivity is directly proportional to the density of FC (M. Chen et al., 2022). Mydin (2011) has explored the thermal conductivity of several FC mixes with different densities. The author has noted that higher porosity can result in lower density and thermal conductivity. In an experimental study, it is reported that the thermal conductivity of mixes with densities ranging from 700 to 1400 kg/m3 swings between 0.24 to 0.74 W/mK (Ganesan et al., 2015). Consequently, FC has been deemed a sustainable building material due to its superior thermal performance, compared to other concrete types, and has been adopted in several applications in buildings (Y. Liu et al., 2020; Qu & Zhao, 2017). FC allows for the incorporation of waste materials in concrete (Hashim & Tantray, 2021), which, in turn, limits its application to non- and semi-structural applications (Amran et al., 2015). Therefore, some environmental concerns associated with natural resource depletion, waste landfills, and CO2 emissions can be addressed (Zimele et al., 2019; Shah et al., 2021). At present, incorporating a wide range of waste materials in FC has been explored, including but not limited to fly ash, silica fume, bottom ash, waste glass, and CDW (She et al., 2018; Kashani et al., 2019).

Based on the findings in the literature, FC has contributed to the energy efficiency of concrete due to its superior thermal performance. However, the integration of FC into new developments, such as additive manufacturing, which improves the sustainability in construction, as confirmed by the results of the SRL shown in Figure 2.6, is still limited. Hence, investigating the foam-incorporated cementitious composites while leveraging new developments in construction is yet to be explored.

2.4.3.4 Incorporating thermal energy storage (TES) materials

To reduce energy consumption, on the one hand, and provide thermal comfort for users, on the other, it is important to minimise heat exchange through concrete (Pop et al., 2018). TES is an effective way to enhance energy efficiency in concrete by increasing its heat storage capacity and adding more thermal mass to concrete (Luo et al., 2019). In this context, the use PCMs can increase energy efficiency in concrete by reducing heating and cooling loads (Achkari & El Fadar, 2020). PCMs store the thermal energy in concrete in latent heat mode, meaning the energy storage occurs when the phase of the storage material is changed from solid to liquid or liquid to gas while the material temperature is not extremely fluctuating, in turn, the peak demand is shifted, as shown in Figure 2.7 (Alptekin & Ezan, 2020). It is reported that the energy storage capacity of PCMs between

18°C to 26°C is 3 to 6 times more than that of water and concrete, respectively (Kuznik et al., 2008).

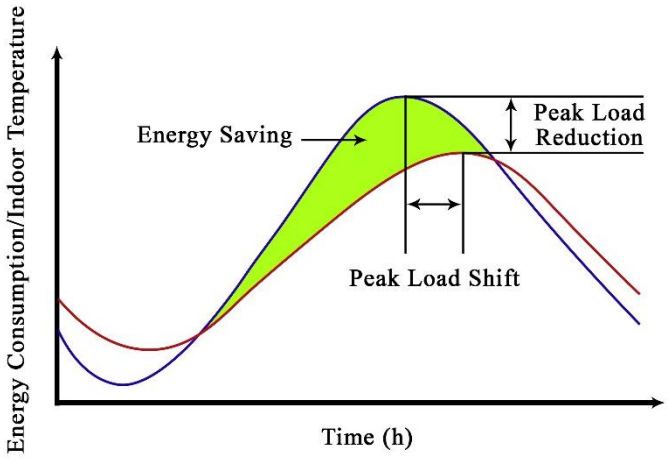

Figure 2.7 The effect of PCM

PCMs are generally categorised into three types: organic, inorganic, and eutectics. The former mainly comprises paraffin and non-paraffin base materials, while inorganic PCMs are usually salt-hydrate and metallics bases. Eutectics PCMs are a mixture of two or more components (Tyagi & Buddhi, 2007). V. D. Cao et al. (2019) have reported that up to 28 to 30% of energy reduction can be achieved in cold climates by utilising PCMs in multi-layer concrete walls. Cabeza et al. (2007) have examined the effect of incorporating microencapsulated PCMs into concrete walls. The results highlight the improved energy efficiency of designed specimens. Reducing the indoor temperature and alleviating the temperature swings are also reported by embedding PCM into concrete walls (Essid et al., 2022). The impacts of PCMs on the energy efficiency in concrete have been widely explored (Faraj et al., 2020; H. Wang et al., 2020). Figure 2.8 shows the classification of thermal energy storage materials and different types of PCMs.

Although several studies have confirmed that embedding PCMs in concrete is an effective way to increase its energy efficiency, researchers have reported long payback periods for this approach (Abu-Hamdeh et al., 2021). Hence, incorporating PCMs in building elements may not be economical due to the higher price of PCMs compared to other insulation methods (Sarı, 2022).

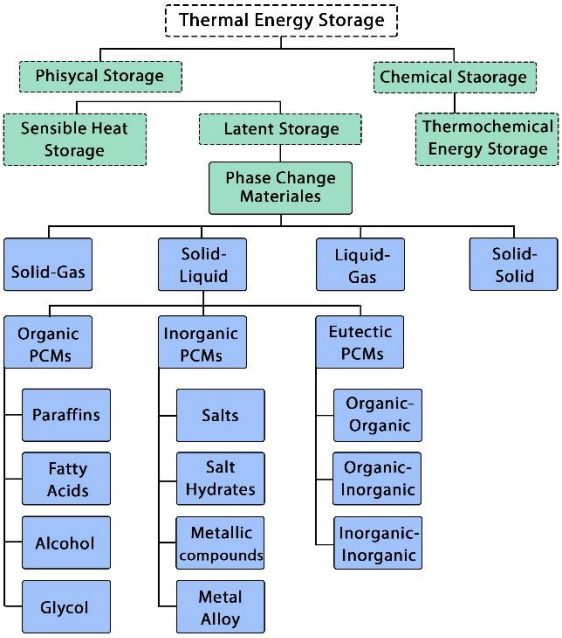

Figure 2.8 Classification of thermal energy storage materials

2.5 Conclusion

The energy use attributed to the concrete industry has raised environmental concerns in recent decades. Thus, various sustainable practices have explored increasing the energy efficiency of concrete concerning its embodied and operating phases. To investigate the evolution of these studies, an SRL is carried out on the documents published between 2000 and 2022, using the Scopus database constrained by a set of pre-defined keywords and criteria. As a result, 283 refined publications are selected. The obtained documents are analysed based on their bibliometrics information to explore contributing institutions, authors, sources, regions, keyword clustering, and the frequency of records over time.

An increasing trend in energy-efficient concrete is noticed from 2017 to 2022, particularly after 2020. China and the United States are the leading countries contributing to the sustainability of buildings. Also, two scholarly venues, the Journals of Cleaner Production and Construction and Building Materials, are found as pioneers in the area of energy-efficient concrete. The analysis of keyword clustering highlights the hotspots that have targeted environmental, mechanical, and thermal objectives. It is found that recycled contents, SCM, aerated concrete, and PCMs are among the most widely researched topics. In this context, several approaches have been of interest, including but not limited to the use of recycled aggregates to produce LWC, incorporation of SCMs as the replacement for cement, introduction of air bubbles to increase the porosity of concrete, and

integration of PCMs into concrete to improve its thermal properties. The latter, however, is reported to be not economical as it is accompanied with long payback periods. Moreover, the current SRL helps identify several research gaps. Addressing these gaps can be deemed as future research pathways contributing to the energy efficiency of concrete. These are summarised as follows:

- Although the significant impact of the thermal performance of concrete during its service life is highlighted in the literature, most studies tend to minimise the environmental implications of concrete considering its embodied phase. This can be attributed to the availability of the embodied values associated with various concrete constituents in reliable standards, facilitating the estimation of the EE for different concrete mixes. In contrast, quantifying the energy use of concrete during its operating phase and the synergetic implications of other parameters add complexity to OE estimation, resulting in limited investigation on the topic. Therefore, more efforts are still needed to shed light on the approaches concerning the operating energy attributed to concrete. Moreover, more investigations on the approaches capable of considering both phases can have a significant promise in energy-efficient concrete.
- The findings show that using RCA can improve the thermal performance of concrete due to its higher porous structure compared to NA, resulting in lower density than normal concrete. However, it can have a detrimental effect on the mechanical properties of concrete mixes. To overcome this shortcoming, replacing cement content with SCMs can help compensate for the weakened mechanical properties. However, replacement beyond certain percentages may lead to a reduction in the mechanical strength of concrete. This study has identified the lack of systematic approaches to design optimised green RAC mixes containing SCMs, considering the replacement thresholds for SCMs and RCA, targeting environmental, mechanical, and thermal aspects.
- Despite the extensive research on the benefits of FC (e.g., promising thermal properties and use of lightweight fillers and SCMs beyond the commonly referenced percentages), research on integrating this approach into new developments in the construction industry, such as additive manufacturing, is limited. Also, the adoption of sustainable practices identified in this study (i.e., using LWA and FC) can help address the limitations associated with this emerging technology. It is worth noting that the results of the SRL highlight the connection between 3D printers and sustainable developments in the construction sector. Hence, research on the thermal properties of green mixes using cutting-edge technologies can contribute to the design of energy-efficient concrete.

- The results of the literature review highlighted the significance of employing sustainable practices to improve the thermal and environmental performance of concrete, neglecting the considerable influence of concrete mix designs on radiant heating systems. Given the proper thermal mass and conductivity of concrete, the heat can be stored and distributed through floors, walls, and ceiling, thus reducing heat costs by creating a responsive and comfortable radiant heating system. Therefore, further investigations into the impact of concrete choice on the thermal efficiency of radiant heating systems can be deemed as a future research avenue.

Chapter 3 A Simplified Predictive Model for Office Building Energy Consumption

3.1 Abstract

The construction sector accounts for 30 to 40% of global energy use and associated carbon emissions. Over 80% of this energy use is attributed to operating phase in buildings, resulting in the development of several approaches to quantify the energy performance of buildings, including numerical, statistical, and data-driven methods. Given the synergetic implications of environmental and design-related parameters on the energy consumption of buildings, minimising the latter requires identifying the most suitable approach to facilitate the preliminary energy evaluations. Existing energy modelling tools can be costly and demand time-consuming modelling based on 3D building models. In addition, assessing data and resources in the early stages of projects can pose remarkable difficulties in detailed modelling. This chapter presents a simplified and accurate operating energy predictive model that requires the least amount and most accessible type of data to accelerate a reliable preliminary understanding of the effects of various design decisions on the overall energy efficiency in buildings. The model is based on over 1.5 million simulations with varying key design factors spanning ten climate zones from 40 cities. Validation is performed with five case studies, resulting in an accuracy of 92.4% in estimating the operating energy consumption of office buildings. The model could assist designers by facilitating energy-related decision-making and achieving energy-optimal design in the preliminary stages of projects, when the impact of available building materials on building operating demand can be significant. The sensitivity analysis enabled by the model showed a potential for up to a 10% enhancement in the thermal properties of exterior walls and roof just by reducing the thermal transmittance of the concrete in those elements. This improvement can lead to up to 6% enhancement in the annual energy performance of buildings.

3.2 Introduction

The construction sector consumes 40% of total energy production worldwide (Nejat et al., 2015) and is responsible for 5.7 billion tons of annual CO_2 emissions: the equivalent of 23% of total global CO_2 emissions (L. Huang et al., 2018).

Energy consumption during a building life cycle can be classified into two main categories: embodied and operating energy (Akbarnezhad & Xiao, 2017). On the one hand, embodied energy accounts for the energy consumed in manufacturing and construction operations, including material

extraction, purification, processing, transportation, installation, construction, and end-of-life processes, such as demolition and landfilling. On the other, operating energy accounts for the energy consumed during the service lives of buildings, including lighting, heating, cooling, ventilation, hot water supply, and equipment (Chiniforush et al., 2018; Hammad et al., 2018). The results of previous studies highlight variations in embodied and operating energy in buildings (E. Wang et al., 2011). For example, life cycle energy analyses of 73 cases, including residential and office applications in 13 countries, indicate that operating energy accounts for between 80 and 90% of total life cycle energy– with embodied energy accounting for the remaining 10 to 20% (Ramesh et al., 2010c). The findings of previous studies also suggest that operating and embodied energy account for approximately 85% and 15% of the life cycle energy, respectively (Khasreen et al., 2009). The amounts of operating and embodied energy, along with their relative share in the total life cycle energy of a building, vary as a function of numerous design-related and environmental factors, and this is reflected in previous studies. As an example of the latter, the share of climatic conditions accounts for 10 to 30% variation in the energy consumption of buildings (Ramesh et al., 2012). Embodied energy varies according to a set of factors, including but not limited to geographical location, material type, manufacturing technology, and construction techniques (Manish K. Dixit, 2017), while variations in operating energy mostly depend on the ambient temperature, thermal properties of materials, and operation of equipment, such as HVAC system, lighting, and occupancy behaviour (Pacheco et al., 2012). The high dependency of embodied and operating energy on design-related and environmental parameters can significantly influence the prediction of energy consumption in buildings. Moreover, uncertainty in various design-related and environmental factors can complicate the accurate measurement of the relative effect of each factor (Feng et al., 2019).

Despite the higher relative share of operating energy compared to embodied energy throughout the life cycle of buildings, the majority of existing quantification methods have explored the embodied energy of materials. This can be ascribed to the availability of embodied values attributed to building materials in reliable standards (Hammond & Jones, 2008). The review of the literature, however, highlights the extensive research on the impact of both environmental and design-related parameters on operating energy in buildings. From the environmental parameter view, Kavousian et al. (2013) reported that weather, location, and floor area are among the most important factors in the energy consumption of residential buildings. Duan et al. (2022) concluded that climatic and socioeconomic conditions dually impact energy consumption in buildings. Nik & Kalagasidis (2013) also explored the effects of climate change on the energy demand of buildings. The authors

reported that the future cooling and heating demands increase and decrease, respectively, over time. In contrast, from the design-related parameters view, Ihara et al. (2015) highlighted the importance of the thermal properties of façade components in buildings. Grynning et al. (2013) also investigated the effect of the thermal properties of windows on energy demand. The authors concluded that a 33% reduction in the u-value of windows could reduce cooling and heating demands by 5-15%. Moreover, several scholars have sought the minimisation of operating energy considering design-related factors. For instance, Najjar et al. (2019) suggested the integration of a mathematical optimisation framework, building information modelling, and life cycle assessment to improve energy efficiency during operating phase. Peippo et al. (1999) utilised an optimisation method to determine the combination of design parameters with the lowest energy demand considering design characteristics and energy demand target. Pisello et al. (2012) presented a method capable of analysing the thermal performance of buildings in a dynamic environment. Other researchers have also studied design strategy modifications to enhance energy efficiency in buildings. Short et al. (2004) concluded that natural ventilation could improve energy efficiency in buildings. Santin (2011) reported that the differences in HVAC systems user behaviour as the most important reason for the mismatch in estimated and actual energy consumption in buildings. It is also stated that using artificial lighting and electro-mechanical systems to meet cooling/heating setpoints can result in high operating energy demands (Praseeda et al., 2016).

By relying on the extensive evidence on the considerable impact of design-related parameters on the energy performance of buildings, the influence of design decisions on embodied and operating energy should be better understood and considered as a part of the design process (Zou et al., 2019). Given the overlapping energy implications of design decisions, the ability to quantify the magnitude of the impact of influential design parameters on operating and embodied energy is required to ensure a holistic minimisation of life cycle energy. The impact of design parameters on embodied energy has been extensively investigated (Dixit et al., 2010). As a result, numerous non-computational estimation methods have been proposed to address the timely estimation of the impact of design-related decisions on embodied energy in buildings. These include input-output, process analysis, and hybrid methods (Crawford & Treloar, 2003). The estimated embodied energy varies in each method due to the differences in data and system boundaries (Venkatraj & Dixit, 2021). On the other hand, to estimate the operating energy in buildings, several studies have been conducted to develop computational approaches which rely on the computer simulation of building operation under various environmental conditions (Yan et al., 2008; Zhong et al., 2019). To quantify operating energy using these computational approaches, a trained engineer/consultant is

required, thereby making the entire process time-consuming and costly (Yigit & Ozorhon, 2018). In addition, accurate and detailed energy-related specifications of building elements are needed as input for these simulations, which may not be available in the early design phases of projects (Roels et al., 2017). The limitations of the available methods, along with the considerably higher relative share of operating energy compared to embodied energy, highlight the importance of developing simplified and reliable non-computational methods to predict operating energy demand in buildings. These could enable not only an estimate of the impact of design-related decisions on operating energy in buildings but also the consideration of different climatic conditions. Our study addresses this gap by proposing a design expression that can provide sufficient accuracy despite its simplicity for estimating operational energy in the early stages of building design. The most influential parameters are included to improve the overall energy performance in buildings. The developed predictive model could allow designers to evaluate the impact of their design decisions on the operating energy demand in a short time. In addition, the model can also be deployed for exploring energy-optimal designs in the preliminary stages of projects.

3.3 Methodology

The process followed to develop the analytical predictive model is depicted in Figure 3.1. The study begun with a comprehensive literature review to identify the 13 most relevant parameters impacting the operating energy consumption of buildings. These include both design and environmental factors. Next, energy simulation scenarios were created by assigning different values to the parameters in 40 cities across the world. The corresponding 1.5 million energy simulations were carried out using EnergyPlus software with an automation process based on the Dynamic Link Library (.dll) file by Gordillo et al. (2020). The collected data was analysed to determine the energy consumption patterns by different contributing sectors, including but not limited to heating, cooling and lighting. The general structure of the predictive model was then developed based on the contribution of each of the identified parameters to the overall energy consumption of buildings. Finally, the coefficients of the model could be calibrated using a genetic algorithm (Ramos Ruiz et al., 2016) to achieve a higher level of accuracy.

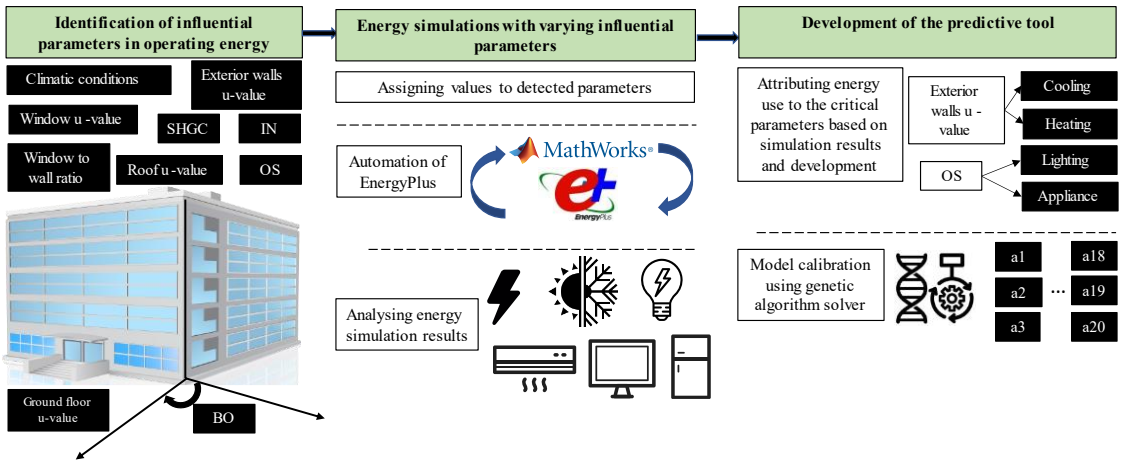

Figure 3.1 Development of the predictive model framework

Results of previous studies show the several design-related and environmental parameters impact operating energy in buildings. These include window to wall ratio (WWR), glass Solar Heat Gain Coefficient (SHGC), glazing u-value (U_{window}), exterior wall u-value (U_{wall}), roof u-value (U_{roof}), ground floor u-value (U_{gf}), infiltration rate (IN), building orientation (BO), operating schedule (OS), and most importantly, environmental indices, e.g., temperature (T), relative humidity (RH), solar radiation (SR), and wind speed (WS) (Najjar et al., 2019; Pisello et al., 2012). In total, 13 parameters were used here to generate energy simulation scenarios.

The energy simulation scenarios were designed to conduct a comprehensive energy analysis. For this purpose, a medium-sized office building provided by the U.S. Department of Energy (DOE) was selected as reference building. The reference rectangular-shaped office building with 15 zones consists of 3 floors with 50 m in length and 33 m in width. The total floor area is 4,982 m^2. The height of each story (floor-to-floor height) is 3.96 m. The set temperature for cooling is assumed to be 24°C and 26.7°C during working and non-working hours, and it is heated at 21°C and 15.6°C during working and non-working hours, respectively. The HVAC system of the building is based on MZVAV with plenum zones. VAV Box Reheat Coil supplies hot water for the building at 60°C, with a maximum capacity of 82°C. The light usage and electricity plug loads are considered to be 10.76 w/m^2. The occupancy schedule is assumed to be 5.38 person/100m^2, which corresponds to a total of 268 people during working hours. Two 20-HP elevators are available in the building. Furthermore, the design factors were given three possible values: lowest, highest, and average (intermediate 1). Additionally, those parameters with significant impact on energy consumption (based on relevant literature findings) were assigned an additional intermediate value (intermediate

2). Table 3.1 lists these values and the corresponding physical definitions of the design-related parameters.

Table 3.1 Considered values for design parameters in energy simulations

Design Parameter	Explanation & Considered Values
Exterior wall u-value (U_{wall})	Heat transfer rate of exterior walls. Min=0.19, Intermediate 1 =0.3, Intermediate 2 = 0.45, Max= 1.75
Ground floor u-value(U_{gf})	Heat transfer rate of ground floor. Min=0.45, Intermediate 1 =0.83, Max=5
Window U-value (U_{window})	Heat transfer rate of window. Min=0.51, Intermediate 1 =2, Intermediate 2 = 3, Max= 4.8
Roof U-value (U_{roof})	Heat transfer rate of roof. Min=0.22, Intermediate 1 =0.3, Intermediate 2 =0.4, Max=0.66
Window Solar Heat Gain Coefficient (SHGC)	Fraction of solar radiation admitted through a window. Min= 0.1, Intermediate 1 =0.4, Intermediate 2 =0.6, Max=0.9
Window to Wall Ratio (WWR)	Area of windows (a) divided by area of exterior walls (b) which is presented in percentage, a/b. Min =17%, Intermediate 1=35%, Intermediate 2=50%, Max=70%
Operating schedule (OS)	Fractional method is utilised that Min=0.25 (using1/4 of the operation capacity), intermediate 1=0.5 (12-hour occupation), Intermediate 2= 0.75 (using ¾ of the operation capacity) and Max=1.0 stands for 24-hour occupation of the building
Building orientation (BO)	The angle between buildings longitudinal axis and the North direction. Min=0º, Intermediate 1=30º, Max=90º
Infiltration rate (IN)	Air exchange rate, known as air change per hour (ACH). Min=0.17, Intermediate 1 =0.4, Intermediate 2 =1.2, Max=2
Ratio of exterior walls area to roof area(α)	For a building with rectangular plan and x,y dimensions with height of h, α is $[2.(x+y).h/(x.y)]$. α usually varies between 0.25 to 15 for medium office buildings. This parameter is considered to be a constant number in this study.

The values of U_{wall}, U_{roof}, U_{gf}, U_{window}, WWR, SHGC, and IN were considered according to the ASHRAE standards (Crawley et al., 2008). Also, a fractional value range (0.25 to 1) and degree were used to quantify OS and BO, respectively. The four most critical environmental indices, i.e. T, RH, SR, and WS were also targeted (Allouhi et al., 2015). It is worth noting that α is assumed to remain constant in energy simulation scenarios due to the unvarying geometry of the reference building.

Energy simulations were carried out in 40 cities to investigate the effects of climatic conditions, as listed in Table 3.2, along with the corresponding values of the targeted environmental parameters. Richards et al. (2019) have classified climate conditions into 10 representative zones, i.e., tropical rainforest (TR), tropical monsoon (TM), savanna (SA), hot desert or arid (HD), cold desert or arid (CD), mediterranean (ME), subtropical (SU), oceanic (OC), hot or warm continental (WC), and cold continental (CC). In this study, four representative cities are considered for each climate zone.

As a result, an average of about 40,000 runs for each city and over 1.5 million total runs were performed by varying the climate zones to represent the selected cities. Moreover, standard and updated weather files containing essential location information, such as latitude, longitude, and daylight savings period, were used to provide the simulation engine with weather data (Crawley et al., 2001).

Table 3.2 Considered climate zones and cities

Climate	City	T (ºC)	RH (%)	SR (Kwh/m2/day)	WS (km/h)
Tropical rainforest (CL01-TR)	Kuala Lumpur	27.5	80.0	5.20	6.40
	Singapore	26.8	84.0	4.30	8.00
	Hilo	23.4	74.0	4.90	18.5
	Kisumu	22.8	61.0	4.80	9.10
Tropical monsoon (CL02-TM)	Miami	25.0	73.0	5.10	14.8
	Qionghai	24.6	85.0	4.50	12.4
	Male	28.6	80.0	5.10	17.0
	San Juan	26.0	75.0	5.00	13.3
Savanna (CL03-SA)	Darwin	27.8	61.5	5.90	15.3
	Accra	26.6	81.0	5.10	7.10
	Havana	24.5	76.0	4.70	17.3
	Brasilia	21.3	68.0	5.00	11.4
Hot desert or arid (CL04-HD)	Riyadh	25.4	29.0	7.00	14.0
	Phoenix	24.5	37.0	6.50	10.0
	Cairo	22.0	56.0	7.10	14.0
	Abu Dhabi	26.8	63.0	6.20	14.1
Cold desert or arid (CL05-CD)	Tabriz	12.5	53.8	4.60	11.0
	Zaragoza	14.7	63.0	5.00	14.5
	Denver	11.0	53.0	4.80	14.0
	Tehran	17.5	40.0	5.00	8.70
Mediterranean (CL06-ME)	Barcelona	15.5	72.0	4.50	12.3
	San Francisco	14.3	73.0	4.30	17.1
	Rome	15.0	75.0	4.00	12.4
	Lisbon	16.9	71.0	4.60	17.5
Subtropical (CL07-SU)	Milan	13.0	75.0	4.70	7.20
	Sydney	17.6	61.3	5.10	12.5
	Shanghai	16.1	80.0	3.20	18.0
	Mexico City	16.6	56.0	4.90	7.50
Oceanic (CL08-OC)	London	11.5	81.0	2.70	11.5
	Amsterdam	10.0	83.0	4.20	20.7
	Melbourne	15.0	56.0	4.20	12.4
	Paris	11.3	78.0	3.20	15.7
Warm continental (CL09-WC)	Moscow	6.00	76.0	3.50	16.0
	Toronto	8.30	71.0	3.90	18.3
	Helsinki	5.10	79.0	3.30	16.0
	Kiev	7.00	76.0	3.20	15.2
Cold continental (CL10-CC)	Yakutsk	-9.00	68.0	2.80	7.00
	Fairbanks	-3.00	65.0	2.90	9.50
	Anchorage	6.00	71.0	3.00	8.60
	Heilongjiang	3.00	63.0	3.00	12.5

3.4 Evolution and calibration of predictive model

The predictive model was formed based on the detailed analysis and interpretation of the results of the energy simulations, focusing on the share of the energy use of the contributing sectors (e.g., heating, cooling, and equipment). The energy demand of the reference building was categorised into two groups, i.e. climate-dependent (e.g., heating and cooling) and climate-independent demands (e.g., equipment electricity use and lighting), which together account for the total operating energy consumption. An analytical expression was proposed to cater for such a categorisation in the energy analysis of the reference building:

$$EUI_E = U_{eq}\Delta T_{eq} OS_{eq} + OS_{eq} EU_{eq}, \quad (3.1),$$

where the first term takes into account climate-dependent energy demands, while the second considers climate-independent demands, which together provide EUI_E, i.e. the annual energy use intensity (EUI). Note that U_{eq} denotes the equivalent heat exchange coefficient of exterior walls, roof, windows, and ground floor; ΔT_{eq} is the difference between the desired indoor and outdoor temperatures; OS_{eq} is the equivalent of OS, i.e., the period during which the building should operate at a desired temperature; EU_{eq} is the equivalent average rate of energy consumption for climate-independent purposes. The predictive model can be further expanded based on the definition of each term as follows. The following subsections present the procedure adopted to expand the terms in Eq. (3.1), followed by the parameterisation and addressing of each term, considering the effects of both design-related and environmental parameters.

3.5 Equivalent heat exchange coefficient (U_{eq})

According to the literature, heat exchange occurs through building elements that are directly exposed to the outside environment, resulting in the transfer of heat/energy (Alghoul et al., 2017). These elements encompass windows, exterior walls, roof, and ground floor. The impact of the heat exchange equivalent of these building elements can be captured by considering their corresponding area on the façades of buildings along with their other thermal properties-e.g., SHGC for windows (Bhatia et al., 2019). Moreover, one of the most contributing factors to heat exchange in buildings is IN, whose role is considerably impacted by RH and WS. With that being said, Eq. (3.2) can represent the equivalent of heat exchange for these elements as follows:

$$U_{eq}=a_1\times\left\{\frac{WWR}{100}\times U_{window}\left(SHGC^2\times a_2+WWR\times a_3\right)\alpha+a_4\times\frac{(100\text{-}WWR)}{100}\times U_{wall}\alpha+a_5U_{roof}+a_6U_{ground}+\right.$$
$$\left.a_7(2+\alpha)(IN+a_8)(RH/100+a_9)(WS+a_{10})\right\} \quad (3.2),$$

In the previous equation, the term U_{eq} comprises the effects of different parameters, including external walls, windows, roof, and ground floor, by multiplying the thermal properties of each element by its corresponding occupied area. To consider the effect of windows, the term $WWR/100\times U_{window}$ indicates the share of window area on the building facade multiplied by its heat transmission coefficient (u-value) (ASHRAE, 2017). Based on the definition of the National Fenestration Rating Council, SHGC is the amount of heat gain derived from the solar radiation transmitted through fenestration, added to the amount gained and re-emitted to the indoor space by fenestration itself (Marinoski et al., 2012). Thus, the term $SHGC^2\times a_2+WWR\times a_3$ captures the effect of the SHGC of windows. Since the thermal performance of vertical and horizontal surfaces are different, the parameter alpha takes into account the proportion of vertical diffuse surfaces (external walls) to their horizontal counterparts (roof and ground floor). To consider the effects of other building surfaces exposed to the outside environment, the term $a_4\times\frac{(100\text{-}WWR)}{100}\times U_{wall}\alpha+a_5U_{roof}+a_6U_{ground}$ denotes the heat exchange coefficient of walls, roof, and ground floor. Moreover, the effect of IN is captured, as IN can cause significant heat exchange through building elements. This factor accelerates the effects of other environmental indices, as it can exchange air with different RH and T, thereby impacting thermal comfort. Further, WS can impact the amount of exchanged air by accelerating the outdoor air penetrating the building (ASHRAE, 2017). Thus, the term $a_7(2+\alpha)(IN+a_8)(RH/100+a_9)(WS+a_{10})$ denotes the heat exchange coefficient of IN. To estimate the heat exchange attributed to windows, exterior walls, roof, ground floor, and IN, the formulated equivalent heat exchange coefficients of these elements are later multiplied by the equivalent of temperature difference (ASHRAE, 2017).

3.5.1 Equivalent temperature difference (ΔT_{eq})

The energy use attributed to heating and cooling loads is significantly impacted by the temperature difference between inside and outside environments. Thus, a detailed consideration of contributing factors to the temperature difference is required. In this sense, several indices, such as the heat caused by occupants and appliances need to be included. Additionally, factors such as OS, BO, and SR can have a notable impact on the temperature difference. Eq. (3.3) describes the equivalent of the temperature difference between the desired setpoint and ambient temperature, as follows:

$$\Delta T_{eq} = abs|T+a_{12}OS+a_{13}SR(1+a_{14}abs(sin|BO+a_{15}|))+a_{16}|\times[1+a_{17}(T+a_{12}OS+a_{13}SR(1+a_{14}abs|BO+a_{15}|)+a_{16})], \quad (3.3),$$

The term ΔT_{eq} considers the effects of factors that cause differences between indoor and outdoor temperatures. To capture the effect of occupant presence, the term $T+a_{12}OS$ includes the heat generated by occupants and utilised equipment during the building operations. The heat generated by equipment during non-working hours is also taken into account by the term a_{16}, with a partial increase in internal temperature. In addition, the term $a_{13}SR(1+a_{14}abs|BO+a_{15}|)$ takes into account the effect of SR, which is impacted by BO with regard to the true north direction (ASHRAE, 2017). Moreover, the term $a_{17}(T+a_{12}OS+a_{13}SR(1+a_{14}abs|BO+a_{15}|)+a_{16})$ includes the direct effect of the temperature difference between the indoor and outdoor environments incurred on the HVAC system. The effect of T is obtained through multiplying the temperature difference by the thermal properties and areas of the building elements, discussed in the previous section.

3.5.2 Equivalent operation schedule (OS_{eq})

The term OS_{eq} presented in Eq. (3.1) captures the effect of OS. In this context, the term $(OS+a_{11})$ is considered to span the energy consumption during operating and non-operating hours, a climate-related relationship. Because most of the energy consumption load occurs in the service time of buildings, all the previous terms are multiplied by OS. The term a_{11} depends on temperature and was considered since heating and cooling loads are not completely zero while the building is not operating, and different temperature setpoints need to be met.

3.5.3 Equivalent non-climate related energy consumption (EU_{eq})

As discussed, a significant bulk of energy use in commercial buildings is ascribed to climate-independent parameters, including OS, lighting, hot water, and power required. For instance, increasing the OS and WWR can increase and decrease the lighting required in buildings, respectively. Such effects can be parameterised in the next equation, where it should be denoted that the energy consumption for non-climate related demands (e.g., interior lighting, equipment, facilities, and so on) is included.

$$EU_{eq} = a_{18}\left(OS+\frac{1}{(WWR\times SHGC\times a_{19})/100}\right)+a_{20}, \quad (3.4),$$

The term $a_{18}(OS+\frac{1}{(WWR\times SHGC\times a_{19})/100})$ includes plug loads and interior light usage, which are impacted by OS and WWR. For instance, if the building is used for an extended period (a greater OS) or natural light gain is limited (small WWR), this term increases the amount of energy consumption due to artificial lighting demand. The term a_{20} considers the energy consumption for the vacant building in a non-operating state. This energy consumption includes facilities and equipment energy use for zero OS, independent of temperature (e.g., fridge usage, security cameras, computers and monitors in stand-by mode, ventilation, water heater, and outdoor lighting).

It is worth mentioning that the average energy consumption of about 1124 MJ/m^2 per year is reported for commercial buildings considering equipment, lighting, heating, cooling and ventilation, according to DOE (IotaComm, 2020). The energy consumption of facilities varies, depending on building applications. Therefore, proper multipliers should be adopted for those buildings with other applications.

By expanding the two main terms in Eq. (3.1) (i.e., climate-dependent and climate-independent) and conducting multiple trial-and-error attempts and modifications, it is concluded that Eq. (3.5) can adequately capture the physics of operating energy consumption for the reference building.

$$EUI_E=a_1\times\left\{\begin{matrix}\frac{WWR}{100}\times U_{window}\left(SHGC^2\times a_2+a_3\times WWR\right)\alpha+a_4\times\frac{(100\text{-}WWR)}{100}\times U_{wall}\alpha+a_5U_{roof}+a_6U_{gf}+\\ a_7(2+\alpha)(IN+a_8)(RH/100+a_9)(WS+a_{10})\end{matrix}\right\}$$

$$\times(OS+a_{11})\times abs|T+a_{12}OS+a_{13}SR(1+a_{14}abs(\sin|BO+a_{15}|))+a_{16}|\times[1+a_{17}(T+a_{12}OS+a_{13}SR(1+a_{14}abs|BO+a_{15}|)+a_{16})]$$

$$+a_{18}(OS+\frac{1}{(WWR\times SHGC\times a_{19})/100})+a_{20}, \qquad (3.5),$$

where EUI_E is the annual operating energy consumption per square meter of the building (MJ/m^2.year), WWR, α , RH, SHGC, and OS carry no unit. In the present study, the α value is 1.19 for all the simulations. The units of IN, WS, SR, BO and T are m^3/hour, km/h, kwh/m^2/day, deg and °C, respectively. Moreover, the unit of the u-values of building elements is $W/(m^2\cdot°K)$.

3.5.4 Calibration of predictive model

By analysing the results of the energy simulations carried out by EnergyPlus, the multipliers a_1 to a_{20} were given a range to limit the search space for calibration process. These multipliers were then calibrated using GA optimisation solver (X. S. Xie et al., 2011). The GA solver continuously adjusts a population of individual solutions within upper and lower limits assigned to the

multipliers. As a result, the population evolves toward an optimal solution while the limits are continuously modified based on the solutions proposed by the GA solver. In this study, the energy simulations performed by the adopted simulation engine described in Section 3.3 were also carried out by the predictive model considering the determined range for the multipliers. The GA solver explored the optimal values of the multipliers by minimising the error between the calculated energy consumption via the simulation engine ($EUI_{R,i}$) and the predicted value through the proposed predictive model ($EUI_{E,i}$). Eq. (3.6) indicates the defined objective function. As a result, the values of the constants were calibrated, as listed in Table 3.3.

$$\text{Objective function}=\sqrt{\sum \frac{\left(\frac{EUI_{E,i}-EUI_{R,i}}{EUI_{R,i}}\right)^2}{n}} \quad (3.6),$$

Figure 3.2 shows the normal distribution of errors between the results of both mentioned methods. Furthermore, a normal distribution curve was calculated for the results, showing -1.5%, 9.6%, and 7.6% for average error, standard deviation, and average absolute error, respectively.

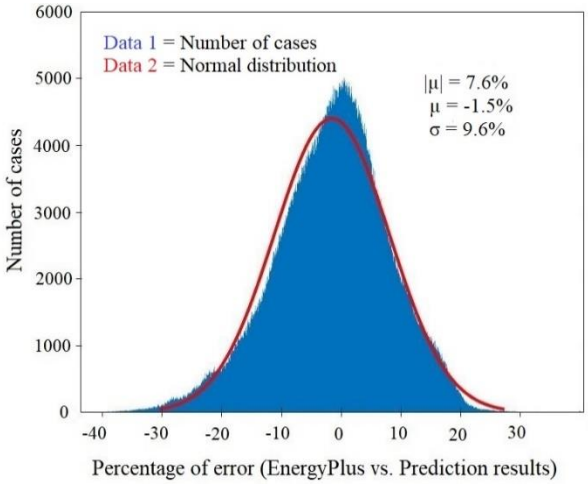

Figure 3.2 Normal Distribution of errors

Table 3.3 Variables optimum values

Variable	Value	Variable	Value
a_1(MJ/(W.yr)	0.08	a_{11}(1.0)	5.43
a_2(1.0)	12.41	a_{12}(°C)	4.22
a_3(1.0)	0.12	a_{13}(m^2.°C.day/kWh)	0.08
a_4(1.0)	14.55	a_{14}(1.0)	-0.22
a_5(1.0)	28.21	a_{15}(deg)	-42.93
a_6(1.0)	-0.52	a_{16}(°C)	-20.43
a_7($W.h^2/(m^5.km.°C)$)	0.09	a_{17}($°C^{-1}$)	-0.02
a_8(m^3/h)	0.14	a_{18}(MJ/m^2 .yr)	668.45
a_9(1.0)	0.60	a_{19}(1.0)	18.45
a_{10}(km/h)	70.25	a_{20}(MJ/m^2 .yr)	680.00

3.6 Validation

In this section, the accuracy of the predictive model is examined in two steps. Firstly, the model proposed was tested in randomly generated cities that were not used in the calibration process to examine the robustness and suitability of its predictions. The predictive tool and simulation engine were used to conduct new energy simulations in these five cities, and the results are compared to validate the accuracy of the model. Secondly, the accuracy of the model was examined for other building applications that were not initially used for calibration. This assessment aimed to assess its robustness and potential need to consider a modification/adaptation of the relevant coefficients and parameters to align with the specific requirements of the desired application.

3.6.1 Commercial application performance

The accuracy of the model was investigated across nine design parameters for commercial application in five targeted cities, as listed in Table 3.4. These cities are considered to span a wide variety of climates, including hot and cold climates (Dakar and Chicago), Mediterranean (Istanbul), Savanna (Manila), and Oceanic (Auckland). Also, maximum and minimum values were considered for the design-related parameters. The variation range (difference between maximum and minimum values) was divided into three equal segments by creating two intermediate values (Int-1 and Int-2) for each parameter, as listed in Table 3.5. The accuracy of the model was explored by assigning column values from Table 3.5 to the corresponding design parameters and sequentially examining the row values for each parameter. The results of the comparisons for the Int-1 and Int-2 are demonstrated for the targeted cities in Figure 3.3 to Figure 3.7. Assigning the values of the Int-1 column can enable swiping the parameters 33% lower and 67% higher than their initial values. Similarly, assigning the values of the Int-2 column can enable swiping the parameters 67% lower and 33% higher than their initial values.

Table 3.4 Considered climate zones and cities for calibration of mathematical model

Climate	City	T (ºC)	RH (%)	SR (Kwh/m2/day)	WS (k*m/h*)
Oceanic	Auckland	15.0	80.0	4.4	16.5
Savanna	Manila	27.3	73.8	5.0	12.8
Mediterranean	Istanbul	15.0	72.0	3.9	16.0
Warm continental	Chicago	10.0	71.0	3.8	16.5
Hot desert or arid	Dakar	25.0	65.8	6.0	14.6

Table 3.5 Different values for design parameters

Design Parameter	Min	Int-1	Int-2	Max
WWR	0.17	0.35	0.50	0.70
SHGC	0.10	0.36	0.63	0.90
U_{window}	0.50	1.66	2.83	4.00
BO	0.00	30.0	60.0	90.0
U_{wall}	0.10	0.73	1.36	2.00
U_{roof}	0.10	0.73	1.36	2.00
U_{gf}	0.10	1.06	2.03	3.00
IN	0.17	0.78	1.39	2.00
OS	0.25	0.50	0.75	1.00

In Figure 3.3 to Figure 3.7, the lines indicate the operating energy predicted by the proposed model, and the markers indicate the operating energy calculated by the simulation engine. The results are comparable in four points in each figure. Also, the EUI results were normalised to the initial values in these figures, thus recognising the difference between the two methods.

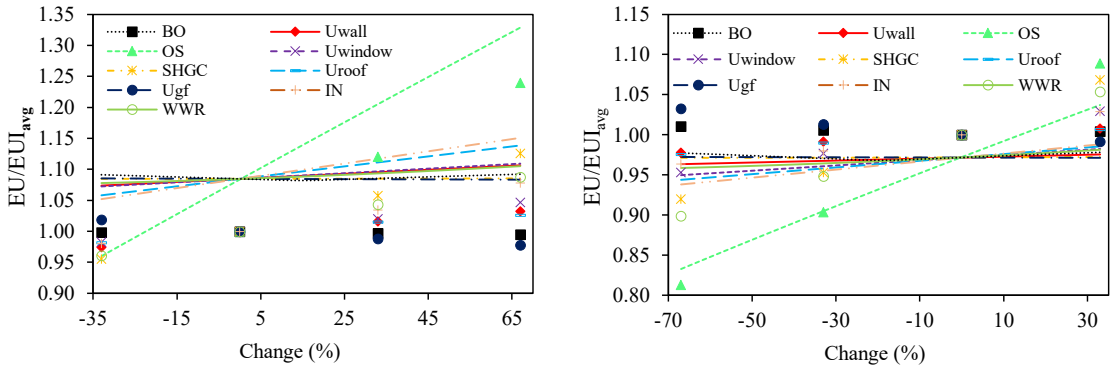

(a) Int-1 *(b) Int-2*

Figure 3.3 Operational energy consumption for Auckland

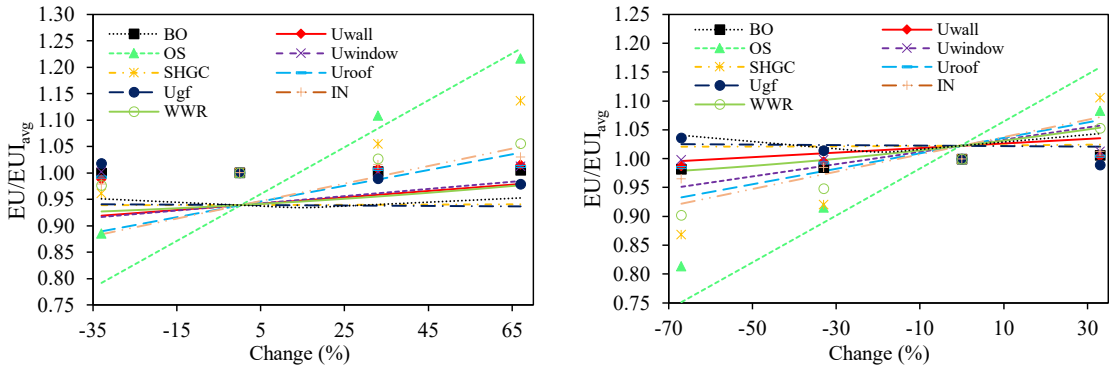

(a) Int-1 *(b) Int-2*

Figure 3.4 Operational energy consumption for Manila

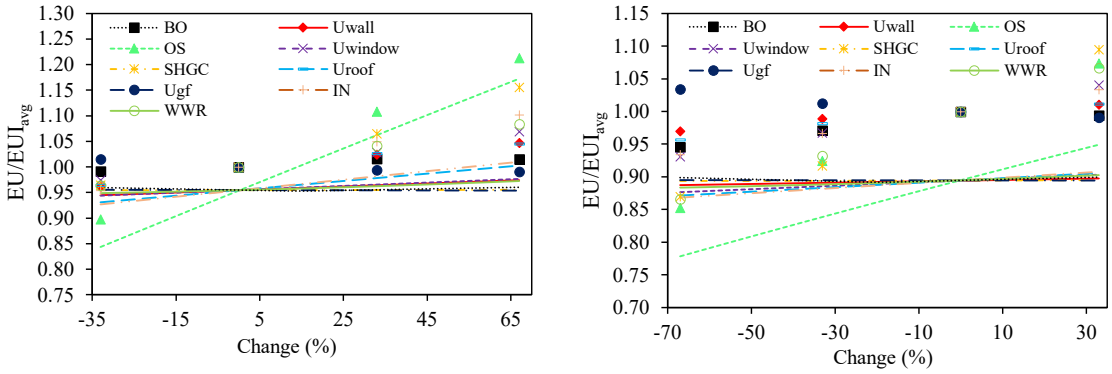

(a) Int-1 *(b) Int-2*

Figure 3.5 Operational energy consumption for Istanbul

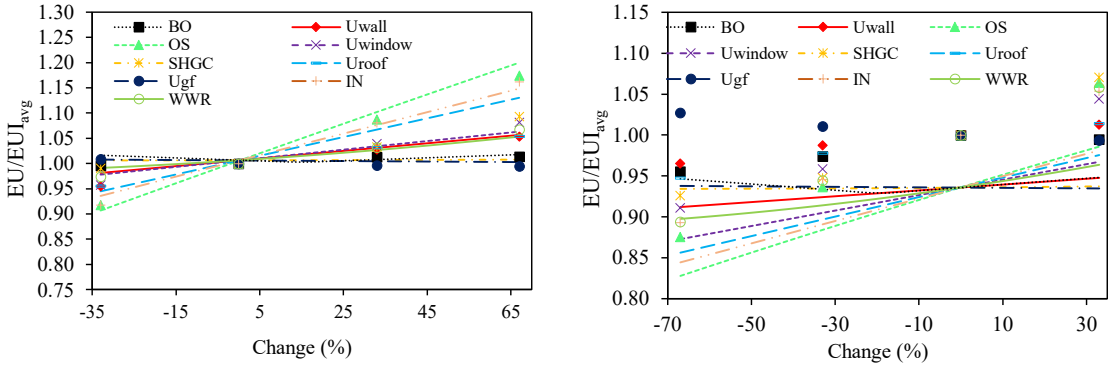

(a) Int-1 *(b) Int-2*

Figure 3.6 Operational energy consumption for Chicago

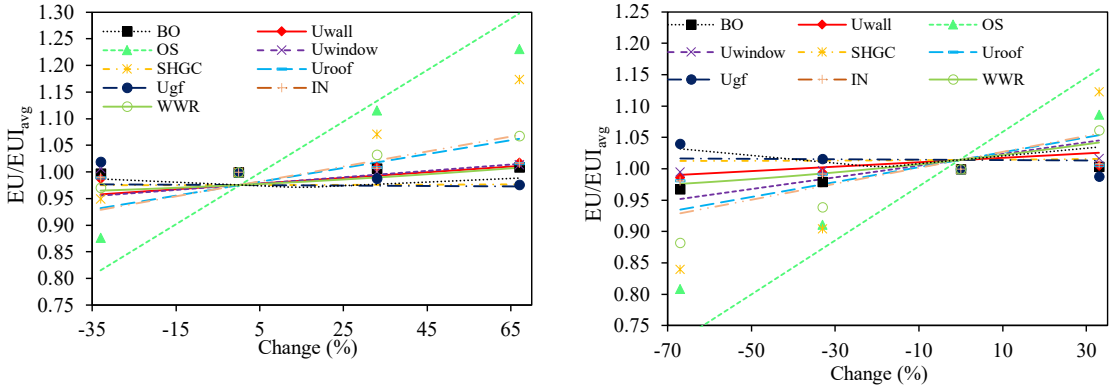

(a) Int-1 *(b) Int-2*

Figure 3.7 Operational energy consumption for Dakar

The results show that the average of the absolute errors for 360 points (considering 36 comparisons in each figure, Int-1 and Int-2, and 5 targeted cities) is 5.06%, indicating that the model predicts the operating energy in commercial buildings with acceptable accuracy. The predictive model shows the highest accuracy in Dakar and Chicago with as much as 3.65% average absolute error,

followed by Manila, Auckland, and Istanbul with 4.85%, 5.65%, and 7.5%, respectively. The results suggest that the model performs more efficiently in severely hot or cold regions due to its minor error rate in Dakar and Chicago – still all errors are within an acceptable range, the results show that the model error is relatively higher in Mediterranean conditions, such as Istanbul. As shown in Figure 3.5, all the markers are placed above their corresponding line, indicating that the EUI results calculated by the simulation engine are slightly higher than those by the predictive model. Therefore, it can be interpreted that the model exhibits slightly lower accuracy in this region compared to other climate zones. The average errors of estimating operating energy corresponding to the column values in Figure 3.5 are depicted in Figure 3.8. The validation result indicates that the model meets a suitable error rate based on the ASHRAE guideline 14-2014, which required the mean of absolute error (MAE) uncertainty indices to be less than 15% (Landsberg et al., 2014).

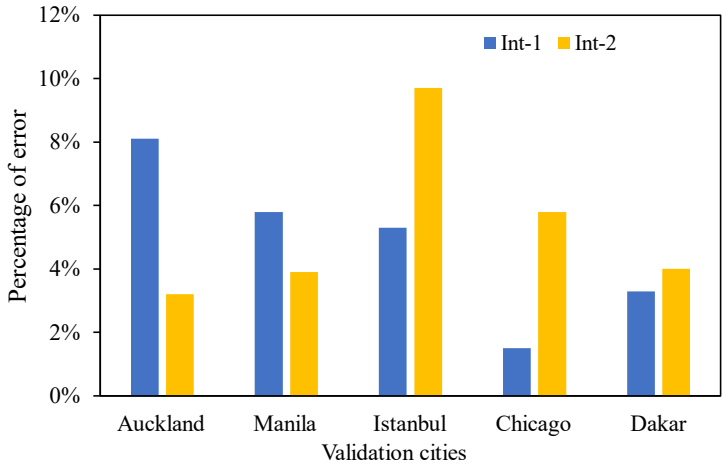

Figure 3.8 Validation errors

3.6.2 Non-commercial application performance

Additionally, a validation of the predictive model was carried out using a random building and climatic zone. A single-family residential building located in Dublin, Ireland and developed by the Pacific Northwest National Laboratory (PNNL) was selected for this purpose. This encompasses an area of 110.26 square meters with two standard levels and exterior walls height of 5.33 meters. Electric resistance heating and crawlspace foundation are employed in the heating pump system and foundation type of the reference building, respectively. Moreover, oceanic climatic conditions and values considered for design-related parameters along with the results obtained from both predictive model and simulation engine are presented in Table 3.6.

Table 3.6 Residential reference building specifications and annual energy consumption

Design Parameter										Climatic Parameters				EP result (MJ/m2)	Predicted result (MJ/m2)
WWR	SHGC	U_{window}	BO	U_{wall}	U_{roof}	U_{gf}	IN	OS	α	T	RH	SR	WS	1202.03	1197.75
0.15	0.33	1.70	0	0.40	0.13	0.22	0.15	0.50	2.05	9.40	0.83	3.00	20		

The results point to the high accuracy in the prediction of the operating energy of the residential building with approximately 1% error. Therefore, the model can also be reliable for residential applications, even though it is not specifically designed for this purpose.

3.7 Sensitivity analysis

The validated model was employed to investigate the magnitude of the impact of each parameter on operating energy in buildings. This was achieved by exploring the impact of variations in the parameters on the EUI, between their minimum and maximum values in 20 equal increments, as listed in Table 3.7. Considering the 14 influencing factors (including α) identified in the present study, this analysis resulted in 588 predictions. Figure 3.9 shows the results of the sensitivity analysis.

Table 3.7 Values considered for sensitivity analysis

Design Parameters										Climatic Parameters			
WWR (%)	SHGC	U_{window} (W/mK)	BO (deg)	U_{wall} (W/mK)	U_{roof} (W/mK)	U_{gf} (W.mK)	IN	OS	α	T (ºC)	RH (%)	SR (Kwh/m2/ day)	WS (Km/h)
10	0.10	0.51	0.00	0.19	0.22	0.45	0.17	0.25	0.25	-9.00	29.00	2.80	7.00
14	0.14	0.72	4.50	0.26	0.24	0.67	0.26	0.28	1.23	-7.12	31.80	3.01	7.68
18	0.18	0.93	9.00	0.34	0.26	0.90	0.35	0.32	2.22	-5.24	34.60	3.23	8.37
22	0.22	1.15	13.50	0.42	0.28	1.13	0.44	0.36	3.21	-3.36	37.40	3.44	9.06
26	0.26	1.36	18.00	0.50	0.30	1.36	0.53	0.40	4.20	-1.48	40.20	3.66	9.75
30	0.30	1.58	22.50	0.58	0.33	1.58	0.62	0.43	5.18	0.40	43.00	3.87	10.44
34	0.34	1.79	27.00	0.65	0.35	1.81	0.71	0.47	6.17	2.28	45.80	4.09	11.12
38	0.38	2.01	31.50	0.73	0.37	2.04	0.81	0.51	7.16	4.16	48.60	4.30	11.81
42	0.42	2.22	36.00	0.81	0.39	2.27	0.90	0.55	8.15	6.04	51.40	4.52	12.50
46	0.46	2.44	40.50	0.89	0.41	2.49	0.99	0.58	9.13	7.92	54.20	4.73	13.19
50	0.50	2.65	45.00	0.97	0.44	2.72	1.08	0.62	10.12	9.80	57.00	4.95	13.88
54	0.54	2.86	49.50	1.04	0.46	2.95	1.17	0.66	11.11	11.68	59.80	5.16	14.56
58	0.58	3.08	54.00	1.12	0.48	3.18	1.26	0.70	12.10	13.56	62.60	5.38	15.25
62	0.62	3.29	58.50	1.20	0.50	3.40	1.35	0.73	13.08	15.44	65.40	5.59	15.94
66	0.66	3.51	63.00	1.28	0.52	3.63	1.45	0.77	14.07	17.32	68.20	5.81	16.63
70	0.70	3.72	67.50	1.36	0.55	3.86	1.54	0.81	15.06	19.20	71.00	6.02	17.32

74	0.74	3.94	72.00	1.43	0.57	4.09	1.63	0.85	16.05	21.08	73.80	6.24	18.00
78	0.78	4.15	76.50	1.51	0.59	4.31	1.72	0.88	17.03	22.96	76.60	6.45	18.69
82	0.82	4.37	81.00	1.59	0.61	4.54	1.81	0.92	18.02	24.84	79.40	6.67	19.38
86	0.86	4.58	85.50	1.67	0.63	4.77	1.90	0.96	19.01	26.72	82.20	6.88	20.07
90	0.90	4.80	90.00	1.75	0.66	5.00	2.00	1.00	20.00	28.60	85.00	7.10	20.76

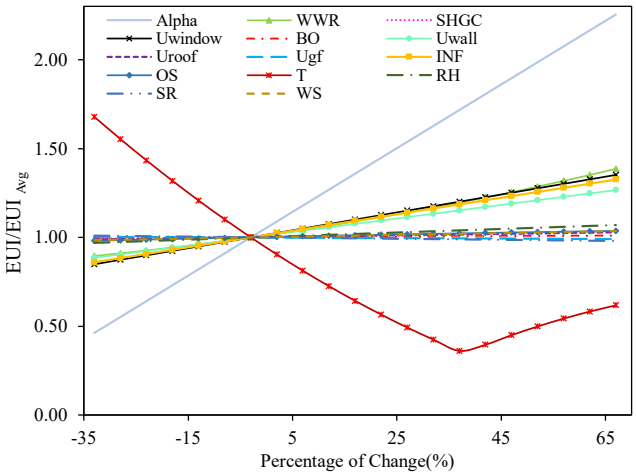

Figure 3.9 Sensitivity analysis of participating factors

Figure 3.9 highlights the significant influence of environmental factors on the EUI. As seen in the figure, an increase in T initially reduces the EUI to a certain point, but from that point onwards, the impact of T on EUI changes, and further increases in T result in increased EUI due to increased cooling load. Figure 3.9 also highlights the significant influence of building massing and mass distribution on operating energy. Also, U_{GF} and BO show minor effects on the energy use of the reference building. The results of the sensitivity analysis agree with the findings in the literature (Zhu et al., 2009). The presented results were obtained from the reference building used in this study, so the results might differ for other building types.

The presented sensitivity analysis was conducted around one intermediate value of environmental indices (e.g., T=x °C, RH=y %, SR=z kwh/m^2/day, and WS=m km/hour), which may not necessarily reflect the behaviour of the design parameters in all climate zones. Hence, additional sensitivity analyses were conducted to investigate the impact of identified factors on the EUI within each climate zone, hereafter. Considering 10 design parameters, 21 values for each parameter, as presented in Table 3.7, and 10 climate zones, these analyses resulted in 2,100 predictions. In these analyses, the design parameters had the same range of value in all the climates, while the environmental indices were assigned considering climate-dependent upper and lower bands, as summarised in Table 3.8. The results of the sensitivity of the identified factors are discussed in the

following paragraphs. Also, the relative importance of the parameters that are out of the scope of this study is discussed in Appendix A.

Table 3.8 Environmental upper and lower bounds for each climate

Climate Zone	ID	Temperature-T (°C)		Relative humidity-RH (%)		Solar radiation-SR (kwh/m^2/day)		Wind speed-WS (km/hour)	
		Min	Max	Min	Max	Min	Max	Min	Max
Tropical rainforest	CL01-TR	22.8	27.5	61.0	84.0	4.30	5.20	8.00	12.5
Tropical monsoon	CL02-TM	24.6	28.6	73.0	85.0	4.50	5.17	12.4	17.0
Savanna	CL03-SA	21.3	27.8	61.5	81.0	4.78	5.90	7.10	17.3
Hot desert	CL04-HD	22.0	26.8	29.0	63.0	6.20	7.10	10.0	14.1
Cold desert	CL05-CD	11.0	17.5	40.0	63.0	4.65	5.00	8.70	14.5
Mediterranean	CL06-ME	14.3	16.9	71.0	75.0	4.03	4.60	12.3	17.5
Subtropical	CL07-SU	13.0	17.6	56.0	80.0	3.20	5.10	7.50	18.0
Oceanic	CL08-OC	10.0	15.0	56.0	81.0	2.79	4.29	11.5	20.7
Warm continental	CL09-WC	6.00	8.30	76.0	79.0	3.20	3.90	15.2	18.3
Cold continental	CL10-CC	-9.00	6.00	63.0	71.0	2.80	3.02	7.00	12.5

3.7.1 Temperature (T)

Figure 3.10 presents the impact of ambient temperature (T) on the energy consumption of the reference building. The results indicate that a 10% increase in T leads to as much as a 6.9% increase in the operating energy demand in CL04-HD, the climate with the highest sensitivity to variations in T. The impact of T is observed to be roughly equal across all climates. Figure 3.10 also reveals that an increase in T in hot climates, such as CL-01, CL-02, Cl-03, and CL-04, leads to an increase in energy use intensity (EUI) due to the additional cooling load imposed on the HVAC system (Cruz Rios et al., 2017). Conversely, in moderate and cold climates, such as CL-05, CL-06, CL-07, Cl-08, CL-09, and CL-10, an increase in T results in a decrease in EUI by reducing the heating load. The results of the sensitivity analysis show that a 10% variation in T leads to an average change of 6.31% in EUI across all climates. These findings are consistent with previous studies in the field (Mirrahimi et al., 2016).

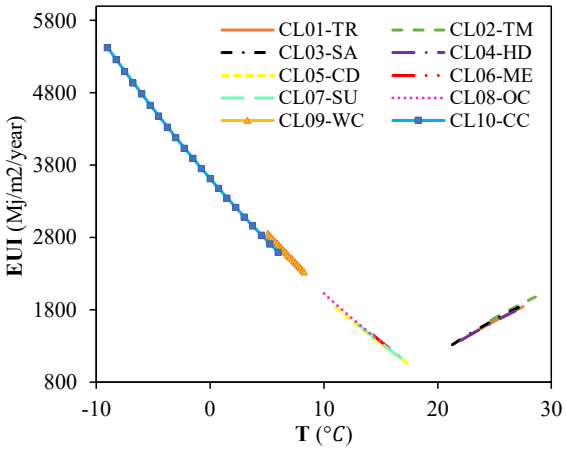

Figure 3.10 Sensitivity analysis for T

3.7.2 Ratio of exterior walls to roof area (α)

As shown in Figure 3.11, the impact of variations in α is more tangible in CL10-CC, with as much as an 8.2% increase in the EUI for a 10% increase in α, followed by CL09-WC and CL08-OC. This can be attributed to the effect of thermal mass on energy consumption in buildings (Reilly & Kinnane, 2017). The results indicate that the impact of variations in α is more significant in severely hot and cold climates. In contrast, the lowest dependency on variations in α is shown in CL06-ME, with a 4% rise in the EUI for a 10% increase in α. This lies in the fact that in moderate climates, the temperature difference between the desired setpoint and ambient temperature is less than that in severely hot or cold climates. As a result, less cooling and heating loads are incurred by variations in the mass of the walls and roof of the reference building.

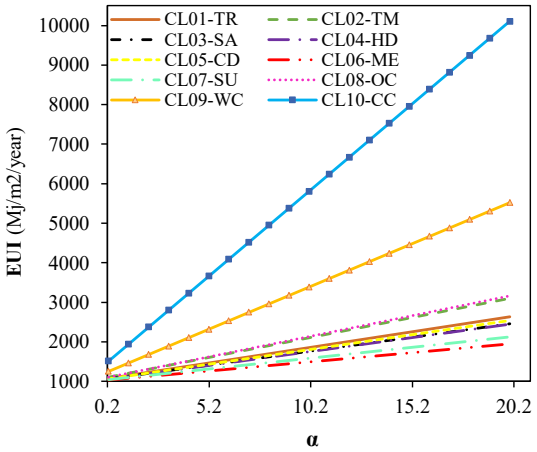

Figure 3.11 Sensitivity analysis for α

3.7.3 Window to wall ratio (WWR)

The sensitivity analysis shows that the operating energy of the reference building consistently increases with an increase in WWR in all the climate zones, as presented in Figure 3.12. The results re-affirms the importance of considering WWR as a critical variable in operating energy demand (X. Cao et al., 2016). The high impact of WWR on the EUI can be ascribed to the higher thermal conductivity and lower thickness of windows compared to other building elements on the façade of buildings. As a result, the u-value of windows is mainly higher than that of exterior walls and roofs, which can cause higher thermal exchange through windows. Further, it is observed that the impact of WWR in cold climates, such as CL10-CC and CL09-WC, is more tangible, as indicated by the exponential growth of the corresponding lines. The results highlight the importance of the relative share of windows and exterior walls in buildings, thus significantly affecting energy consumption in buildings (Sang et al., 2014). In particular, the results indicate that a 10% increase in WWR can increase the EUI with as much as 3.8%, on average.

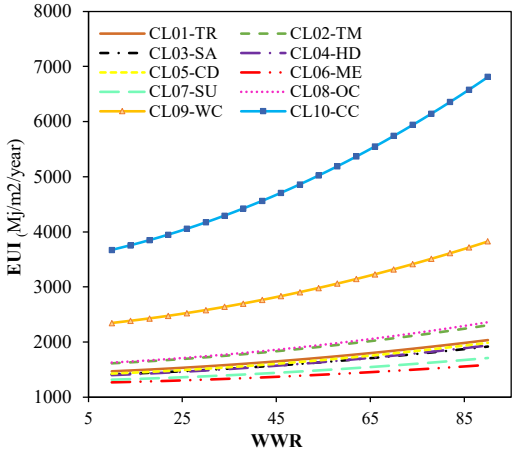

Figure 3.12 Sensitivity analysis for WWR

3.7.4 Exterior wall U-value (U_{Wall})

The impact of variations in U_{wall} on the operating energy of the reference building is shown in Figure 3.13. The results show that the EUI increases with an increase in U_{wall} in all the climate zones. Because exterior walls share a considerable area with the outside environment, the thermal properties of this element play a central role in the operating energy of buildings (Ralegaonkar & Gupta, 2010). Figure 3.13 also shows that the operating energy in CL10-CC and CL09-WC are impacted more than other climate zones, with as much as 4.8% and 4% swing for 10% variation in U_{wall}, respectively. Similar to α and WWR, the lowest dependency on this factor is identified in CL06-ME. This is due to the effects of these factors on the temperature difference between the

indoor and outdoor zones, which is larger in hot and cold climates and less in moderate climates. Aside from the environmental parameters, which cannot be optimised by designers, U_{wall} appears to be a highly influential factor (Lizana et al., 2017). This is also indirectly reflected in the sensitivity analysis results of α, where the importance of the thermal mass of exterior walls is highlighted.

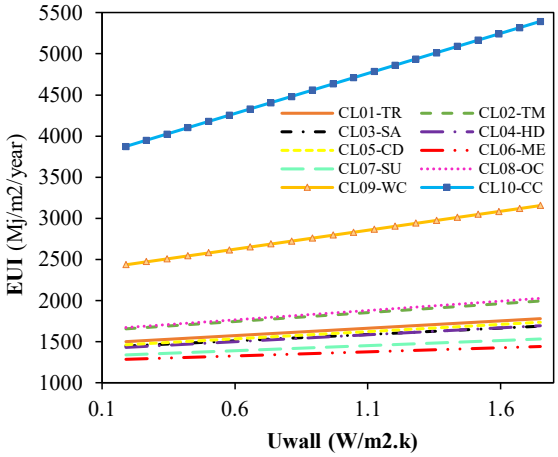

Figure 3.13 Sensitivity analysis for U_{wall}

3.7.5 Roof U-value (U_{roof})

In light of the definition of α in this study, there is an interaction between α and U_{roof}. The impact of U_{roof} on the EUI increases when α decreases and vice versa. Considering the rectangular shape building with x as length, y as width, and h as height, an increase in the x and y, without changing the height of the building, can decrease α since the increase in the roof area is more tangible than that in the exterior wall area. Therefore, the energy performance of the reference building becomes more sensitive to U_{roof}. In contrast, an increase in the height of the building, without changing the x and y values, can increase α since the exterior wall area increases with no change in the roof area. As a result, the sensitivity level of energy consumption to U_{roof} decreases. The results of the sensitivity analysis show that the effect of 10% variations in U_{roof} on the EUI is more significant in cold climates, with as much as 2.3%, followed by hot and moderate ones. This can be attributed to a considerable amount of heat transmitted through roofs in buildings (Sadineni et al., 2011).

3.7.6 GF U-value (U_{gf})

The results obtained from the sensitivity analysis show that variations in U_{gf} slightly impact the operating energy of the reference building. Based on the findings of this study, variation in U_{gf} has

the second lowest impact on the EUI after BO. In particular, the results indicate that a 10% increase in U_{gf} can decrease the EUI, with as much as 0.83%, on average, in hot and moderate climates. This relationship can be attributed to the existence of moisture in the different layers of soil, thereby preventing significant fluctuations in its temperature. As a result, the ground temperature remains between the desired setpoint and the ambient temperature. Therefore, an excessive insulation of ground floor deprives the building of the cooling benefits of the underneath soil in hot and moderate climates (Goswami & Biseli, 1993; Staszczuk et al., 2017). However, the results show that a poor insulation of the ground floor can increase the EUI by increasing the heating load in cold climates.

Figure 3.14 summarises the level of the influence of 10% variation in the six presented factors on the EUI in all the climate zones.

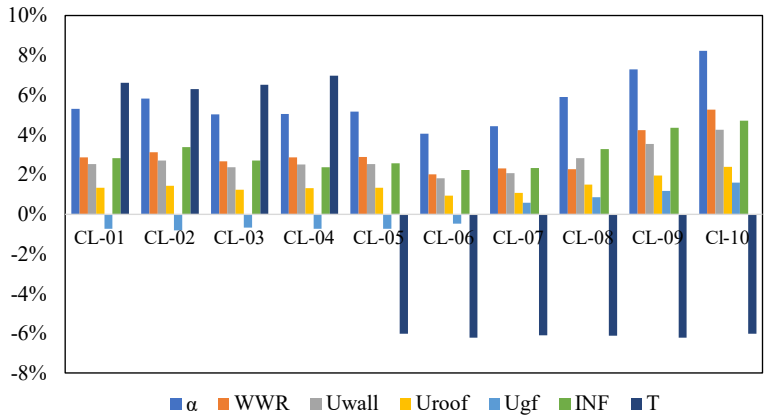

Figure 3.14 Level of influence for 10% change on the EUI

3.8 Conclusion

The current study proposed a novel, non-computational model for predicting the operating energy of office buildings as office and retail building types are responsible for about 50% of energy consumption in developed countries. The model was developed through the analysis of over 1.5 million simulations which involves varying key design factors obtained through a comprehensive literature review. The input data required for the model include readily available information on the thermal properties of building elements. By conducting extensive energy simulations across 40 cities, representing ten distinct climate zones (four zones each), a comprehensive analysis of the results was carried out. This analysis led to the development of an operating energy predictive model specifically focused on the energy consumption of different sections within buildings, including heating, cooling, and lighting. Further, the model was calibrated using a genetic algorithm solver, which could increase the model accuracy to 92.4%. The model developed was further

validated by examining its accuracy across five randomly selected cities. Additionally, the applicability of the model was explored in other building types, such as residential. The results confirmed that the accuracy of the predictive model falls within an acceptable range for the reference residential building. Nevertheless, generalising the model for other applications requires a modification/adaptation of the relevant coefficients and parameters, including those considered for wwr, lighting, and hot water to align with the desired requirements. The proposed model can bridge the gap between simulation results in academia and real-world calculations in the construction sector, assisting designers in evaluating the impact of various design decisions on the operating energy of buildings. Furthermore, the mathematical nature of the model enables its direct integration as the objective function in the optimisation processes, thus enabling the identification of optimal design choices and the design of more energy-efficient buildings.

The parametric study using the model also highlights the significant impact of environmental indices, such as ambient temperature, on the energy performance of buildings. Indeed, a 10% variation in four environmental parameters can potentially impact the operating energy demand by as much as 12%. Additionally, the model also confirmed the central role of the thermal properties of building envelopes, including exterior walls and roofs, in the operating energy of buildings. In was shown that improving the thermal properties of these elements by just 10% can lead to a 6% overall energy use enhancement. The results of the sensitivity analysis of exterior walls to roof areas (α) and window-to-wall ratio (WWR) reflect the importance of improving the thermal performance of building envelopes in reducing energy demand. Also, the analysis highlights the cooling effect of the ground floor in buildings located in hot and moderate climates. It was shown that the excessive insulation of the ground floor hinders the building from harnessing the cooling advantages offered by the underlying soil. Despite the relevant results and indications found, it is important to denote that this study can be further improved in future research by including the non-generalisability of the trends reported for the reference building. Furthermore, it is worth noting that this study has certain limitations, such as capturing the impact of user behaviour and the aging process of building elements, along with the effect of wall-to-floor ratio on the energy use in buildings. To achieve more accurate and precise energy consumption predictions, further studies may consider the effects of parameters such as window shade control and HVAC usage, as well as the impact of climate change on energy consumption.

Chapter 4 AI-Assisted optimisation of energy-efficient concrete mixes incorporating recycled concrete aggregates

4.1 Abstract

Maximising the content of supplementary cementitious materials and recycled concrete aggregates as a partial to full replacement for Portland cement and coarse aggregates are among the widely adopted strategies to increase energy efficiency in concrete, considering both operating and embodied phases. Both approaches improve the insulation capacity and negative environmental implications attributed to concrete by reducing the thermal conductivity and environmental footprints of concrete. However, the synergetic implications of adopting these approaches on concrete properties add complexity to the design of energy-efficient mixes. This chapter proposes a novel AI-based multi-objective optimisation framework addressing the lack of a systematic method to formulate these concretes and solves the common multi-objective mix design problems. The framework is developed for the mix proportioning of energy-efficient concrete mixes containing recycled concrete aggregates and commonly used supplementary cementitious materials while ensuring the desired compressive strength. The proposed optimisation model leverages a dataset of about 2,120 mixes and employs an extreme gradient boosting machine to model the compressive strength requirements as a mechanical constraint throughout the optimsiation process. Given the impact of thermal objectives on environmental performance of concrete, a set of objectives spanning the life cycle of recycled aggregate concrete, including minimising thermal conductivity, global warming, acidification, fossil fuel depletion potential, and the cost of production, are targeted. The effectiveness of the framework is validated through case studies across different strength ranges. The results indicate a significant improvement in thermal and environmental sustainability indicators, including an 11.3%, 28.9% and 28% reduction in thermal conductivity, global warming, and acidification potentials, besides considerable cost savings of up to 24.4% without compromising the mechanical performance of concrete.

4.2 Introduction

Concrete is the most commonly used material in the construction industry, with more than 10 billion tons of annual production (Ahmad, et al., 2021). Concrete manufacturing contributes to 3% of global of energy use, 8% of global greenhouse gas emissions, and significant natural resource depletion (S. A. Miller & Moore, 2020). However, the energy use attributed to concrete is not limited to its environmental performance (i.,e. embodied energy) as the thermal properties of

concrete considerably impact operating energy in buildings (Pérez-Lombard et al., 2008). Therefore, improving both operating and embodied energy performance of concrete holds significant promise in a transition towards energy efficient buildings and eco-friendly concrete products (Y. Wu et al., 2015).

Significant energy loss through building envelopes (Y. Wu et al., 2015) and environmental footprints attributed to concrete production (Turner & Collins, 2013) highlight the importance of the types of aggregates and cementitious materials, along with the quantity and distribution of pore structure, on the energy performance of concrete throughout its life cycle, (K.-H. Kim et al., 2003). Therefore, sustainable practices tend to improve the thermal properties, particularly thermal conductivity (TC) and thermal mass (TM) and carbon equivalent emissions of concrete mixes, thereby improving the energy efficiency in buildings. Most practical and viable approaches considering both operating and embodied phases include i) minimising the Portland cement (C) content of concrete through its partial to complete replacement with supplementary cementitious materials (SCMs), including but not limited to Fly Ash (FA), Silica Fume (SF), and Ground Granulated Blast-Furnace slag (GGBFS) (Gettu et al., 2019; C. T. Tam, 2021), and ii) maximising the porosity of concrete mixes through partial or complete replacement of coarse aggregates (Cagg) with recycled concrete aggregates (RCA) that contain more pore structure than natural aggregates (V. W. Y. Tam et al., 2020; H. Wu et al., 2019). The mentioned sustainable practices have shown significant potential in improving the thermal properties (i.,e. thermal insulation capacity) (Sargam et al., 2020), and environmental footprints of concrete (Napolano et al., 2016), (i.,e. diverting waste from landfills, and mitigating the need for extracting natural resources attributed to the construction industry). In this sense, incorporating only RCA in concrete mixes can adversely impact the mechanical properties of concrete due to its higher water absorption, porosity, and weaker bond between the old and new paste (V. W. Y. Tam et al., 2020; H. Wu et al., 2019), despite thermal and environmental benefits that it offers (T. Ding et al., 2016; Francioso et al., 2021). To tackle this shortcoming, incorporating SCMs into concrete mixes resulting in recycled aggregate concrete (RAC) has been extensively explored (Guo et al., 2020b; W. Zhang et al., 2019), which can further improve the energy performance of RAC (Sargam et al., 2020). However, incorporating SCM and RCA beyond a certain replacement percentage aiming to maximise the energy efficiency of concrete is generally accompanied with adverse effects on the mechanical performance of concrete (C. Liang et al., 2021). To provide an example, Qin et al. (2022) conducted an experimental study to investigate the combined effects of replacing Cagg (50 and 100% by volume) and C content (50

and 75% by weight) with RCA and SCMs, respectively. The results showed a compressive strength (CS) reduction in all mixes with more than 50% replacement of RCA and SCMs.

To effectively incorporate SCMs and RCA into concrete mixes, it is crucial to strike a balance between the desired mechanical, thermal, and environmental objectives. This is because these approaches have synergistic effects on concrete properties, which adds complexity to the mix design process. However, investigations on RAC mixes containing SCMs have mainly focused on their mechanical properties. While some researchers have studied the CS of these green concrete mixes (Topc, 2008; T. Xie et al., 2020), others have explored strength and fresh state properties (Faysal et al., 2020; W. Feng et al., 2021), or the combination of strength and durability properties (Guo et al., 2020b). From an environmental perspective, although several experimental studies have recently considered the environmental performance of RAC (Habibi et al., 2021; Majhi & Nayak, 2020), exploring the environmental performance of RAC containing SCMs is mainly limited to predicting carbonation depth (Nunez & Nehdi, 2021), its chloride threshold (Y. Wang et al., 2022), and resistance against sulfate attack (Corral Higuera et al., 2011). Additionally, while the individual effects of incorporating RCA (H. Zhao et al., 2018b) and SCMs (Demirboğa, 2007) on the thermal performance of concrete have been studied, there is a lack of research on their combined impact, and the few available studies require costly experimental trials (Al Martini et al., 2023). Nevertheless, designing RAC containing SCMs requires considering the overlapping effects of mix constituents on the desired objectives. This can be achieved using systematic concrete mix design techniques managing a set of design variables and objectives. However, existing approaches, including those recommended by the British Department of Environment, American Concrete Institute and the Murdock method, have not been designed for thermal and environmental objectives (Penido et al., 2022), despite considering performance-based objectives. In addition, designing green concrete mixtures can become more challenging due to the increased number of design variables and the need to monitor multiple performance measures. As a result, the inherently laborious and time-consuming trial-based approaches to concrete mix design tend to be even less efficient (Soudki et al., 2001).

In this context, multi-objective computational techniques can effectively overcome the mentioned challenges by satisfying the objectives required during the life cycle of green concrete mixes while finding near-optimal solutions at lower computational costs (DeRousseau et al., 2018). These optimisation methods, particularly metaheuristic approaches, are capable of handling numerous design variables and objectives under non-linear constraints required in sustainable concrete mixes (Cakiroglu et al., 2021; Naseri et al., 2020). Given the advances in mix optimisation modelling,

data-driven modelling techniques have also been recently used and integrated into the optimisation process, where the properties of concrete can be predicted through artificial intelligence models trained with large datasets (Kandiri et al., 2020). This approach can develop more realistic models based on relevant performance data, effectively replacing the empirical models calibrated on relatively limited experimental datasets. Following the focus of the conventional methods of designing concrete mixes on mechanical properties, multi-objective computational techniques reported in previous studies, e.g., data-driven and empirical-based concrete optimisation models, have targeted one or more mechanical objectives (Elemam et al., 2020), as well as cost and CO2 emissions (J. Zhang et al., 2020), while neglecting the thermal properties and important environmental concerns associated with RAC production. Reviewing the literature shows that multi-objective optimisation (MOO) methods targeting the life cycle of RAC containing SCMs are missing. With this in mind, our study is the first attempt in the literature to apply a MOO metaheuristic algorithm simultaneously satisfying economic, operating, and embodied-related objectives of green RAC mixes.

The present study aims to bridge the existing gap by proposing a novel optimisation framework for RAC mixes containing SCMs, integrating data-driven modelling and MOO techniques to achieve a set of objectives affecting the energy performance of RAC mixes throughout their life cycle. The developed framework optimises RAC mixes with respect to their strength requirements, given the significant effect of the targeted mechanical properties on thermal and environmental objectives. The framework targets TC and the three most commonly adopted environmental objectives, i.e. the global warming potential (GWP), acidification potential (ACDP), and fossil fuel depletion potential (FFDP), along with the production cost as an economic objective, without compromising the mechanical performance of concrete. A dataset inventory from the literature containing approximately 2,120 mixes is leveraged for the data-driven modelling of CS. To achieve this goal, seven machine learning algorithms are trained and tested on the dataset to identify the most accurate model. The selected predictive model is then integrated into a metaheuristic optimisation framework to determine the desired CS, thereby identifying optimal concrete mixtures based on mechanical design objectives, which can facilitate the optimisation process. The following sections present the methodology used to develop the MOO framework and the results of case studies adopted, indicating the effectiveness and benefits of the framework.

4.3 Methodology

Figure 4.1 presents the schematic structure of the key components of the framework developed in this study for the optimal mix design of energy-efficient RAC mixes containing commonly used SCMs (FA and SF). In the design, two main components operate on the collected dataset. The first component – data-driven modelling – uses the collected dataset to predict the strength of concrete mixes. Recently, AI-based predictive models have been extensively used to predict concrete properties (Kaloop et al., 2020). Thus, several machine learning algorithms are trained and tested on the collected dataset where mix proportions for different ingredients are considered as input variables and CS as the only output (Hafez et al., 2023). The performances of the machine learning algorithms are evaluated using a set of error metrics to identify the most accurate algorithm, and the most accurate model is used in the optimisation process (Imran et al., 2023). Previous studies have included the designed machine learning model as an objective function (Naseri et al., 2020). In contrast, the present study integrated the developed model as a mechanical constraint determining the desired CS range for the optimal mixes considering the correlation between the thermal, environmental, and mechanical performance of the RAC (Lakhiar et al., 2022). This approach can improve the efficiency of the optimisation process by circumventing unnecessary objective function evaluations and limiting the search space, thereby reducing the computational resources and time required (Helwig & Wanka, 2007). In the second component –the optimisation phase –minimising a set of thermal, environmental, and economic objectives, namely TC, GWP, ACDP, FFDP, and production cost of RAC mixes, is targeted (Asadi Shamsabadi et al., 2023) using a MOO metaheuristic algorithm and a set of constraints, including the developed model as a mechanical constraint.

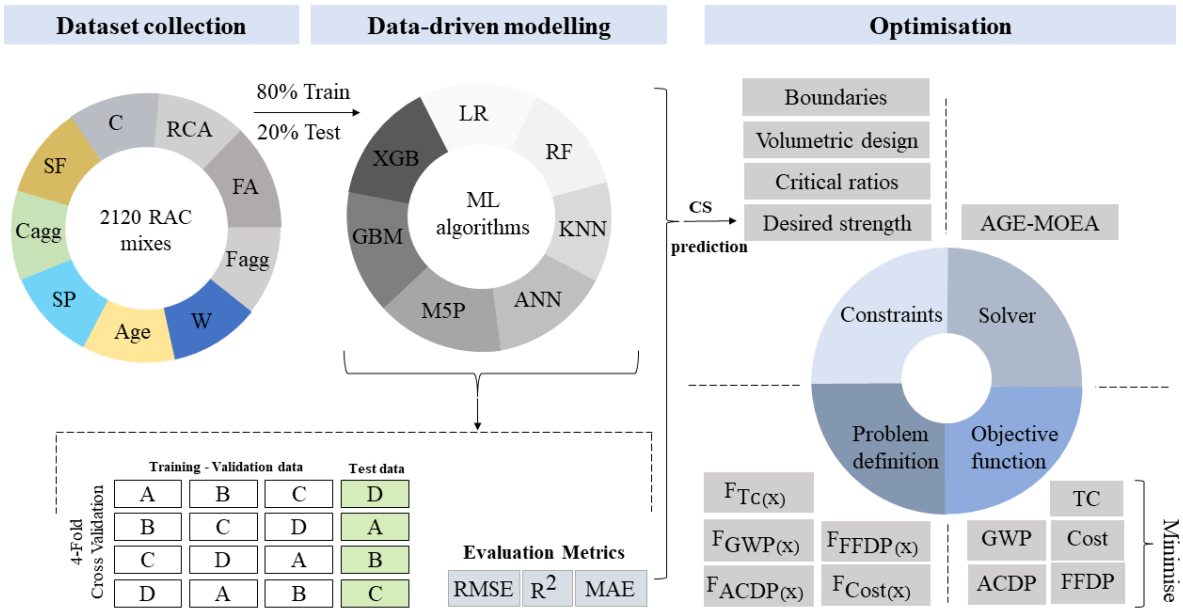

Figure 4.1 Mix design optimisation framework

4.3.1 Data-driven modelling

Several data-driven modelling techniques have been explored in previous studies to predict the mechanical properties of concrete (Mohammadi et al., 2021), (T. Gupta et al., 2019). With the objective of identifying the most suitable machine learning algorithm for the given dataset, the ones showing the best performance in the literature are investigated in a five-step sequential trial of growing complexity of algorithms. The first step is based on multiple linear regression (MLR) (Witten et al., 2005). This is commonly used to find the correlation between a set of input and output variables and has been widely adopted to predict mechanical characteristics (Bhanja & Sengupta, 2002), (L. Chen, 2010). The second step tests K-nearest neighbours (KNN). The KNN is a non-parametric method that suits both classification and regression problems (Haworth & Cheng, 2012). This is then followed by investigating the effectiveness of the M5P technique in the third trial step. This technique integrates a traditional decision tree with linear regression function found in the literature to solve engineering problems (Fatih & Burhan, 2015). In the fourth step, the effectiveness of Artificial Neural Network (ANN) and Random Forest (RF) as widely used methods to predict the CS of concrete (Farooq et al., 2020) are explored. The last step investigates the Gradient Boosting Machine (GBM) and Extreme Gradient Boosting (Xgboost) methods. The former is an efficient machine learning algorithm that enhances prediction accuracy by combining various base models (Friedman, 2001), while Xgboost is an ensemble machine learning algorithm

known as an advanced version of GBM in which the model variants are alleviated through normalising the loss function (T. Chen & Guestrin, 2016). The performances of the above mentioned methods are evaluated to identify the most effective algorithm which is then used in the optimisation phase. In all machine learning trials, 70% of the dataset was used to train parameters, 10% for the validation process, in which the hyperparameters were tuned, and 20% to test the predictive model developed. It is worth noting that the performances of the employed methods were optimised using random search and Bayesian optimisation methods to tune hyperparameters. More information on the structure of the used machine learning approaches can be found in Appendix B.

4.3.2 Evaluating the performances of machine learning-based models using error metrics

After training, testing, and optimising the machine learning algorithms presented in the previous section, their performances are assessed using standard error metrics found in other works, such as (L. Ji & Gallo, 2006). These are the coefficient of determination (R^2), root mean squared error (RMSE), and mean absolute error (MAE).

4.3.3 Multi-objective optimisation (MOO)

The impact of mechanical strength on the thermal (Kazmi et al., 2021) and environmental properties (J. Xiao et al., 2018) of RAC highlights the need for integrating the predictive model into a MOO framework to identify the optimal RAC mixes by constraining the CS of mixes. Based on existing studies, metaheuristic approaches, such as evolutionary algorithms including Non-dominated Sorting Genetic Algorithm II (NSGA-II) (Deb et al., 2002), Multi-objective Particle Swarm Optimisation (MOPSO) (Tao et al., 2019), and Multi-objective Differential Evolution (MODE) (Babu & Gujarathi, 2007), can provide competitive solutions to MOO problems. Most studies, however, have focused on complying with defined constraints, whereas dealing with conflicting objectives may require maintaining population diversity (Tian et al., 2018). As a result, in the optimisation process, the population is typically pushed toward locally feasible optimal or infeasible areas before considering the balance between proximity and diversity within the feasible region. To overcome this limitation, adaptive geometry estimation based many-objective evolutionary algorithm (AGE-MOEA) can be adopted. This method aims to achieve the Pareto frontier by considering both proximity and diversity, while keeping a relatively reduced computational cost (Panichella, 2019). By relying on the good performance of AGE-MOEA as compared to the two-archive evolutionary algorithm for constrained MOO, NSGA-II, and NSGA-III methods (de Melo et al., 2022), AGE-MOEA is adopted for the metaheuristic optimisation phase in this study.

4.4 Dataset description

A robust data inventory is required for the deployment of data-driven modelling techniques. A dataset of about 2,120 RAC mixes is, therefore, developed based on the literature. The collected data are composed of concrete mixes (design variables) in green mixes containing RCA and SCMs. The gathered dataset has the available proportions of 8 components, i.e. C, SF, FA, water (W), superplasticiser (SP), Cagg, fine aggregate (Fagg), and coarse RCA, therefore resulting in different concrete mixes. The other data collected refers to the curing age and CS of the mixes. The following criteria are considered while collecting the data from peer-reviewed publications:

- Two types of SCMs, including FA and SF are considered in the references.
- Only normal weight aggregate is considered as the Cagg.
- All the specimens are produced in laboratory conditions and have open-air curing.

After reviewing over 56 publications and eliminating outliers in the initial analysis using three standard deviations from the mean value method (empirical rule), approximately 2,120 mixes are collected from the peer-reviewed publications listed in Table 4.1 to develop the dataset. Figure 4.2 shows the scatterplots of the independent variables against the CS and the distribution of CS within the dataset.

Table 4.1 Dataset references

Reference	Data number	Reference	Data number
(Domingo-Cabo et al., 2009)	8	(Medina et al., 2014)	12
(Casuccio et al., 2008)	9	(Pedro et al., 2015)	12
(Poon et al., 2007)	30	(S. Ismail & Ramli, 2013)	12
(Carneiro et al., 2014)	2	(Gómez-Soberón, 2002)	15
(Limbachiya et al., 2000)	4	(López Gayarre et al., 2014)	16
(Etxeberria, Marí, et al., 2007)	4	(Wardeh et al., 2015)	16
(Fathifazl et al., 2011)	4	(Kumutha & Vijai, 2010)	20
(Chakradhara Rao et al., 2011)	4	(C. Thomas et al., 2018)	24
(Folino & Xargay, 2014)	4	(V. W. Y. Tam et al., 2015)	24
(Etxeberria, Vázquez, et al., 2007)	7	(A. B. Ajdukiewicz & Kliszczewicz, 2007)	24
(Butler et al., 2013)	8	(Sato et al., 2007)	26
(Belén et al., 2011)	8	(Çakır & Sofyanlı, 2015)	27
(Beltrán, Barbudo, et al., 2014)	8	(Abd Elhakam et al., 2012)	30
(Pepe et al., 2014)	8	(Andreu & Miren, 2014)	30
(Matias et al., 2013)	9	(Somna et al., 2012)	36
(Malešev et al., 2010)	9	(Lin et al., 2004)	48
(Beltrán, Agrela, et al., 2014)	9	(Graybeal & Tanesi, 2008)	48
(Manzi et al., 2013)	10	(C. Thomas et al., 2013)	72
(Nepomuceno et al., 2018)	10	(A. Ajdukiewicz & Kliszczewicz, 2002)	175
(C. Zheng et al., 2018)	10	(K. Kim et al., 2013)	11
(Corinaldesi, 2010)	10	(Dilbas et al., 2014)	12
(Taffese, 2018)	10	(Haitao & Shizhu, 2015)	20
(Kisku et al., 2020)	1	(Altun & Oltulu, 2020)	4
(Lesovik et al., 2021)	6	(Ajmani et al., 2019)	12
(Çakır & Dilbas, 2021)	14	(Dilbas & Çakır, 2021)	21
(Mukharjee & Barai, 2014)	24	(Paulson et al., 2019)	27
(Pedro et al., 2017)	36	(Dilbas et al., 2014)	12
(M. Van Tran & Chau, 2021)	54	(Golafshani & Behnood, 2019)	1030

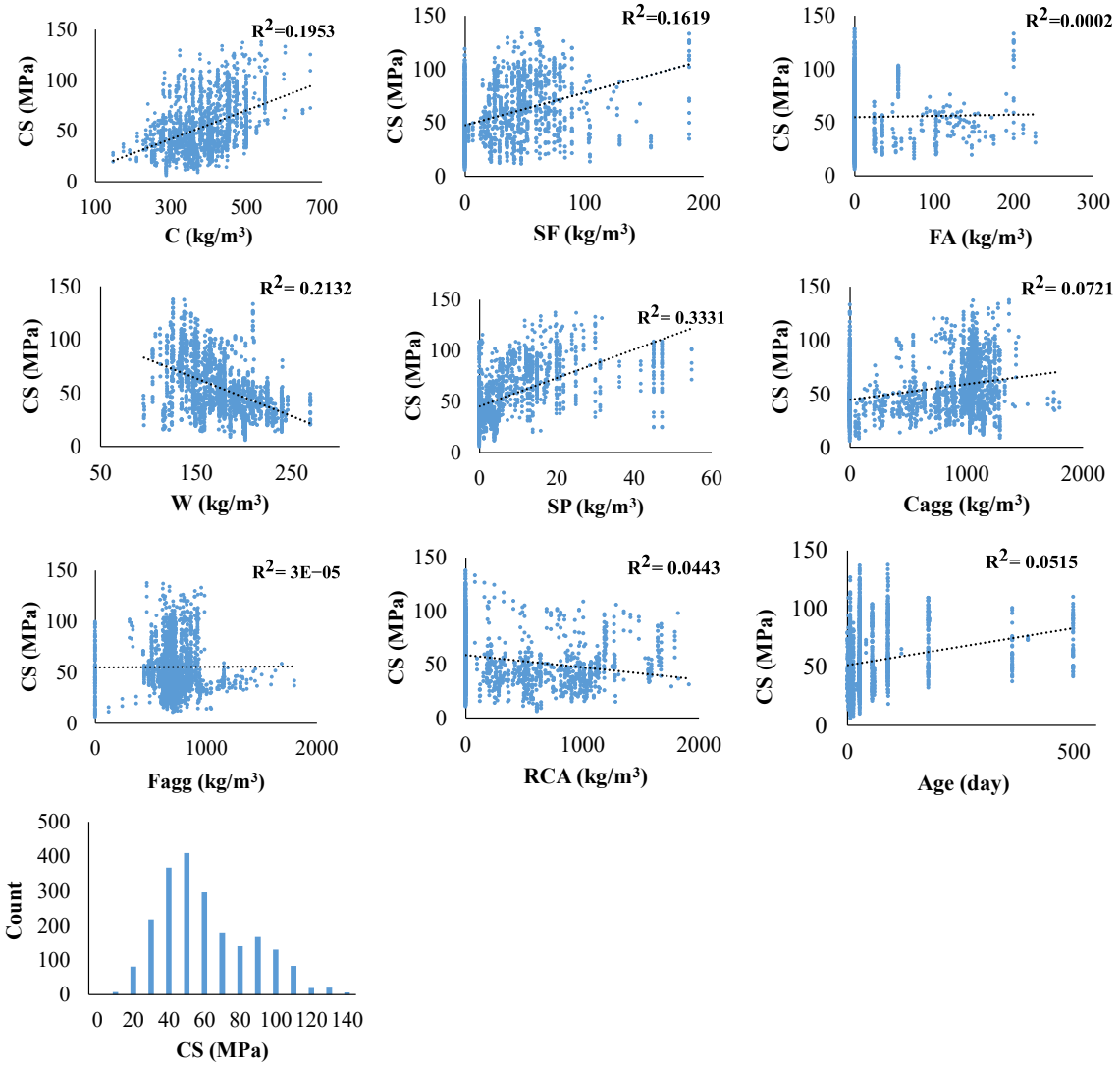

Figure 4.2 Scatterplots of independent variables against CS & CS distribution

As shown in Figure 4.2, the dataset provides a wide range of values for the input variables, including W, C, RCA, Cagg, Fagg contents, and age. This figure also shows that the CS of the mixtures mainly ranges between 20 and 100 MPa. The statistical properties of the dataset are summarised in Table 4.2. It is worth noting that the unit kg/m^3 refers to the proportion of components in each cubic meter of concrete.

Table 4.2 Statistics of Input and output parameters

Input variable	Minimum	Maximum	Mean	Std deviation	Unit
Cement	147.5	670	393.17	79.15	(kg/m^3)
Silica Fume	0	188	24.86	33.35	(kg/m^3)
Fly Ash	0	227.5	10.28	34.8	(kg/m^3)
Water	95.4	270	174.82	32.88	(kg/m^3)
Superplasticizer	0	55	7.04	10.451	(kg/m^3)
Coarse aggregate	0	1800	731.89	465.13	(kg/m^3)
Fine Aggregate	0	1800	695.46	221.19	(kg/m^3)
RCA	0	1917	315.39	463.69	(kg/m^3)
Age	1	500	54.80	89.94	days
Output					
CS	5.84	137.4	55.22	25.24	MPa

4.5 Data-driven modelling performance

The performance of the selected machine learning-based algorithms is evaluated using the three error metrics identified in Section 4.3.2. A sensitivity analysis is also carried out to evaluate the sensitivity of the model to variations in the design variables. Table 4.3 compares the performances of the selected machine learning methods considering the error metrics. Further, Figure 4.3 presents the scatterplots of the observed versus predicted values of the test dataset for each algorithm.

Table 4.3 Error metrics evaluation

machine learning algorithm	R^2	RMSE	MAE
Xgboost	0.956	5.13	3.372
GBM	0.951	5.39	3.305
M5P	0.820	10.81	7.875
ANN	0.90	7.4	4.068
KNN	0.75	12.2	8.477
RF	0.92	6.6	4.173
LR	0.57	15.8	12.141

In the results shown above, the Xgboost and GBM algorithms have significantly higher R^2 compared to the other machine learning algorithms, with Xgboost having the best performance (R^2 = 95.6%). The superior performance of this model is consistent with the findings from previous studies on its efficiency in predicting the CS of RAC and ultra-high performance concrete (J. Duan et al., 2021),. Such a performance can be attributed to the continuous optimisation of the objective functions which reduces the variants in the model. This simplifies the model and avoids overfitting (T. Chen & Guestrin, 2016). The results also indicate that the gradient boosting algorithms can perform better than neural networks and decision tree-based algorithms for the RAC dataset.

Therefore, Xgboost is selected for feature importance analysis. The low accuracy of LR confirms that the relationship between the inputs and output is less likely to be detected by a linear pattern.

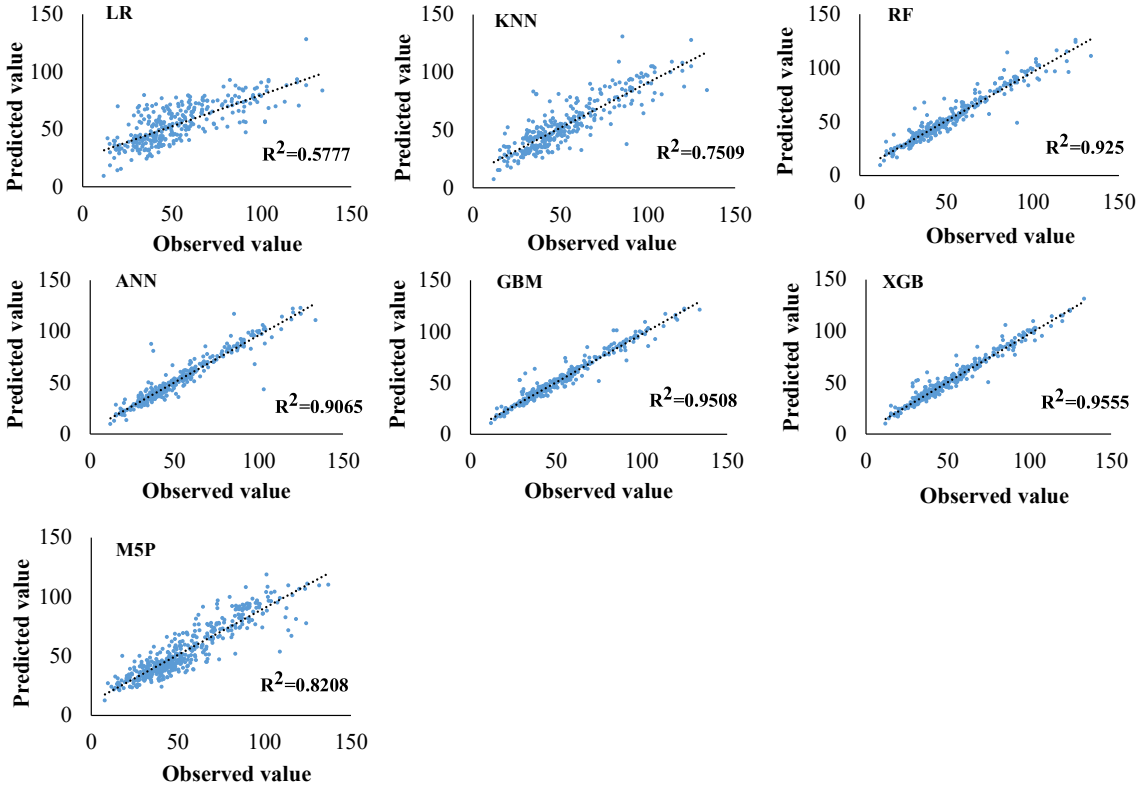

Figure 4.3 Predicted Vs. Observed values for machine learning algorithms

The corresponding level of importance and the impact range for each input variable on CS is demonstrated in the SHAP summary plot presented in Figure 4.4. Each point on the plot shows an instance in the dataset, where the y-axis denotes the input variables in the order of descending level of impact, while the x-axis indicates the impact of each feature on the output. The concentration of points represents the density of the Shapley values of features. The colours show the value position of the feature within its range from high to low. Accordingly, the model finds a strong impact of SP, age, C, W, and SF contents on CS compared to other features. It can also be observed that the model integrates the information provided by the aggregates, RCA, and FA contents into the prediction of CS. The same figure also indicates the increment or decrement of a feature on the dependent variable. For instance, an increase in the C content increases CS, while an increase in the W content decreases CS. In addition, a lower curing age reduces CS significantly, as expected from common knowledge about the behaviour of concrete mixes.

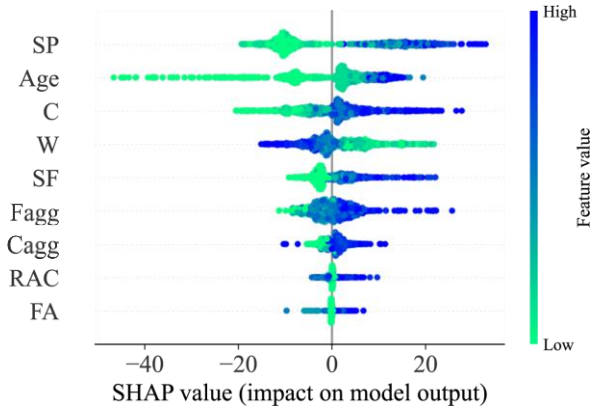

Figure 4.4 Feature importance analysis using Xgboost and SHAP method

4.6 Multi-objective RAC mix optimisation components

This section describes the construction of the MOO algorithm and its components. It also shows how the predictive tool is integrated into the metaheuristic optimisation process. The construction of the MOO algorithm requires the definition of the problems to be solved in mathematical terms. The relevant objective functions are then targeted to address the defined problems. Several types of constraints including CS-related constraint are also considered to determine the required margins of optimal solutions. In this study, CS is constrained using the developed strength prediction function and a solver is employed to undertake the full optimisation process.

4.6.1 Problem definition

As noted, the present study targets to optimise three types of objectives: thermal, environmental and economic objectives. For an environmental perspective, a number of growing environmental concerns, including global warming, acidification, and fossil fuel depletion are deemed to be minimised while the cost of production is included to address economic concerns. For thermal objectives, reviewing the literature shows that the TC and TM of concrete play central roles in its energy performance (Balaras, 1996; Zhu et al., 2015). Therefore, this study carries out a case study to explore the magnitude of impacts of TC and TM on the energy performance of a reference building (medium size office building) provided by the Department of Energy (DOE). For this purpose, a wide range of TC (0.3-0.7 W/m.K) and specific heat (SH) (500-900 J/kg.K) are assigned to the exterior walls and roof of the reference building and the impact of their variations on the annual energy consumption of the reference building is shown in Figure 4.5. Given the fact that TM of concrete elements is a function of their SH, density and volume, variations in SH represents variations in TM of concrete in this case study as the density and dimensions of exterior walls and

roof are considered to be constant. The case study is caried out for four cities (Cairo, Istanbul, London, Fairbanks), representing hot, Mediterranean, oceanic, and cold climatic conditions, respectively.

While no direct relationship between TC and TM has been found in the literature, they can be related in certain cases. For instance, some materials with high TM typically exhibit high TC, as they are usually dense and composed of substances that conduct heat well. On the other hand, materials with high thermal mass but low thermal conductivity can be found as well, such as insulation materials designed to conserve heat while resisting its transfer. Thus, the value of TC is considered constant when TM is increasing and vice versa, given the absence of a clear relationship between TC and TM.

The reference rectangular-shaped office building with 15 zones consists of 3 floors with 50 m in length and 33 m in width. The total floor area is 4,982 m^2. The height of each story (floor-to-floor height) is 3.96 m. The set temperature for cooling is assumed to be 24°C and 26.7°C during working and non-working hours, and it is heated at 21°C and 15.6°C during working and non-working hours, respectively. The HVAC system of the building is based on MZVAV with plenum zones. VAV Box Reheat Coil supplies hot water for the building at 60°C, with a maximum capacity of 82°C. The light usage and electricity plug loads are considered to be 10.76 w/m^2. The occupancy schedule is assumed to be 5.38 person/100 m^2, which corresponds to a total of 268 people during working hours. Two 20-HP elevators are available in the building.

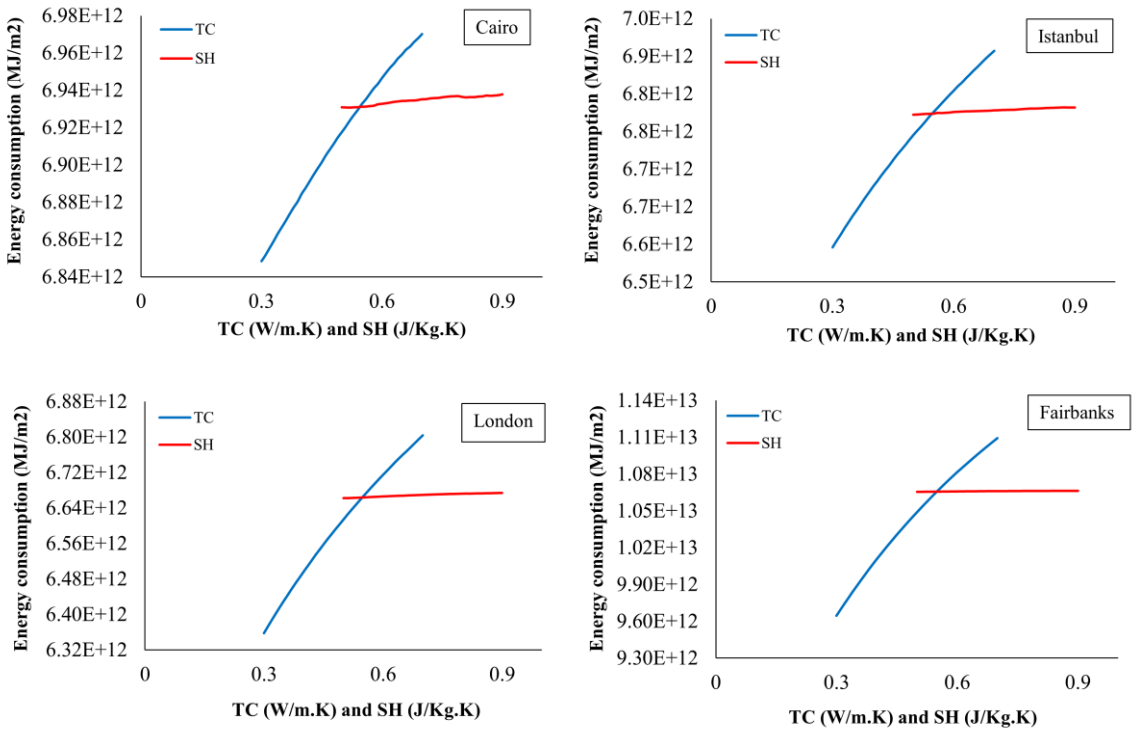

Figure 4.5 Impact of TC and SH on energy performance of concrete

The results of the case study show that increasing the TC of concrete mixes, by up to 50% can increase the energy performance of the case building with as much as 0.7%, 2.1%, 3.5%, and 6.8% in Cairo, Istanbul, London, and Fairbanks, respectively. Meanwhile, the effect of 50% increment in SH of concrete mixes on energy consumption of the reference building is found to be 0.07%, 0.11%, 0.12%, 0.05% in the four selected climatic condition. The results show that the impact of TC on the annual energy performance of the building is considerably higher compared to TM. The findings in the literature also confirm the significant impact of TC on the heating and cooling loads caused by concrete thermal properties (Vangeem et al., 2013). Thus, TC is chosen as a thermal objective for the optimisation phase due to its tangible impact on the energy performance of building. The MOO problem is defined as:

$$\text{Minimise: } \begin{cases} F_{cost(x)} \\ F_{TC(x)} \\ F_{GWP(x)} \\ F_{ACDP(x)} \\ F_{FFDP(x)} \end{cases}$$

Subject to: $l_i \leq x_i \leq u_i$, $i=1, 2, 3, \ldots, n$,

where $F_{cost(x)}$ is the cost function, and $F_{TC(x)}$, $F_{GWP(x)}$, $F_{AP(x)}$, and $F_{FFDP(x)}$ denote the thermal and environmental objectives defined in the next sections. Note that the factors l_i and u_i indicate the lower and upper bounds of variable x_i, respectively, while n is the number of objective variables. In this study, FA, SF, and RCA are taken as the by-products of other industries, and, therefore, there are no GWP, AP, and FFDP values attributed to them.

4.6.2 Objective functions

The first objective is related to the minimisation of the cost of mixes. This is defined as follows:

$$\text{Min } F_{cost(x)} = P_cC_c + P_{SF}C_{SF}+P_{FA}C_{FA}+P_WC_W+P_{SP}C_{SP}+P_{Cagg}C_{Cagg}+P_{Fagg}C_{Fagg}+P_{RCA}C_{RCA}, \quad (4.1)$$

where P_c, P_{SF}, P_{FA}, P_W, P_{SP}, P_{Cagg}, P_{Fagg}, and P_{RCA} are the unit prices of C, SF, FA, W, SP, Cagg, Fagg, and RCA (in this study, in Australian Dollars – AUD), respectively. The used unit prices are given in Table 4.4 and are based on retailor quotes, while C_C, C_{SF}, C_{FA}, C_W, C_{SP}, C_{Cagg}, C_{Fagg}, and C_{RCA} represent the corresponding content in the mix.

Table 4.4 Cost of mix design components

Component	Cost ($/kg)
Cement – C	0.2
Silica fume – SF	0.4
Fly ash – FA	0.11
Water – W	0.005
Superplasticiser – SP	2.9
Coarse aggregate – Cagg	0.06
Fine aggregate – Fagg	0.05
Recycled concrete aggregate – RCA	0.02

In addition to the cost function (Eq 4.1), the minimisation of TC is defined as follows:

$$\text{Min } F_{TC(x)=} VF_{CTC_C}+VF_{SF}TC_{SF}+VF_{FA}TC_{FA}+VF_WTC_W+VF_{SP}TC_{SP}+VF_{Cagg}TC_{Cagg}+VF_{Fagg}TC_{Fagg} +VF_{RCA}TC_{RCA}, \quad (4.2)$$

Where VF_C, VF_{SF}, VF_{FA}, VF_W, VF_{SP}, VF_{Cagg}, VF_{Fagg},and VF_{RCA} denote the volume fraction of C, SF, FA, W, SP, Cagg, Fagg, and RCA, respectively, while TC_C, TC_{SF}, TC_{FA}, TC_W, TC_{SP}, TC_{Cagg}, TC_{Fagg}, and TC_{RCA} indicate the TC of the corresponding components. The TC values of the components are obtained from the literature and are presented in Table 4.5.

Third objective function considered in this study is GWP minimisation defined as follows:

$$\text{Min } F_{GWP(x)}=G_C C_C+G_{SF}C_{SF} + G_{FA}C_{FA}+G_W C_W+G_{SP}C_{SP}+G_{Cagg}C_{Cagg}+G_{Fagg}C_{Fagg}+G_{RCA}C_{RCA}, \quad (4.3)$$

where G_C, G_{SF}, G_{FA}, G_W, G_{SP}, G_{Cagg}, G_{Fagg}, and G_{RCA} indicate the GWP associated with C, SF, FA, W, SP, Cagg, Fagg, and RCA, respectively. All the 100-year GWP values shown in Table 4.5 are collected according to the Integrated Pollution Prevention and Control (IPPC) guidelines.

Table 4.5 GWP and TC of mix design components

Component	$GWP_{100\text{-year}}$ production	TC (W/m.K)
Cement – C	0.885	0.9
Silica fume – SF	-	0.1
Fly ash – FA	-	0.2
Water – W	0.0025	0.6
Superplasticiser – SP	1.11	0.4
Coarse aggregate – Cagg	0.0032	0.3
Fine aggregate – Fagg	0.0032	0.6
Recycled concrete aggregate – RCA	-	0.4

The second environmental objective is the minimisation of ACDP. This can be represented by the following equation:

$$\text{Min } F_{AP(x)}= A_c C_c+ A_{SF}C_{SF}+A_{FA}C_{FA}+A_W C_W+A_{SP}C_{SP}+A_{Cagg}C_{Cagg}+A_{Fagg}C_{Fagg}+A_{RCA}C_{RCA}, \quad (4.4)$$

where A_C, A_{SF}, A_{FA}, A_W, A_{SP}, A_{Cagg}, A_{Fagg}, and A_{RCA} indicate the ACDP of C, SF, FA, W, SP, Cagg, Fagg, and RCA, respectively – see the adopted values in Table 4.6.

The last environmental objective function minimises the FFDP of mixes. This can be written as:

$$\text{Min } F_{FFDP(x)}= F_c C_c+F_{SF}C_{SF}+F_{FA}C_{FA}+F_W C_W+F_{SP}C_{SP}+F_{Cagg}C_{Cagg}+F_{Fagg}C_{Fagg}+F_{RCA}C_{RCA}, \quad (4.5)$$

where F_C, F_{SF}, F_{FA}, F_W, F_{SP}, F_{Cagg}, F_{Fagg}, and F_{RCA} indicate the FFDP of C, SF, FA, W, SP, Cagg, Fagg, and RCA, respectively. The values attributed to the FFDP of the constitutes can also be found in Table 4.6.

Table 4.6 Acidification and fossil fuel depletion potential of mix design components

Component	ACDP	FFDP
Cement – C	0.0053	1.49
Silica fume – SF	-	-
Fly ash – FA	-	-
Water – W	0.0045	0.01
Superplasticiser – SP	0.00481	83.97
Coarse aggregate – Cagg	0.00002	0.0063
Fine aggregate – Fagg	0.00002	0.0063
Recycled concrete aggregate – RCA	-	-

4.6.3 Constraints

The required constraints in the optimisation of concrete mixes are provided in this section. The first group of constraints takes into account the upper and lower bounds of mix ingredients written as:

$$C_{i.L} \leq C_i \leq C_{i.U}, \tag{4.6}$$

where $C_{i.L}$ and $C_{i.U}$ indicate the lower and upper content for the i^{th} component of mixes.

The second group of constraints considers the critical proportions in concrete mixes, such as the ratio of W to the binder (C_W/B) and the SP to C ratio (C_{sp}/C_C). The critical ratios considered in this study are listed in Table 4.7.

The third group of constraints accounts for the volumetric design of optimal mixes. This is ensured by the next equation, where the volumetric design of the optimal mixes is constrained to 1:

$$\frac{C_C}{U_C} + \frac{C_{SF}}{U_{SF}} + \frac{C_{FA}}{U_{FA}} + \frac{C_W}{U_W} + \frac{C_{SP}}{U_{SP}} + \frac{C_{Cagg}}{U_{Cagg}} + \frac{C_{Fagg}}{U_{Fagg}} + \frac{C_{RCA}}{U_{RCA}} + V_A = 1, \tag{4.7}$$

where C_i, U_i, and V_A represent the content of each component, density, and air volume in concrete mixes, respectively. Table 4.7 shows the boundaries, critical ratios, and densities for each constituent.

Table 4.7 Boundaries and ratio constraints

Input	Min	Max	Critical ratios	Critical ratios		Density (kg/m^3)
				Min	Max	
Cement – C	300	500	C_W/B	0.2	0.8	3150
Silica fume – SF	0	40	C_{FA}/B	0	0.5	2300
Fly ash – FA	0	150	C_{SF}/B	0	0.3	2500
Water – W	150	300	$C_{Fagg}/Total_{agg}$	0	1	1000
Superplasticiser – SP	1	15	C_{Cagg}/B	0	6	1350
Coarse aggregate – Cagg	200	1800	C_{SP}/C_C	0	0.13	2500
Fine aggregate – Fagg	500	1800				2650
Recycled concrete aggregate – RCA	200	1800				1200
Age	1	90				-

Ultimately, the fourth category of constraints is to determine the desired range of CS. This is formulated based on the machine learning-based model described in the data-driven modelling section. Hereby, the developed CS predictive function is integrated into the designed framework using the following constraint:

$$CS_L \leq CS_i \leq CS_U, \quad (4.8)$$

where CS_L and CS_U indicate the lower and upper bounds of the desired CS range.

4.6.4 Solver

To successfully solve a constrained multi-objective problem, it is important to establish a balance between proximity and diversity. This can be achieved by adopting the AGE-MOEA technique, where the iterative estimation and approximation of the geometry of the Pareto frontier is considered to help achieve solutions close enough to the reference points and diverse enough to provide various alternatives. This MOO approach follows a similar workflow to the NSGA-II with the main difference that it replaces the crowding distance operator with a survival score that automatically integrates diversity and proximity (Panichella, 2022). Compared to the common optimisation algorithms, the AGE-MOEA has two main advantages (Fang et al., 2021). First, it utilises a quick procedure to estimate the geometry of the generated front, and second, it combines the diversity and proximity of non-dominant fronts. Therefore, unlike the commonly used optimisation algorithms in providing population for the next generations, solutions are adopted according to their contribution to the diversity and proximity of non-dominated fronts with respect to the estimated geometry. As a result, more accurate and diverse alternatives can be obtained.

The optimisation algorithm starts with the determination of an initial set of randomly generated solutions (N). Further, utilising crossover and mutations generates a new set of solutions

(offspring), and a new population is obtained by merging the offspring and current populations. Next, this algorithm utilises the non-dominated sorting algorithm to divide the new population into several non-dominated fronts (F1, F2, F3, ...). Then, the obtained non-dominated fronts are normalised. Next, the L_p norm (geometry) of the first non-dominated front are computed and a survival score that combines diversity and proximity is attributed to the solutions in the first front (F1). In this optimisation approach, diversity and proximity are calculated using L_p norm. The distance between each population member and the ideal point denotes the proximity, whereas diversity is estimated using the distance between population members. In the next step, a new population of solutions is obtained by collecting solutions from the non-dominated fronts starting from the F_1, F_2 and so forth. The procedure ends when adding the solutions of the current non-dominated front surpasses the number of objectives. Eventually, the solutions are ranked based on their survival score, and the one with the highest survival score is the winner (Panichella, 2019). The survival score is calculated based on the value of the L_p norm (geometry of the first non-dominated front), while L_p norm can be obtained using the following equation:

$$\|v\|_p = \left(\sum_{i=1}^{m} x_i^p \right)^{1/p} \tag{4.9}$$

The value of p indicates the geometry of the hyper-surface, while m and v denote the number of objective functions and the set of points in an m-dimensional space, respectively. Since the value of p is calculated continuously, the solutions have the same distances to the origin in the normalised solution space (Panichella, 2019).

4.7 Case study

The proposed data-driven RAC mix optimisation framework is applied to a set of case studies designed to explore its efficiency. For this purpose, three classes of CS (representing RACs with 28-day CS, ranging from 23-27 MPa, 33-37 MPa, and 43-47 MPa) are targeted to evaluate the framework performance in proposing optimal RAC mixes. Furthermore, in order to explore the sensitivity of the optimal solutions to variations in the relative importance of the different objectives, another case study is carried out using Technique Order Preference by Similarity to an Ideal Solution (TOPSIS) analysis. This is of particular relevance, as the priority of economic, thermal, and environmental objectives may vary from one project to another.

4.7.1 Optimal mix

Table 4.8 represents the optimal mixes proposed by the framework and mixes selected from the dataset along with the corresponding values of the targeted objectives within three CS ranges (23-27 MPa, 33-37 MPa, and 43-47 MPa). Moreover, to evaluate the efficiency of the proposed framework, the values of the cost, thermal, and environmental objectives are calculated for all the mixes in the dataset and are compared with the optimal solutions proposed by the optimisation framework. Figure 4.6 shows the results of the paired comparisons of the optimal and calculated objective values with red and blue dots, respectively. For this comparison, equal weights are considered for all the objectives. As the results indicate, by replacing C and Cagg contents with SCMs (SF and FA) and RCA-which have lower TC values-the average TC of the proposed concrete mixes has improved by 7.8%, 10.9%, and 15.3% for the three different CS classes of 25±2, 35±2, and 45±2 MPa respectively. Similar findings on the effectiveness of replacing C with SCMs in improving the TC of concrete mixes are reported in the literature. For instance, Demirboğa and Gül (Demirbog, 2003) have reported a significant improvement of up to 53% in TC of lightweight mixes by replacing C content with expanded perlite aggregate, SF and FA, in varying proportions. In addition, it is found that replacing 30% of C content with FA has reduced the TC of mixes by up to 23% (Demirboğa, 2007). Th findings of the present study suggest that the reduction in TC increases with an increase in the CS ranges, which can be attributed to the higher replacement percentage of SCMs with C in higher CS ranges. From an environmental perspective, the contents of the environmentally expensive constituents, such as C and SP, are reduced in the mixes proposed by the framework, while more SF and FA are incorporated, both of which are environmentally less expensive. In addition, more RCA is introduced as the replacement of the Cagg, as it can help achieve the same properties with concretes containing ordinary aggregate types. As the results suggest, the environmental footprints of the mixes proposed by the developed framework are improved. Moreover, reducing SP and adding RCA contents compensate for the relatively high cost of SF. These have resulted in improvements in the environmental footprints, thermal, and economic objectives of the mixes proposed by the developed framework. The findings of the literature corroborate the effectiveness of SCMs and RCA in improving the cost and environmental performance of concrete. For instance, Majhi et al. (Majhi & Nayak, 2020) studied the effects of incorporating two types of SCMs (i.,e. slag and lime) into RAC. The results showed that including these SCMs (to certain percentages) led to a 7.15 – 11.80% and 32.5%–67.0% reduction in the production cost and environmental properties of RAC, including GWP and ACDP. Habibi et al. (Habibi et al., 2021) highlighted the significant effects of SF and slag on reducing the GWP

associated with concrete mixes, while the impact of RCA on the GWP minimisation was reported to be minor. Cassiani et al. (Cassiani et al., 2021) also indicated the impact of incorporating FA, SF, and slag on improving the sustainability measures of concrete mixes in an experimental study. In addition, the use of RCA up to certain percentages has been shown to reduce the cost of production (Tošić et al., 2015). It is worth noting that the unit kg/m^3 refers to the proportion of components in each cubic meter of concrete.

Table 4.8 Designed mixes Vs. mixes from the dataset for three classes of CS

	CS (MPa)	Cement (kg/m^3)	SF (kg/m^3)	FA (kg/m^3)	W (kg/m^3)	SP (kg/m^3)	Cagg (kg/m^3)	Fagg (kg/m^3)	RCA (kg/m^3)	Age	GWP	Cost ($/kg)	ACDP	FFDP	TC (W/m.K)
Optimised mixes	23-27	208	5.95	1.36	117	1.14	169	237	1344	28	187.10	96.95	1.64	409.94	0.44
		208	1.44	74.84	112	2.08	95	126	1096	28	179.92	105.29	1.61	486.60	0.44
		221	4.64	67.34	114	2.32	93	261	1347	28	185.07	95.05	1.62	372.27	0.45
		198	5.96	1.36	120	2.22	172	226	1344	28	179.90	97.82	1.61	486.41	0.44
	33-37	213	23.46	45.56	133	0.01	1258	566	12	28	195.12	161.78	1.77	331.75	0.54
		189	25.95	15.01	102	2.35	119	375	1316	28	172.33	109.50	1.49	484.00	0.43
		213	21.45	101.50	117	0.35	1183	518	268	28	194.10	166.26	1.69	359.02	0.51
		204	23.10	15.69	102	0.84	106	335	1316	28	183.30	104.16	1.55	378.69	0.43
	43-47	266	42.97	23.02	197	1.05	12	1279	61	28	241.62	142.95	2.33	495.60	0.43
		315	45.69	105.23	185	0.44	20	188	1054	28	281.16	126.90	2.51	510.68	0.45
		267	42.93	25.05	168	0.88	122	1279	54	28	242.60	149.21	2.21	482.97	0.43
		266	44.49	24.36	160	1.19	437	1279	54	28	243.10	169.27	2.17	509.36	0.45
Dataset mixes	23-27	210	0	0	206	0	0	943	977	28	189.38	109.72	2.06	319.05	0.43
		258	0	75	159	0	742	691	273	28	233.31	145.18	2.11	393.61	0.49
		250	0	0	150	4.37	858	762	286	28	231.67	158.74	2.05	750.22	0.50
		250	0	0	150	4.37	770	762	286	28	231.38	153.46	2.05	749.67	0.50
	33-37	354	35.46	0	117	3.91	1145	716	0	28	324.40	201.50	2.46	867.68	0.54
		378	42	0	240	0	1030	650	0	28	340.51	187.90	3.12	574.04	0.55
		315	105	0	240	0	1030	650	0	28	284.75	200.50	2.78	480.17	0.54
		332	17.52	0	175	2.82	764	747	295	28	302.67	171.66	2.59	742.44	0.51
	43-47	401	0	0	173	0.2	911	574	303	28	360.29	171.06	2.93	623.81	0.53
		401	0	0	173	0.71	585	574	585	28	359.80	158.60	2.93	663.89	0.50
		397	0	0	198	0	1071	714	0	28	357.26	180.29	3.03	602.48	0.56
		380	0	0	190	0.41	640	1163	0	28	342.99	174.67	2.91	611.64	0.51

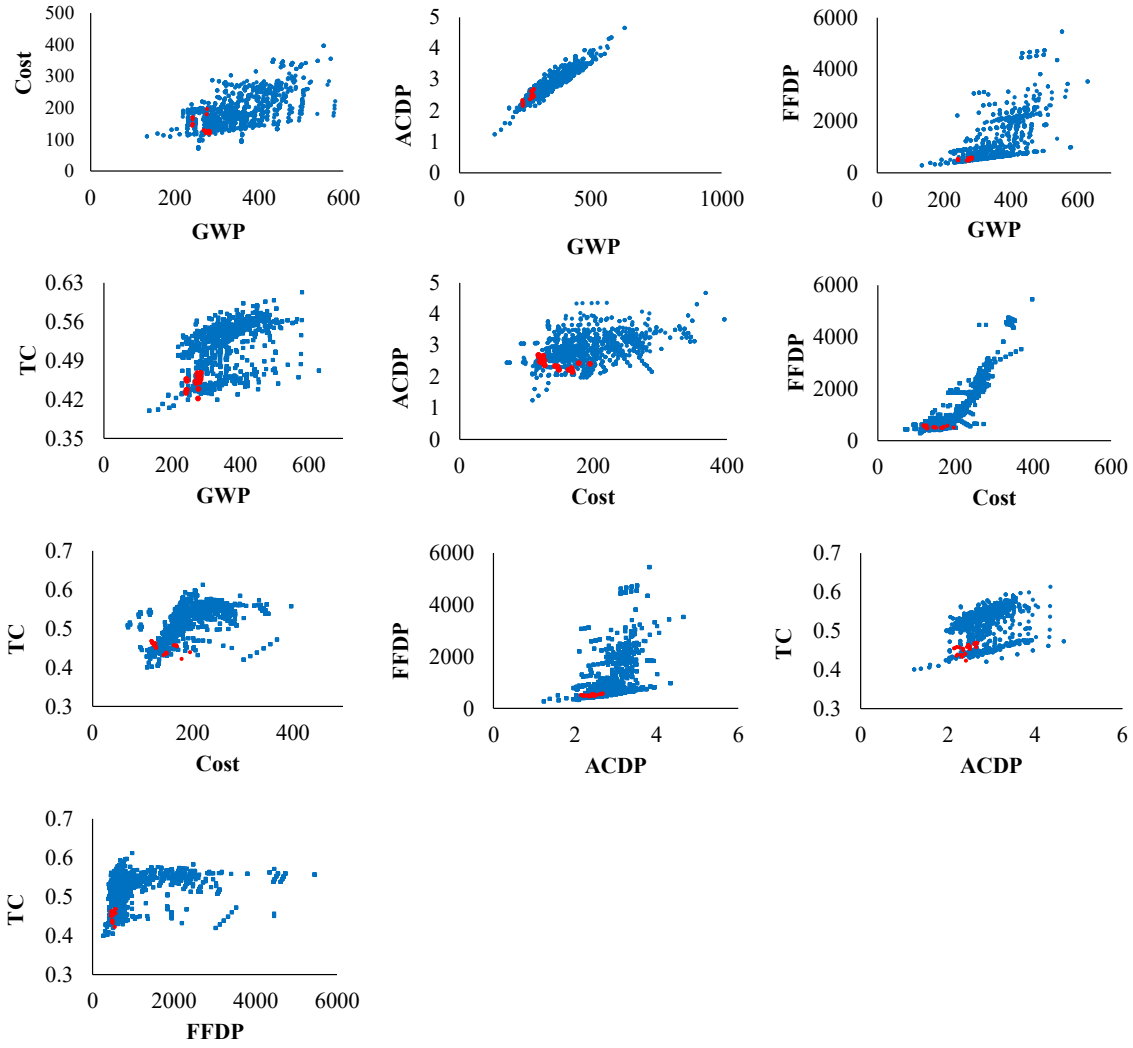

Figure 4.6 Objective functions paired comparison

4.7.2 Multi-criteria decision making analysis

Different weights can be attributed to thermal, environmental and economic indices based on their relative importance according to organisational, regional, and project-specific priorities (Lippiatt, 2002). To identify the optimal solutions by considering a specific set of relative importance weights assigned to the economic, thermal, and environmental indices, TOPSIS is adopted in this study. Thanks to the importance of cost as a key decision criterion, four scenarios are defined by varying the weight associated with the cost index from 0.2 to 0.4, 0.6, and 0.8. Accordingly, the equal weights of 0.2, 0.15, 0.1, and 0.05 are assigned to the four thermal and environmental objectives in scenarios 1 to 4, respectively. Figure 4.7 shows the sensitivity of each objective to the variation of the assigned weights when applied to the final solutions for the CS range between 43 and 47 MPa.

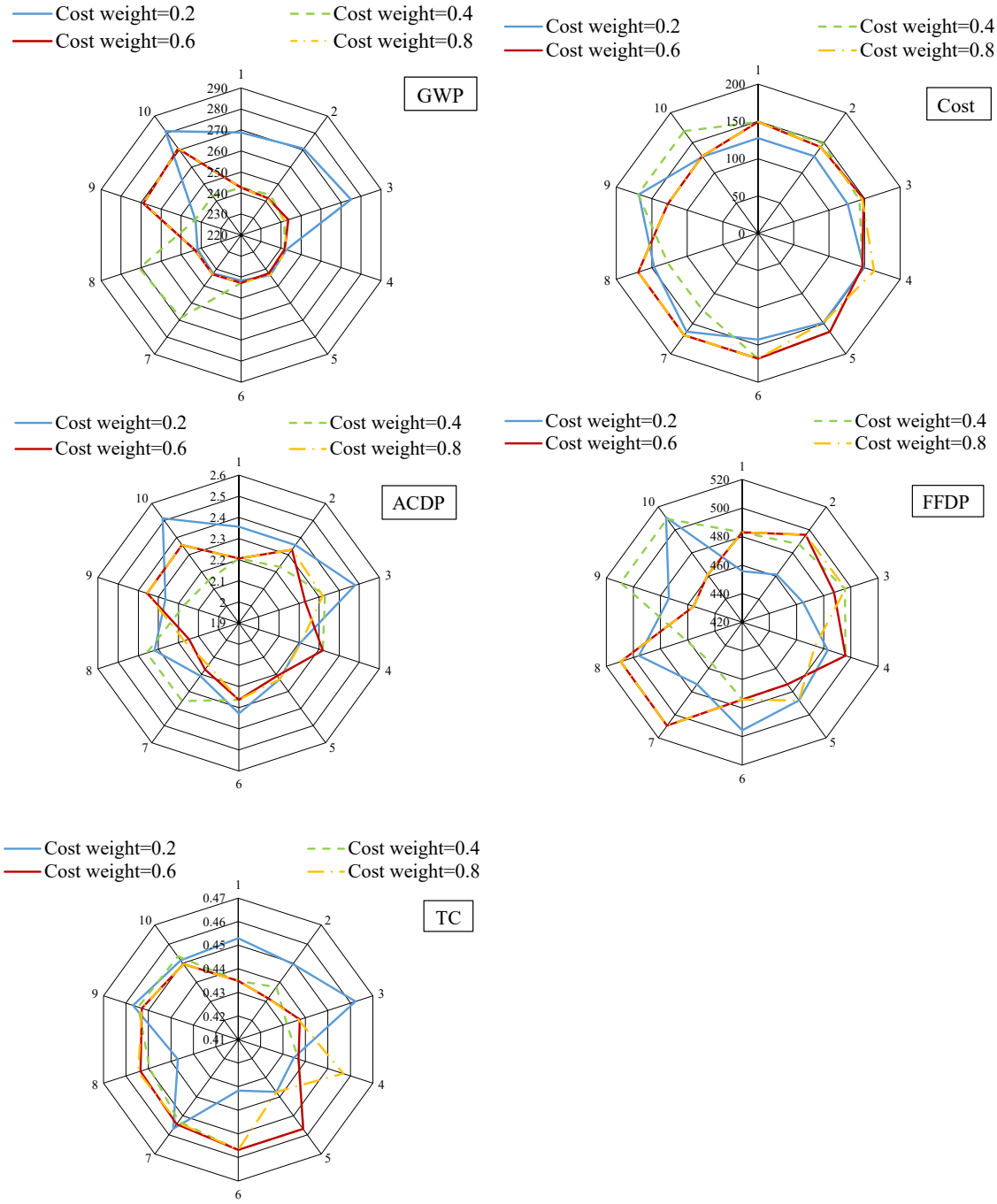

Figure 4.7 TOPSIS analysis on optimal objectives

The relatively low sensitivity of the optimal solutions to variations in the importance of cost can be attributed to the narrow chosen CS range. The variation in the relative importance of cost is, however, found to significantly impact the values of thermal and environmental objectives. These results, therefore, highlight the importance of clarity on the relative importance of thermal, environmental, and economic objectives within an organisation to ensure that concrete mixes are designed to maximise their intended impacts. Further, the sensitivity of the optimal solutions to the

weighting of objectives highlights the risks associated with generalising the findings of a particular case study and project to another without accounting for the specific requirements of projects.

4.8 Conclusions

A multi-objective concrete mix optimisation framework is developed to increase the energy efficiency of concrete throughout its lifecycle leveraging the benefits of incorporating RCA and SCMs into concrete mixes to meet thermal, environmental and economic objectives, including TC, GWP, and cost of production. The MOO framework is designed using a set of machine learning-based techniques, including linear, decision tree-based, neural network, and gradient boosting algorithms. The machine learning algorithms are trained and tested using a dataset of about 2,120 mixes collected from the literature by relying on the experimental data correlating the mix proportions and curing age to predict the CS of RAC mixtures. The accuracy of the data-driven models is evaluated using a group of error metrics, and the best-performing algorithm, Xgboost, is integrated into the MOO framework as a mechanical constraint to limit the desired CS range, thereby increasing the efficiency of the optimisation process. The proposed optimisation framework can significantly reduce the time and resources required for mix optimisation by automating the process, thereby mitigating the need for time-consuming and trial-based mix optimisation attempts. The main findings of this study are summarised as follows:

- This study highlights the efficiency of gradient boosting algorithms in predicting the non-linear relationship between the constituents of concrete and its CS, as Xgboost and GBM techniques outperform other algorithms, with respective 95.6% and 95.1% precision in predicting the CS of the mixes.
- In line with the widely accepted fact that using RCA can improve the thermal and environmental performance of concrete at the cost of its mechanical performance, the present study shows that incorporating SCMs can effectively compensate for the reduced strength of RAC, while simultaneously improving its operating and embodied energy efficiency.
- Considering the high sensitivity of the Xgboost predictive model highlighted through the feature importance analysis using the SHAP method, variables age, SP, C, and W can be deemed the most influential factors impacting the CS of RAC mixtures. These findings provide valuable insights into the optimisation of RAC mixes to improve their mechanical properties, particularly CS.

- The results of the study highlight the effectiveness of integrating advanced data-driven modelling techniques and MOO algorithms in facilitating the design of energy-efficient concrete mixes containing RCA and SCMs by automating the process. This is shown through case studies, where the CS ranges between 25±2, 35±2, and 45±2 MPa to examine the framework performance across different strength ranges. In addition, the sensitivity of results to variations in the relative importance of objectives confirms the efficiency of the proposed method in improving the thermal and environmental properties as well as the production cost of RAC mixes. In particular, the results show that up to 24.4% cost reduction can be achieved using the optimised RAC mix, while at the same time leading to 11.3% and 28.9% improvements in TC and GWP, respectively.

While the framework presented in this study offers a practical approach to designing energy-efficient RAC mixes containing SCMs, a number of limitations can be considered. First, the data used for the training and testing of the machine learning models developed in this study are derived from laboratory experiments reported in the literature with instances of missing information on the temperature and humidity during the curing methods, material quality, type, and gradation, as well as mixing procedure. Second, including the durability performance of mixes can increase the reliability of the MOO, which can be achieved by reporting the durability properties of mixes in the literature. Third, the environmental impact multipliers used in this thesis may not accurately represent all the materials used in the concrete mixes considered in the dataset. Therefore, the precision of the optimisation framework may improve by utilising local environmental impact inventories representing locally used mix constituents. It is believed that addressing the mentioned limitations can improve the accuracy and reliability of data-driven approaches.

This thesis conducted an in-depth investigation of the influential factors in the energy efficiency of buildings, spanning environmental and design-related parameters. The findings of the study highlighted the importance of the thermal performance of building materials, particularly concrete, throughout its operating life due to its widespread use in building envelopes, including roof and exterior walls. Therefore, this research aimed to contribute to the body of literature by optimising concrete mixes with improved thermal properties. However, to ensure the practicality of proposed mixes along with the importance of the mechanical properties and environmental footprints of concrete mixes, a few mechanical and environmental indicators were considered, resulting in the data-driven based multi-objective optimisation framework for thermal and energy performance under mechanical constraints proposed in Chapter 4. It is worth noting that the commonly used sustainable practices found in the literature appealing to improve the energy efficiency of concrete, including replacing fine aggregates with recycled materials, could address some limitations associated with the emerging technology of concrete 3D printing. For instance, substituting lightweight fillers such as recycled materials with NA can reduce the weight of mixes, thereby helping them to bear their self-weight, which is highly required in concrete 3D printed elements. It can also reduce the need for natural aggregates, thus mitigating the environmental consequences attributable to the concrete industry. Therefore, Chapter 5 aims to experimentally adopt such an approach to examine its effectiveness in improving the printability and thermal properties of mixes.

Chapter 5 Pathways to formulate lightweight and ultra-lightweight 3D printable cementitious composites

5.1 Abstract

This chapter studies the pathways to formulate lightweight and ultra-lightweight 3D printable cementitious composites. A hybrid approach was proposed by combining the advantages of traditional chemical-induced foaming (foaming approach) and lightweight particulate inclusions (synthetic foam approach). A comprehensive experimental program was carried out to evaluate the impacts of foaming agents and fly ash cenosphere (FAC) on the printability, microstructure, mechanical and thermal properties of 3D printed samples. The results showed that the hybrid approach could produce a mixture with a density as low as 470 kg/m^3 while ensuring good flowability and buildability owing to the lubricating effect of foaming and supporting skeleton formed by FAC. In addition, a three-step homogenization procedure was also developed to predict the effective elastic modulus and thermal conductivity of 3D printable cementitious composites and cementitious foam. The findings of the study highlighted the effectiveness of the hybrid approach in formulating 3D printable ultra-lightweight cementitious composites in thermal insulation and acoustic applications.

5.2 Introduction

Large-scale concrete 3D printing and digital construction have brought enormous potential to expand the design space of buildings and other forms of infrastructure (He et al., 2020). One of the most striking features of additively constructed (i.e., 3D printed) concrete structures is its ability to interactively design and produce materials and architectural forms that are otherwise unachievable by conventional casting (Ooms et al., 2021). This new paradigm of construction allows an unprecedented approach for materials and structures co-design – i.e., the materials and components (e.g., geometry) can be parametrically designed attuning to the optimal performance and functionalities. Numerous research efforts are still underway in various areas including properties of 3D printable cementitious materials (Wolfs et al., 2018a) – mechanical and rheological properties (Al-Qutaifi et al., 2018), material design optimization (Z. Liu et al., 2019), as well as behaviors of the 3D printed elements (Wolfs et al., 2018a), including reinforcing strategies (Asprone et al., 2018). However, fewer efforts have been concerted around functional materials that may enable various functionalities in buildings and other infrastructures (He et al., 2020; M. S. Khan et al., 2020).

Lightweight and ultra-lightweight cementitious composites (LCC/ULCC) have been found promising in a number of applications in concrete 3D printing. First, the reduction of material density significantly reduces the tendency of plastic and viscoplastic buckling (i.e., when concrete is still 'green') that would lead to printing failure during the printing process (Perrot et al., 2021). By reducing the self-weight of printed materials, the self-weight imposed on the underlaying layers will be reduced, thereby reducing the filament deformation and the likelihood of buckling failure (Wolfs et al., 2018b). Secondly, since most current cement-based 3D printing materials are formulated and shipped in the form of 'pre-mixes', the incorporation of lightweight/ultra-lightweight filler can effectively reduce the weight and, therefore, the shipping costs of printing materials. Thirdly, in order to ensure proper printing parameters (e.g., flowability, extrudability, and buildability), mixtures dedicated for printing typically consist of high volumes of cement, fine fractions and special admixtures, which in turn results in higher costs and carbon footprint (Flatt & Wangler, 2022). Therefore, various strategies have been sought to lower the cement and natural sand contents in 3D printing mixtures (Bhattacherjee et al., 2021; T. Ding, Xiao, Zou, et al., 2020). This can be achieved by replacing either the binder with various supplementary cementitious materials (SCMs) or including (lightweight) fillers that have less impact on printing parameters (Bai et al., 2021).

Aside from reduced structural weight, LCCs/ULCCs also improve the thermal and sound insulation performance of building components (Tinoco et al., 2022), alongside other benefits such as improved fire resistance (Suntharalingam et al., 2021) and increased flexibility in strength design (Pasupathy et al., 2022a). The exploration of lightweight cementitious materials for 3D printing has been on-going over the recent years. Araújo et al. (Araújo et al., 2022) explored the impact of incorporating light expanded clay aggregate on the thermal performance of cementitious composites. The results showed that the density and thermal conductivity of 3D printable cementitious composites were reduced to 1770 kg/m^3 and 0.61 W/mk by partially replacing sand content with lightweight fine aggregates. Similarly, Mohammad et al. (Mohammad et al., 2020) investigated the feasibility of partial to full replacement of natural fine aggregates with expanded perlite aggregate for designing lightweight 3D printable concrete mixtures with improved thermal properties. In addition, Weger et al. (Weger et al., 2020) examined the potential of using expanded glass beads as the partial replacement of sand for 3D printable mixtures, where a cementitious composite with the density of 1015 kg/m^3 was obtained. The findings in the literature highlight the effectiveness of replacing sand with lightweight fillers in reducing the density of 3D printable

cementitious composites. Such a reduction, however, seems to be limited and the lowest density achieved was around 1000 kg/m^3.

To tackle these limitations, applying foaming agents to further reduce the density of 3D printable cementitious composites has been investigated (C. Liu et al., 2021; Markin, Sahmenko, Nerella, Näther, et al., 2019). Foaming agents generate a significant amount of air bubbles, resulting in low-density materials that are suitable for non-structural applications (i.e., insulation and acoustic)(Yuanliang et al., 2021). Markin et al. (Markin, Nerella, et al., 2019) proposed a pro-foaming process to design 3D printable foam concrete mixtures, resulting in a cementitious composite with a density and thermal conductivity of 980 kg/m^3 and 0.24 W/mK respectively. Moreover, Markin et al. (Markin et al., 2021) explored the thermal and mechanical properties of several 3D printable foam concretes. Their results indicated that mixtures with density and thermal conductivity ranging from 800 to 1200 kg/m^3 and 0.17 to 0.35 W/mK, respectively were obtained. On the other hand, Cho et al. (Cho et al., 2021) highlighted the impact of foam concentration on the rheological properties of cementitious composites, elucidating the rheology and printability of three foam concrete mixtures with densities around 700, 1000, and 1400 kg/m^3.

In light of the negative impacts of incorporating foaming agents on the printability of cementitious composites, in particular buildability (Cho et al., 2021), the effectiveness of this approach in density reduction is constrained by certain limitations. Previous studies by the authors indicated that cementitious composite materials containing micro- and meso-size lightweight particulate inclusions may have significant promise in addressing the printability issue of light weight cementitious composites (Brooks et al., 2018; Shen et al., 2021; H. Zhou & Brooks, 2019). This class of materials include LCC/ULCC made from hollow FAC, hollow glass microspheres (HGM), and expanded plastic (Shen et al., 2021; H. Zhou & Brooks, 2019). These materials can achieve reduced density while maintaining relatively high mechanical properties (i.e., elastic modulus and strength). However, to date, few studies have investigated the viability of lightweight fillers and chemical foaming for LCC. Leveraging the synergetic effects of lightweight fillers capable of improving printability and foaming agents to drastically reduce the density of cementitious composites for 3D printing applications has shown significant promise.

Motivated by this knowledge gap, the present study investigates the pathways to formulate lightweight and ultra-lightweight 3D printable cementitious composites by proposing a hybrid approach combining the advantages of traditional chemical-induced foaming and micro-sized

lightweight particulate inclusions (synthetic foam approach). A comprehensive experimental program was carried out to evaluate the impacts of foaming agents and FAC on the printability, microstructure, mechanical and thermal properties of 3D printed samples. In addition, the elastic modulus and thermal conductivity of different mixtures were modeled through a three-step homogenization approach for property predictions and to enable future computational material design. The present study highlights the effectiveness of the proposed hybrid approach in formulating 3D printable LCC and ULCCs for a number of possible architectural applications.

5.3 Pathways to formulate lightweight and ultralightweight cement-based composites for 3D printing

Traditionally, lightweight concretes were produced by incorporating lightweight aggregates (LWA) such as expanded perlite (Lanzón & García-Ruiz, 2008), shale, and expanded clay (Chandra & Berntsson, 2002) into concrete. Mixtures formulated for 3D printing, however, rarely incorporate coarse aggregates. In addition, the irregular shape and high porosity of LWAs often have significant adverse impact on the printing parameters of the mixtures. Therefore, the LCCs and ULCCs for 3D printing are typically formulated through one of the two pathways: (*i*) Foaming: both chemically induced foaming (Markin, Nerella, et al., 2019) and the mixture of cement paste with preformed foam pastes (Markin, Sahmenko, Nerella, Nather, et al., 2019) have been incorporated to produce 3D printable LCC in the density range of 700-1400 kg/m^3 (Marais et al., 2021a). While it is straightforward to achieve reduced density through foaming, drawbacks of this method include weak interlayer bonds, low mechanical strengths, and poor buildability during printing (Pasupathy et al., 2022b). In addition, the air voids formed by chemical foaming agents can easily deform, coalesce, and collapse under gravitational load when the printed filaments are fresh, see Figure 5.1 (a), leading to excessive plastic and viscoplastic deformation of the printed filaments. (*ii*) Synthetic foam: the second approach to form LCC and ULCC for 3D printing is through the addition of micro-size particulate lightweight inclusion including expanded polystyrene and polyurethane beads (Pavel & Blagoeva, 2018), FACs, expanded glass microsphere, and expanded plastic microsphere. It is worth mentioning that the addition of FAC will form synthetic foam composites (Brooks et al., 2020; He et al., 2023). At higher loading fractions of the lightweight inclusion, the rigid shell inclusions will form a strong skeleton to resist gravity-induced deformation at fresh state, see Figure 5.1 (b). However, due to the effect of FAC (and other similar micro-sized lightweight inclusions) on the rheological properties of cementitious composites (B. Lu et al., 2020), the mixtures with high volume fractions of the inclusion phase are not easily flowable and extrudable, thereby limiting the density range can be achieved by this method.

Combining the benefits of both chemical-induced foaming and lightweight particulate inclusions, this research investigates a hybrid approach, see Figure 5.1 (c), to form 3D printable LCC and ULCC, where the density of cementitious composites was reduced both by using the chemical foaming approach and the (partial to full) replacement of sand content with lightweight inclusions such as FAC to simultaneously lower the density and compensate for the weakened printability parameters of cementitious composites. By having the synergistic effects of micro-size particulate inclusions and the foaming agent on density reduction, flowability, and strength, this approach could reduce the density of mixtures to an unprecedented level without significantly compromising their printability parameters. This approach may create material design spaces that are appealing to building designers seeking functional building elements with unique architectural attributes (e.g., energy efficiency, attuned acoustic and water retention properties). Moreover, adopting the hybrid approach facilitated the inclusion of more lightweight fillers that can help mitigate the negative environmental footprints of natural resource exploitation and landfill waste.

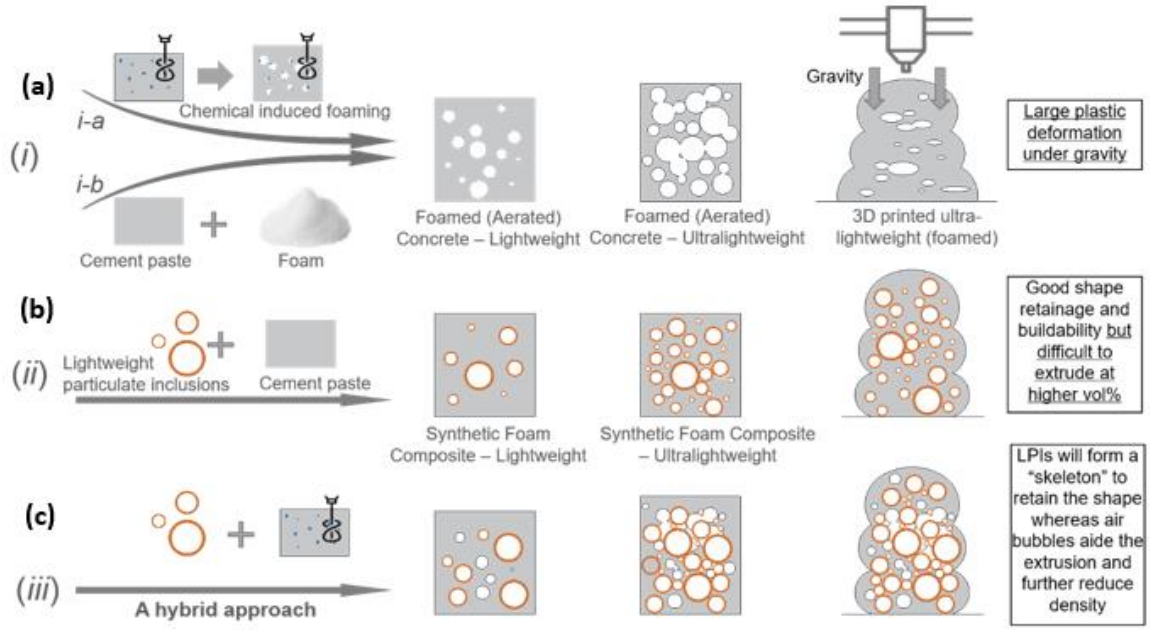

Figure 5.1 Lightweight and ultra-lightweight formulation of cementitious composites: (a) foaming; (b) synthetic foam; and (c) hybrid approach

5.4 Experiment program

5.4.1 Materials and preparation

In this research, eight (8) 3D printable mixtures were designed as enlisted in Table 5.1. The reference mix (Ref) was formulated using two types of cement (blended), i.e., ordinary Portland cement (OPC) and calcium sulfoaluminate (CSA), silica sand, superplasticizer (SP), cellulose ether (CE) as viscosity modifier, and water. To reduce the density of the mixture, two different dosage of a highly concentrated foaming agent (MasterCell® 30) were added, resulting in FA32 and FA34. In addition, the sand content of the Ref mix was replaced with 50% and 75% FAC by volume (i.e., noted as FAC50 and FAC75, respectively). To investigate the synergistic effect of both approaches, two different dosages of the foaming agent were introduced, where FAC75-FA13 and FAC75-FA29 mixes represent 75% sand replacement by FAC plus 12.7 kg/m^3 and 29.4 kg/m^3 foaming agent contents, respectively. It is worth noting that the unit kg/m^3 refers to the proportion of components in each cubic meter of mix designs in Table 5.1. Finally, the one mix with the entire sand content replaced by FAC was designed, and an additional dosage of foaming agent (36.4 kg/m^3) was added, resulting in the FAC100-FA36 mixture. The FAC used in this experiment is grade ES-106 with an average particle size of 85 μm (D_{10}= 44.9 μm, D_{90}= 155.4 μm), and a true density of 910 kg/m^3 tested by a gas pycnometer. It is worth noting that the optimal dosage for the foaming agents depends on the objective density, which usually requires multiple trial-and-error attempts. Also, due to the varied contents of FAC and the liquid nature of foaming agent, the amounts of water, cement, and SP were slightly adjusted, as shown in Table 5.1.

Table 5.1 Mixture design

Mix ID	OPC	CSA	Sand	FAC	SP	CE	FA*	Water	Density
	(kg/m^3)	(kg/m^3)	(kg/m^3)	(kg/m^3)	(kg/m^3)	(kg/m^3)	(kg/m^3)	(kg/m^3)	(kg/m^3)
Ref	981.1	9.9	991.0	0.0	1.7	1.4	0.00	306.4	2200
FA32	973.8	16.2	869.9	0.0	0.0	8.5	32.3	304.3	1310
FA34	968.2	16.1	864.9	0.0	0.0	8.5	33.9	306.6	1040
FAC50	977.4	9.9	493.7	169.5	6.5	1.4	0.0	305.3	1840
FAC75	974.0	9.8	246.0	253.4	11.0	1.4	0.0	304.2	1680
FAC75-FA13	1014.4	16.9	229.0	235.9	10.1	0.9	12.7	304.3	1160
FAC75-FA29	980.6	16.3	221.3	228.0	4.9	4.1	29.4	306.5	840
FAC100-FA36	950.2	15.8	0.0	293.8	0.0	8.3	36.4	313.9	470

*FA denotes foaming agent for labeling the mixtures

All the mixtures were prepared following the same mixing procedure: First, all the dry powder constituents (i.e., cement, sand, FAC) were mixed on a low speed (107 RPM) setting for one

minute. Then, water and SP were added to the mixes and mixing for one more minute, followed by another 3 minutes medium speed (198 RPM) mixing. For mixtures that incorporated foaming agent, MasterCell® 30 was added to the mixtures along with water and SP. To better activate the foaming agent, a paint mixer was used to mix the mixture at a higher rotation rate (800-1000 RPM) for three minutes. The mixing process is shown in Figure 5.2. A screw-driven extrusion type 3D concrete printer was utilized for the printing tests, as shown in Figure 5.3. The benchtop concrete 3D printer is comprised of a screw-driven extruder, a printing platform (length 75cm, width: 67cm, height: 67cm), and three motion sliders that enable the movement of printheads in three directions of X, Y, and Z. The screw-driven extruder contains a two-liter hopper, an auger driven by a servo motor with adjustable speeds and extrusion rates, and four nozzle sizes of 5, 10, 20, and 35 mm.

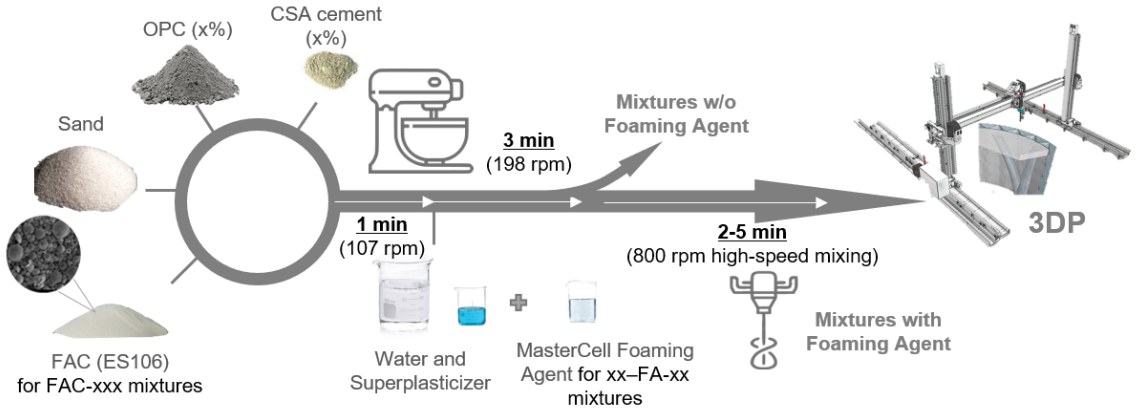

Figure 5.2 Process of preparing ultra-lightweight 3D printable concrete

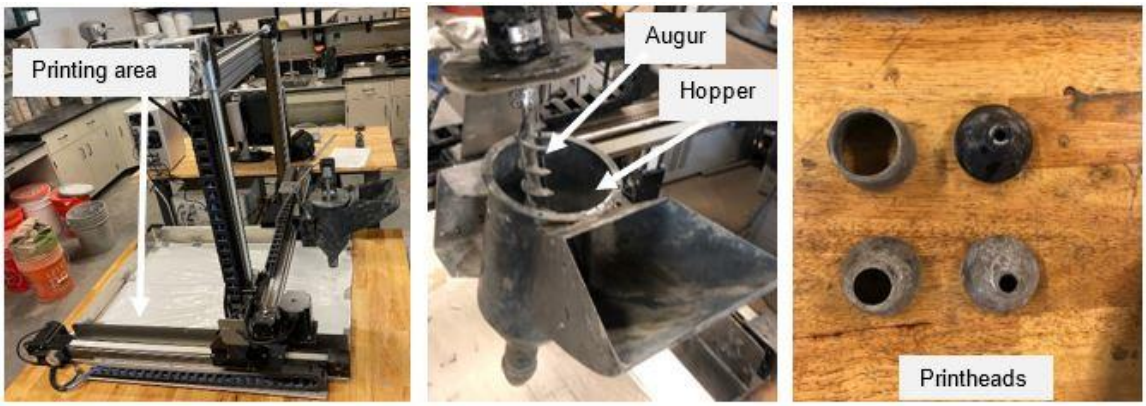

Figure 5.3 Benchtop extrusion type concrete 3D printer used for testing

5.4.2 Fresh state properties and printability indicators

The printability of the mixtures was characterized by flowability, extrudability, and buildability, within 30-minute windows. The printing parameter settings were the same for all the mixtures

within each printability test (i. e., extrudability and buildability). Mechanical samples were also produced.

5.4.2.1 Flowability

Flowability tests were carried out to ensure the proper delivery of material from the mixer to the hopper and the suitable state of material in the hopper. These tests were carried out using a flow table according to ASTM C230 specifications to evaluate the flowability of the mixtures within a 30-minute window once the mixing process was completed. A bronze casting cone mold was used, which has a top diameter, bottom diameter, and height of 69.85, 101.6, and 20.8 mm, respectively. The cone mold was placed on a flat circular table and filled with mortar. The mortar was properly compacted before removing the cone mold. Then, the table was dropped 25 times within 60 seconds. The diameter of the spread mortars was measured in two perpendicular directions, and the average value was used as the flowability indicator.

Figure 5.4 presents the flowability of the mixtures in the fresh and 30-minute after mixing, representing the allowable time for printing. The results show that the flowability in all the mixtures was reduced after 30 minutes, which was mainly attributed to the cement hydration over time (Jiao et al., 2017) . The reduction was negligible in the FAC75 and FAC100-FA36 mixes, around 1.4% and 1.8%, respectively, followed by the FAC75-FA29 mix. This was mainly owing to the presence of the high dosage of FAC and the foaming agent in these mixes. The inclusion of the FAC reduces the flowability of the mixtures due to particle packing (Sun et al., 2018); while introducing the foaming agent increased the cohesion due to higher air content, thus reducing the flowability of the mixtures, which agrees with the findings in the literature (Makul & Sua-Iam, 2016). Therefore, increasing the volume percentage of FAC or the dosage of foaming agent will lead to a decrease in flowability. Aside from the high cohesiveness of FA32 and FA34, their lower flowability when compared to the Ref, FAC50, and FAC75 were also due to the lower water-solid ratio in these mixtures (Sun et al., 2018). Overall, all mixtures retained acceptable flowability within the 30 minutes window tested after the mixing was completed.

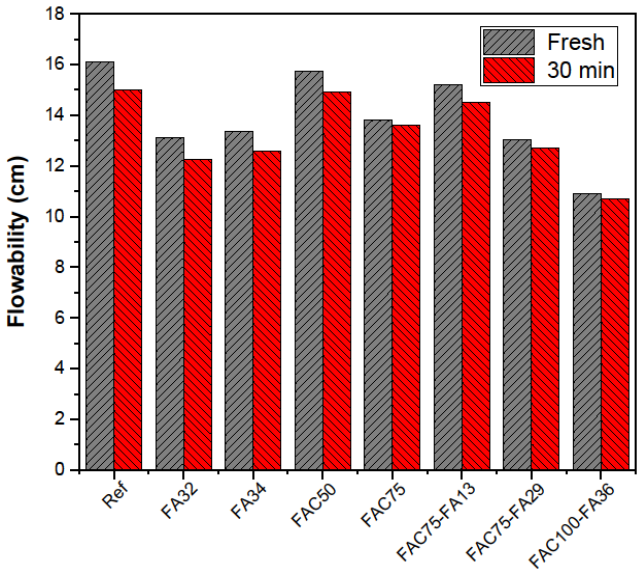

Figure 5.4 Results showing the flowability

5.4.2.2 Extrudability

Extrudability refers to the workability of the material when extruding through a 3D printer nozzle. It plays a critical role in the 3D printing process because improper extrudability may clog the nozzle, leading to discontinuously shaped material or even no material is extruded (Z. Li et al., 2020). A 10 mm nozzle was utilized in this study to quantify the extrudability of the mixtures by measuring the width of the printed mortar in an S-shape at the fresh state and after 30 min. The mortar was printed with a continuous length of 3.5 m in an S-shape, and the length of each leg is 50 cm. The print head velocity and extrusion rate were set to 45 mm/s and 1 round per second (RPS), respectively. A caliper was used to measure the width of the printed lines.

The extrudability was characterized by the width of printed lines and was categorized into three classes: 1) extrudable (E): the mixture extruded with no flows and the width of the printed lines was not exceeded 1.7 times of the nozzle size (17 mm); 2) over extruded (O): the mixture spread excessively and exceeded 1.7 times of the nozzle size; and 3) breakage (B): the printed mixture was extruded discontinuously. The extrudability along with the average width and the standard deviations of the printed lines are summarized in Table 5.2, where seven measurements were conducted for each mixture. Selected images representing typical sample of each class are shown in Figure 5.5. In the fresh state, FA34 and FAC75-FA29 exhibited the highest average width about 18.1 mm and 17.6 mm (Falliano et al., 2019). The result indicated that high dosage of foaming agent contents would increase the printed line width, resulting in the potential over-extrusion of the

cementitious composites (B. Lu et al., 2019). On the other hand, FAC75 showed the best extrudability properties with an average width of 10.5 mm, which was related to the packing of FAC, thereby preventing the over-extrusion of printed filaments (Danish & Mosaberpanah, 2021). The extrudability of FAC100-FA36 was also improved by the full replacement of sand with FAC. After 30 min, the Ref showed the best extrudability with an average width of 12.3 mm. Similar to the fresh state, incorporating foaming agent increased the line width in FA32 and FA34, while FAC50 and FAC75 mixtures were not extrudable after 30 min as they were printed with breakage, see Figure 5.5 (a). This was owing to the high content of FAC, resulting in high water absorption which dries the mixtures after 30 minutes (Satpathy et al., 2019). The results highlighted the effectiveness of the hybrid approach as incorporating FAC improved the extrudability of the foam incorporated mixtures. Nevertheless, it was also indicated that we need to be cautious of over-extrusion when combining foaming agents and FAC, especially using a relatively high dosage.

Table 5.2 Extrudability test results

Mixture	Fresh	30 min	Fresh		30 min	
			Avg (mm)	Std (mm)	Avg (mm)	Std (mm)
Ref	E	E	16.0	1.0	12.3	1.8
FA32	E	E	16.2	0.3	14.9	0.4
FA34	O	O	18.1	1.6	17.1	1.3
FAC50	E	B	11.9	0.8	NA*	NA
FAC75	E	B	10.5	0.0	NA	NA
FAC75-FA13	O	E	17.0	0.8	14.1	0.5
FAC75-FA29	O	E	17.6	1.5	16.1	1.6
FAC100-FA36	E	E	15.3	0.4	14.1	0.5

*NA: Not Available

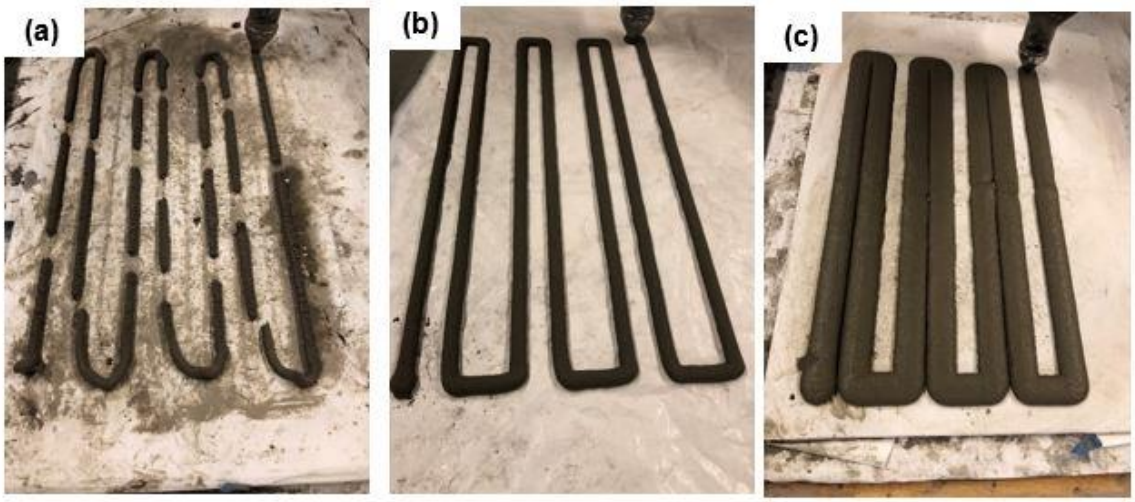

Figure 5.5 Extrudability test samples at 30 min after mixing: (a) FAC75 (B); (b) FAC75-FA29 (E); and (c) FA34 (O)

5.4.2.3 Buildability

Buildability has usually been deemed as one of the most critical indicators in concrete 3D printing because it indicates the ability of a material to bear the weight of top layers without significant deformation or plastic collapse in the fresh state (Muthukrishnan et al., 2021). In the buildability test, several layers were stacked, where the height to width ratio represents the buildability of the mixes. The buildability tests were carried out by vertically depositing six 250 mm-long layers in straight lines using a 20 mm nozzle. The layers were printed at 3-minute intervals for all the mixtures to allow sufficient time for the layer surfaces to slightly dry before the next layer was deposited. Throughout the buildability tests, print head velocity, extrusion rate, and layer height were set to 25 mm/s, 1.8 RPS, and 12mm, respectively. The height of the layers was also recorded at the fresh state and after 30 minutes to record the height change of the samples.

The height to width ratio of stacked print samples was used to quantify the buildability of the samples. The results for both fresh state and after 30 minutes are shown in Figure 5.6 (a), and the pictures of printed example samples are shown in Figure 5.6 (b) and (c). The results are in a good agreement with the discussion presented in section 5.3. The results showed that increasing the concentration of the foaming agent negatively impacted the buildability. Introducing excessive foaming agent (FA32 and FA34) significantly reduced the buildability where the sample failed due to plastic and viscoplastic deformation, as shown in Figure 5.6 (c). Meanwhile, the same figure highlighted the effectiveness of FAC in improving the buildability of FAC50 and FAC75 mixtures as their buildability was improved (better than the reference benchmark) with increments in the FAC content. Despite the positive effects of FAC in FAC50 and FAC75, these mixes were not extrudable after the 30-minute window, which limited the printability of FAC-incorporated mixtures to their fresh states. By introducing the synergetic effect between foaming agent and FAC, the challenges of buildability and extrudability are successfully addressed, as evidenced by the improved buildability of FAC100-FA36. The adverse impact of foaming agent on buildability was also reflected in the reductions of the buildability from FAC75 to FAC75-FA13 and from FAC75-FA13 to FAC75-FA29 – replacing sand with FAC effectively improved the buildability of the mixtures. These findings are consistence with those in the literature (B. Lu et al., 2019).

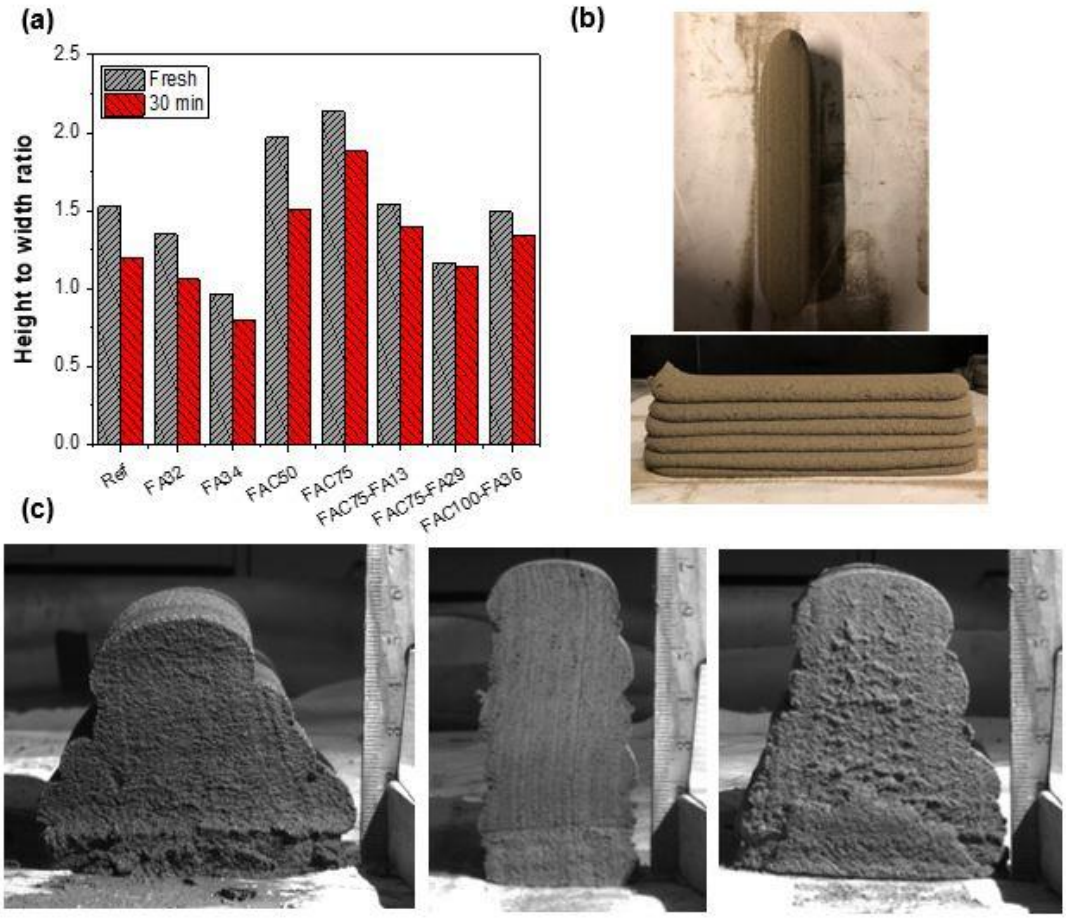

Figure 5.6 Buildability: (a) height to width ratio, (b) top and side view of FAC100-FA36 mix, (c) buildability evaluation for FA34, FAC75, and FAC100-FA36 mixes

5.4.3 Microstructures

5.4.3.1 Micro-CT analysis

X-ray microtomography (Micro-CT) was used to carry out the 3D microstructure analysis. A high-resolution 3D micro-CT system (*Carl Zeiss Versa 620*) with an isotropic voxel size of 9um was used for micro-CT scanning. In computed tomography, X-ray imaging was repeated by slow rotation of the sample to obtain a three-dimensional image, a digital copy of which was stored as a set of pixel matrices, and the 3D reconstruction of the microstructure was conducted using the Dragonfly 2020 software (*Object Research System*). Figure 5.7 presents the micro-CT scan of FAC75-FA29, where the orange areas represent sand and FAC (Figure 5.7 (a)). In the cross-section view (Figure 5.7 (b)), heterogeneous white particles and spherical gray parts denoted sand particles and FAC, respectively; the dark areas in the cross-section view denotes the air voids generated through chemical foaming. For this mix 75% of sand content was replaced with FAC, as evidenced

by the higher fraction of 'gray' over 'white' particles. It can be seen that the FAC particles forms a 'skeleton' to support the self-weight of the printed object while the mix was still fresh. The results of micro-CT analysis showed the highly porous microstructure of the 3D printed mixture, where the hybrid lightweighting approach results in a microstructure that resemble our hypothesis discussed in section 5.3. Phase segmentation analysis showed a porosity of 44.35% was achieved. It is noted that this porosity obtained by CT data may not include the internal void space of FAC due to the limited penetration capacity of the X-ray beam.

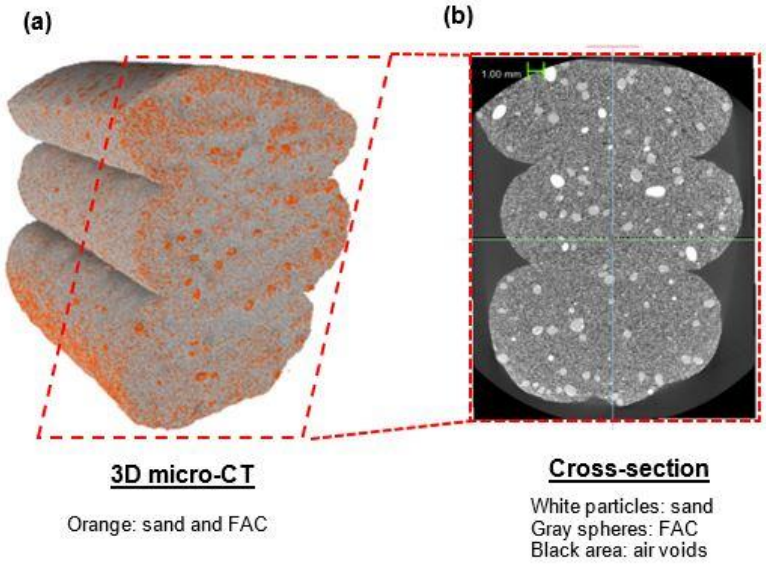

Figure 5.7 Micro-CT scan of FAC75-FA29 shows the phases of sand, FAC, and air voids: (a) 3D micro-CT; and (b) one cross-section.

5.4.3.2 Scanning electron microscopy (SEM) analysis

Further microstructure analysis was carried out using scanning electron microscopy (SEM). The SEM images were obtained using a Hitachi TM3030 Tabletop SEM. The samples were first cut from casted cylinders and polished using a Buehler variable speed polisher (120 to 1200 grit). Then, the samples were kept in an oven (100-110 °C) for four hours to reduce moisture contents. After that, they were taken out to reach room temperature before running the SEM test.

Figure 5.8 presents the microstructure of the Ref, FAC75, FA32, and FAC100-FA36 mixtures, with a focus on the effects of FAC and the foaming agent on pore structure. The Ref sample (Figure 5.8 (a)) serves as a benchmark for comparing with other samples, given its absence of FAC and foaming agent components. For the Ref sample, low air content and homogenous distribution of the sand particles were observed, indicating the sample was well extruded. For the FAC75 sample, the SEM images show that the substitution of sand with FAC led to an increased air void contents

as shown in Figure 5.8 (b). The introduction of foaming agent (FA32) changed the microstructure of the cement matrix, as reflected by the increased porosity as shown in Figure 5.8 (c). It can be seen that due to increased porosity, the sand particles are 'loosely bonded' as the air voids percolate, creating weak links that adversely affect both the 'green' and hardened strength of the printed cement composites. On the other hand, the mixture prepared by the hybrid method exhibited the highest porosity among all the samples, as shown in Figure 5.8 (d). Although a small amount of FACs were entrapped within air voids, but the FACs formed a skeleton with complete "force chain" to support the material system.

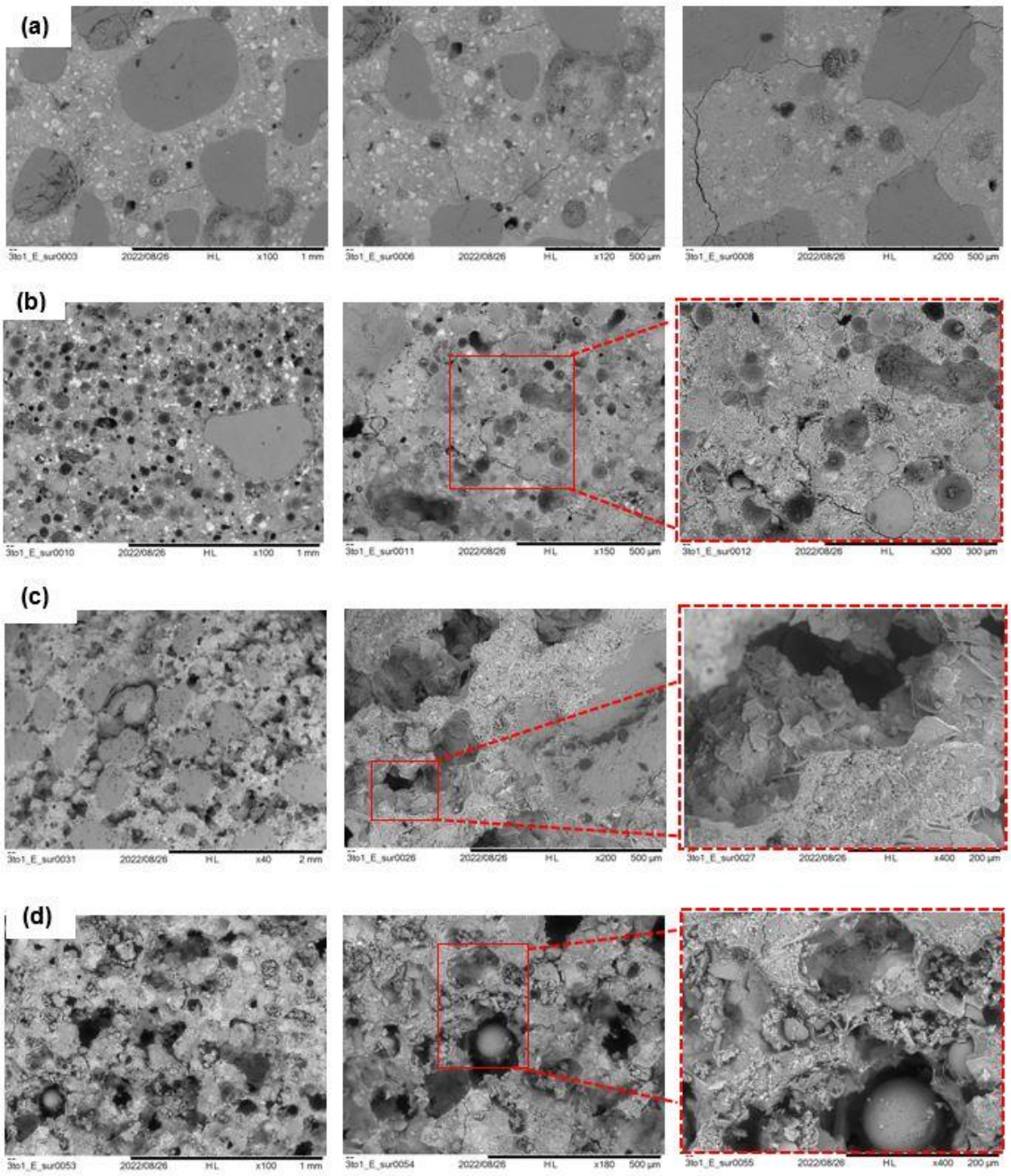

Figure 5.8 SEM images: (a) Ref; (b) FAC75; (c) FA32; and (d) FAC100-FA36

5.4.4 Mechanical properties

The mechanical properties, including compressive strength, elastic modulus, and inter-filament shear strength, of the printed samples were tested. A printed layer of each sample having the height of 12mm was used in the test. Different print head velocities (25-32 mm/sec) and extrusion rates (1-2.5 RPS) were used in preparing the samples, adjusted based on the extrudability, buildability,

and workability of the mixtures. The samples for mechanical tests were printed with the dimensions approximately 500 mm × 60 mm × 70 mm (length × width × height), as shown in Figure 5.9 (a). Aside from the printed samples, four 50.8 mm cubic samples and four 101.6 mm (height) × 50.8 mm (diameter) cylinders of the mixtures denoted in Table 5.1 were casted for compression, elastic modulus, and thermal tests. For the mixtures without foaming agent, a vibration table was used to compact the samples. For mixtures with foaming agent, the samples were repeatedly tapped on the table after lift. In addition, twelve 50.8 mm cubic samples were cut from printed bars, nine of which were used to measure the compressive strength in the X, Y, and Z axes (three samples for each axis), and the remaining three were used for the direct shear test to evaluate the inter-filament bonding. All the specimens were cured for 28 days under controlled conditions of 98% humidity and 25℃ temperature in a concrete curing room prior to mechanical tests.

The compression tests were conducted using a 500kN INSTRON servo-hydraulic universal system, as shown in Figure 5.9 (d). The mechanical loading was carried out in a displacement-control mode at the loading rate of 0.5 mm/min. The samples were placed between two metal bearing caps (Figure 5.9 (b)). For the direct shear test, a pair of caps were designed and used, as illustrated in Figure 5.9 (c). A loading rate of 0.02 mm/min was used in the pre-test setting process to ensure the samples were properly settled into the bearing caps. A high-resolution Charge Coupled Device (CCD) camera was used to capture the progressive failure of the compressive and direct shear test samples. For the elastic modulus test, a pair of clamp-on extensometers (*Epsilon Tech*) with a gauge length of 50mm was used to measure the compressive strain that will be used for elastic modulus calculations, as shown in Figure 5.9 (e).

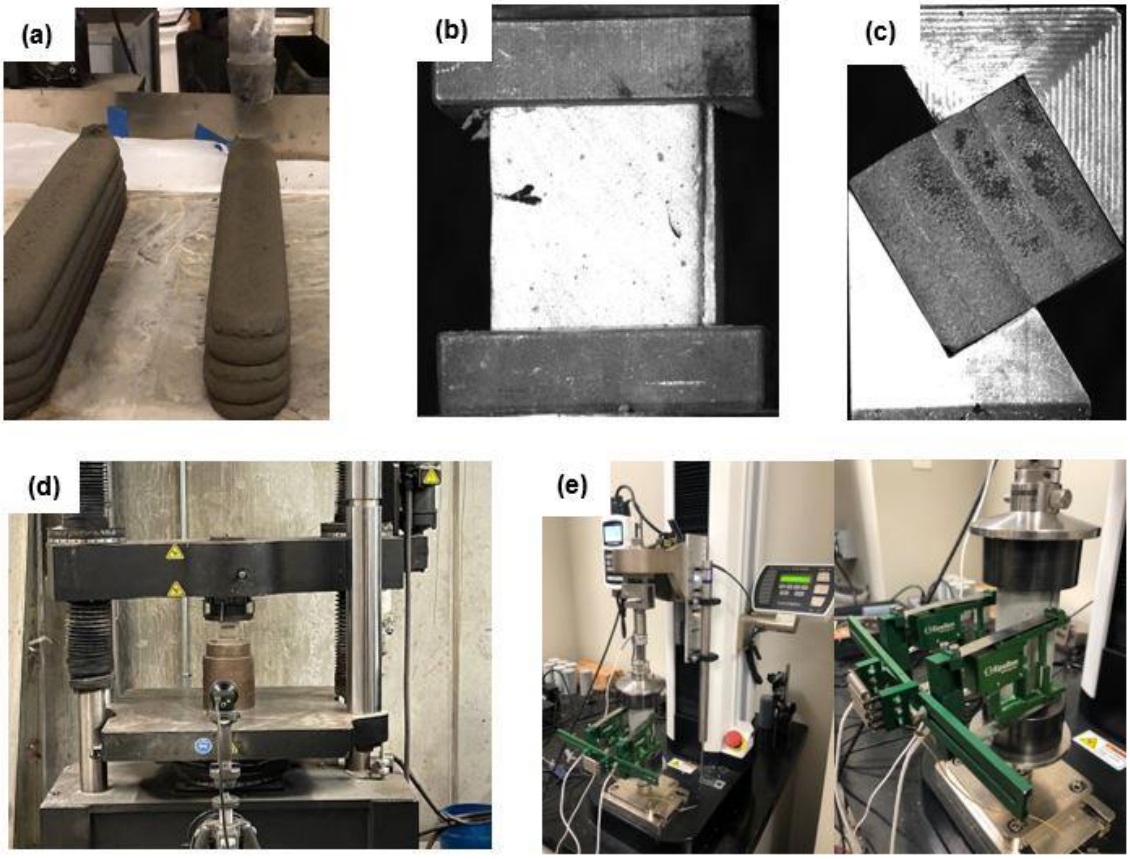

Figure 5.9 Mechanical test sample preparation and test setup: (a) printing mechanical test bars; (b) compression test setup; (c) direct shear test setup; (d) INSTRON servo-hydraulic universal system; (e) elastic modulus test setup

The density, elastic modulus, and compressive and interlayer bond strength test results of the 3D printed cementitious composites are summarized in Table 5.3. Selected 3D printed samples for the compression tests and their failure modes are shown in Figure 5.10 (a). The printed samples generally had lower compressive strength compared to the casted counterparts due to their weak interlayer bonds. In addition, the compressive strengths along the X and Z directions are usually slightly lower than their counterpart along the Y direction because it is assumed that the inter-filament interfaces (weak points) are perpendicular to the applied force in the Y direction. The discrepancy is likely attributed to the failure modes of the samples, where compression under the X and Z directions loading mostly causes failure at the interfaces between two successive printed layer, whereas compression under the Y direction is likely to cause failure at the shear zone through the bulk mortar, as shown in Figure 5.10 (b) (Brooks et al., 2022). It is worth noting that FA34 was not printable (NP) due to the high concentration of the foaming agent causing excessive deformation at fresh state. Thus, only its casted samples were used for compression test.

Figure 5.10 (b) compares the compressive strength of the printed samples under X, Y, Z loading directions. Foam incorporated samples, i.e., FA32 and FA34, showed significant reduction in compressive strength due to the introduction of the foaming agent, which significantly increased the porosity. The compressive strength of FA32 was reduced by 67%, 64%, and 79% along the X, Y, and Z directions, respectively, compared to Ref, which is consistence with the findings in (Pasupathy et al., 2021). For the FAC samples, i.e., FAC50 and FAC75, the compressive strength reduces as FAC replacement of sand. The FAC50 shows a slight reduction in the compressive strength over the Ref sample mainly due to the weaker strength of the FAC compared with sand. The FAC75 experienced more significant compressive strength reduction, by 40%, 34%, and 40% along the X, Y, and Z directions, respectively. This is mainly because the formation of weaker interlayer bonds as increased amounts of sand replaced by FAC. For the hybrid samples, i.e., FAC75-FA13, FAC75-FA29, and FAC100-FA36, a drastic compressive reduction was observed due to the combined effects of FAC and foaming agent. However, they still have enough compressive strength to be used as non-structural components. The results confirm the findings in the related studies in the field, incorporating foaming agents and lightweight supplementary cementitious materials (Markin, Nerella, et al., 2019). For example, FAC100-FA36 yielded the compressive strength of 2.33, 2.79, and 1.76 MPa along the X, Y, and Z directions respectively. The results of elastic modulus tests shown in Figure 5.10 (c) follow a similar trend as compressive strength test. How materials' elastic moduli change as a function of the sample density will be discussed in detail in Section 5.5. For the samples tested, FAC100-FA36 achieves the lowest density around 470 kg/m^3 which supports our hypothesis that the hybrid approach could reduce the density of mixtures to an unprecedented level without significantly compromising their printability parameters.

Direct shear tests were also carried out to evaluate the impacts of FAC and the foaming agent on the interlayer bond strengths of the samples. All the samples failed due to the breakage in interlayer bonds during the direct shear tests as shown in Figure 5.10 (d). The addition of both FAC and the foaming agent led to a significant reduction in the direct shear strength similar to the compression test results. Failed direct shear samples are shown in Figure 5.10 (e).

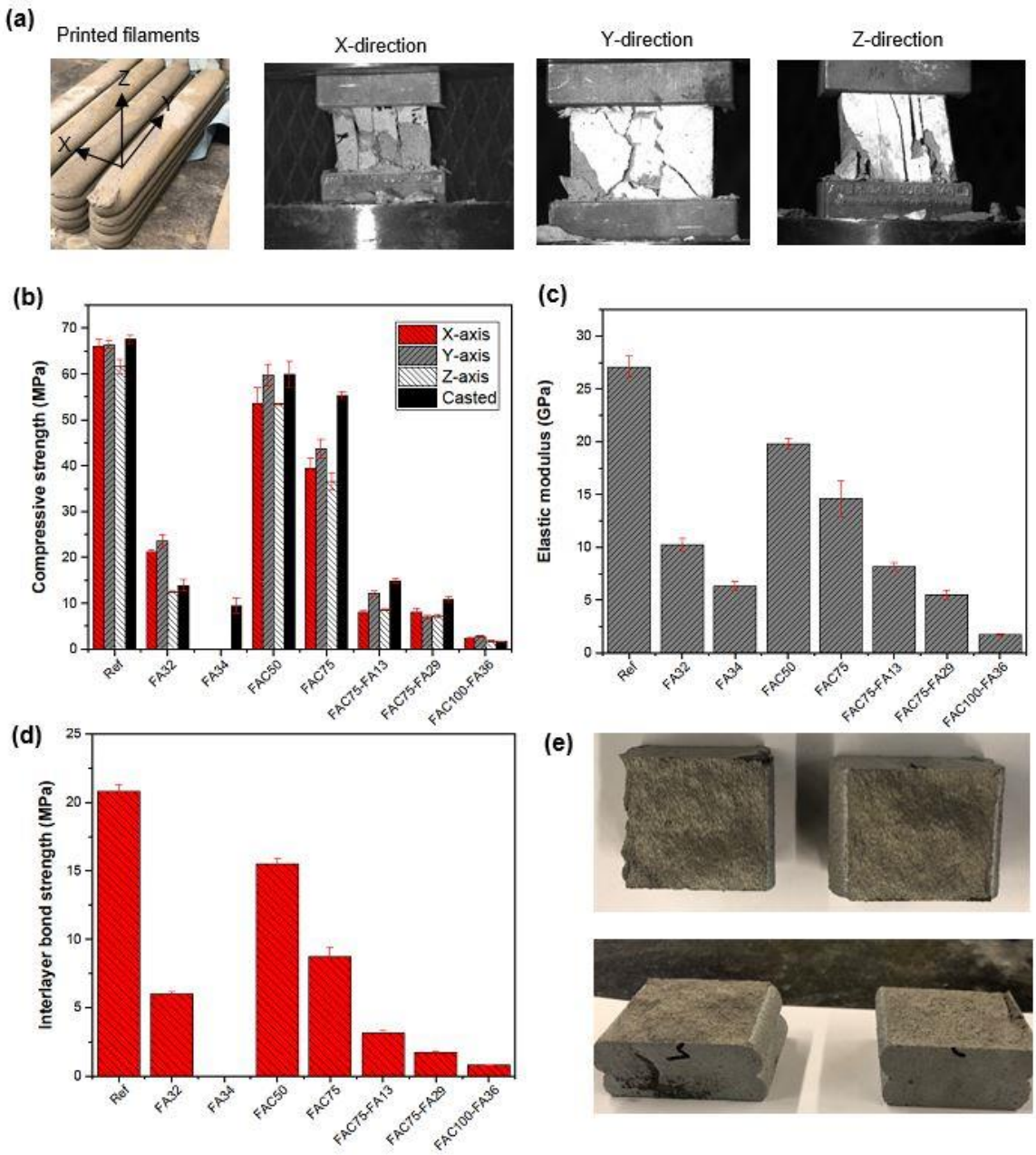

Figure 5.10 Compression, elastic modulus, and direct shear test results: (a) printed filaments and cut cubic samples for compression tests and their failure modes; (b) compression test results; (c) elastic modulus test results; (d) direct shear test results; and (e)

Table 5.3 Density and mechanical properties of the mixtures

Mix ID	FAC replacement	Density (casted)	Elastic modulus (cast)	Compressive strength (cast)	Compressive strength (x-axis)	Compressive strength (y-axis)	Compressive strength (z-axis)	Direct shear strength
	(%)	(kg/m^3)	(GPa)	(MPa)	(MPa)	(MPa)	(MPa)	(MPa)
Ref	0	2220 ± 9	27.06 ± 1.00	67.61 ± 0.82	66.03 ± 1.59	66.40 ± 0.91	61.60 ± 1.55	20.79 ± 0.51
FA32	0	1310 ± 12	10.23 ± 0.68	23.91 ± 1.31	21.23 ± 0.47	23.50 ± 1.46	12.54 ± 0.17	6.01 ± 0.14
FA34	0	1040 ± 14	6.32 ± 0.46	9.48 ± 1.65	NP	NP	NP	NP
FAC50	50%	1840 ± 10	19.80 ± 0.54	59.95 ± 2.81	53.65 ± 3.44	59.75 ± 2.47	53.46 ± 0.21	15.49 ± 0.41
FAC75	75%	1680 ± 9	14.58 ± 1.77	55.36 ± 0.77	39.48 ± 2.14	43.69 ± 2.08	36.57 ± 1.87	8.75 ± 0.68
FAC75-FA13	75%	1160 ± 10	8.19 ± 0.37	14.88 ± 0.44	8.30 ± 0.30	12.11 ± 0.53	8.19 ± 0.18	3.14 ± 0.17
FAC75-FA29	75%	840 ± 12	5.50 ± 0.45	10.80 ± 0.59	8.07 ± 0.80	8.30 ± 0.44	7.23 ± 0.36	1.74 ± 0.09
FAC100-FA36	100%	470 ± 10	1.70 ± 0.07	1.72 ± 0.08	2.33 ± 0.20	2.79 ± 0.14	1.76 ± 0.15	0.79 ± 0.02

5.4.5 Thermal properties

The transient plane source (TPS) method was used to characterize the thermal properties of the mixtures. First, the casted cylinders were cut into three parts along the height, which was polished to ensure the surfaces were flat and smooth. Then, the samples were set in an oven with 43^{o}C for 12 hours to eliminate moisture content and were kept at room temperature for 10 hours before testing. During TPS test, a Kapton supported by double-spiraled nickel metal sensors was placed between two samples to serve as both the main heat source and heat measurement device, as shown in Figure 5.11 (a) and (b). In the test, the initial electrical resistance of the TPS element was balanced in a Wheatstone bridge, and subsequently, the unbalanced voltage drop, $\Delta V(t)$, was captured as the function of time using a high-impedance digital voltmeter. As a result, an iteration was carried out to measure the thermal conductivity (k) and thermal diffusivity (κ).

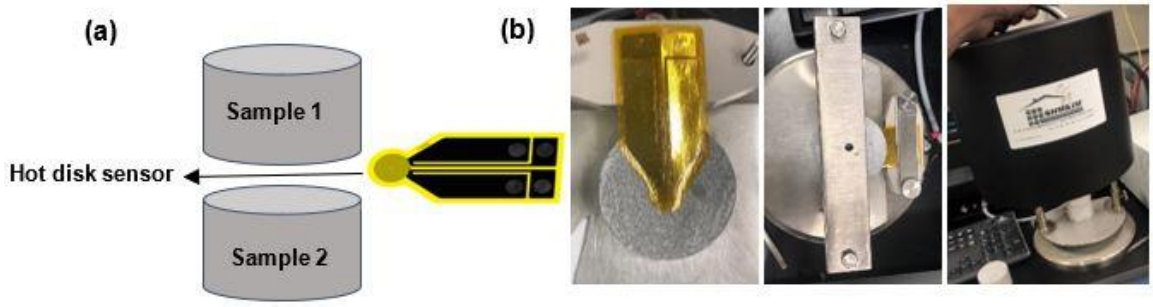

Figure 5.11 TPS test: (a) sensor and sample locations; and (b) setup

Table 5.4 presents the results of the TPS method used to evaluate the thermal properties of the 3D printable mixtures, including thermal conductivity, thermal diffusivity, and specific heat. The thermal conductivity and specific heat also plotted in Figure 5.12 for comparison purposes. It is observed that the replacement of sand with FAC and the introduction of the foaming agent significantly impacted the thermal properties of the mixtures. In particular, the FAC100-FA36 sample exhibited an 88.8% reduction in thermal conductivity, compared to the Ref sample. The replacement of 75% of sand content with FAC led to a 58.3% reduction in thermal conductivity (FAC75), while introducing the foaming agent without sand replacement resulted in a 49% reduction in thermal conductivity (FA32). Previous research by Marais et al. (2021b) has also shown that the incorporation FAC and foaming agents can reduce the thermal conductivity of concrete.

Notably, the sensitivity of the thermal conductivity to FAC content was relatively higher than in the mechanical tests. However, it is worth mentioning that the density of the mixtures is the most significant factor affecting the mechanical properties, i.e., higher density usually led to higher mechanical measures. This is not necessarily the case when considering the relationship between thermal properties and densities. For example, the density of FA32 and FA34 were lower than FAC75 and FAC75-FA13, but their thermal conductivities were higher. This discrepancy is primarily owing to the higher thermal conductivity of sand compared to FAC.

Table 5.4 Results of thermal properties

Mix ID	Thermal conductivity (Printed)	Thermal diffusivity (Printed)	Specific heat capacity (Printed)
	W/mK	m^2/s	MJ/m^3K
Ref	1.44 ± 0.03	0.87 ± 0.010	1.66 ± 0.060
FA32	0.73 ± 0.02	0.67 ± 0.009	1.09 ± 0.050
FA34	0.54 ± 0.01	0.54 ± 0.007	1.00 ± 0.050
FAC50	0.81 ± 0.02	0.54 ± 0.007	1.50 ± 0.050
FAC75	0.60 ± 0.01	0.46 ± 0.006	1.30 ± 0.007
FAC75-FA13	0.45 ± 0.01	0.46 ± 0.005	1.03 ± 0.040
FAC75-FA29	0.32 ± 0.01	0.40± 0.005	0.91 ± 0.004
FAC100-FA36	0.16 ± 0.01	0.32 ± 0.005	0.50 ± 0.004

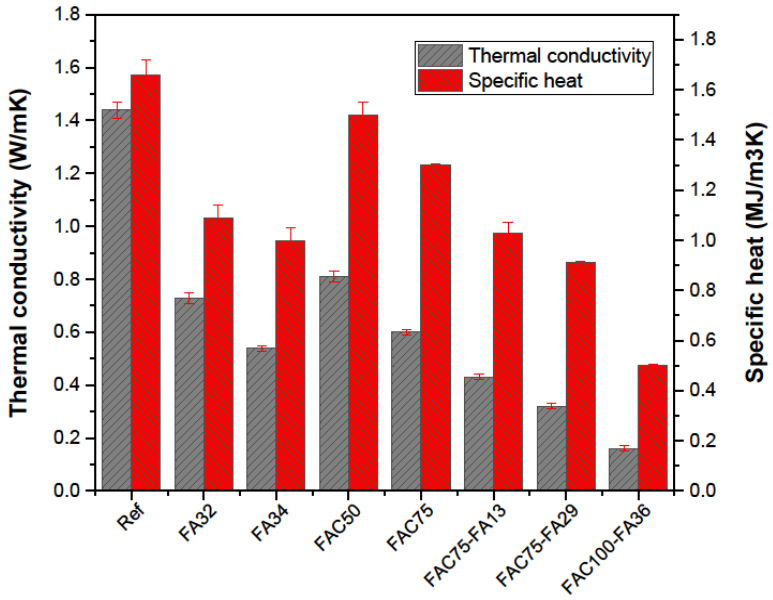

Figure 5.12 Thermal conductivity and specific heat

5.5 Predicting the effective elastic modulus and effective thermal conductivity of FAC-incorporated and cementitious foam composites

Both the effective thermal conductivity (χ_{eff}) and the effective elastic modulus (E_{eff}) of the 3D printable cementitious foam materials can be estimated by a three-step homogenization procedure, as evidenced by the authors' previous works (Brooks et al., 2020; Shen & Zhou, 2020), as shown in Figure 5.13. In the first step, effective medium theory (EMT) was used to estimate the equivalent elastic modulus and thermal conductivity of the hollow FAC particles. The second step used the Mori-Tanaka model (MT) to estimate the effective elastic modulus and effective thermal conductivity of the cementitious composites, which was a mixture of cement, sand, and FAC. As for the cement foam, the two-layer embedded model (Z. Zhou et al., 2022) and the Eucken model (Eucken, 1932) were applied to calculate the effective elastic modulus and effective thermal conductivity in step 3.

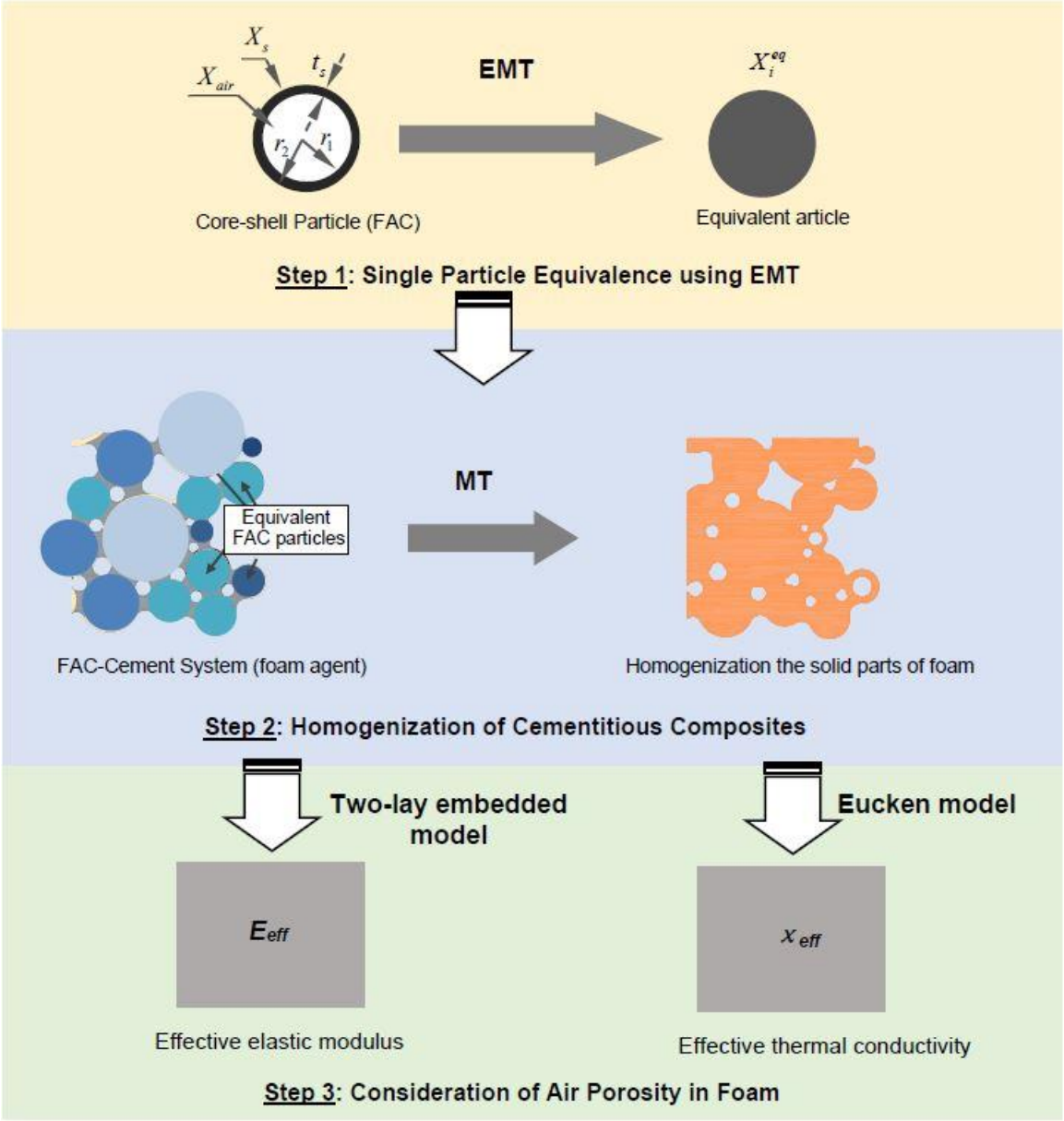

Figure 5.13 A three-step homogenization procedure to obtain the effective elastic modulus and effective thermal conductivity for 3D printable ultralight weight cementitious composites and cementitious foam

5.5.1 Modeling of core-shell inclusions

In the mixture, cenosphere was used to substitute silica sand which can reduce both density and thermal conductivity. Cenosphere has a core-shell configuration with fly ash as the shell material and air as the core material. Cenosphere can be equivalented to a solid particle due to having the same dimension with equivalent elastic and thermal properties, see Step 1 in Figure 5.13. The

equivalent elastic modulus can be estimated through the equivalent bulk modulus and equivalent shear modulus. The equivalent bulk modulus of the inclusion, K_I^{eq}, is (Christensen & Lo, 1979):

$$K_I^{eq} = K_{shell} + \frac{\left(K_{core} - K_{shell}\right)\delta}{1+\left(1-\delta\right)\left[\left(K_{core} - K_{shell}\right) \Big/ \left(K_{shell} + \frac{4}{3}G_{shell}\right)\right]} \tag{5.1}$$

where $\delta = \left(r_1/r_2\right)^3$ is the volumetric ratio of the core in a core-shell particle, where r_1 is the inner radius and r_2 is the outer radius; K_{shell}, G_{shell}, and K_{core}, G_{core} are the bulk and shear moduli of the shell and core materials, respectively.

The equivalent shear modulus of a core-shell particle, G_I^{eq}, can be obtained by solving:

$$A_1\left(\frac{G_I^{eq}}{G_{shell}}\right)^2 + A_2\left(\frac{G_I^{eq}}{G_{shell}}\right) + A_3 = 0 \tag{5.2}$$

where coefficients A_1, A_2, and A_3 are the functions of the core/shell material elastic properties and the volumetric ratio of the core is δ. The formulations of A_1, A_2, and A_3 can be found in (Shen & Zhou, 2020).

The equivalent thermal conductivity of a core-shell particle is (Jia et al., 2018):

$$\chi_I^{eq} = \frac{2\left(1-\delta\right)\chi_{shell} + \left(1+2\delta\right)\chi_{core}}{\left(2+\delta\right)\chi_{shell} + \left(1-\delta\right)\chi_{core}}\chi_{shell} \tag{5.3}$$

where χ_{core} and χ_{shell} are the thermal conductivities of the core and shell, respectively.

5.5.2 Homogenization of cementitious composites

The second step (Step 2 in Figure 5.13) estimated the homogenized properties, i.e., effective elastic properties and thermal conductivity, of the cementitious composites by using the Mori-Tanaka model (Klusemann & Svendsen, 2010). The cementitious composites were considered as the mixture of cement paste, aggregates, and functional inclusions. Cement paste was used as the matrix and particles such as cenosphere and sand were used as functional inclusions. The elastic properties of the effective elastic tensor, $\mathbf{C}_{cc}$, of a cementitious composite system containing n classes inclusions (the i^{th}) may be estimated as:

$$\mathbf{C}_{cc} = \mathbf{C}_m + \sum_{i=1}^{n}\phi_i\left(\mathbf{C}_{I,i} - \mathbf{C}_m\right)\mathbf{\Gamma}^{\mathrm{C}}_{(\mathrm{MT}),i} \tag{5.4}$$

where $\mathbf{C}_m$ is the elastic tensors of the matrix; ϕ_i and $\mathbf{C}_{I,i}$ are the volume fraction and the elastic tensor

of the i^{th} class inclusion. $\mathbf{\Gamma}^{C}_{(MT),i}$ is the Mori-Tanaka strain concentration tensor of the i^{th} inclusion:

$$\mathbf{\Gamma}^{C}_{(MT),i} = \left[\phi_i \mathbf{I} + \phi_m \left(\mathbf{\Gamma}^{C}_{dil,i} \right)^{-1} + \sum_{j=1}^{N} \phi_j \mathbf{\Gamma}^{C}_{dil,j} \left(\mathbf{\Gamma}^{C}_{dil,i} \right)^{-1} \right]^{-1}, \quad j \neq i \tag{5.5}$$

where ϕ_m is the volume fraction of the matrix, and $\mathbf{I}$ is the fourth order identity tensor. $\mathbf{\Gamma}^{C}_{dil,i} = \left[\mathbf{I} + \mathbf{S}^{C}_{m} \mathbf{C}_m^{-1} \left(\mathbf{C}_{I,i} - \mathbf{C}_m \right) \right]^{-1}$ is the strain concentration tensor of the i^{th} inclusion under dilute scheme (Klusemann & Svendsen, 2010), where $\mathbf{S}^{C}_{m}$ is the Eshelby's tensor and can be found in (Eshelby, 1957). Similarly, the effective thermal conductivity tensor of cementitious composites, χ_{cc}, can be estimated by:

$$\boldsymbol{\chi}_{cc} = \boldsymbol{\chi}_m + \sum_{i=1}^{N} \phi_i \left(\boldsymbol{\chi}_{I,i} - \boldsymbol{\chi}_m \right) \mathbf{\Gamma}^{\chi}_{(MT),i} \tag{5.6}$$

where $\chi_{I,i}$, χ_m are the thermal conductivity tensors of the i^{th} class inclusion and matrix, respectively, and $\mathbf{\Gamma}^{\chi}_{(MT),i}$ is the temperature gradient concentration tensor (Stránský et al., 2011).

5.5.3 Homogenization for cementitious foam

In the third step, the effective elastic modulus and effective thermal conductivity of the cementitious foam were estimated by the two-layer embedded model and the Eucken model, respectively, as shown in the Step 3 in Figure 5.13. The two-layer embedded model has been recently proposed by Zhou et al. (2022) and has the form of:

$$E_{foam} = \frac{E_{cc}\left(1-\phi_{pore}\right)\left(1-\nu_{foam}\right)}{x_1 - \dfrac{4E_{ss}\phi_{pore}}{E_{cc}\left(1-\phi_{pore}\right)\left(1-\nu_{foam}\right) + E_{ss}x_2}} \tag{5.7}$$

where, $x_1 = \phi_{pore}\left(1+\nu_{cc}\right) + \left(1-\nu_{cc}\right)$ and $x_2 = \left(1+\nu_{cc}\right) + \phi_{pore}\left(1-\nu_{cc}\right)$; E_{cc} and ν_{cc} are the elastic modulus and Poisson's ratio of the cementitious composites estimated in the second step; ϕ_{pore} is the volume fraction of the pore not including the air volume in the FAC inner cavity; E_{ss} is the elastic modulus of the spherical shell, which can be estimated by the Washer formula (Walsh, 1965) through $E_{ss} = E_{cc} - \dfrac{2\phi_{pore}(1-\nu_{ss})E_{cc}}{1-2\nu_{ss}+(2-\nu_{ss})\phi_{pore}}$. In addition, the shear modulus of the foam, G_{foam}, can be estimated by Equation 2. The Poisson's ratio of the foam, ν_{foam}, can be expressed as the function of E_{foam} and G_{foam} by the basics of elasticity, i.e., $\nu_{foam} = E_{foam}/2G_{foam} - 1$.

Additionally, the effective thermal conductivity of the cementitious foam can be calculated using the Eucken model (Eucken, 1932):

$$\chi_{foam} = \chi_{cc}\left(\frac{1+2\phi_{pore}\left(1-\chi_{cc}/\chi_{air}\right)/\left(1+2\chi_{cc}/\chi_{a}\right)}{1-\phi_{pore}\left(1-\chi_{cc}/\chi_{air}\right)/\left(1+2\chi_{cc}/\chi_{a}\right)}\right) \tag{5.8}$$

where χ_{air} is the thermal conductivity of air.

5.5.4 Modeling results and discussion

The effective elastic modulus and effective thermal conductivity of the 3D printable cementitious composites and cementitious foam can be estimated by Equations 5.1-5.8. Figure 5.14 compares the predicted effective elastic modulus and predicted effective thermal conductivity as a function of the measured density of the experimental data. Overall, the effective properties predicted by the three-step homogenization procedure matched well with the experimental data. It was observed that both the effective elastic modulus and effective thermal conductivity increased as the density increases, and these patterns almost followed a linear relationship. For the cementitious foam, the increase is lower than the cementitious composites. This is mainly because cementitious foam usually has an open cell structure, see Figure 5.8. Compared with closed cell structure, composites having an open cell structure usually leads to lower elastic modulus and thermal conductivity (Pabst et al., 2018). It should be noted that the elastic modulus of the cement paste for cementitious composites and cementitious foam is different when considering the effects of foam agents, see Table 5.5.

Table 5.5 Elastic and thermal properties of the constituents of cementitious composites and cementitious foam

Material properties	**Cement paste (composite)**	**Cement paste (foam)**	**Sand**	**FAC**	
				Core	Shell
E (GPa)	20	10	72	0	96
ν (-)	0.25	0.25	0.17	0.5	0.25
χ (W/mK)	1	1	4	0.026	1.6

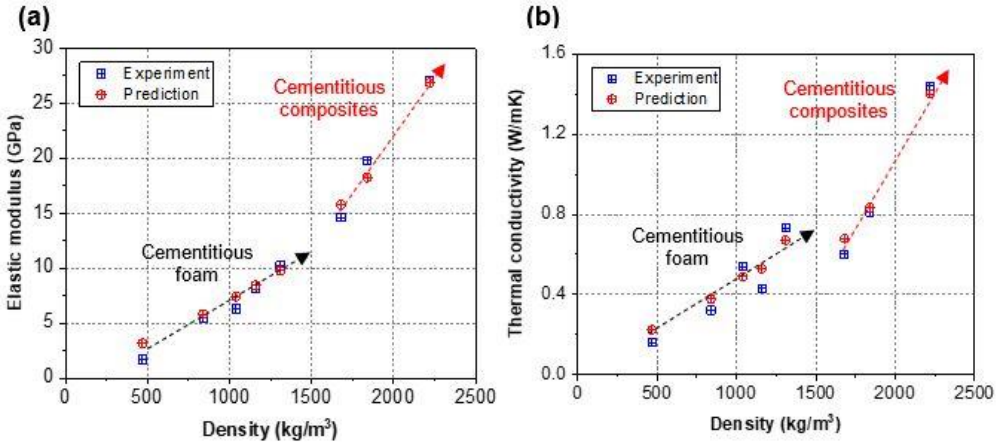

Figure 5.14 Comparison between predicted and experimental effective properties: (a) effective elastic modulus; and (b) effective thermal conductivity

5.6 Conclusions

This chapter aims to study the pathways to formulate lightweight and ultra-lightweight 3D printable cementitious composites by combining the advantages of traditional chemical-induced foaming (foaming approach) and lightweight particulate inclusions (synthetic foam approach) through a hybrid approach. A comprehensive experimental program was conducted to estimate the printability, microstructure, mechanical and thermal properties of 3D printed samples. Totally, eight different mixtures were formulated through varying the replacement percentages of sand with FAC (50%, 75%, and 100%) and introducing the various dosage of a foaming agent. For printability, performance indicators of flowability, extrudability, and buildability were measured; for microstructure, both 3D micro-CT analysis and SEM analysis were conducted; for mechanical properties, compressive strength, direct shear strength, and elastic modulus were measured; for thermal properties, thermal conductivity, thermal diffusivity, and specific heat capacity were tested. Additionally, a three-stage homogenization method was proposed to estimate the effective elastic modulus and effective thermal conductivity for 3D printable ultra-lightweight cement-based composites and cement foam. Based on the presented results, the following conclusions can be drawn.

- The concentration of foaming agent and FAC content highly impacted the printability of the mixtures prepared by traditional foaming and synthetic foam approaches. For the foaming approach, increase foam content will reduce the buildability because it introduces excessive air voids make the sample can hardly support its self-weight. For the synthetic foam approach, increase the replacement percentage of sand with FAC to a certain amount

could reduce the flowability and extrudability because its high water absorption which dries the mixtures after a certain amount of time (e.g., 30 min).

- The mixture prepared by the hybrid approach combines the advantages of foaming and synthetic foam approaches which has good flowability and buildability thanks to the lubricating effect of foaming and support skeleton formed by FAC. This has been confirmed by examining the microstructures of samples prepared by different approaches. In addition, the hybrid approach can produce mixtures with unprecedent low density. The lowest density achieved in this study was 470 kg/m^3, indicating a 78% density reduction compared to the Ref sample.
- The mechanical properties, including compressive strength, direct shear strength, and elastic modulus, of the 3D printed samples were lower than their casted counterparts due to their weak interlayer bonds. In addition, the mechanical properties reduce as the increase of foam agent dosage and FAC replacement percentage. The usage of excessive foam agent may lead to unbuildable due to loss of compressive strength. On the other hand, the replacement of sand with FAC will not significantly reduce its mechanical performance. For the cast samples, the results showed that FAC50 and FAC75 have a compressive strength of 59.85 and 55.36 MPa respectively, indicating only a 11.3% and 18.1% reduction compared with the Ref (67.61 MPa). For the 3D printed sample, the compressive strength reduced to 59.75 and 43.69 MPa for FAC50 and FAC75 along Y direction. For the mixture prepared by the hybrid approach, the compressive strength has been significantly reduced but still able to be used as nonstructural purpose such as concrete foam insulation. For example, FAC100-FA36 has the compressive strength of 2.33, 2.79, and 1.76 MPa along the X, Y, and Z directions respectively.
- The mixtures produced by the hybrid approach are good candidate for building or industry insulation applications especially constructions may prone to fire hazard. The results show that FAC100-FA36 achieves the lowest thermal conductivity 0.16 W/mK with a relatively low thermal diffusivity 0.32 m^2/s.
- The effective elastic modulus and effective thermal conductivity of both 3D printable ultra-lightweight cement-based and cement foam composites were successfully predicted by a three-step homogenization procedure. The results indicate that the developed model could capture the effect of incorporating FAC and the foaming agent very well.

Chapter 6 Conclusions and Recommendations

6.1 Summary and conclusions

This dissertation proposed innovative numerical and experimental concrete mix design approaches to optimise the energy efficiency of concrete in buildings. The main focus was given to improving the energy efficiency of concrete throughout its service life by adopting a range of sustainable practices within concrete mix designs, including incorporating SCMs, RCAs, and foaming agents. Meanwhile, the environmental and mechanical performance of concrete mixes, along with cost efficiency were considered as key requirements in the optimisation process. This was motivated by the synergetic effects that minimising embodied and operating phase-related implications of concrete may have on its mechanical properties, as well as the importance of achieving a balanced combination of thermal, environmental, mechanical and economical indices during the concrete mix design process. The efficiency and accuracy of the developed approaches were examined through a range of numerical and experimental methods. The main findings of this dissertation are summarised as follows:

- A systematic review of the literature on the energy efficiency of concrete choices in buildings over the past two decades, as presented in Chapter 2, shed light on the growing research trends focusing on the thermal properties of concrete. However, the effect of mix design choices on the environmental implications of concrete during its embodied phase has received more research attention compared to the operating energy efficiency of concrete. A set of sustainable strategies, including the incorporation of SCMs, RCAs, foaming agents, and PCMs, were identified to improve the energy performance of concrete throughout its embodied and operating phases. The correlation between the novel additive manufacturing technology and sustainable developments was shown by exploring the evolution of knowledge on energy-efficient concrete in the construction sector.
- In Chapter 3, ambient temperature was found to be most influential while gauging the impacts of environmental and design-related parameters on the operating energy performance of buildings, followed by building geometry and the thermal properties of windows and concrete. The thermal mass and mass distribution of concrete, along with window to wall ratio, were shown to be critical design parameters. It was also concluded that a 10% improvement in the thermal properties of concrete used in exterior walls and

roofs could reduce the operating energy by 6% in commercial buildings. Moreover, the time-consuming and costly processes of computational energy simulations can be mitigated by the operating energy predictive model developed. The proposed model enables studying the magnitude of the impact of influential factors, including concrete mix choices on the overall operating energy consumption in buildings under different climatic conditions. The streamlined model proposed can facilitate the energy estimation of buildings in the design process using readily available data, thereby contributing to more efficient design choices.

- Given the overlapping effects of SCMs and RCAs on the thermal and mechanical properties of concrete, the problem of the reduced mechanical strength associated with replacing cement and NA contents with SCMs and RCA was addressed by proposing a data-driven RAC mix optimisation framework in Chapter 4. It was shown that gradient boosting algorithms can yield the highest accuracy in predicting the compressive strength of RAC mixes containing SCMs (FA and SF). Additionally, the sensitivity analysis of the proposed predictive model highlighted the significant impact of superplasticiser and curing age on the mechanical performance of RAC, followed by cement and water contents. The optimisation framework was shown to provide a reliable alternative to the time-consuming, expensive, and laborious process of lab-based optimisation, which is currently adopted. Additionally, the AI-based multi-objective optimisation framework addresses the lack of a systematic method to formulate green concrete mixes containing recycled concrete aggregates and solves the common multi-objective mix design problems. It was concluded that the operating and embodied-related objectives of RAC, including thermal conductivity, global warming potential as well as the cost of production, can potentially improve by about 11%, 29%, and 24%, respectively, without compromising the mechanical performance of RAC mixes using the proposed framework.

- The thermal properties of concrete mixes were further improved by fully replacing NA (sand) with an LWA (fly ash cenosphere) and incorporating various concentrations of a foaming agent, resulting in LWC and ULWC concrete mix designs. The mix designs proposed in Chapter 5, were found to be appealing to the novel technology of concrete 3D printing. This was owing to the reduced density of printed elements using the formulated LWC and ULWC mixes. It was highlighted that the load-bearing properties of the mixes were improved by reducing their density to as low as 470 kg/m^3 using LWA and a foaming

agent. It was also shown that the thermal conductivity and specific heat of 3DP foam concrete could be enhanced by as much as 89% and 70%, respectively. It was found that increasing the recycled content and the amount of foaming agents can lead to an increase in porosity, which could play a key role in improving the insulation capacity and mitigating the negative environmental impacts of concrete production. This enhancement, however, is achieved at the expense of decreased mechanical performance. It was concluded that the thermal performance of 3D printable mixes is primarily determined by the thermal conductivity of their constituents, rather than their density. It was also concluded that the environmental footprints associated with waste landfills and natural resource depletion can be alleviated using foaming agents as they allow a replacement of natural aggregates with recycled contents beyond the ratios commonly reported in the literature. A three-step homogenization procedure was also developed to predict the impact of incorporating FAC and the foaming agent into 3D printable cementitious composites. The formulated ultra-lightweight and lightweight 3D printable cementitious composites offer thermal performance improvements to the built environment. The proposed approach can contribute to sustainable construction by reducing the need for natural aggregates while enhancing thermal efficiency and design versatility, thereby fostering more sustainable building elements.

- The results presented in this thesis demonstrated that the proposed data-driven optimisation framework can effectively decrease the density of concrete without compromising its mechanical performance and cost efficiency. Moreover, the formulated lightweight and ultra-lightweight concrete mixes can considerably improve the thermal properties and environmental consequences attributed to concrete 3D printing. Therefore, adopting the proposed mix optimisation methods can be used in practice to format concrete mixes that meet thermal, environmental, economic and mechanical criteria, as well as the project-specific performance requirements required by specifications.

The findings of the study have practical applications, emphasizing the energy implications of material choices. For instance, the energy use of office buildings can be estimated in the very early stages of projects using the predictive model developed and the impact of material choices on energy use can be evaluated depending on the climatic condition. Moreover, optimal green concrete mixes containing RCA and SCMs can be proposed as per the mechanical performance requirements. Also, the formulated 3DP cementitious composites can

be employed for acoustic and insulation purposes where high mechanical performance is not required.

6.2 Recommendations and future developments

Despite the effects of the proposed approaches in reducing the energy consumption and carbon emissions of concrete throughout its operating and embodied phases, contributing to the sustainability of buildings, a few areas can be further explored in future studies. The limitations of the present study and recommended future research to address these gaps are highlighted in the following:

- Although this dissertation targeted several design-related indices to develop an operating energy predictive model, the effect of occupant behaviour was not considered. User behaviour significantly impacts the energy consumption associated with the use of appliances, lighting, and HVAC. Thus, further developments in operating energy minimisation could include anomaly detection based on occupancy modelling.

- The impact of aging on the thermal performance of building elements has not been considered in this study and can be a topic of future research . Variations in the behaviour of building elements during their service life would need to be considered in addition to the potential effects of changes in the environmental parameters. For example, there is a lack of knowledge on the effects of climate change on building energy performance. It is anticipated that by capturing the effect of variations in both environmental and design-related factors, more effective energy-related decisions can be taken.

- The effects of detailed information on mixing, material quality and type, and curing period have not been included in this study and can be considered in future investigations. The accuracy of data-driven mix optimisation frameworks could be further enhanced if more information regarding curing conditions, material gradation, and mixing procedures were made available. In addition, leveraging the systematic mix optimisation approaches to develop simple and reliable User Interfaces (UI) could enable engineers and building designers to easily evaluate the mechanical, environmental and economic consequences of their decisions in the design phases of projects.

- The applicability of the green concrete optimisation framework can be further improved by considering the impact of advanced sustainable solutions, such as PCMs. Therefore, enhanced optimisation models can contribute to designing PCM-incorporated mixtures to improve the energy efficiency of concrete choices across several aspects, including embodied, operation, and thermal energy storage capacity.

- Balancing conflicting printing properties, particularly pumpability and buildability, in the design of concrete mixes has not been considered in this research. However, addressing this aspect can accelerate the formulation of energy-efficient 3D printable mixtures. For instance, incorporating lightweight fillers and insulative materials such as recycled contents and foaming agents can improve the rheological and pumpability properties of mixes while posing challenges to their buildability. Therefore, integrating the mixing parameters to align with the appropriate printing parameters holds the potential for fostering more sustainable productions.

- Although low-density 3D printed cementitious composites have the potential to serve as effective insulation materials in buildings, this particular aspect was not targeted in this research. The improved thermal properties of low-density 3D printed elements could improve the overall energy performance of buildings. Therefore, further research on this topic and its integration into building codes and construction practices could be deemed as valuable future developments.

Appendices

Appendix A

A1 Window U-value (U_{window})

The following figure presents the sensitivity analysis conducted using the predictive model to analyse the impact of U_{window} variation as the third influencing factor on the EUI of the reference building. The results indicate the variations of U_{window} mostly impact the energy demand in CL10-CC and CL09-WC with as much as 5.1% and 4.3% for a 10% variation of U_{window}, respectively. In contrast, the lowest dependency on operating energy consumption for a 10% variation of U_{window} belongs to CL06-ME with as much as 2.2%. Given that windows are critical sources of heat transmission, the predictive model shows the high impact of the thermal properties of windows on the EUI (Tan et al., 2020).

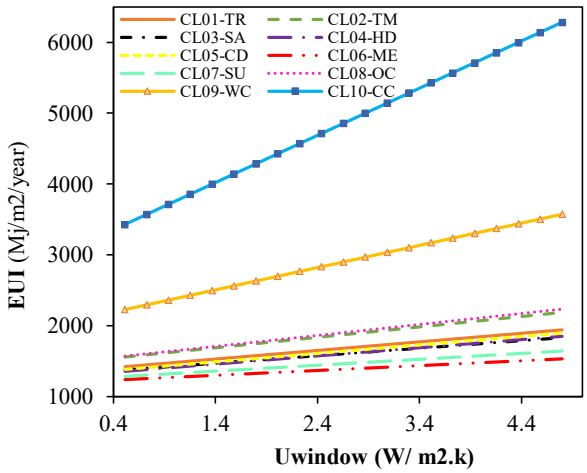

Sensitivity analysis for U_{window}

A2 Infiltration rate (IN)

The results of the sensitivity analysis indicate a 10% variation in IN impacts the EUI in CL10-CC and CL09-WC with as much as 4.7% and 4.3%, respectively. Also, the minor dependency of CL06-ME on the variation of IN is observed by a 2.2% increase for a 10% increment of this factor. Given that IN allows the outdoor air, with different T and RH, to be mixed with the indoor space environment, this factor can highly impact the EUI (G. Han et al., 2015). The findings show that this parameter is highly impacted by environmental parameters such as T, WS, and RH (Y. Ji et al., 2020).

A3 Relative humidity (RH)

Based on the findings of this study, RH is the second influential environmental parameter. The results indicate that CL10-CC and CL09-WC are the most sensitive climates to the variation in RH. The results indicate that EUI fluctuates by 3.6% and 3.2% for a 10% variation in RH in the mentioned climates. Further observations show that the average change in EUI is 2.3% for a 10% increment in RH in all the climates. As the following figure shows, an increase in RH increases energy consumption in both hot and cold climates, which matches the findings of the previous studies (Vellei et al., 2017).

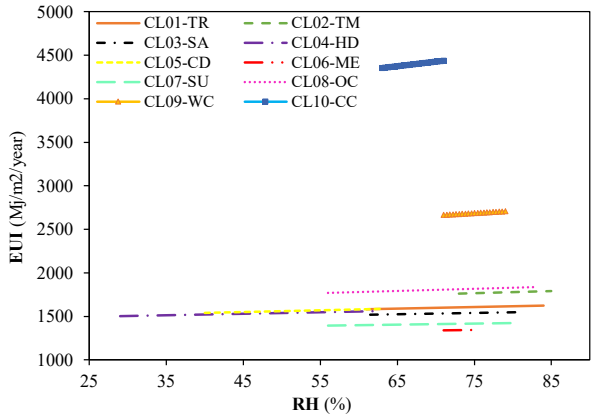

Sensitivity analysis for RH

A4 Operating schedule (OS)

The results indicate that energy demand continuously rises with an increase in OS. The predictive model analysis reveals that CL03-SA and CL04-HD are the most sensitive climates to this factor with as much as 3.4% and 3.35% for 10% variation in OS, respectively. Increasing the operating hours increases the energy demand for cooling, heating, equipment, and lighting. The conclusion that can be drawn from the results is that this increment is more tangible in hot climates as the cooling load is drastically increased with working hour increments (Azar & Menassa, 2012). In contrast, in cold climates, the energy demand for cooling is much less due to the lower ambient temperature, while the heating load is required mostly in mornings, and it is decreased in noon and afternoon as the ambient temperature becomes warmer in the mentioned period. This is also reflected in the following figure, as the growth in the EUI is sharper in hot climates such as CL01-TR, CL02-TM, CL03-SA, and CL04-HD.

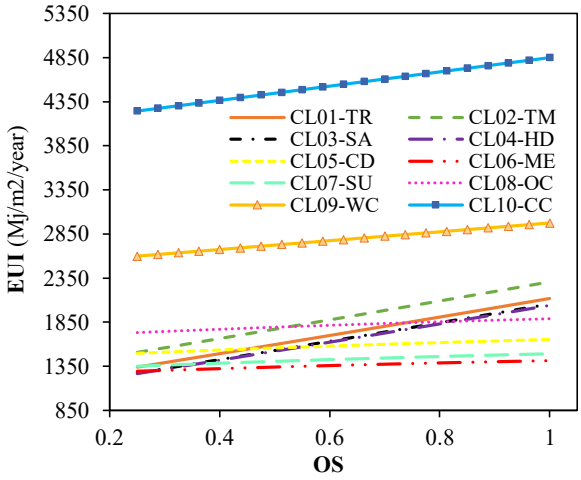

Sensitivity analysis for OS

A5 Wind speed (WS)

The results of the sensitivity analysis show that variation in WS is more tangible in climates with severe climatic conditions. Further, it is observed that the most impacted climate for a 10% variation of WS is CL10-CC with as much as 2.3%, while the least sensitive climates are CL04-HD and CL05-CD with 0.73% variation. Particularly, the results highlight that EUI is increased with an increase in WS in all climate zones. This factor accelerates the outdoor air to enter inside and can increase the energy demand in hot and cold climates (Kalamees et al., 2012). Results indicate that the average impact of WS on operating energy demand is 1.3% for a 10% increase in WS.

A6 Solar Heat Gain Coefficient (SHGC)

The results from the predictive model show that an increase in SHGC impacts the energy demand of the reference building in the cold climates more than in moderate and hot climates. In cold climates such as CL-09-WC and CL10-CC, a slight increment at very low values of SHGC decreases the energy demand as gaining solar heat through windows allows more solar radiation to pass windows and reduces energy consumption by reducing the heating loads. On the other hand, high SHGC increases the EUI by increasing the cooling loads in both hot and climate zones (J. W. Lee et al., 2013).

A7 Solar radiation (SR)

As the following figure shows, an increase in SR decreases the energy demand in moderate and cold climates by decreasing the heating load, while this factor behaves differently in hot climates by increasing the cooling load. This factor impacts the energy performance mostly in CL10-CC and CL06-ME, with as much as 3.1% and 0.03% for a 10% variation in SR. In this study, the impact of SR is found to be less than T and RH, which is in a fair correlation with the findings of previous studies (Neto & Fiorelli, 2008).

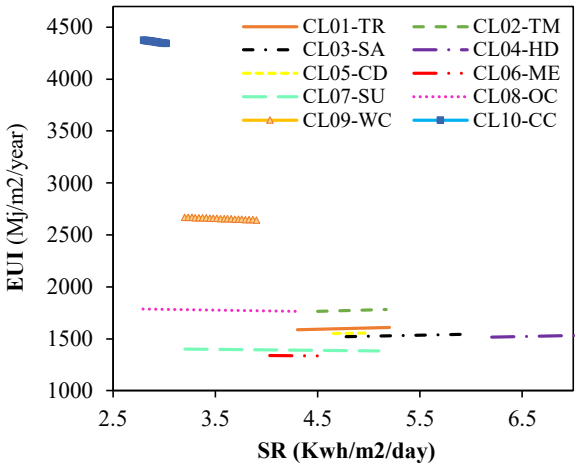

Sensitivity analysis for SR

A8 Building Orientation (BO)

The findings show that BO has the lowest impact on the energy demand of the reference building, among others. This can be attributed to the fact that variations in BO only impact the angle at which exterior walls and windows are exposed to solar radiation (Mottahedi et al., 2015). In particular, the results indicate that the EUI increases by 0.44% on average for a 10% increase in BO.

Appendix B

B1 Multiple linear regression (MLR)

This model is the improved version of simple linear regression. This approach is known as the most common linear regression method (Khademi et al., 2016; Neter et al., 1996; H. Liang & Song, 2009). The general form of the MLR model is as follows:

$$Y=\beta_0+\beta_1 x_1+\beta_2 x_2+...+\beta_n x_{n+}\varepsilon, \quad (1)$$

where Y is the response factor, β_0, β_1, β_2, ..., and β_n are the regression coefficients, and $x_1, x_2,..., x_n$ are independent input variables. Linear regression is usually fitted using the least squares approach, minimising the lack of fit and penalised version of the least squares loss function. This algorithm seeks a relationship in terms of a straight line that has the best estimation of all individual data points, including both target and output variables (Khademi et al., n.d.).

B2 K-nearest neighbour (KNN)

As a non-parametric method, KNN is a predictive algorithm based on an intuitive hypothesis (Altman, 1992; Bronshtein, 2017). In this technique, new samples are categorised based on their k-nearest neighbours. In other words, values that are close in input space are assumed to be close in objective space, as well (Myatt, 2007). The KNN algorithms measure the closeness of data using different metrics; however, the Euclidean distance function is the most widely used metric for determining the distance between the training and test dataset (Shakhnarovich et al., 2006).

$$d(x_t,x_i)=\sqrt{\sum_{n=1}^{N}(x_{t,n}-x_{i,n})^2}, \quad (2)$$

where x_i and x_t denote the training and testing sample, respectively. N, $x_{t,n}$, and $x_{i,n}$ represent the feature number, values of the n^{th} features of the testing, and training samples, respectively. The output of x_t is the mean of the outputs of the k-nearest neighbours:

$$f(x_t)=\frac{1}{k}\sum_{i\in N_k(x_i)} f(x_i), \quad (3)$$

where $N_{k(x_t)}$ includes the indices of the k-nearest neighbours of x_t.

B3 M5P model tree

In the M5P model, the traditional decision tree is coupled with a linear regression function to the nodes of leaves. This technique includes 4 main phases of data splitting, generating linear regression, pruning, and smoothing. Throughout the data splitting process, the branches and leaves of the decision tree are formed. Then, linear regression is developed at each node for prediction purposes. Next, the pruning process is implemented to enhance the calculation efficiency and prevent overfitting. Eventually, the smoothing process takes place to offset the potential severe branching discontinuities (Behnood et al., 2015). To develop the regression tree, splitting space using the standard deviation reduction (SDR) factor is performed as follows:

$$SDR=sd(p)-\sum_j \frac{|p_j|}{p} sd(p_j), \quad (4)$$

where P is the set of data points that reach the node, Pj is the data point that results from splitting at node based on the determined splitting parameter, while sd is the standard deviation. The error measurement for data points is performed using the standard deviation. The following equation is used for the smoothing process:

$$p'=\frac{(np+kq)}{(n+k)}, \quad (5)$$

where P' indicates the prediction passed to the upper node, n is the number of training instances, p is the prediction passed from below to the existing node, q is the predicted value by the model at the current node, and k denotes the smoothing constant (Y. Wang & Witten, 1996).

B4 Artificial neural network (ANN)

ANN is known as a nonlinear mathematical approach which determines the correlations between input variables and response factor. ANN consists of neurons and weighted nodes that simulate the human brain structure. Basically, an ANN structure contains three layers of input, hidden, and output, while each layer encompasses at least a node, as shown in the figure below. The input layers receive information from the external world and convey data to hidden layers through connecting neurons. Next, the hidden nodes process the data to determine the relationship among the inputs. During the information processing, step weights, sum function, and activation function are important factors that are undertaken by hidden layers (Topçu et al., 2008). The level of importance of information is determined by its attributed weight. Each neuron combines its current information with receiving data from other neurons and transfers it to the next neuron. This cycle continues

until the fitting process is performed accurately or the error rate and defined iteration number are met. Finally, output layers reveal the predictions (Ben Chaabene et al., 2020).

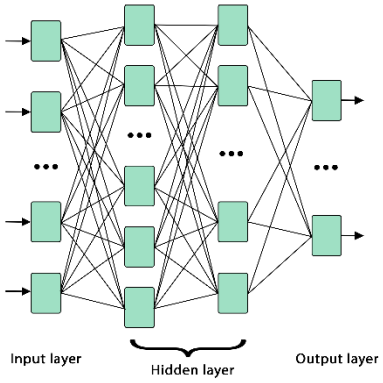

ANN model structure

B5 Random Forest (RF)

The RF method has been widely adopted for predicting the CS of concretes by researchers (Farooq et al., 2020). During the training process, several trees are formed usually by using two-thirds of the dataset. To better randomize data distribution, different dimensions of rows and columns are used (Grömping, 2009). Then, the bagging method is used to integrate all trees to enhance the prediction accuracy. Randomly selected data samples comprise a bootstrap sample and a sample that is not encompassed by the bootstrap, also known as the out of bag sample. The remaining one-third of data from the first phase is used to estimate the out of bag error for all trees. Each tree generates a regression which results in a prediction. Finally, the last prediction is obtained by averaging the predictions of all trees (Han et al., 2019). Among the advantages of this approach are smooth and fast formation of correlation between inputs and response variables, capability to manage large datasets, and diversity of applications. The structure of the RF method is shown in the following figure.

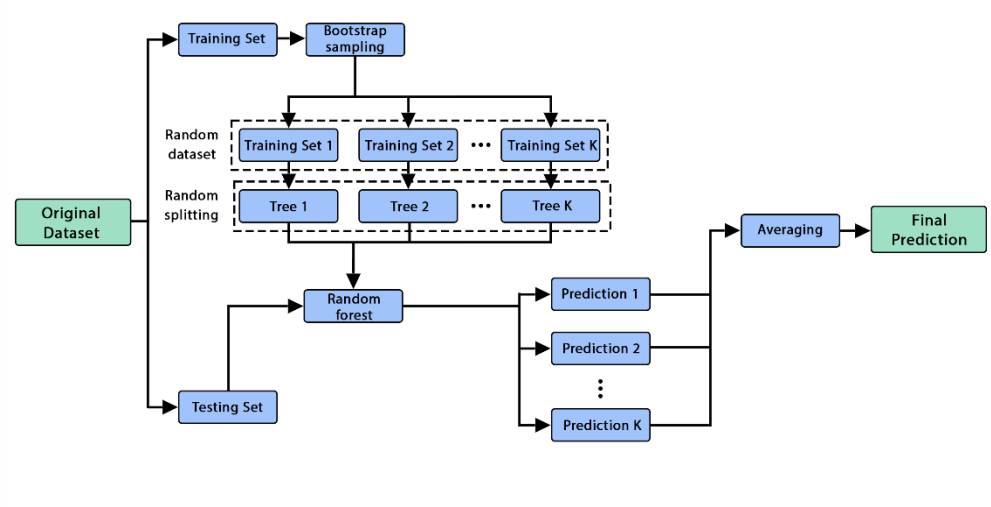

Random forest model structure

B6 Gradient boosting machine (GBM)

GBM is known as an efficient machine learning algorithm that is widely employed in engineering problems (Qi & Tang, 2018). In gradient boosting machine algorithms, new base models are continuously fitted to the dataset to improve the accuracy of predictions. The mission of the new base model is to reduce the loss function by considering its negative gradient in each cycle. Similar to other boosting approaches, GBM forms in a stage-wise fashion and reforms by the optimisation of the loss function (Natekin & Knoll, 2013). GBM adds the basis function in a way that lowers the error function. The following figure shows the GBM algorithm structure based on the regression tree.

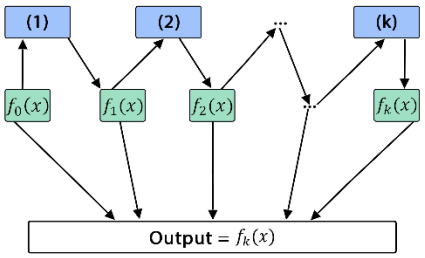

GBM model structure

B7 Extreme gradient boosting (Xgboost)

As a cutting-edge boosting approach, Xgboost is an ensemble machine learning algorithm. In Xgboost, model variants are alleviated through normalising the loss function. As a result, the model

is simplified, and overfitting is minimised (Xia et al., 2017). Xgboost utilises various additive functions to predict results as follows:

$$\bar{y_i}=y_i^0+\eta\sum_{k=1}^{M} f_k(x_i), \quad (6)$$

where $\bar{y_i}$ and y_i^0 are the predicted result and initial guess which are obtained from mean measured values in training set, respectively. η is shrinkage factor which smooths the model, while adding new trees and preventing overfitting. M is the number of estimators, and f_k indicates an independent tree structure. X_i denotes input vector. Xgboost evaluates the "goodness" of the model by using a regularisation function, as the equation below shows:

$$\Omega(f)=\gamma T+\frac{1}{2}\lambda||\omega||^2, \quad (7)$$

where Ω_f,γ, λ, and ω denote regularisation term, minimum required loss to partition leaf node, regularisation parameter, and the score vector of leaves, respectively (J. Fan et al., 2018; T. Chen & Guestrin, 2016).

Bibliography

Abbasi, S., & Noorzai, E. (2021). The BIM-Based multi-optimization approach in order to determine the trade-off between embodied and operation energy focused on renewable energy use. *Journal of Cleaner Production*, *281*, 125359. https://doi.org/10.1016/j.jclepro.2020.125359

Abd Elhakam, A., Mohamed, A. E., & Awad, E. (2012). Influence of self-healing, mixing method and adding silica fume on mechanical properties of recycled aggregates concrete. *Construction and Building Materials*, *35*, 421–427. https://doi.org/10.1016/j.conbuildmat.2012.04.013

Abden, J., Tao, Z., Alim, M. A., Pan, Z., George, L., & Wuhrer, R. (2022). Combined use of phase change material and thermal insulation to improve energy efficiency of residential buildings. *Journal of Energy Storage*, *56*(PA), 105880. https://doi.org/10.1016/j.est.2022.105880

Abreu, V., Evangelista, L., & de Brito, J. (2018). The effect of multi-recycling on the mechanical performance of coarse recycled aggregates concrete. *Construction and Building Materials*, *188*, 480–489. https://doi.org/10.1016/j.conbuildmat.2018.07.178

Abu-Hamdeh, N. H., Melaibari, A. A., Alquthami, T. S., Khoshaim, A., Oztop, H. F., & Karimipour, A. (2021). Efficacy of incorporating PCM into the building envelope on the energy saving and AHU power usage in winter. *Sustainable Energy Technologies and Assessments*, *43*(November 2020), 100969. https://doi.org/10.1016/j.seta.2020.100969

Achkari, O., & El Fadar, A. (2020). Latest developments on TES and CSP technologies – Energy and environmental issues, applications and research trends. *Applied Thermal Engineering*, *167*(December 2019), 114806. https://doi.org/10.1016/j.applthermaleng.2019.114806

Adesanya, D. A., & Raheem, A. A. (2009). Development of corn cob ash blended cement. *Construction and Building Materials*, *23*(1), 347–352. https://doi.org/10.1016/j.conbuildmat.2007.11.013

Adesina, A. (2019). Use of phase change materials in concrete: current challenges. *Renewable Energy and Environmental Sustainability*, *4*, 9.

Adewoyin, O., Adesina, A., & Das, S. (2022). Physico-thermal and microstructural properties of thermal-efficient mortars made with low cement content. *Construction and Building Materials*, *325*(January), 126850. https://doi.org/10.1016/j.conbuildmat.2022.126850

Adhikary, S. K., & Rudzionis, Z. (2020). Influence of expanded glass aggregate size, aerogel and binding materials volume on the properties of lightweight concrete. *Materials Today:*

Proceedings, *32*, 712–718. https://doi.org/10.1016/j.matpr.2020.03.323

Afgan, S., & Bing, C. (2021). Scientometric review of international research trends on thermal energy storage cement based composites via integration of phase change materials from 1993 to 2020. *Construction and Building Materials*, *278*, 122344. https://doi.org/10.1016/j.conbuildmat.2021.122344

Ahmad, M. R., Chen, B., & Farasat Ali Shah, S. (2019). Investigate the influence of expanded clay aggregate and silica fume on the properties of lightweight concrete. *Construction and Building Materials*, *220*, 253–266. https://doi.org/10.1016/j.conbuildmat.2019.05.171

Ahmad, W., Ahmad, A., Ostrowski, K. A., Aslam, F., & Joyklad, P. (2021). A scientometric review of waste material utilization in concrete for sustainable construction. *Case Studies in Construction Materials*, *15*(July), e00683. https://doi.org/10.1016/j.cscm.2021.e00683

Ahmad, W., Ahmad, A., Ostrowski, K. A., Aslam, F., Joyklad, P., & Zajdel, P. (2021). Sustainable approach of using sugarcane bagasse ash in cement-based composites: A systematic review. *Case Studies in Construction Materials*, *15*(August), e00698. https://doi.org/10.1016/j.cscm.2021.e00698

Ahmed, H. U., Faraj, R. H., Hilal, N., Mohammed, A. A., & Sherwani, A. F. H. (2021). Use of recycled fibers in concrete composites: A systematic comprehensive review. *Composites Part B: Engineering*, *215*(November 2020), 108769. https://doi.org/10.1016/j.compositesb.2021.108769

Airaksinen, M., & Matilainen, P. (2011). A Carbon footprint of an office building. *Energies*, *4*(8), 1197–1210. https://doi.org/10.3390/en4081197

Ajayi, S. O., Oyedele, L. O., & Ilori, O. M. (2019). Changing significance of embodied energy: A comparative study of material specifications and building energy sources. *Journal of Building Engineering*, *23*(May 2018), 324–333. https://doi.org/10.1016/j.jobe.2019.02.008

Ajdukiewicz, A. B., & Kliszczewicz, A. T. (2007). Comparative Tests of Beams and Columns Made of Recycled Aggregate Concrete and Natural Aggregate Concrete. *Journal of Advanced Concrete Technology*, *5*(2), 259–273. https://doi.org/10.3151/jact.5.259

Ajdukiewicz, A., & Kliszczewicz, A. (2002). Influence of recycled aggregates on mechanical properties of HS/HPC. *Cement and Concrete Composites*, *24*(2), 269–279. https://doi.org/10.1016/S0958-9465(01)00012-9

Ajmani, H. Al, Suleiman, F., Abuzayed, I., & Tamimi, A. (2019). Evaluation of concrete strength made with recycled aggregate. *Buildings*, *9*(3), 1–14. https://doi.org/10.3390/buildings9030056

Akande, O. K., Fabiyi, O., & Mark, I. C. (2015). Sustainable Approach to Developing Energy Efficient Buildings for Resilient Future of the Built Environment in Nigeria. *American Journal of Civil Engineering and Architecture*, *3*(4), 144–152. https://doi.org/10.12691/ajcea-3-4-5

Akbarnezhad, A., & Xiao, J. (2017). Estimation and minimization of embodied carbon of buildings: A review. *Buildings*, *7*(1), 5.

Akeiber, H., Nejat, P., Majid, M. Z. A., Wahid, M. A., Jomehzadeh, F., Zeynali Famileh, I., Calautit, J. K., Hughes, B. R., & Zaki, S. A. (2016). A review on phase change material (PCM) for sustainable passive cooling in building envelopes. *Renewable and Sustainable Energy Reviews*, *60*, 1470–1497. https://doi.org/10.1016/j.rser.2016.03.036

Al-Qutaifi, S., Nazari, A., & Bagheri, A. (2018). Mechanical properties of layered geopolymer structures applicable in concrete 3D-printing. *Construction and Building Materials*, *176*, 690–699. https://doi.org/10.1016/j.conbuildmat.2018.04.195

Al Martini, S., Khartabil, A., & Sabouni, R. (2023). Evaluation of Thermal Conductivity of Sustainable Concrete Having Supplementary Cementitious Materials (SCMs) and Recycled Aggregate (RCA) Using Needle Probe Test. *Sustainability (Switzerland)*, *15*(1). https://doi.org/10.3390/su15010109

Alghoul, S. K., Rijabo, H. G., & Mashena, M. E. (2017). Energy consumption in buildings: A correlation for the influence of window to wall ratio and window orientation in Tripoli, Libya. *Journal of Building Engineering*, *11*(April), 82–86. https://doi.org/10.1016/j.jobe.2017.04.003

Ali, M. R., Maslehuddin, M., Shameem, M., & Barry, M. S. (2018). Thermal-resistant lightweight concrete with polyethylene beads as coarse aggregates. *Construction and Building Materials*, *164*, 739–749. https://doi.org/10.1016/j.conbuildmat.2018.01.012

Allouhi, A., El Fouih, Y., Kousksou, T., Jamil, A., Zeraouli, Y., & Mourad, Y. (2015). Energy consumption and efficiency in buildings: current status and future trends. *Journal of Cleaner Production*, *109*, 118–130. https://doi.org/10.1016/j.jclepro.2015.05.139

Alptekin, E., & Ezan, M. A. (2020). Performance investigations on a sensible heat thermal energy storage tank with a solar collector under variable climatic conditions. *Applied Thermal Engineering*, *164*(September 2019), 114423. https://doi.org/10.1016/j.applthermaleng.2019.114423

Altman, N. S. (1992). An introduction to kernel and nearest-neighbor nonparametric regression. *American Statistician*, *46*(3), 175–185. https://doi.org/10.1080/00031305.1992.10475879

Altun, M. G., & Oltulu, M. (2020). Effect of different types of fiber utilization on mechanical properties of recycled aggregate concrete containing silica fume. *Journal of Green Building*, *15*(1), 119–136. https://doi.org/10.3992/1943-4618.15.1.119

Amran, Y. H. M., Farzadnia, N., & Ali, A. A. A. (2015). Properties and applications of foamed concrete; A review. *Construction and Building Materials*, *101*, 990–1005. https://doi.org/10.1016/j.conbuildmat.2015.10.112

Anand, C. K., & Amor, B. (2017). Recent developments, future challenges and new research directions in LCA of buildings: A critical review. *Renewable and Sustainable Energy Reviews*, *67*, 408–416. https://doi.org/10.1016/j.rser.2016.09.058

Andreu, G., & Miren, E. (2014). Experimental analysis of properties of high performance recycled aggregate concrete. *Construction and Building Materials*, *52*, 227–235. https://doi.org/10.1016/j.conbuildmat.2013.11.054

Aprianti, E., Shafigh, P., Bahri, S., & Farahani, J. N. (2015a). Supplementary cementitious materials origin from agricultural wastes - A review. *Construction and Building Materials*, *74*, 176–187. https://doi.org/10.1016/j.conbuildmat.2014.10.010

Aprianti, E., Shafigh, P., Bahri, S., & Farahani, J. N. (2015b). Supplementary cementitious materials origin from agricultural wastes - A review. *Construction and Building Materials*, *74*, 176–187. https://doi.org/10.1016/j.conbuildmat.2014.10.010

Araújo, R. A., Martinelli, A. E., Cabral, K. C., F. O. A. Dantas, A., F. D. Silva, I., A. C. Xavier, A., & Santos, A. L. (2022). Thermal performance of cement-leca composites for 3D printing. *Construction and Building Materials*, *349*(July 2021). https://doi.org/10.1016/j.conbuildmat.2022.128771

Arce, P., Medrano, M., Gil, A., Oró, E., & Cabeza, L. F. (2011). Overview of thermal energy storage (TES) potential energy savings and climate change mitigation in Spain and Europe. *Applied Energy*, *88*(8), 2764–2774. https://doi.org/10.1016/j.apenergy.2011.01.067

Asadi, I., Baghban, M. H., Hashemi, M., Izadyar, N., & Sajadi, B. (2022). Phase change materials incorporated into geopolymer concrete for enhancing energy efficiency and sustainability of buildings: A review. *Case Studies in Construction Materials*, *17*(March), e01162. https://doi.org/10.1016/j.cscm.2022.e01162

Asadi, I., Shafigh, P., Abu Hassan, Z. F. Bin, & Mahyuddin, N. B. (2018a). Thermal conductivity of concrete – A review. *Journal of Building Engineering*, *20*(April), 81–93. https://doi.org/10.1016/j.jobe.2018.07.002

Asadi, I., Shafigh, P., Abu Hassan, Z. F. Bin, & Mahyuddin, N. B. (2018b). Thermal conductivity

of concrete – A review. *Journal of Building Engineering*, *20*(July), 81–93. https://doi.org/10.1016/j.jobe.2018.07.002

Asadi, I., Shafigh, P., Abu Hassan, Z. F. Bin, & Mahyuddin, N. B. (2018c). Thermal conductivity of concrete – A review. *Journal of Building Engineering*, *20*(July), 81–93. https://doi.org/10.1016/j.jobe.2018.07.002

Asadi, I., Shafigh, P., Hashemi, M., Akhiani, A. R., Maghfouri, M., Sajadi, B., Mahyuddin, N., Esfandiari, M., Rezaei Talebi, H., & Metselaar, H. S. C. (2021). Thermophysical properties of sustainable cement mortar containing oil palm boiler clinker (OPBC) as a fine aggregate. *Construction and Building Materials*, *268*, 121091. https://doi.org/10.1016/j.conbuildmat.2020.121091

Asadi Shamsabadi, E., Salehpour, M., Zandifaez, P., & Dias-da-Costa, D. (2023). Data-driven multicollinearity-aware multi-objective optimisation of green concrete mixes. *Journal of Cleaner Production*, *390*(October 2022), 136103. https://doi.org/10.1016/j.jclepro.2023.136103

Ashish, D. K. (2019). Concrete made with waste marble powder and supplementary cementitious material for sustainable development. *Journal of Cleaner Production*, *211*, 716–729. https://doi.org/10.1016/j.jclepro.2018.11.245

ASHRAE. (2017). Hvac System Design Software. *Ashrae*, *2nd*. http://www.carrier.com/commercial/en/us/software/hvac-system-design/

Asprone, D., Menna, C., Bos, F. P., Salet, T. A. M., Mata-Falcón, J., & Kaufmann, W. (2018). Rethinking reinforcement for digital fabrication with concrete. *Cement and Concrete Research*, *112*(June), 111–121. https://doi.org/10.1016/j.cemconres.2018.05.020

Assiego De Larriva, R., Calleja Rodríguez, G., Cejudo López, J. M., Raugei, M., & Fullana I Palmer, P. (2014). A decision-making LCA for energy refurbishment of buildings: Conditions of comfort. *Energy and Buildings*, *70*, 333–342. https://doi.org/10.1016/j.enbuild.2013.11.049

Azar, E., & Menassa, C. C. (2012). A comprehensive analysis of the impact of occupancy parameters in energy simulation of office buildings. *Energy & Buildings*, *55*, 841–853. https://doi.org/10.1016/j.enbuild.2012.10.002

Babu, B. V., & Gujarathi, A. M. (2007). Multi-Objective Differential Evolution (MODE) for optimization of supply chain planning and management. *2007 IEEE Congress on Evolutionary Computation, CEC 2007*, 2732–2739. https://doi.org/10.1109/CEC.2007.4424816

Bai, G., Wang, L., Ma, G., Sanjayan, J., & Bai, M. (2021). 3D printing eco-friendly concrete containing under-utilised and waste solids as aggregates. *Cement and Concrete Composites*, *120*(February), 104037. https://doi.org/10.1016/j.cemconcomp.2021.104037

Bajpai, R., Choudhary, K., Srivastava, A., & Singh, K. (2020). Environmental impact assessment of fl y ash and silica fume based geopolymer concrete. *Journal of Cleaner Production*, *254*, 120147. https://doi.org/10.1016/j.jclepro.2020.120147

Balaras, C. A. (1996). The role of thermal mass on the cooling load of buildings. An overview of computational methods. *Energy and Buildings*, *24*(1), 1–10. https://doi.org/10.1016/0378-7788(95)00956-6

Balaras, C. A., Droutsa, K., Dascalaki, E., & Kontoyiannidis, S. (2005). Heating energy consumption and resulting environmental impact of European apartment buildings. *Energy and Buildings*, *37*(5), 429–442. https://doi.org/10.1016/j.enbuild.2004.08.003

Barcelo, L., Kline, J., Walenta, G., & Gartner, E. (2014). Cement and carbon emissions. *Materials and Structures/Materiaux et Constructions*, *47*(6), 1055–1065. https://doi.org/10.1617/s11527-013-0114-5

Becchio, C., Corgnati, S. P., Kindinis, A., & Pagliolico, S. (2009). Improving environmental sustainability of concrete products: Investigation on MWC thermal and mechanical properties. *Energy and Buildings*, *41*(11), 1127–1134. https://doi.org/10.1016/j.enbuild.2009.05.013

Behnood, A., Olek, J., & Glinicki, M. A. (2015). Predicting modulus elasticity of recycled aggregate concrete using M5 0 model tree algorithm. *Construction and Building Materials*, *94*, 137–147. https://doi.org/10.1016/j.conbuildmat.2015.06.055

Belén, G. F., Fernando, M. A., Diego, C. L., & Sindy, S. P. (2011). Stress-strain relationship in axial compression for concrete using recycled saturated coarse aggregate. *Construction and Building Materials*, *25*(5), 2335–2342. https://doi.org/10.1016/j.conbuildmat.2010.11.031

Beltrán, M. G., Agrela, F., Barbudo, A., Ayuso, J., & Ramírez, A. (2014). Mechanical and durability properties of concretes manufactured with biomass bottom ash and recycled coarse aggregates. *Construction and Building Materials*, *72*, 231–238. https://doi.org/10.1016/j.conbuildmat.2014.09.019

Beltrán, M. G., Barbudo, A., Agrela, F., Galvín, A. P., & Jiménez, J. R. (2014). Effect of cement addition on the properties of recycled concretes to reach control concretes strengths. *Journal of Cleaner Production*, *79*, 124–133. https://doi.org/10.1016/j.jclepro.2014.05.053

Ben Chaabene, W., Flah, M., & Nehdi, M. L. (2020). Machine learning prediction of mechanical

properties of concrete: Critical review. *Construction and Building Materials*, *260*, 119889. https://doi.org/10.1016/j.conbuildmat.2020.119889

Berardi, U., Tronchin, L., Manfren, M., & Nastasi, B. (2018). On the effects of variation of thermal conductivity in buildings in the Italian construction sector. *Energies*, *11*(4), 1–17. https://doi.org/10.3390/en11040872

Berndt, M. L. (2009). Properties of sustainable concrete containing fly ash, slag and recycled concrete aggregate. *Construction and Building Materials*, *23*(7), 2606–2613. https://doi.org/10.1016/j.conbuildmat.2009.02.011

Bhanja, S., & Sengupta, B. (2002). Investigations on the compressive strength of silica fume concrete using statistical methods. *Cement and Concrete Research*, *32*(9), 1391–1394. https://doi.org/10.1016/S0008-8846(02)00787-1

Bhatia, A., Sangireddy, S. A. R., & Garg, V. (2019). An approach to calculate the equivalent solar heat gain coefficient of glass windows with fixed and dynamic shading in tropical climates. *Journal of Building Engineering*, *22*(April 2018), 90–100. https://doi.org/10.1016/j.jobe.2018.11.008

Bhattacherjee, S., Basavaraj, A. S., Rahul, A. V., Santhanam, M., Gettu, R., Panda, B., Schlangen, E., Chen, Y., Copuroglu, O., Ma, G., Wang, L., Basit Beigh, M. A., & Mechtcherine, V. (2021). Sustainable materials for 3D concrete printing. *Cement and Concrete Composites*, *122*(June), 104156. https://doi.org/10.1016/j.cemconcomp.2021.104156

Bogas, J. A., De Brito, J., & Cabaço, J. (2014). Long-term behaviour of concrete produced with recycled lightweight expanded clay aggregate concrete. *Construction and Building Materials*, *65*, 470–479. https://doi.org/10.1016/j.conbuildmat.2014.05.003

Bon, R., & Hutchinson, K. (2000). Sustainable construction: Some economic challenges. *Building Research and Information*, *28*(5–6), 310–314. https://doi.org/10.1080/096132100418465

Bonoli, A., Zanni, S., & Serrano-Bernardo, F. (2021). Sustainability in building and construction within the framework of circular cities and european new green deal. The contribution of concrete recycling. *Sustainability (Switzerland)*, *13*(4), 1–16. https://doi.org/10.3390/su13042139

Boobalan, S. C., Salman Shereef, M., Saravanaboopathi, P., & Siranjeevi, K. (2022). Studies on green concrete – A review. *Materials Today: Proceedings*, *65*, 1404–1409. https://doi.org/10.1016/j.matpr.2022.04.392

Boquera, L., Castro, J. R., Pisello, A. L., & Cabeza, L. F. (2021). Research progress and trends on

the use of concrete as thermal energy storage material through bibliometric analysis. *Journal of Energy Storage*, *38*(November 2020), 102562. https://doi.org/10.1016/j.est.2021.102562

Borri, E., Zsembinszki, G., & Cabeza, L. F. (2021). Recent developments of thermal energy storage applications in the built environment: A bibliometric analysis and systematic review. *Applied Thermal Engineering*, *189*(January), 116666. https://doi.org/10.1016/j.applthermaleng.2021.116666

Bronshtein, A. (2017). A quick introduction to K-Nearest Neighbors Algorithm. *Noteworthy-The Journal Blog*.

Brooks, A. L., He, Y., Farzadnia, N., Seyfimakrani, S., & Zhou, H. (2022). Incorporating PCM-enabled thermal energy storage into 3D printable cementitious composites. *Cement and Concrete Composites*, *129*(March), 104492. https://doi.org/10.1016/j.cemconcomp.2022.104492

Brooks, A. L., Shen, Z., & Zhou, H. (2020). Development of a high-temperature inorganic synthetic foam with recycled fly-ash cenospheres for thermal insulation brick manufacturing. *Journal of Cleaner Production*, *246*, 118748. https://doi.org/10.1016/j.jclepro.2019.118748

Brooks, A. L., Zhou, H., & Hanna, D. (2018). Comparative study of the mechanical and thermal properties of lightweight cementitious composites. *Construction and Building Materials*, *159*, 316–328. https://doi.org/10.1016/j.conbuildmat.2017.10.102

Burbano-Garcia, C., Hurtado, A., Silva, Y. F., Delvasto, S., & Araya-Letelier, G. (2021). Utilization of waste engine oil for expanded clay aggregate production and assessment of its influence on lightweight concrete properties. *Construction and Building Materials*, *273*, 121677. https://doi.org/10.1016/j.conbuildmat.2020.121677

Busch, P., Kendall, A., Murphy, C. W., & Miller, S. A. (2022). Literature review on policies to mitigate GHG emissions for cement and concrete. *Resources, Conservation and Recycling*, *182*(November 2021), 106278. https://doi.org/10.1016/j.resconrec.2022.106278

Butler, L., West, J. S., & Tighe, S. L. (2013). Effect of recycled concrete coarse aggregate from multiple sources on the hardened properties of concrete with equivalent compressive strength. *Construction and Building Materials*, *47*, 1292–1301. https://doi.org/10.1016/j.conbuildmat.2013.05.074

Cabeza, L. F., Castellón, C., Nogués, M., Medrano, M., Leppers, R., & Zubillaga, O. (2007). Use of microencapsulated PCM in concrete walls for energy savings. *Energy and Buildings*,

39(2), 113–119. https://doi.org/10.1016/j.enbuild.2006.03.030

Cakiroglu, C., Islam, K., Bekdaş, G., Kim, S., & Geem, Z. W. (2021). CO2 emission optimization of concrete-filled steel tubular rectangular stub columns using metaheuristic algorithms. *Sustainability (Switzerland)*, *13*(19), 1–26. https://doi.org/10.3390/su131910981

Çakır, Ö., & Dilbas, H. (2021). Durability properties of treated recycled aggregate concrete: Effect of optimized ball mill method. *Construction and Building Materials*, *268*. https://doi.org/10.1016/j.conbuildmat.2020.121776

Çakır, Ö., & Sofyanlı, Ö. Ö. (2015). Influence of silica fume on mechanical and physical properties of recycled aggregate concrete. *HBRC Journal*, *11*(2), 157–166. https://doi.org/10.1016/j.hbrcj.2014.06.002

Calderón, A., Barreneche, C., Hernández-Valle, K., Galindo, E., Segarra, M., & Fernández, A. I. (2020). Where is Thermal Energy Storage (TES) research going? – A bibliometric analysis. *Solar Energy*, *200*(January 2019), 37–50. https://doi.org/10.1016/j.solener.2019.01.050

Cao, V. D., Bui, T. Q., & Kjøniksen, A. L. (2019). Thermal analysis of multi-layer walls containing geopolymer concrete and phase change materials for building applications. *Energy*, *186*, 115792. https://doi.org/10.1016/j.energy.2019.07.122

Cao, X., Dai, X., & Liu, J. (2016). Building energy-consumption status worldwide and the state-of-the-art technologies for zero-energy buildings during the past decade. *Energy and Buildings*, *128*, 198–213. https://doi.org/10.1016/j.enbuild.2016.06.089

Cárdenas-Ramírez, C., Jaramillo, F., & Gómez, M. (2020). Systematic review of encapsulation and shape-stabilization of phase change materials. *Journal of Energy Storage*, *30*(52), 101495. https://doi.org/10.1016/j.est.2020.101495

Carneiro, J. A., Lima, P. R. L., Leite, M. B., & Toledo Filho, R. D. (2014). Compressive stress-strain behavior of steel fiber reinforced-recycled aggregate concrete. *Cement and Concrete Composites*, *46*, 65–72. https://doi.org/10.1016/j.cemconcomp.2013.11.006

Cassiani, J., Martinez-Arguelles, G., Peñabaena-Niebles, R., Keßler, S., & Dugarte, M. (2021). Sustainable concrete formulations to mitigate Alkali-Silica reaction in recycled concrete aggregates (RCA) for concrete infrastructure. *Construction and Building Materials*, *307*(March). https://doi.org/10.1016/j.conbuildmat.2021.124919

Casuccio, M., Torrijos, M. C., Giaccio, G., & Zerbino, R. (2008). Failure mechanism of recycled aggregate concrete. *Construction and Building Materials*, *22*(7), 1500–1506. https://doi.org/10.1016/j.conbuildmat.2007.03.032

Cavalline, T. L., Castrodale, R. W., Freeman, C., & Wall, J. (2017). Impact of lightweight

aggregate on concrete thermal properties. *ACI Materials Journal*, *114*(6), 945–956. https://doi.org/10.14359/51701003

Chakradhara Rao, M., Bhattacharyya, S. K., & Barai, S. V. (2011). Influence of field recycled coarse aggregate on properties of concrete. *Materials and Structures/Materiaux et Constructions*, *44*(1), 205–220. https://doi.org/10.1617/s11527-010-9620-x

Chandra, S., & Berntsson, L. (2002). *Lightweight Aggregate Concrete: Science, Technology, and Applications*. Noyes Publications.

Chen, L. (2010). A multiple linear regression prediction of concrete compressive strength based on physical properties of electric arc furnace oxidizing slag. *Iternational Journal of Applied Science and Engineering*, *7,2*, 153–158.

Chen, M., Liu, P., Kong, D., Wang, Y., Wang, J., Huang, Y., Yu, K., & Wu, N. (2022). Influencing factors of mechanical and thermal conductivity of foamed phosphogypsum-based composite cementitious materials. *Construction and Building Materials*, *346*(May). https://doi.org/10.1016/j.conbuildmat.2022.128462

Chen, M., Wang, S., Lu, L., Zhao, P., & Gong, C. (2016). Effect of matrix components with low thermal conductivity and density on performances of cement-EPS/VM insulation mortar. *Journal of Thermal Analysis and Calorimetry*, *126*(3), 1123–1132. https://doi.org/10.1007/s10973-016-5718-x

Chen, T., & Guestrin, C. (2016). Xgboost: A scalable tree boosting system. *Proceedings of the 22nd Acm Sigkdd International Conference on Knowledge Discovery and Data Mining*, 785–794.

Chiniforush, A. A., Akbarnezhad, A., Valipour, H., & Xiao, J. (2018). Energy implications of using steel-timber composite (STC) elements in buildings. *Energy and Buildings*, *176*, 203–215. https://doi.org/10.1016/j.enbuild.2018.07.038

Cho, S., Kruger, J., van Rooyen, A., & van Zijl, G. (2021). Rheology and application of buoyant foam concrete for digital fabrication. *Composites Part B: Engineering*, *215*(October 2020), 108800. https://doi.org/10.1016/j.compositesb.2021.108800

Christensen, R. M., & Lo, K. H. (1979). Solutions for Effective Shear Properties in Three Phase Sphere and Cylinder Models. *Journal of Mechanics and Physics of Solids*, *27*, 315–330.

Chua, K. J., Chou, S. K., Yang, W. M., & Yan, J. (2013). Achieving better energy-efficient air conditioning - A review of technologies and strategies. *Applied Energy*, *104*, 87–104. https://doi.org/10.1016/j.apenergy.2012.10.037

Cioffi, R., Travaglioni, M., Piscitelli, G., Petrillo, A., & Parmentola, A. (2020). Smart

manufacturing systems and applied industrial technologies for a sustainable industry: A systematic literature review. *Applied Sciences (Switzerland)*, *10*(8). https://doi.org/10.3390/APP10082897

Cobo, M. J., López-Herrera, A. G., Herrera-Viedma, E., & Herrera, F. (2011). Science mapping software tools: Review, analysis, and cooperative study among tools. *Journal of the American Society for Information Science and Technology*, *62*(7), 1382–1402.

Colangelo, F., Petrillo, A., Cioffi, R., Borrelli, C., & Forcina, A. (2018). Life cycle assessment of recycled concretes: A case study in southern Italy. *Science of the Total Environment*, *615*, 1506–1517. https://doi.org/10.1016/j.scitotenv.2017.09.107

Collivignarelli, M. C., Cillari, G., Ricciardi, P., Miino, M. C., Torretta, V., Rada, E. C., & Abbà, A. (2020). The production of sustainable concrete with the use of alternative aggregates: A review. *Sustainability (Switzerland)*, *12*(19), 1–34. https://doi.org/10.3390/SU12197903

Cordero, A. S., Melgar, S. G., & Márquez, J. M. A. (2019). Green building rating systems and the new framework level(s): A critical review of sustainability certification within Europe. *Energies*, *13*(1), 1–25. https://doi.org/10.3390/en13010066

Corinaldesi, V. (2010). Mechanical and elastic behaviour of concretes made of recycled-concrete coarse aggregates. *Construction and Building Materials*, *24*(9), 1616–1620. https://doi.org/10.1016/j.conbuildmat.2010.02.031

Corral Higuera, R., Arredondo Rea, S. P., Flores, N., Gómez Soberón, J. M. V., Almeraya Calderón, F., Castorena González, J. H., & Almaral Sánchez, J. L. (2011). Sulfate attack and reinforcement corrosion in concrete with recycled concrete aggregates and supplementary cementing materials. *International Journal of Electrochemical Science*, *6*, 613–621.

Crawford, R. H., & Treloar, G. J. (2003). Validation of the use of Australian input output data for building embodied energy simulation. *Eighth International IBPSA Conference*, 235–242.

Crawley, D. B., Lawrie, L. K., Winkelmann, F. C., Buhl, W. F., Huang, Y. J., Pedersen, C. O., Strand, R. K., Liesen, R. J., Fisher, D. E., Witte, M. J., & Glazer, J. (2001). EnergyPlus: Creating a new-generation building energy simulation program. *Energy and Buildings*, *33*(4), 319–331. https://doi.org/10.1016/S0378-7788(00)00114-6

Crawley, D. B., Rees, S. J., Witte, M. J., Kennedy, S. D., Crowther, H. F., Baker, R. G., Beda, M. F., Cooper, K. W., Cummings, S. D., Dean, K. W., Doerr, R. G., Howard, E. P., & Newman, H. M. (2008). *Standard Method of Test for the Evaluation of Building Energy Analysis Computer Programs*. *4723*, 1–77. https://www.ashrae.org/file library/technical resources/standards and guidelines/standards addenda/140_2007_b.pdf

Cruz Rios, F., Naganathan, H., Chong, W. K., Lee, S., & Alves, A. (2017). Analyzing the Impact of Outside Temperature on Energy Consumption and Production Patterns in High-Performance Research Buildings in Arizona. *Journal of Architectural Engineering*, *23*(3), 1–12. https://doi.org/10.1061/(asce)ae.1943-5568.0000242

Cseh, Á., Balázs, G. L., Kekanović, M., & Miličić, I. M. (2021). Effect of SCMs on heat transfer properties of LWAC. *Journal of Thermal Analysis and Calorimetry*, *144*(4), 1095–1108. https://doi.org/10.1007/s10973-020-09631-w

Damdelen, O. (2019). Influences of construction material type and water-cement ratio reduction on thermal transmittance of sustainable concrete mixes. *Construction and Building Materials*, *196*, 345–353. https://doi.org/10.1016/j.conbuildmat.2018.11.133

Danish, A., & Mosaberpanah, M. A. (2021). Influence of cenospheres and fly ash on the mechanical and durability properties of high-performance cement mortar under different curing regimes. *Construction and Building Materials*, *279*, 122458. https://doi.org/10.1016/j.conbuildmat.2021.122458

de Lassio, J., França, J., Espirito Santo, K., & Haddad, A. (2016). Case Study: LCA Methodology Applied to Materials Management in a Brazilian Residential Construction Site. *Journal of Engineering*, *2016*, 1–9. https://doi.org/10.1155/2016/8513293

de Melo, S. A., Pereira, R. B. D., da Silva Reis, A. F., Lauro, C. H., & Brandão, L. C. (2022). Multi-objective evolutionary optimization of unsupervised latent variables of turning process. *Applied Soft Computing*, 108713. https://doi.org/10.1016/j.asoc.2022.108713

Deb, K., Pratap, A., Agarwal, S., & Meyarivan, T. (2002). A fast and elitist multiobjective genetic algorithm: NSGA-II. *IEEE Transactions on Evolutionary Computation*, *6*(2), 182–197. https://doi.org/10.1109/4235.996017

Debieb, F., Courard, L., Kenai, S., & Degeimbre, R. (2010). Mechanical and durability properties of concrete using contaminated recycled aggregates. *Cement and Concrete Composites*, *32*(6), 421–426. https://doi.org/10.1016/j.cemconcomp.2010.03.004

Demirbog, R. (2003). *The effects of expanded perlite aggregate , silica fume and fly ash on the thermal conductivity of lightweight concrete*. *33*, 723–727. https://doi.org/10.1016/S0008-8846(02)01032-3

Demirboğa, R. (2003). Influence of mineral admixtures on thermal conductivity and compressive strength of mortar. *Energy and Buildings*, *35*(2), 189–192. https://doi.org/10.1016/S0378-7788(02)00052-X

Demirboğa, R. (2007). Thermal conductivity and compressive strength of concrete incorporation

with mineral admixtures. *Building and Environment*, *42*(7), 2467–2471. https://doi.org/10.1016/j.buildenv.2006.06.010

Demirboğa, R., & Gül, R. (2003). Thermal conductivity and compressive strength of expanded perlite aggregate concrete with mineral admixtures. *Energy and Buildings*, *35*(11), 1155–1159. https://doi.org/10.1016/j.enbuild.2003.09.002

Deng, Z., Huang, H., Ye, B., Xiang, P., & Li, C. (2020). Mechanical Performance of RAC under True-Triaxial Compression after High Temperatures. *Journal of Materials in Civil Engineering*, *32*(8). https://doi.org/10.1061/(asce)mt.1943-5533.0003231

DeRousseau, M. A., Kasprzyk, J. R., & Srubar, W. V. (2018). Computational design optimization of concrete mixtures: A review. *Cement and Concrete Research*, *109*(December 2017), 42–53. https://doi.org/10.1016/j.cemconres.2018.04.007

Dilbas, H., & Çakır, Ö. (2021). Physical and Mechanical Properties of Treated Recycled Aggregate Concretes: Combination of Mechanical Treatment and Silica Fume. *Journal of Materials in Civil Engineering*, *33*(6), 04021096. https://doi.org/10.1061/(asce)mt.1943-5533.0003658

Dilbas, H., Şimşek, M., & Çakir, Ö. (2014). An investigation on mechanical and physical properties of recycled aggregate concrete (RAC) with and without silica fume. *Construction and Building Materials*, *61*(March 2006), 50–59. https://doi.org/10.1016/j.conbuildmat.2014.02.057

Dinelli, G., Belz, G., Majorana, C. E., & Schrefler, B. A. (1996). Experimental investigation on the use of fly ash for lightweight precast structural elements. *Materials and Structures/Materiaux et Constructions*, *29*(10), 632–638. https://doi.org/10.1007/bf02485971

Ding, G., & Ying, X. (2019). Embodied and operating energy assessment of existing buildings e Demolish or rebuild. *Energy*, *182*, 623–631. https://doi.org/10.1016/j.energy.2019.06.056

Ding, T., Xiao, J., Qin, F., & Duan, Z. (2020). Mechanical behavior of 3D printed mortar with recycled sand at early ages. *Construction and Building Materials*, *248*, 118654.

Ding, T., Xiao, J., & Tam, V. W. Y. (2016). A closed-loop life cycle assessment of recycled aggregate concrete utilization in China. *Waste Management*, *56*, 367–375. https://doi.org/10.1016/j.wasman.2016.05.031

Ding, T., Xiao, J., Zou, S., & Wang, Y. (2020). Hardened properties of layered 3D printed concrete with recycled sand. *Cement and Concrete Composites*, *113*(May), 103724. https://doi.org/10.1016/j.cemconcomp.2020.103724

Dixit, M. K. (2017). Life cycle embodied energy analysis of residential buildings: A review of literature to investigate embodied energy parameters. *Renewable and Sustainable Energy Reviews*, *79*(May), 390–413. https://doi.org/10.1016/j.rser.2017.05.051

Dixit, M. K., Fernández-solís, J. L., Lavy, S., & Culp, C. H. (2012). Need for an embodied energy measurement protocol for buildings : A review paper. *Renewable and Sustainable Energy Reviews*, *16*(6), 3730–3743. https://doi.org/10.1016/j.rser.2012.03.021

Dixit, M. K., Fernández-Solís, J. L., Lavy, S., & Culp, C. H. (2010). Identification of parameters for embodied energy measurement: A literature review. *Energy and Buildings*, *42*(8), 1238–1247. https://doi.org/10.1016/j.enbuild.2010.02.016

Domingo-Cabo, A., Lázaro, C., López-Gayarre, F., Serrano-López, M. A., Serna, P., & Castaño-Tabares, J. O. (2009). Creep and shrinkage of recycled aggregate concrete. *Construction and Building Materials*, *23*(7), 2545–2553. https://doi.org/10.1016/j.conbuildmat.2009.02.018

dos Santos, C. P., & Matias, L. M. C. (2006). Coeficientes de Transmissão Térmica da Envolvente dos Edif{\'\i}cios, Lisboa. *LNEC-ICT Informação Técnica de Edif{\'\i}cios-ITE*, *50*.

Dossche, C., Boel, V., De Corte, W., & De Belie, N. (2015). Green concrete: optimization of high-strength concrete based on LCA. *International Workshop on Durability and Sustainability of Concrete Structures (IW-DSCS)*, 357–366.

Drissi, S., Ling, T. C., Mo, K. H., & Eddhahak, A. (2019). A review of microencapsulated and composite phase change materials: Alteration of strength and thermal properties of cement-based materials. *Renewable and Sustainable Energy Reviews*, *110*(April), 467–484. https://doi.org/10.1016/j.rser.2019.04.072

Duan, H., Chen, S., & Song, J. (2022). Characterizing regional building energy consumption under joint climatic and socioeconomic impacts. *Energy*, *245*, 123290. https://doi.org/10.1016/j.energy.2022.123290

Duan, J., Asteris, P. G., Nguyen, H., Bui, X. N., & Moayedi, H. (2021). A novel artificial intelligence technique to predict compressive strength of recycled aggregate concrete using ICA-XGBoost model. *Engineering with Computers*, *37*(4), 3329–3346. https://doi.org/10.1007/s00366-020-01003-0

Duchesne, J. (2021). Alternative supplementary cementitious materials for sustainable concrete structures: a review on characterization and properties. *Waste and Biomass Valorization*, *12*, 1219–1236.

Elchalakani, M., Basarir, H., & Karrech, A. (2017). Green Concrete with High-Volume Fly Ash and Slag with Recycled Aggregate and Recycled Water to Build Future Sustainable Cities. *Journal of Materials in Civil Engineering*, *29*(2). https://doi.org/10.1061/(asce)mt.1943-5533.0001748

Elemam, W. E., Abdelraheem, A. H., Mahdy, M. G., & Tahwia, A. M. (2020). Optimizing fresh properties and compressive strength of self-consolidating concrete. *Construction and Building Materials*, *249*, 118781. https://doi.org/10.1016/j.conbuildmat.2020.118781

Elshahawi, M., Hückler, A., & Schlaich, M. (2021). Infra lightweight concrete: A decade of investigation (a review). *Structural Concrete*, *22*(S1), E152–E168. https://doi.org/10.1002/suco.202000206

Eshelby, J. D. (1957). The Determination of the Elastic Field of an Ellipsoidal Inclusion, and Related Problems. *Proceedings of the Royal Society of London, Series A, Matchematical and Physical Science*, *241*(1226), 376–396.

Essid, N., Eddhahak, A., & Neji, J. (2022). Experimental and numerical analysis of the energy efficiency of PCM concrete wallboards under different thermal scenarios. *Journal of Building Engineering*, *45*(October 2021), 103547. https://doi.org/10.1016/j.jobe.2021.103547

Etxeberria, M., Marí, A. R., & Vázquez, E. (2007). Recycled aggregate concrete as structural material. *Materials and Structures/Materiaux et Constructions*, *40*(5), 529–541. https://doi.org/10.1617/s11527-006-9161-5

Etxeberria, M., Vázquez, E., Marí, A., & Barra, M. (2007). Influence of amount of recycled coarse aggregates and production process on properties of recycled aggregate concrete. *Cement and Concrete Research*, *37*(5), 735–742. https://doi.org/10.1016/j.cemconres.2007.02.002

Eucken, A. (1932). Thermal conductivity of ceramic refractory materials; calculation from thermal conductivity of constituents. *Ceramic Abstracts*, *11*. https://doi.org/10.1007/s10853-006-7637-x

Falliano, D., De Domenico, D., Ricciardi, G., & Gugliandolo, E. (2020). 3D-printable lightweight foamed concrete and comparison with classical foamed concrete in terms of fresh state properties and mechanical strength. *Construction and Building Materials*, *254*, 119271. https://doi.org/10.1016/j.conbuildmat.2020.119271

Falliano, D., Gugliandolo, E., De Domenico, D., & Ricciardi, G. (2019). Experimental investigation on the mechanical strength and thermal conductivity of extrudable foamed

concrete and preliminary views on its potential application in 3D printed multilayer insulating panels. *First RILEM International Conference on Concrete and Digital Fabrication--Digital Concrete 2018*, 277–286.

Falliano, D., Restuccia, L., & Gugliandolo, E. (2021). A simple optimized foam generator and a study on peculiar aspects concerning foams and foamed concrete. *Construction and Building Materials*, *268*, 121101. https://doi.org/10.1016/j.conbuildmat.2020.121101

Fan, J., Wang, X., Wu, L., Zhou, H., Zhang, F., Yu, X., Lu, X., & Xiang, Y. (2018). Comparison of Support Vector Machine and Extreme Gradient Boosting for predicting daily global solar radiation using temperature and precipitation in humid subtropical climates: A case study in China. *Energy Conversion and Management*, *164*(March), 102–111. https://doi.org/10.1016/j.enconman.2018.02.087

Fang, X., Shen, Y. X., & Zhang, X. F. (2021). Multi-objective evolutionary algorithm based on decomposition with integration strategy. *ACM International Conference Proceeding Series*, *1*, 216–222. https://doi.org/10.1145/3507548.3507581

Faraj, K., Khaled, M., Faraj, J., Hachem, F., & Castelain, C. (2020). Phase change material thermal energy storage systems for cooling applications in buildings: A review. *Renewable and Sustainable Energy Reviews*, *119*(May 2019), 109579. https://doi.org/10.1016/j.rser.2019.109579

Farooq, F., Ahmed, W., Akbar, A., Aslam, F., & Alyousef, R. (2021). Predictive modeling for sustainable high-performance concrete from industrial wastes: A comparison and optimization of models using ensemble learners. *Journal of Cleaner Production*, *292*, 126032. https://doi.org/10.1016/j.jclepro.2021.126032

Farooq, F., Amin, M. N., Khan, K., Sadiq, M. R., Javed, M. F., Aslam, F., & Alyousef, R. (2020). A comparative study of random forest and genetic engineering programming for the prediction of compressive strength of high strength concrete (HSC). *Applied Sciences (Switzerland)*, *10*(20), 1–18. https://doi.org/10.3390/app10207330

Farooq, F., Jin, X., Faisal Javed, M., Akbar, A., Izhar Shah, M., Aslam, F., & Alyousef, R. (2021). Geopolymer concrete as sustainable material: A state of the art review. *Construction and Building Materials*, *306*(September), 124762. https://doi.org/10.1016/j.conbuildmat.2021.124762

Fathifazl, G., Ghani Razaqpur, A., Burkan Isgor, O., Abbas, A., Fournier, B., & Foo, S. (2011). Creep and drying shrinkage characteristics of concrete produced with coarse recycled concrete aggregate. *Cement and Concrete Composites*, *33*(10), 1026–1037.

https://doi.org/10.1016/j.cemconcomp.2011.08.004

Fatih, A., & Burhan, M. (2015). *Modeling of compressive strength and UPV of high-volume mineral-admixtured concrete using rule-based M5 rule and tree model M5P classifiers Yas*. *94*, 235–240. https://doi.org/10.1016/j.conbuildmat.2015.06.029

Favaretto, P., Hidalgo, G. E. N., Sampaio, C. H., de Almeida Silva, R., & Lermen, R. T. (2017). Characterization and use of construction and demolition waste from South of Brazil in the production of foamed concrete blocks. *Applied Sciences (Switzerland)*, *7*(10). https://doi.org/10.3390/app7101090

Faysal, R., Maslehuddin, M., Shameem, M., & Ahmad, S. (2020). Effect of mineral additives and two - stage mixing on the performance of recycled aggregate concrete. *Journal of Material Cycles and Waste Management*, *22*(5), 1587–1601. https://doi.org/10.1007/s10163-020-01048-9

Feng, W., Tang, Y., Zhang, Y., & Qi, C. (2021). Partially fly ash and nano-silica incorporated recycled coarse aggregate based concrete : Constitutive model and enhancement mechanism. *Journal of Materials Research and Technology*, *17*, 192–210. https://doi.org/10.1016/j.jmrt.2021.12.135

Feng, Y., Gong, D., Zhang, Q., Jiang, S., Zhao, L., & Cui, N. (2019). Evaluation of temperature-based machine learning and empirical models for predicting daily global solar radiation. *Energy Conversion and Management*, *198*(July), 111780. https://doi.org/10.1016/j.enconman.2019.111780

Figueiredo, A., Lapa, J., Vicente, R., & Cardoso, C. (2016). Mechanical and thermal characterization of concrete with incorporation of microencapsulated PCM for applications in thermally activated slabs. *Construction and Building Materials*, *112*, 639–647. https://doi.org/10.1016/j.conbuildmat.2016.02.225

Flatt, R. J., & Wangler, T. (2022). On sustainability and digital fabrication with concrete. *Cement and Concrete Research*, *158*(April), 106837. https://doi.org/10.1016/j.cemconres.2022.106837

Folino, P., & Xargay, H. (2014). Recycled aggregate concrete - Mechanical behavior under uniaxial and triaxial compression. *Construction and Building Materials*, *56*, 21–31. https://doi.org/10.1016/j.conbuildmat.2014.01.073

Francioso, V., Moro, C., & Velay-Lizancos, M. (2021). Effect of recycled concrete aggregate (RCA) on mortar's thermal conductivity susceptibility to variations of moisture content and ambient temperature. *Journal of Building Engineering*, *43*(July), 103208.

https://doi.org/10.1016/j.jobe.2021.103208

Friedman, J. (2001). Greedy Function Approximation : A Gradient Boosting Machine Author (s): Jerome H . Friedman Source : The Annals of Statistics , Vol . 29 , No . 5 (Oct ., 2001), pp . 1189-1232 Published by : Institute of Mathematical Statistics Stable URL : http://www. *The Annals of Statistics*, *29*(5), 1189–1232. https://www.jstor.org/stable/2699986

Fu, Y., Wang, X., Wang, L., & Li, Y. (2020). *Foam Concrete : A State-of-the-Art and State-of-the-Practice Review*. *2020*.

Ganesan, S., Othuman Mydin, M. A., Mohd Yunos, M. Y., & Mohd Nawi, M. N. (2015). Thermal properties of foamed concrete with various densities and additives at ambient temperature. *Applied Mechanics and Materials*, *747*, 230–233.

Gedam, B. A., Singh, S., Upadhyay, A., & Bhandari, N. M. (2019). Improved durability of concrete using supplementary cementitious materials. *Sustainable Construction Materials and Technologies*, *3*. https://doi.org/10.18552/2019/idscmt5151

George Baird, Andrew Alcorn, & Phil Haslam. (1997). The energy embodied in building materials - updated New Zealand coefficients and their significance. *IPENZ Transactions*, *24*(1), 46–54.

Gettu, R., Patel, A., Rathi, V., Prakasan, S., Basavaraj, A. S., Palaniappan, S., & Maity, S. (2019). Influence of supplementary cementitious materials on the sustainability parameters of cements and concretes in the Indian context. *Materials and Structures*, *52*(1), 1–11. https://doi.org/10.1617/s11527-019-1321-5

Giama, E., & Papadopoulos, A. M. (2015). Assessment tools for the environmental evaluation of concrete, plaster and brick elements production. *Journal of Cleaner Production*, *99*, 75–85. https://doi.org/10.1016/j.jclepro.2015.03.006

Gökçe, H. S., Hatungimana, D., & Ramyar, K. (2019). Effect of fly ash and silica fume on hardened properties of foam concrete. *Construction and Building Materials*, *194*, 1–11. https://doi.org/10.1016/j.conbuildmat.2018.11.036

Golafshani, E. M., & Behnood, A. (2019). Estimating the optimal mix design of silica fume concrete using biogeography-based programming. *Cement and Concrete Composites*, *96*(October 2018), 95–105. https://doi.org/10.1016/j.cemconcomp.2018.11.005

Gómez-Soberón, J. M. V. (2002). Porosity of recycled concrete with substitution of recycled concrete aggregate: An experimental study. *Cement and Concrete Research*, *32*(8), 1301–1311. https://doi.org/10.1016/S0008-8846(02)00795-0

Gordillo, G. C., Ruiz, G. R., Stauffer, Y., Dasen, S., & Bandera, C. F. (2020). EplusLauncher: An

API to Perform Complex EnergyPlus Simulations in MATLAB® and C#. *Sustainability*, *12*(2), 672. https://doi.org/10.3390/su12020672

Goswami, D. Y., & Biseli, K. M. (1993). Use of underground air tunnels for heating and cooling agricultural and residential buildings. *Fact Sheet EES*, *78*, 1–4.

Graybeal, B., & Tanesi, J. (2008). A cementitious long-life wearing course to reduce frequency of maintenance works on high-traffic roads. *Transport Research Arena Europe 2008*, *1561*(February), 454–461. https://doi.org/10.1061/(ASCE)0899-1561(2007)19

Grömping, U. (2009). Variable importance assessment in regression: Linear regression versus random forest. *American Statistician*, *63*(4), 308–319. https://doi.org/10.1198/tast.2009.08199

Grynning, S., Gustavsen, A., Time, B., & Petter, B. (2013). Windows in the buildings of tomorrow : Energy losers or energy gainers ? *Energy & Buildings*, *61*, 185–192. https://doi.org/10.1016/j.enbuild.2013.02.029

Guo, Z., Jiang, T., Zhang, J., Kong, X., Chen, C., & Lehman, D. E. (2020a). Mechanical and durability properties of sustainable self-compacting concrete with recycled concrete aggregate and fly ash, slag and silica fume. *Construction and Building Materials*, *231*, 117115. https://doi.org/10.1016/j.conbuildmat.2019.117115

Guo, Z., Jiang, T., Zhang, J., Kong, X., Chen, C., & Lehman, D. E. (2020b). Mechanical and durability properties of sustainable self-compacting concrete with recycled concrete aggregate and fly ash, slag and silica fume. *Construction and Building Materials*, *231*, 117115. https://doi.org/10.1016/j.conbuildmat.2019.117115

Guo, Z., Tu, A., Chen, C., & Lehman, D. E. (2018). Mechanical properties, durability, and life-cycle assessment of concrete building blocks incorporating recycled concrete aggregates. *Journal of Cleaner Production*, *199*, 136–149. https://doi.org/10.1016/j.jclepro.2018.07.069

Gupta, S., & Chaudhary, S. (2022). State of the art review on supplementary cementitious materials in India – II: Characteristics of SCMs, effect on concrete and environmental impact. *Journal of Cleaner Production*, *357*(November 2021), 131945. https://doi.org/10.1016/j.jclepro.2022.131945

Gupta, T., Patel, K. A., Siddique, S., Sharma, R. K., & Chaudhary, S. (2019). Prediction of mechanical properties of rubberised concrete exposed to elevated temperature using ANN. *Measurement*, *147*, 106870. https://doi.org/10.1016/j.measurement.2019.106870

Habert, G., & Roussel, N. (2009). Study of two concrete mix-design strategies to reach carbon mitigation objectives. *Cement and Concrete Composites*, *31*(6), 397–402.

https://doi.org/10.1016/j.cemconcomp.2009.04.001

Habibi, A., Ramezanianpour, A. M., & Mahdikhani, M. (2021). RSM-based optimized mix design of recycled aggregate concrete containing supplementary cementitious materials based on waste generation and global warming potential. *Resources, Conservation and Recycling*, *167*(January), 105420. https://doi.org/10.1016/j.resconrec.2021.105420

Hafez, H., Kassim, D., Kurda, R., Silva, R. V., & de Brito, J. (2021). Assessing the sustainability potential of alkali-activated concrete from electric arc furnace slag using the ECO2 framework. *Construction and Building Materials*, *281*, 122559. https://doi.org/10.1016/j.conbuildmat.2021.122559

Hafez, H., Teirelbar, A., Tošić, N., Ikumi, T., & de la Fuente, A. (2023). Data-driven optimization tool for the functional, economic, and environmental properties of blended cement concrete using supplementary cementitious materials. *Journal of Building Engineering*, *67*(January). https://doi.org/10.1016/j.jobe.2023.106022

Haitao, Y., & Shizhu, T. (2015). Preparation and properties of high-strength recycled concrete in cold areas. *Materiales de Construcción*, *65*(318), e050--e050.

Hamad, M. A., Nasr, M., Shubbar, A., Al-Khafaji, Z., Al Masoodi, Z., Al-Hashimi, O., Kot, P., Alkhaddar, R., & Hashim, K. (2021). Production of ultra-high-performance concrete with low energy consumption and carbon footprint using supplementary cementitious materials instead of silica fume: A review. *Energies*, *14*(24), 1–26. https://doi.org/10.3390/en14248291

Hammad, A. W., Akbarnezhad, A., & Oldfield, P. (2018). Optimising embodied carbon and U-value in load bearing walls: A mathematical bi-objective mixed integer programming approach. *Energy and Buildings*, *174*, 657–671. https://doi.org/10.1016/j.enbuild.2018.05.061

Hammond, G. P., & Jones, C. I. (2008). Embodied energy and carbon in construction materials. *Proceedings of the Institution of Civil Engineers-Energy*, *161*(2), 87–98.

Han, G., Srebric, J., & Enache-pommer, E. (2015). Different modeling strategies of infiltration rates for an office building to improve accuracy of building energy simulations. *Energy & Buildings*, *86*, 288–295. https://doi.org/10.1016/j.enbuild.2014.10.028

Han, Q., Gui, C., Xu, J., & Lacidogna, G. (2019). A generalized method to predict the compressive strength of high-performance concrete by improved random forest algorithm. *Construction and Building Materials*, *226*, 734–742. https://doi.org/10.1016/j.conbuildmat.2019.07.315

Hasanbeigi, A., Price, L., & Lin, E. (2012). Emerging energy-efficiency and CO 2 emission-reduction technologies for cement and concrete production: A technical review. *Renewable and Sustainable Energy Reviews*, *16*(8), 6220–6238. https://doi.org/10.1016/j.rser.2012.07.019

Hashim, M., & Tantray, M. (2021). Developing and optimizing foam concrete using industrial waste materials. *Innovative Infrastructure Solutions*, *6*(4), 1–10. https://doi.org/10.1007/s41062-021-00572-3

Haworth, J., & Cheng, T. (2012). Non-parametric regression for space-time forecasting under missing data. *Computers, Environment and Urban Systems*, *36*(6), 538–550. https://doi.org/10.1016/j.compenvurbsys.2012.08.005

He, Y., Brooks, A., Li, Y., & Zhou, H. (2023). Towards building homeostasis through a low-cost biomimetic synthetic foam for building surface cooling and energy saving. *Journal of Cleaner Production*, *385*(November 2022), 135626. https://doi.org/10.1016/j.jclepro.2022.135626

He, Y., Zhang, Y., Zhang, C., & Zhou, H. (2020). Energy-saving potential of 3D printed concrete building with integrated living wall. *Energy and Buildings*, *222*, 110110. https://doi.org/10.1016/j.enbuild.2020.110110

Heier, J., Bales, C., & Martin, V. (2015). Combining thermal energy storage with buildings - A review. *Renewable and Sustainable Energy Reviews*, *42*, 1305–1325. https://doi.org/10.1016/j.rser.2014.11.031

Helwig, S., & Wanka, R. (2007). *Particle Swarm Optimization in High-Dimensional Bounded Search Spaces*. *Sis*, 198–205.

Hernández-Pérez, I., Álvarez, G., Xamán, J., Zavala-Guillén, I., Arce, J., & Simá, E. (2014). Thermal performance of reflective materials applied to exterior building components - A review. *Energy and Buildings*, *80*, 81–105. https://doi.org/10.1016/j.enbuild.2014.05.008

Ho, L. S., & Huynh, T. P. (2022). Recycled waste medical glass as a fine aggregate replacement in low environmental impact concrete: Effects on long-term strength and durability performance. *Journal of Cleaner Production*, *368*(February), 133144. https://doi.org/10.1016/j.jclepro.2022.133144

Holm, T. A., & Bremner, T. W. (2000). *State-of-the-Art Report on High-Strength , High-Durability Structural Low-Density Concrete for Applications in Severe Marine Environments Structures Laboratory*. *August*.

Hossain, M. U., Poon, C. S., Lo, I. M. C., & Cheng, J. C. P. (2016). Comparative environmental

evaluation of aggregate production from recycled waste materials and virgin sources by LCA. *Resources, Conservation and Recycling*, *109*, 67–77. https://doi.org/10.1016/j.resconrec.2016.02.009

Hosseini, M. R., Maghrebi, M., Akbarnezhad, A., Martek, I., & Arashpour, M. (2018). Analysis of Citation Networks in Building Information Modeling Research. *Journal of Construction Engineering and Management*, *144*(8), 1–13. https://doi.org/10.1061/(asce)co.1943-7862.0001492

Howlader, M. K., Rashid, M. H., Mallick, D., & Haque, T. (2012). Effects of aggregate types on thermal properties of concrete. *ARPN Journal of Engineering and Applied Sciences*, *7*(7), 900–907.

Huang, B., Wang, Y., Lu, W., & Cheng, M. (2022). Fabrication and energy efficiency of translucent concrete panel for building envelope. *Energy*, *248*, 123635. https://doi.org/10.1016/j.energy.2022.123635

Huang, L., Krigsvoll, G., Johansen, F., Liu, Y., & Zhang, X. (2018). Carbon emission of global construction sector. *Renewable and Sustainable Energy Reviews*, *81*(June 2016), 1906–1916. https://doi.org/10.1016/j.rser.2017.06.001

Humar, I., Ge, X., Xiang, L., Jo, M., Chen, M., & Zhang, J. (2011). Rethinking energy efficiency models of cellular networks with embodied energy. *IEEE Network*, *25*(2), 40–49. https://doi.org/10.1109/MNET.2011.5730527

Huntzinger, D. N., & Eatmon, T. D. (2009). A life-cycle assessment of Portland cement manufacturing: comparing the traditional process with alternative technologies. *Journal of Cleaner Production*, *17*(7), 668–675. https://doi.org/10.1016/j.jclepro.2008.04.007

Ibn-Mohammed, T., Greenough, R., Taylor, S., Ozawa-Meida, L., & Acquaye, A. (2013). Operational vs. embodied emissions in buildings - A review of current trends. *Energy and Buildings*, *66*, 232–245. https://doi.org/10.1016/j.enbuild.2013.07.026

Ihara, T., Gustavsen, A., & Petter, B. (2015). Effect of facade components on energy efficiency in office buildings. *Applied Energy*, *158*, 422–432. https://doi.org/10.1016/j.apenergy.2015.08.074

Imbabi, M. S., Carrigan, C., & McKenna, S. (2012). Trends and developments in green cement and concrete technology. *International Journal of Sustainable Built Environment*, *1*(2), 194–216. https://doi.org/10.1016/j.ijsbe.2013.05.001

Imran, M., Khushnood, R. A., & Fawad, M. (2023). A hybrid data-driven and metaheuristic optimization approach for the compressive strength prediction of high-performance

concrete. *Case Studies in Construction Materials*, *18*, e01890. https://doi.org/10.1016/j.cscm.2023.e01890

IotaComm. (2020). *Benchmarking Commercial Building Energy Use Per Square Foot | Iota*. https://www.iotacommunications.com/blog/benchmarking-commercial-building-energy-use-per-square-foot/

Ismail, H. B., Mahmud, K., Daniel, Anuar, N. H., Azman, N. S., Wahab, M. A. A., Ibrahim, M. J. M., Saripudin, S. S., Nawi, N. M., & Jamal, M. H. (2018). Evaluation on the mechanical properties of concrete using clay Brick as Sand substituation. *International Journal of Engineering and Technology(UAE)*, *7*(3.14 Special Issue 14), 403–406.

Ismail, S., & Ramli, M. (2013). Engineering properties of treated recycled concrete aggregate (RCA) for structural applications. *Construction and Building Materials*, *44*, 464–476. https://doi.org/10.1016/j.conbuildmat.2013.03.014

Jaillon, L., & Poon, C. S. (2008). Sustainable construction aspects of using prefabrication in dense urban environment: A Hong Kong case study. *Construction Management and Economics*, *26*(9), 953–966. https://doi.org/10.1080/01446190802259043

Ji, L., & Gallo, K. (2006). An agreement coefficient for image comparison. *Photogrammetric Engineering and Remote Sensing*, *72*(7), 823–833. https://doi.org/10.14358/PERS.72.7.823

Ji, Y., Duanmu, L., Liu, Y., & Dong, H. (2020). Air infiltration rate of typical zones of public buildings under natural conditions. *Sustainable Cities and Society*, *61*(June 2019), 102290. https://doi.org/10.1016/j.scs.2020.102290

Jia, Z., Wang, Z., Hwang, D., & Wang, L. (2018). Prediction of the Effective Thermal Conductivity of Hollow Sphere Foams. *ACS Applied Energy Materials*, *1*(3), 1146–1157. https://doi.org/10.1021/acsaem.7b00264

Jiang, X., Xiao, R., Bai, Y., Huang, B., & Ma, Y. (2022). Influence of waste glass powder as a supplementary cementitious material (SCM) on physical and mechanical properties of cement paste under high temperatures. *Journal of Cleaner Production*, *340*(January), 130778. https://doi.org/10.1016/j.jclepro.2022.130778

Jiao, D., Shi, C., Yuan, Q., An, X., Liu, Y., & Li, H. (2017). Effect of constituents on rheological properties of fresh concrete-A review. *Cement and Concrete Composites*, *83*, 146–159. https://doi.org/10.1016/j.cemconcomp.2017.07.016

Johra, H., Margheritini, L., Ivanov Antonov, Y., Meyer Frandsen, K., Enggrob Simonsen, M., Møldrup, P., & Lund Jensen, R. (2021). Thermal, moisture and mechanical properties of Seacrete: A sustainable sea-grown building material. *Construction and Building Materials*,

266, 121025. https://doi.org/10.1016/j.conbuildmat.2020.121025

Jones, M. R., & McCarthy, A. (2006). Heat of hydration in foamed concrete: Effect of mix constituents and plastic density. *Cement and Concrete Research*, *36*(6), 1032–1041. https://doi.org/10.1016/j.cemconres.2006.01.011

Kalamees, T., Jylhä, K., Tietäväinen, H., Jokisalo, J., Ilomets, S., Hyvönen, R., & Saku, S. (2012). Development of weighting factors for climate variables for selecting the energy reference year according to the en ISO 15927-4 standard. *Energy and Buildings*, *47*, 53–60. https://doi.org/10.1016/j.enbuild.2011.11.031

Kaloop, M. R., Kumar, D., Samui, P., Hu, J. W., & Kim, D. (2020). Compressive strength prediction of high-performance concrete using gradient tree boosting machine. *Construction and Building Materials*, *264*, 120198. https://doi.org/10.1016/j.conbuildmat.2020.120198

Kandiri, A., Mohammadi Golafshani, E., & Behnood, A. (2020). Estimation of the compressive strength of concretes containing ground granulated blast furnace slag using hybridized multi-objective ANN and salp swarm algorithm. *Construction and Building Materials*, *248*, 118676. https://doi.org/10.1016/j.conbuildmat.2020.118676

Karimpour, M., Belusko, M., Xing, K., & Bruno, F. (2014). Minimising the life cycle energy of buildings: Review and analysis. *Building and Environment*, *73*, 106–114. https://doi.org/10.1016/j.buildenv.2013.11.019

Kashani, A., Ngo, T. D., & Hajimohammadi, A. (2019). Effect of recycled glass fines on mechanical and durability properties of concrete foam in comparison with traditional cementitious fines. *Cement and Concrete Composites*, *99*(October 2017), 120–129. https://doi.org/10.1016/j.cemconcomp.2019.03.004

Kavousian, A., Rajagopal, R., & Fischer, M. (2013). Determinants of residential electricity consumption : Using smart meter data to examine the effect of climate , building characteristics , appliance stock , and occupants ' behavior. *Energy*, *55*, 184–194. https://doi.org/10.1016/j.energy.2013.03.086

Kazmi, S. M. S., Munir, M. J., Wu, Y. F., Lin, X., & Ahmad, M. R. (2021). Investigation of thermal performance of concrete incorporating different types of recycled coarse aggregates. *Construction and Building Materials*, *270*, 121433. https://doi.org/10.1016/j.conbuildmat.2020.121433

Ke, Y., Beaucour, A. L., Ortola, S., Dumontet, H., & Cabrillac, R. (2009). Influence of volume fraction and characteristics of lightweight aggregates on the mechanical properties of concrete. *Construction and Building Materials*, *23*(8), 2821–2828.

https://doi.org/10.1016/j.conbuildmat.2009.02.038

Khademi, F., Behfarnia, K., & Engineering, S. (n.d.). *EVALUATION OF CONCRETE COMPRESSIVE STRENGTH c r v i h o e f*.

Khademi, F., Mohammadmehdi, S., & Deshpande, N. (2016). Predicting strength of recycled aggregate concrete using Artificial Neural Network , Adaptive Neuro-Fuzzy Inference System and Multiple Linear Regression. *International Journal of Sustainable Built Environment*, *5*(2), 355–369. https://doi.org/10.1016/j.ijsbe.2016.09.003

Khan, M. S., Sanchez, F., & Zhou, H. (2020). 3-D printing of concrete: Beyond horizons. *Cement and Concrete Research*, *133*(December 2019), 106070. https://doi.org/10.1016/j.cemconres.2020.106070

Khan, S. A., Koç, M., & Al-Ghamdi, S. G. (2021). Sustainability assessment, potentials and challenges of 3D printed concrete structures: A systematic review for built environmental applications. *Journal of Cleaner Production*, *303*, 127027. https://doi.org/10.1016/j.jclepro.2021.127027

Khasreen, M. M., Banfill, P. F. G., & Menzies, G. F. (2009). Life-cycle assessment and the environmental impact of buildings: A review. *Sustainability*, *1*(3), 674–701. https://doi.org/10.3390/su1030674

Khedari, J., Suttisonk, B., Pratinthong, N., & Hirunlabh, J. (2001). New lightweight composite construction materials with low thermal conductivity. *Cement and Concrete Composites*, *23*(1), 65–70. https://doi.org/10.1016/S0958-9465(00)00072-X

Kim, K.-H., Jeon, S.-E., Kim, J.-K., & Yang, S. (2003). An experimental study on thermal conductivity of concrete. *Cement and Concrete Research*, *33*(3), 363–371.

Kim, K., Shin, M., & Cha, S. (2013). Combined effects of recycled aggregate and fly ash towards concrete sustainability. *Construction and Building Materials*, *48*, 499–507. https://doi.org/10.1016/j.conbuildmat.2013.07.014

Kishore, R. A., Bianchi, M. V. A., Booten, C., Vidal, J., & Jackson, R. (2020). Optimizing PCM-integrated walls for potential energy savings in U.S. Buildings. *Energy and Buildings*, *226*, 110355. https://doi.org/10.1016/j.enbuild.2020.110355

Kisku, N., Rajhans, P., Panda, S. K., Nayak, S., & Pandey, V. (2020). Development of durable concrete from C&D waste by adopting identical mortar volume method in conjunction with two-stage mixing procedure. *Construction and Building Materials*, *256*, 119361. https://doi.org/10.1016/j.conbuildmat.2020.119361

Klusemann, B., & Svendsen, B. (2010). Homogenization methods formulti-phase elastic

composites: Comparisons and benchmarks. *Technische Mechanik*, *30*(4), 374–386.

Kossecka, E., & Kosny, J. (2002). Influence of insulation configuration on heating and cooling loads in a continuously used building. *Energy and Buildings*, *34*(4), 321–331. https://doi.org/10.1016/S0378-7788(01)00121-9

Kovacic, I., & Zoller, V. (2015). Building life cycle optimization tools for early design phases. *Energy*, *92*, 409–419. https://doi.org/10.1016/j.energy.2015.03.027

Kumanayake, R., & Luo, H. (2018). A tool for assessing life cycle CO2 emissions of buildings in Sri Lanka. *Building and Environment*, *128*(October 2017), 272–286. https://doi.org/10.1016/j.buildenv.2017.11.042

Kumutha, R., & Vijai, K. (2010). Strength of concrete incorporating aggregates recycled from demolition waste. *Journal of Engineering and Applied Sciences*, *5*(5), 64–71.

Kurda, R., de Brito, J., & Silvestre, J. D. (2019). CONCRETop method: Optimization of concrete with various incorporation ratios of fly ash and recycled aggregates in terms of quality performance and life-cycle cost and environmental impacts. *Journal of Cleaner Production*, *226*, 642–657. https://doi.org/10.1016/j.jclepro.2019.04.070

Kusuma, G. H., Budidarmawan, J., & Susilowati, A. (2015). Impact of concrete quality on sustainability. *Procedia Engineering*, *125*, 754–759. https://doi.org/10.1016/j.proeng.2015.11.122

Kuznik, F., Virgone, J., & Noel, J. (2008). Optimization of a phase change material wallboard for building use. *Applied Thermal Engineering*, *28*(11–12), 1291–1298. https://doi.org/10.1016/j.applthermaleng.2007.10.012

Lakhiar, M. T., Kong, S. Y., Bai, Y., Susilawati, S., Zahidi, I., Paul, S. C., & Raghunandan, M. E. (2022). Thermal and Mechanical Properties of Concrete Incorporating Silica Fume and Waste Rubber Powder. *Polymers*, *14*(22). https://doi.org/10.3390/polym14224858

Landsberg, D. R., Shonder, J. A., Barker, K. A., Haberl, J. S., Judson, S. A., Jump, D. A., Koran, W. E., Hall, R. L., Reindl, D. T., Anderson, J. R., Barnaby, C. S., Clark, J. A., Dunlap, J. F., Earley, J. W., Emmerich, S. J., & Graef, P. T. (2014). Measurement of Energy, Demand, and Water Savings. *ASHRAE Guideline 14-2014*, *4*, 1–150. www.ashrae.org%0Awww.ashrae.org/technology.

Lanzón, M., & García-Ruiz, P. A. (2008). Lightweight cement mortars: Advantages and inconveniences of expanded perlite and its influence on fresh and hardened state and durability. *Construction and Building Materials*, *22*(8), 1798–1806. https://doi.org/10.1016/j.conbuildmat.2007.05.006

Lee, J. M., Kim, M. J., Kim, S. K., & Yang, H. J. (2022). Enhancing CO2 balance in concrete through carbonation during a service life using organic liquid emitting diode (OLED) as a binder. *Journal of Cleaner Production*, *343*(February), 130936. https://doi.org/10.1016/j.jclepro.2022.130936

Lee, J. W., Jung, H. J., Park, J. Y., Lee, J. B., & Yoon, Y. (2013). Optimization of building window system in Asian regions by analyzing solar heat gain and daylighting elements. *Renewable Energy*, *50*, 522–531. https://doi.org/10.1016/j.renene.2012.07.029

Lesovik, V. S., Lesovik, R. V., & Albo Ali, W. S. (2021). Effect of recycled course aggregate from concrete debris on the strength of concrete. *Journal of Physics: Conference Series*, *1926*(1). https://doi.org/10.1088/1742-6596/1926/1/012002

Li, Q., Ju, Z., Wang, Z., Ma, L., Jiang, W., Li, D., & Jia, J. (2022). Thermal performance and economy of PCM foamed cement walls for buildings in different climate zones. *Energy and Buildings*, *277*, 112470. https://doi.org/10.1016/j.enbuild.2022.112470

Li, X., Qin, D., Hu, Y., Ahmad, W., Ahmad, A., Aslam, F., & Joyklad, P. (2022). A systematic review of waste materials in cement-based composites for construction applications. *Journal of Building Engineering*, *45*(October 2021), 103447. https://doi.org/10.1016/j.jobe.2021.103447

Li, Z., Hojati, M., Wu, Z., Piasente, J., Ashrafi, N., Duarte, J. P., Nazarian, S., Bilén, S. G., Memari, A. M., & Radlińska, A. (2020). Fresh and hardened properties of extrusion-based 3D-printed cementitious materials: A review. *Sustainability (Switzerland)*, *12*(14), 1–33. https://doi.org/10.3390/su12145628

Liang, C., Cai, Z., Wu, H., Xiao, J., Zhang, Y., & Ma, Z. (2021). Chloride transport and induced steel corrosion in recycled aggregate concrete: A review. *Construction and Building Materials*, *282*, 122547. https://doi.org/10.1016/j.conbuildmat.2021.122547

Liang, H., & Song, W. (2009). Improved estimation in multiple linear regression models with measurement error and general constraint. *Journal of Multivariate Analysis*, *100*(4), 726–741. https://doi.org/10.1016/j.jmva.2008.08.003

Limbachiya, M. C., Leelawat, T., & Dhir, R. K. (2000). Use of recycled concrete aggregate in high-strength concrete. *Materials and Structures/Materiaux et Constructions*, *33*(9), 574–580. https://doi.org/10.1007/bf02480538

Lin, Y. H., Tyan, Y. Y., Chang, T. P., & Chang, C. Y. (2004). An assessment of optimal mixture for concrete made with recycled concrete aggregates. *Cement and Concrete Research*, *34*(8), 1373–1380. https://doi.org/10.1016/j.cemconres.2003.12.032

Ling, T. C., & Poon, C. S. (2013). Use of phase change materials for thermal energy storage in concrete: An overview. *Construction and Building Materials*, *46*, 55–62. https://doi.org/10.1016/j.conbuildmat.2013.04.031

Lippiatt, B. C. (2002). BEES®3.0. *Building for Environmental and Economic Sustainability Technical Manual and User Guide", NISTIR*, *6916*, 8–28.

Liu, C., Wang, X., Chen, Y., Zhang, C., Ma, L., Deng, Z., Chen, C., Zhang, Y., Pan, J., & Banthia, N. (2021). Influence of hydroxypropyl methylcellulose and silica fume on stability, rheological properties, and printability of 3D printing foam concrete. *Cement and Concrete Composites*, *122*(June), 104158. https://doi.org/10.1016/j.cemconcomp.2021.104158

Liu, M. Y. J., Alengaram, U. J., Jumaat, M. Z., & Mo, K. H. (2014). Evaluation of thermal conductivity, mechanical and transport properties of lightweight aggregate foamed geopolymer concrete. *Energy and Buildings*, *72*, 238–245. https://doi.org/10.1016/j.enbuild.2013.12.029

Liu, Y., Chen, G., Wang, Z., Chen, Z., Gao, Y., & Li, F. (2020). On the seismic performance of autoclaved aerated concrete self-insulation block walls. *Materials*, *13*(13), 1–13. https://doi.org/10.3390/ma13132942

Liu, Y., Huang, S., Li, L., Xiao, H., Chen, Z., & Mao, H. (2021). Experimental and numerical studies on the direct shear behavior of sand–rca (Recycled concrete aggregates) mixtures with different contents of rca. *Materials*, *14*(11). https://doi.org/10.3390/ma14112909

Liu, Z., Li, M., Weng, Y., Wong, T. N., & Tan, M. J. (2019). Mixture Design Approach to optimize the rheological properties of the material used in 3D cementitious material printing. *Construction and Building Materials*, *198*, 245–255. https://doi.org/10.1016/j.conbuildmat.2018.11.252

Lizana, J., Chacartegui, R., Barrios-Padura, A., & Valverde, J. M. (2017). Advances in thermal energy storage materials and their applications towards zero energy buildings: A critical review. *Applied Energy*, *203*, 219–239. https://doi.org/10.1016/j.apenergy.2017.06.008

Loonen, R. C. G. M., Trčka, M., Cóstola, D., & Hensen, J. L. M. (2013). Climate adaptive building shells: State-of-the-art and future challenges. *Renewable and Sustainable Energy Reviews*, *25*, 483–493. https://doi.org/10.1016/j.rser.2013.04.016

López-Alonso, M., Mart\'\in-Morales, M., Mart\'\inez-Echevarr\'\ia, M. J., Agrela, F., & Zamorano, M. (2021). Residual biomasses as aggregates applied in cement-based materials. In *Waste and Byproducts in Cement-Based Materials* (pp. 89–137). Elsevier.

López, E., Manuel, F., Ramírez, D., & Ballester, F. (2013). *Thermal evaluation of structural*

concretes for construction of biodigesters. *58*, 310–318. https://doi.org/10.1016/j.enbuild.2012.11.036

López Gayarre, F., López-Colina Pérez, C., Serrano López, M. A., & Domingo Cabo, A. (2014). The effect of curing conditions on the compressive strength of recycled aggregate concrete. *Construction and Building Materials*, *53*, 260–266. https://doi.org/10.1016/j.conbuildmat.2013.11.112

Lu, B., Qian, Y., Li, M., Weng, Y., Leong, K. F., Tan, M. J., & Qian, S. (2019). Designing spray-based 3D printable cementitious materials with fly ash cenosphere and air entraining agent. *Construction and Building Materials*, *211*, 1073–1084. https://doi.org/10.1016/j.conbuildmat.2019.03.186

Lu, B., Zhu, W., Weng, Y., Liu, Z., Yang, E. H., Leong, K. F., Tan, M. J., Wong, T. N., & Qian, S. (2020). Study of MgO-activated slag as a cementless material for sustainable spray-based 3D printing. *Journal of Cleaner Production*, *258*, 120671. https://doi.org/10.1016/j.jclepro.2020.120671

Lu, W., Tam, V. W. Y., Chen, H., & Du, L. (2020). A holistic review of research on carbon emissions of green building construction industry. *Engineering, Construction and Architectural Management*, *27*(5), 1065–1092. https://doi.org/10.1108/ECAM-06-2019-0283

Lu, Y., Wang, S., & Shan, K. (2015). Design optimization and optimal control of grid-connected and standalone nearly/net zero energy buildings. *Applied Energy*, *155*, 463–477. https://doi.org/10.1016/j.apenergy.2015.06.007

Luo, Y., Zhang, L., Bozlar, M., Liu, Z., Guo, H., & Meggers, F. (2019). Active building envelope systems toward renewable and sustainable energy. *Renewable and Sustainable Energy Reviews*, *104*(February), 470–491. https://doi.org/10.1016/j.rser.2019.01.005

M.I. Khan. (2002). Factors affecting the thermal properties of concrete and applicability of its prediction models. *Building and Environment*, *37*, 607–614.

MacDonald, I., & Strachan, P. (2001). Practical application of uncertainty analysis. *Energy and Buildings*, *33*(3), 219–227. https://doi.org/10.1016/S0378-7788(00)00085-2

Mah, C. M., Fujiwara, T., & Ho, C. S. (2018). Life cycle assessment and life cycle costing toward eco-efficiency concrete waste management in Malaysia. *Journal of Cleaner Production*, *172*, 3415–3427. https://doi.org/10.1016/j.jclepro.2017.11.200

Mahadevan, M., Francis, A., & Thomas, A. (2020). A simulation-based investigation of sustainability aspects of 3D printed structures. *Journal of Building Engineering*, *32*(August),

101735. https://doi.org/10.1016/j.jobe.2020.101735

Majdi, H. M. A., & Li, Z. (2016). Mechanical and thermal insulation properties of high volume fly ash fiber reinforced cement composite (HVFA-FRCC) manufactured by extrusion technique. *Sustainable Construction Materials and Technologies*, *2016-Augus*, 1–7. https://doi.org/10.18552/2016/scmt4s152

Majhi, R. K., & Nayak, A. N. (2020). Production of sustainable concrete utilising high-volume blast furnace slag and recycled aggregate with lime activator. *Journal of Cleaner Production*, *255*, 120188. https://doi.org/10.1016/j.jclepro.2020.120188

Majumdar, K., Thakur, B., & Majumdar, A. (2022). Natural Fiber Reinforced Concrete: Bibliometric and Network Analyses to Delineate the Current Status and Future Pathways. *Journal of Natural Fibers*, *19*(17), 1–21. https://doi.org/10.1080/15440478.2022.2140323

Makul, N., & Sua-Iam, G. (2016). Characteristics and utilization of sugarcane filter cake waste in the production of lightweight foamed concrete. *Journal of Cleaner Production*, *126*, 118–133. https://doi.org/10.1016/j.jclepro.2016.02.111

Małek, M., Jackowski, M., Łasica, W., & Kadela, M. (2021). Influence of polypropylene, glass and steel fiber on the thermal properties of concrete. *Materials*, *14*(8). https://doi.org/10.3390/ma14081888

Malešev, M., Radonjanin, V., & Marinković, S. (2010). Recycled concrete as aggregate for structural concrete production. *Sustainability*, *2*(5), 1204–1225. https://doi.org/10.3390/su2051204

Manzi, S., Mazzotti, C., & Bignozzi, M. C. (2013). Short and long-term behavior of structural concrete with recycled concrete aggregate. *Cement and Concrete Composites*, *37*(1), 312–318. https://doi.org/10.1016/j.cemconcomp.2013.01.003

Marais, H., Christen, H., Cho, S., De Villiers, W., & Van Zijl, G. (2021a). Computational assessment of thermal performance of 3D printed concrete wall structures with cavities. *Journal of Building Engineering*, *41*(December 2020). https://doi.org/10.1016/j.jobe.2021.102431

Marais, H., Christen, H., Cho, S., De Villiers, W., & Van Zijl, G. (2021b). Computational assessment of thermal performance of 3D printed concrete wall structures with cavities. *Journal of Building Engineering*, *41*(February). https://doi.org/10.1016/j.jobe.2021.102431

Marinoski, D. L., Güths, S., & Lamberts, R. (2012). Development of a calorimeter for determination of the solar factor of architectural glass and fenestrations. *Building and Environment*, *47*(1), 232–242. https://doi.org/10.1016/j.buildenv.2011.07.017

Markin, V., Krause, M., Otto, J., Schröfl, C., & Mechtcherine, V. (2021). 3D-printing with foam concrete: From material design and testing to application and sustainability. *Journal of Building Engineering*, *43*(June). https://doi.org/10.1016/j.jobe.2021.102870

Markin, V., Nerella, V. N., Schröfl, C., Guseynova, G., & Mechtcherine, V. (2019). Material design and performance evaluation of foam concrete for digital fabrication. *Materials*, *12*(15). https://doi.org/10.3390/ma12152433

Markin, V., Sahmenko, G., Nerella, V. N., Nather, M., & Mechtcherine, V. (2019). Investigations on the foam concrete production techniques suitable for 3D-printing with foam concrete. *IOP Conference Series: Materials Science and Engineering*, *660*(1). https://doi.org/10.1088/1757-899X/660/1/012039

Markin, V., Sahmenko, G., Nerella, V. N., Näther, M., & Mechtcherine, V. (2019). Investigations on the foam concrete production techniques suitable for 3D-printing with foam concrete. *IOP Conference Series: Materials Science and Engineering*, *660*(1), 12039.

Martinez, C. M., del Bosque, I. F. S., Medina, G., Fr\'\ias, M., & de Rojas, M. I. S. (2022). Thermal performance of concrete with recycled concrete powder as partial cement replacement and recycled CDW aggregate. *The Structural Integrity of Recycled Aggregate Concrete Produced with Fillers and Pozzolans*, 105–143.

Matias, D., De Brito, J., Rosa, A., & Pedro, D. (2013). Mechanical properties of concrete produced with recycled coarse aggregates - Influence of the use of superplasticizers. *Construction and Building Materials*, *44*, 101–109. https://doi.org/10.1016/j.conbuildmat.2013.03.011

May Tzuc, O., Rodríguez Gamboa, O., Aguilar Rosel, R., Che Poot, M., Edelman, H., Jiménez Torres, M., & Bassam, A. (2021). Modeling of hygrothermal behavior for green facade's concrete wall exposed to nordic climate using artificial intelligence and global sensitivity analysis. *Journal of Building Engineering*, *33*(July 2020). https://doi.org/10.1016/j.jobe.2020.101625

Medina, C., Zhu, W., Howind, T., Sánchez De Rojas, M. I., & Frías, M. (2014). Influence of mixed recycled aggregate on the physical-mechanical properties of recycled concrete. *Journal of Cleaner Production*, *68*, 216–225. https://doi.org/10.1016/j.jclepro.2014.01.002

Meglin, R., & Kytzia, S. (2019). Environmental assessment in the building materials industry: How are the results of life-cycle-assessment (LCA) for concrete influenced by technology and regulations? *Sustainable Construction Materials and Technologies*, *2*. https://doi.org/10.18552/2019/idscmt5108

Meho, L. I., & Rogers, Y. (2008). Citation counting, citation ranking, and h-index of human-computer interaction researchers: a comparison of Scopus and Web of Science. *Journal of the American Society for Information Science and Technology*, *59*(11), 1711–1726.

Mehta, P. K. (2010). Sustainable cements and concrete for the climate change era - A review. *2nd International Conference on Sustainable Construction Materials and Technologies*, 1–10.

Memon, S. A., Cui, H., Lo, T. Y., & Li, Q. (2015). Development of structural-functional integrated concrete with macro-encapsulated PCM for thermal energy storage. *Applied Energy*, *150*, 245–257. https://doi.org/10.1016/j.apenergy.2015.03.137

Meyer, C. (2006). Aerated Concrete as a Green Building Material. *Aerated Concrete*, *1*(October), 10.

Miller, D., Doh, J. H., & Mulvey, M. (2015). Concrete slab comparison and embodied energy optimisation for alternate design and construction techniques. *Construction and Building Materials*, *80*, 329–338. https://doi.org/10.1016/j.conbuildmat.2015.01.071

Miller, S. A. (2018). Supplementary cementitious materials to mitigate greenhouse gas emissions from concrete: can there be too much of a good thing? *Journal of Cleaner Production*, *178*, 587–598. https://doi.org/10.1016/j.jclepro.2018.01.008

Miller, S. A., & Moore, F. C. (2020). production. *Nature Climate Change*, *10*(May). https://doi.org/10.1038/s41558-020-0733-0

Mirrahimi, S., Mohamed, M. F., Haw, L. C., Ibrahim, N. L. N., Yusoff, W. F. M., & Aflaki, A. (2016). The effect of building envelope on the thermal comfort and energy saving for high-rise buildings in hot-humid climate. *Renewable and Sustainable Energy Reviews*, *53*, 1508–1519. https://doi.org/10.1016/j.rser.2015.09.055

Mithraratne, N., & Vale, B. (2004). Life cycle analysis model for New Zealand houses. *Building and Environment*, *39*(4), 483–492. https://doi.org/10.1016/j.buildenv.2003.09.008

Mo, K. H., Ling, T. C., Alengaram, U. J., Yap, S. P., & Yuen, C. W. (2017). Overview of supplementary cementitious materials usage in lightweight aggregate concrete. *Construction and Building Materials*, *139*, 403–418. https://doi.org/10.1016/j.conbuildmat.2017.02.081

Mohamad, N., Muthusamy, K., Embong, R., Kusbiantoro, A., & Hashim, M. H. (2021). Environmental impact of cement production and Solutions: A review. *Materials Today: Proceedings*, *48*, 741–746. https://doi.org/10.1016/j.matpr.2021.02.212

Mohammad, M., Masad, E., Seers, T., & Al-Ghamdi, S. G. (2020). High-performance light-weight concrete for 3D printing. *Second RILEM International Conference on Concrete and Digital Fabrication: Digital Concrete 2020 2*, 459–467.

Mohammadi, E., Arashpour, M., & Kashani, A. (2021). Green mix design of rubbercrete using machine learning-based ensemble model and constrained multi-objective optimization. *Journal of Cleaner Production*, *327*(February), 129518. https://doi.org/10.1016/j.jclepro.2021.129518

Mottahedi, M., Mohammadpour, A., Amiri, S. S., Riley, D., & Asadi, S. (2015). Multi-linear Regression Models to Predict the Annual Energy Consumption of an Office Building with Different Shapes. *Procedia Engineering*, *118*, 622–629. https://doi.org/10.1016/j.proeng.2015.08.495

Mukharjee, B. B., & Barai, S. V. (2014). Influence of Nano-Silica on the properties of recycled aggregate concrete. *Construction and Building Materials*, *55*, 29–37. https://doi.org/10.1016/j.conbuildmat.2014.01.003

Mukherjee, S. P., & Vesmawala, G. (2013). Literature Review on Technical Aspect of Sustainable Concrete. *International Journal of Engineering Science Invention*, *2*(8), 1–9. www.ijesi.org

Mullett, P. (2022). Innovation in construction. A practical guide to transforming the construction industry. In *The Handbook of Innovation and Services: A Multi-disciplinary Perspective*. https://doi.org/10.1007/978-3-030-95798-8

Muñoz-Ruiperez, C., Rodríguez, A., Gutiérrez-González, S., & Calderón, V. (2016). Lightweight masonry mortars made with expanded clay and recycled aggregates. *Construction and Building Materials*, *118*, 139–145. https://doi.org/10.1016/j.conbuildmat.2016.05.065

Muthukrishnan, S., Ramakrishnan, S., & Sanjayan, J. (2021). Technologies for improving buildability in 3D concrete printing. *Cement and Concrete Composites*, *122*(May), 104144. https://doi.org/10.1016/j.cemconcomp.2021.104144

Myatt, G. J. (2007). *Making sense of data: a practical guide to exploratory data analysis and data mining*. John Wiley \& Sons.

Mydin, M. A. O. (2011). Effective thermal conductivity of foamcrete of different densities. *Concrete Research Letters*, *2*(1), 181–189. www.crl.issres.net

N H Zahari, I. A. R. and A. M. H. Z. (2009). Foamed Concrete: Potential Application in Thermal Insulation. *Muceet*, 47–52. http://eprints.uthm.edu.my/1759/1/Muceet_2009.pdf

Najjar, M., Figueiredo, K., Hammad, A. W. A., & Haddad, A. (2019). Integrated optimization with building information modeling and life cycle assessment for generating energy efficient buildings. *Applied Energy*, *250*(April), 1366–1382. https://doi.org/10.1016/j.apenergy.2019.05.101

Napolano, L., Menna, C., Graziano, S. F., Asprone, D., D'Amore, M., De Gennaro, R., & Dondi, M. (2016). Environmental life cycle assessment of lightweight concrete to support recycled materials selection for sustainable design. *Construction and Building Materials*, *119*, 370–384. https://doi.org/10.1016/j.conbuildmat.2016.05.042

Narayanan, N., & Ramamurthy, K. (2000). Microstructural investigations on aerated concrete. *Cement and Concrete Research*, *30*(3), 457–464. https://doi.org/10.1016/S0008-8846(00)00199-X

Naseri, H., Jahanbakhsh, H., Hosseini, P., & Moghadas Nejad, F. (2020). Designing sustainable concrete mixture by developing a new machine learning technique. *Journal of Cleaner Production*, *258*, 120578. https://doi.org/10.1016/j.jclepro.2020.120578

Natekin, A., & Knoll, A. (2013). Gradient boosting machines, a tutorial. *Frontiers in Neurorobotics*, *7*(DEC). https://doi.org/10.3389/fnbot.2013.00021

Nejat, P., Jomehzadeh, F., Taheri, M. M., Gohari, M., & Muhd, M. Z. (2015). A global review of energy consumption, CO2 emissions and policy in the residential sector (with an overview of the top ten CO2 emitting countries). *Renewable and Sustainable Energy Reviews*, *43*, 843–862. https://doi.org/10.1016/j.rser.2014.11.066

Nepomuceno, M. C. S., Isidoro, R. A. S., & Catarino, J. P. G. (2018). Mechanical performance evaluation of concrete made with recycled ceramic coarse aggregates from industrial brick waste. *Construction and Building Materials*, *165*, 284–294. https://doi.org/10.1016/j.conbuildmat.2018.01.052

Neter, J., Kutner, M. H., Nachtsheim, C. J., Wasserman, W., & others. (1996). *Applied linear statistical models*.

Neto, A. H., & Fiorelli, F. A. S. (2008). Comparison between detailed model simulation and artificial neural network for forecasting building energy consumption. *Energy and Buildings*, *40*(12), 2169–2176. https://doi.org/10.1016/j.enbuild.2008.06.013

Nguyen, L. H., Beaucour, A. L., Ortola, S., & Noumowé, A. (2014). Influence of the volume fraction and the nature of fine lightweight aggregates on the thermal and mechanical properties of structural concrete. *Construction and Building Materials*, *51*, 121–132. https://doi.org/10.1016/j.conbuildmat.2013.11.019

Nik, V. M., & Kalagasidis, A. S. (2013). Impact study of the climate change on the energy performance of the building stock in Stockholm considering four climate uncertainties. *Building and Environment*, *60*, 291–304. https://doi.org/10.1016/j.buildenv.2012.11.005

Nunez, I., & Nehdi, M. L. (2021). Machine learning prediction of carbonation depth in recycled

aggregate concrete incorporating SCMs. *Construction and Building Materials*, *287*, 123027. https://doi.org/10.1016/j.conbuildmat.2021.123027

Oh, B. K., Park, J. S., Choi, S. W., & Park, H. S. (2016). Design model for analysis of relationships among CO2 emissions, cost, and structural parameters in green building construction with composite columns. *Energy and Buildings*, *118*, 301–315. https://doi.org/10.1016/j.enbuild.2016.03.015

Oladinrin, O. T., Arif, M., Rana, M. Q., & Gyoh, L. (2022). Interrelations between construction ethics and innovation: a bibliometric analysis using VOSviewer. *Construction Innovation*. https://doi.org/10.1108/CI-07-2021-0130

Omer, A. M. (2008). *Energy , environment and sustainable development*. *12*, 2265–2300. https://doi.org/10.1016/j.rser.2007.05.001

Ooms, T., Vantyghem, G., Van Coile, R., & De Corte, W. (2021). A parametric modelling strategy for the numerical simulation of 3D concrete printing with complex geometries. *Additive Manufacturing*, *38*(December 2020), 101743. https://doi.org/10.1016/j.addma.2020.101743

Ordoñez, A., Carreras, J., Korolija, I., Zhang, Y., & Coronas, A. (2014). Impact Of Building Geometry On Its Energy Performance Depending On Climate Zones. *BSO 14 - Building Simulation and Optimisation, the Second IBPSA England Conference, June 23-24, 2014, UCL, February 2016*.

Oyebisi, S., & Alomayri, T. (2022). Cement-based concrete modified with Vitellaria Paradoxa ash: A lifecycle assessment. *Construction and Building Materials*, *342*(PA), 127906. https://doi.org/10.1016/j.conbuildmat.2022.127906

Pabst, W., Uhlířová, T., Gregorová, E., & Wiegmann, A. (2018). Young's modulus and thermal conductivity of closed-cell, open-cell and inverse ceramic foams – model-based predictions, cross-property predictions and numerical calculations. *Journal of the European Ceramic Society*, *38*(6), 2570–2578. https://doi.org/10.1016/j.jeurceramsoc.2018.01.019

Pachauri, R. K. (2016). The Intergovernmental Panel on Climate Change (IPCC) fifth assessment report and its implications for human health and urban areas. *Climate Health Risks in Megacities: Sustainable Management and Strategic Planning*, 7–12. https://doi.org/10.1201/9781315367323-3

Pacheco, R., Ordóñez, J., & Martínez, G. (2012). Energy efficient design of building: A review. *Renewable and Sustainable Energy Reviews*, *16*(6), 3559–3573. https://doi.org/10.1016/j.rser.2012.03.045

Pacheco Torgal, F., Miraldo, S., Labrincha, J. A., & De Brito, J. (2012). An overview on concrete carbonation in the context of eco-efficient construction: Evaluation, use of SCMs and/or RAC. *Construction and Building Materials*, *36*, 141–150. https://doi.org/10.1016/j.conbuildmat.2012.04.066

Palomar, I., Barluenga, G., & Puentes, J. (2015). Lime-cement mortars for coating with improved thermal and acoustic performance. *Construction and Building Materials*, *75*, 306–314. https://doi.org/10.1016/j.conbuildmat.2014.11.012

Panayiotou, G. P., Kalogirou, S. A., & Tassou, S. A. (2016). Evaluation of the application of Phase Change Materials (PCM) on the envelope of a typical dwelling in the Mediterranean region. *Renewable Energy*, *97*, 24–32. https://doi.org/10.1016/j.renene.2016.05.043

Panchabikesan, K., Vellaisamy, K., & Ramalingam, V. (2017). Passive cooling potential in buildings under various climatic conditions in India. *Renewable and Sustainable Energy Reviews*, *78*(May), 1236–1252. https://doi.org/10.1016/j.rser.2017.05.030

Panesar, D. K., & Zhang, R. (2020). Performance comparison of cement replacing materials in concrete: Limestone fillers and supplementary cementing materials – A review. *Construction and Building Materials*, *251*, 118866. https://doi.org/10.1016/j.conbuildmat.2020.118866

Panichella, A. (2019). An adaptive evolutionary algorithm based on non-euclidean geometry for many-objective optimization. *GECCO 2019 - Proceedings of the 2019 Genetic and Evolutionary Computation Conference*, 595–603. https://doi.org/10.1145/3321707.3321839

Panichella, A. (2022). An improved Pareto front modeling algorithm for large-scale many-objective optimization. *GECCO 2022 - Proceedings of the 2022 Genetic and Evolutionary Computation Conference*, *Lm*, 565–573. https://doi.org/10.1145/3512290.3528732

Park, H. S., Kwon, B., Shin, Y., Kim, Y., Hong, T., & Choi, S. W. (2013). Cost and CO2 emission optimization of steel reinforced concrete columns in high-rise buildings. *Energies*, *6*(11), 5609–5624. https://doi.org/10.3390/en6115609

Park, S. B., Yoon, E. S., & Lee, B. I. (1999). Effects of processing and materials variations on mechanical properties of lightweight cement composites. *Cement and Concrete Research*, *29*(2), 193–200. https://doi.org/10.1016/S0008-8846(98)00221-X

Pasupathy, K., Ramakrishnan, S., & Sanjayan, J. (2021). Formulating eco-friendly geopolymer foam concrete by alkali-activation of ground brick waste. *Journal of Cleaner Production*, *325*(September), 129180. https://doi.org/10.1016/j.jclepro.2021.129180

Pasupathy, K., Ramakrishnan, S., & Sanjayan, J. (2022a). Enhancing the properties of foam

concrete 3D printing using porous aggregates. *Cement and Concrete Composites*, *133*(July), 104687. https://doi.org/10.1016/j.cemconcomp.2022.104687

Pasupathy, K., Ramakrishnan, S., & Sanjayan, J. (2022b). Enhancing the properties of foam concrete 3D printing using porous aggregates. *Cement and Concrete Composites*, *133*(May), 104687. https://doi.org/10.1016/j.cemconcomp.2022.104687

Patel, D., Shrivastava, R., Tiwari, R. P., & Yadav, R. K. (2020). Properties of cement mortar in substitution with waste fine glass powder and environmental impact study. *Journal of Building Engineering*, *27*(December 2018), 100940. https://doi.org/10.1016/j.jobe.2019.100940

Paul, S. C., Tay, Y. W. D., Panda, B., & Tan, M. J. (2018). Fresh and hardened properties of 3D printable cementitious materials for building and construction. *Archives of Civil and Mechanical Engineering*, *18*(1), 311–319.

Paulson, A. J., Prabhavathy, R. A., Rekh, S., & Brindha, E. (2019). Application of neural network for prediction of compressive strength of silica fume concrete. *International Journal of Civil Engineering and Technology*, *10*(2), 1859–1867.

Pavel, C. C., & Blagoeva, D. T. (2018). Competitive landscape of the EU's insulation materials industry for energy-efficient buildings. *Publications Office of the European Union*, *EUR 28816*, 1–24. https://doi.org/10.2760/750646

Pec, I. B., & Milovanovic, B. (2020). *Recycled aggregate concrete for nearly zero-energy buildings*. *67*(11).

Pedro, D., de Brito, J., & Evangelista, L. (2015). Performance of concrete made with aggregates recycled from precasting industry waste: influence of the crushing process. *Materials and Structures/Materiaux et Constructions*, *48*(12), 3965–3978. https://doi.org/10.1617/s11527-014-0456-7

Pedro, D., de Brito, J., & Evangelista, L. (2017). Mechanical characterization of high performance concrete prepared with recycled aggregates and silica fume from precast industry. *Journal of Cleaner Production*, *164*, 939–949. https://doi.org/10.1016/j.jclepro.2017.06.249

Peippo, K., Lund, P. D., & Vartiainen, E. (1999). Multivariate optimization of design trade-offs for solar low energy buildings. *Energy and Buildings*, *29*(2), 189–205. https://doi.org/10.1016/s0378-7788(98)00055-3

Penadés-Plà, V., García-Segura, T., & Yepes, V. (2019). Accelerated optimization method for low-embodied energy concrete box-girder bridge design. *Engineering Structures*,

179(November 2018), 556–565. https://doi.org/10.1016/j.engstruct.2018.11.015

Penido, R. E.-K., da Paixão, R. C. F., Costa, L. C. B., Peixoto, R. A. F., Cury, A. A., & Mendes, J. C. (2022). Predicting the compressive strength of steelmaking slag concrete with machine learning – Considerations on developing a mix design tool. *Construction and Building Materials*, *341*(May), 127896. https://doi.org/10.1016/j.conbuildmat.2022.127896

Pepe, M., Toledo Filho, R. D., Koenders, E. A. B., & Martinelli, E. (2014). Alternative processing procedures for recycled aggregates in structural concrete. *Construction and Building Materials*, *69*, 124–132. https://doi.org/10.1016/j.conbuildmat.2014.06.084

Pérez-Bella, J. M., Domínguez-Hernández, J., Cano-Suñén, E., Del Coz-Díaz, J. J., & Álvarez Rabanal, F. P. (2015). A correction factor to approximate the design thermal conductivity of building materials. Application to Spanish façades. *Energy and Buildings*, *88*, 153–164. https://doi.org/10.1016/j.enbuild.2014.12.005

Pérez-Lombard, L., Ortiz, J., & Pout, C. (2008). A review on buildings energy consumption information. *Energy and Buildings*, *40*(3), 394–398. https://doi.org/10.1016/j.enbuild.2007.03.007

Perrot, A., Pierre, A., Nerella, V. N., Wolfs, R. J. M., Keita, E., Nair, S. A. O., Neithalath, N., Roussel, N., & Mechtcherine, V. (2021). From analytical methods to numerical simulations: A process engineering toolbox for 3D concrete printing. *Cement and Concrete Composites*, *122*(June), 104164. https://doi.org/10.1016/j.cemconcomp.2021.104164

Pisello, A. L., Goretti, M., & Cotana, F. (2012). A method for assessing buildings' energy efficiency by dynamic simulation and experimental activity. *Applied Energy*, *97*, 419–429. https://doi.org/10.1016/j.apenergy.2011.12.094

Pokorný, J., Ševčík, R., Šál, J., & Zárybnická, L. (2021). Lightweight blended building waste in the production of innovative cement-based composites for sustainable construction. *Construction and Building Materials*, *299*. https://doi.org/10.1016/j.conbuildmat.2021.123933

Poon, C. S., Kou, S. C., & Lam, L. (2007). Influence of recycled aggregate on slump and bleeding of fresh concrete. *Materials and Structures/Materiaux et Constructions*, *40*(9), 981–988. https://doi.org/10.1617/s11527-006-9192-y

Pop, O. G., Fechete Tutunaru, L., Bode, F., Abrudan, A. C., & Balan, M. C. (2018). Energy efficiency of PCM integrated in fresh air cooling systems in different climatic conditions. *Applied Energy*, *212*(September 2017), 976–996. https://doi.org/10.1016/j.apenergy.2017.12.122

Potbhare, V., Syal, M., & Korkmaz, S. (2009). Adoption of green building guidelines in developing countries based on u.s. and india experiences. *Journal of Green Building*, *4*(2), 158–174. https://doi.org/10.3992/jgb.4.2.158

Praseeda, K. I., Reddy, B. V. V., & Mani, M. (2016). Embodied and operational energy of urban residential buildings in India. *Energy and Buildings*, *110*, 211–219. https://doi.org/10.1016/j.enbuild.2015.09.072

Proshin, A. P., Beregovoi, V. A., Beregovoi, A. M., & Eremkin, A. I. (2005). Unautoclaved foam concrete and its constructions adapted to regional conditions. *Use of Foamed Concrete in Construction: Proceedings of the International Conference Held at the University of Dundee, Scotland, UK on 5 July 2005*, 113–120.

Qi, C., & Tang, X. (2018). Slope stability prediction using integrated metaheuristic and machine learning approaches: A comparative study. *Computers and Industrial Engineering*, *118*(August 2017), 112–122. https://doi.org/10.1016/j.cie.2018.02.028

Qin, D., Dong, C., Zong, Z., & Guo, Z. (2022). *Shrinkage and Creep of Sustainable Self-Compacting Concrete with Recycled Concrete Aggregates , Fly Ash , Slag , and Silica Fume*. *34*(9), 1–14. https://doi.org/10.1061/(ASCE)MT.1943-5533.0004393

Qu, X., & Zhao, X. (2017). Previous and present investigations on the components, microstructure and main properties of autoclaved aerated concrete – A review. *Construction and Building Materials*, *135*, 505–516. https://doi.org/10.1016/j.conbuildmat.2016.12.208

Qureshi, L. A., Ali, B., & Ali, A. (2020). Combined effects of supplementary cementitious materials (silica fume, GGBS, fly ash and rice husk ash) and steel fiber on the hardened properties of recycled aggregate concrete. *Construction and Building Materials*, *263*(2020), 120636. https://doi.org/10.1016/j.conbuildmat.2020.120636

Radhi, H. (2011). Viability of autoclaved aerated concrete walls for the residential sector in the United Arab Emirates. *Energy and Buildings*, *43*(9), 2086–2092. https://doi.org/10.1016/j.enbuild.2011.04.018

Rahla, K. M., Mateus, R., & Bragança, L. (2019). Comparative sustainability assessment of binary blended concretes using Supplementary Cementitious Materials (SCMs) and Ordinary Portland Cement (OPC). *Journal of Cleaner Production*, *220*, 445–459. https://doi.org/10.1016/j.jclepro.2019.02.010

Raj, A., Sathyan, D., & Mini, K. M. (2019). Physical and functional characteristics of foam concrete: A review. *Construction and Building Materials*, *221*, 787–799. https://doi.org/10.1016/j.conbuildmat.2019.06.052

Rajagopalan, N., Bilec, M. M., & Landis, A. E. (2010). Residential life cycle assessment modeling: Comparative case study of insulating concrete forms and traditional building materials. *Journal of Green Building*, *5*(3), 95–106. https://doi.org/10.3992/jgb.5.3.95

Ralegaonkar, R. V., & Gupta, R. (2010). Review of intelligent building construction: A passive solar architecture approach. *Renewable and Sustainable Energy Reviews*, *14*(8), 2238–2242. https://doi.org/10.1016/j.rser.2010.04.016

Ramamurthy, K., Kunhanandan Nambiar, E. K., & Indu Siva Ranjani, G. (2009). A classification of studies on properties of foam concrete. *Cement and Concrete Composites*, *31*(6), 388–396. https://doi.org/10.1016/j.cemconcomp.2009.04.006

Ramesh, T., Prakash, R., & Shukla, K. K. (2010a). *Life cycle energy analysis of buildings : An overview*. *42*, 1592–1600. https://doi.org/10.1016/j.enbuild.2010.05.007

Ramesh, T., Prakash, R., & Shukla, K. K. (2010b). Life cycle energy analysis of buildings: An overview. In *Energy and Buildings* (Vol. 42, Issue 10, pp. 1592–1600). Elsevier Ltd. https://doi.org/10.1016/j.enbuild.2010.05.007

Ramesh, T., Prakash, R., & Shukla, K. K. (2010c). Life cycle energy analysis of buildings: An overview. *Energy and Buildings*, *42*(10), 1592–1600.

Ramesh, T., Prakash, R., & Shukla, K. K. (2012). Life cycle energy analysis of a residential building with different envelopes and climates in Indian context. *Applied Energy*, *89*(1), 193–202. https://doi.org/10.1016/j.apenergy.2011.05.054

Ramos Ruiz, G., Fernández Bandera, C., Gómez-Acebo Temes, T., & Sánchez-Ostiz Gutierrez, A. (2016). Genetic algorithm for building envelope calibration. *Applied Energy*, *168*, 691–705. https://doi.org/10.1016/j.apenergy.2016.01.075

Rashad, A. M. (2018). Lightweight expanded clay aggregate as a building material – An overview. *Construction and Building Materials*, *170*, 757–775. https://doi.org/10.1016/j.conbuildmat.2018.03.009

Real, S., Bogas, J. A., Gomes, M. da G., & Ferrer, B. (2016). Thermal conductivity of structural lightweight aggregate concrete. *Magazine of Concrete Research*, *68*(15), 798–808.

Real, S., Gomes, M. G., Moret Rodrigues, A., & Bogas, J. A. (2016). Contribution of structural lightweight aggregate concrete to the reduction of thermal bridging effect in buildings. *Construction and Building Materials*, *121*, 460–470. https://doi.org/10.1016/j.conbuildmat.2016.06.018

Real, S., Maia, C., Bogas, J. A., & Da Gl ria Gomes, M. (2021). Thermal conductivity modelling of structural lightweight aggregate concrete. *Magazine of Concrete Research*, *73*(15), 798–

809. https://doi.org/10.1680/jmacr.19.00320

Reilly, A., & Kinnane, O. (2017). The impact of thermal mass on building energy consumption. *Applied Energy*, *198*, 108–121. https://doi.org/10.1016/j.apenergy.2017.04.024

Richards, D., Masoudi, M., Oh, R. R. Y., Yando, E. S., Zhang, J., Friess, D. A., Grêt-Regamey, A., Tan, P. Y., & Edwards, P. J. (2019). Global Variation in Climate, Human Development, and Population Density Has Implications for Urban Ecosystem Services. *Sustainability*, *11*(22), 6200. https://doi.org/10.3390/su11226200

Rivera, F., Martínez, P., Castro, J., & López, M. (2015). Massive volume fly-ash concrete: A more sustainable material with fly ash replacing cement and aggregates. *Cement and Concrete Composites*, *63*, 104–112. https://doi.org/10.1016/j.cemconcomp.2015.08.001

Robati, M., Kokogiannakis, G., & McCarthy, T. J. (2017). Impact of structural design solutions on the energy and thermal performance of an Australian office building. *Building and Environment*, *124*, 258–282. https://doi.org/10.1016/j.buildenv.2017.08.018

Roberz, F., Loonen, R. C. G. M., Hoes, P., & Hensen, J. L. M. (2017). Ultra-lightweight concrete : Energy and comfort performance evaluation in relation to buildings with low and high thermal mass. *Energy & Buildings*, *138*, 432–442. https://doi.org/10.1016/j.enbuild.2016.12.049

Rodrigues, C., & Freire, F. (2017). Environmental impact trade-offs in building envelope retrofit strategies. *International Journal of Life Cycle Assessment*, *22*(4), 557–570. https://doi.org/10.1007/s11367-016-1064-2

Roels, S., Bacher, P., Bauwens, G., Castaño, S., Jiménez, M. J., & Madsen, H. (2017). On site characterisation of the overall heat loss coefficient: Comparison of different assessment methods by a blind validation exercise on a round robin test box. *Energy and Buildings*, *153*, 179–189. https://doi.org/10.1016/j.enbuild.2017.08.006

Rwelamila, P. D., Talukhaba, A. A., & Ngowi, A. B. (2000). Project procurement systems in the attainment of sustainable construction. *Sustainable Development*, *8*(1), 39–50. https://doi.org/10.1002/(SICI)1099-1719(200002)8:1<39::AID-SD127>3.0.CO;2-Z

Saad, M., Abo-El-Enein, S. A., Hanna, G. B., & Kotkata, M. F. (1996). Effect of temperature on physical and mechanical properties of concrete containing silica fume. *Cement and Concrete Research*, *26*(5), 669–675.

Sadineni, S. B., Madala, S., & Boehm, R. F. (2011). Passive building energy savings: A review of building envelope components. *Renewable and Sustainable Energy Reviews*, *15*(8), 3617–3631. https://doi.org/10.1016/j.rser.2011.07.014

Saffari, M., De Gracia, A., Ushak, S., & Cabeza, L. F. (2016). Economic impact of integrating PCM as passive system in buildings using Fanger comfort model. *Energy and Buildings*, *112*, 159–172. https://doi.org/10.1016/j.enbuild.2015.12.006

Sagara, A., Tjondro, J. A., & Putri, D. K. (2017). Experimental Study of Fly Ash Density Effect to the Mortar Compressive Strength with Recycled Fine Aggregate. *Procedia Engineering*, *171*, 620–626. https://doi.org/10.1016/j.proeng.2017.01.395

Sakai, K. (2015). From the "Old" to a "New" construction industry-Sustainability design of structures. *Special Publication*, *305*, 40–41.

Salah Alaloul, W., Al Salaheen, M., Malkawi, A. B., Alzubi, K., Al-Sabaeei, A. M., & Ali Musarat, M. (2021). Utilizing of oil shale ash as a construction material: A systematic review. *Construction and Building Materials*, *299*, 123844. https://doi.org/10.1016/j.conbuildmat.2021.123844

Saleh, A. N., Attar, A. A., Ahmed, O. K., & Mustafa, S. S. (2021). Improving the thermal insulation and mechanical properties of concrete using Nano-SiO2. *Results in Engineering*, *12*(June), 100303. https://doi.org/10.1016/j.rineng.2021.100303

Samad, S., & Shah, A. (2017). Role of binary cement including Supplementary Cementitious Material (SCM), in production of environmentally sustainable concrete: A critical review. *International Journal of Sustainable Built Environment*, *6*(2), 663–674. https://doi.org/10.1016/j.ijsbe.2017.07.003

Samson, G., Phelipot-Mardelé, A., & Lanos, C. (2017). A review of thermomechanical properties of lightweight concrete. *Magazine of Concrete Research*, *69*(4), 201–216. https://doi.org/10.1680/jmacr.16.00324

Sandanayake, M., Gunasekara, C., Law, D., Zhang, G., & Setunge, S. (2018). Greenhouse gas emissions of different fly ash based geopolymer concretes in building construction. *Journal of Cleaner Production*, *204*, 399–408. https://doi.org/10.1016/j.jclepro.2018.08.311

Sandanayake, M., Zhang, G., Setunge, S., Luo, W., & Li, C. Q. (2017). Estimation and comparison of environmental emissions and impacts at foundation and structure construction stages of a building – A case study. *Journal of Cleaner Production*, *151*, 319–329. https://doi.org/10.1016/j.jclepro.2017.03.041

Sang, X., Pan, W., & Kumaraswamy, M. M. (2014). Informing energy-efficient building envelope design decisions for Hong Kong. *Energy Procedia*, *62*(September), 123–131. https://doi.org/10.1016/j.egypro.2014.12.373

Santamouris, M., Papanikolaou, N., Livada, I., Koronakis, I., Georgakis, C., Argiriou, A., &

Assimakopoulos, D. N. (2001). On the impact of urban climate on the energy consuption of building. *Solar Energy*, *70*(3), 201–216. https://doi.org/10.1016/S0038-092X(00)00095-5

Santin, O. G. (2011). Behavioural patterns and user profiles related to energy consumption for heating. *Energy and Buildings*, *43*(10), 2662–2672. https://doi.org/10.1016/j.enbuild.2011.06.024

Sargam, Y., Wang, K., & Alleman, J. E. (2020). Effects of Modern Concrete Materials on Thermal Conductivity. *Journal of Materials in Civil Engineering*, *32*(4), 1–11. https://doi.org/10.1061/(asce)mt.1943-5533.0003026

Sarı, A. (2022). *Materials Today : Proceedings A review on phase change materials (PCMs) for thermal energy storage implementations*. *58*, 1360–1367. https://doi.org/10.1016/j.matpr.2022.02.231

Sassine, E., Kinab, E., Cherif, Y., Antczak, E., & Nasrallah, M. (2021). Thermal performance of lightweight concrete applications in building envelopes in Lebanon. *Building Simulation*, *14*, 1359–1375.

Sato, R., Maruyama, I., Sogabe, T., & Sogo, M. (2007). Flexural behavior of reinforced recycled concrete beams. *Journal of Advanced Concrete Technology*, *5*(1), 43–61. https://doi.org/10.3151/jact.5.43

Satpathy, H. P., Patel, S. K., & Nayak, A. N. (2019). Development of sustainable lightweight concrete using fly ash cenosphere and sintered fly ash aggregate. *Construction and Building Materials*, *202*, 636–655. https://doi.org/10.1016/j.conbuildmat.2019.01.034

Sebaibi, N., & Boutouil, M. (2020). Reducing energy consumption of prefabricated building elements and lowering the environmental impact of concrete. *Engineering Structures*, *213*(April), 110594. https://doi.org/10.1016/j.engstruct.2020.110594

Šefflová, M., Volf, M., & Pavl\uu, T. (2014). Thermal properties of concrete with recycled aggregate. *Advanced Materials Research*, *1054*, 227–233.

Senaratne, S., Lambrousis, G., Mirza, O., Tam, V. W. Y., & Kang, W. H. (2017a). Recycled Concrete in Structural Applications for Sustainable Construction Practices in Australia. *Procedia Engineering*, *180*(0), 751–758. https://doi.org/10.1016/j.proeng.2017.04.235

Senaratne, S., Lambrousis, G., Mirza, O., Tam, V. W. Y., & Kang, W. H. (2017b). Recycled Concrete in Structural Applications for Sustainable Construction Practices in Australia. *Procedia Engineering*, *180*(0), 751–758. https://doi.org/10.1016/j.proeng.2017.04.235

Sereewatthanawut, I., & Prasittisopin, L. (2020). Environmental evaluation of pavement system incorporating recycled concrete aggregate. *International Journal of Pavement Research and*

Technology, *13*(5), 455–465. https://doi.org/10.1007/s42947-020-0002-7

Shadram, F., Johansson, T. D., Lu, W., Schade, J., & Olofsson, T. (2016). An integrated BIM-based framework for minimizing embodied energy during building design. *Energy and Buildings*, *128*, 592–604. https://doi.org/10.1016/j.enbuild.2016.07.007

Shadram, F., & Mukkavaara, J. (2018). An integrated BIM-based framework for the optimization of the trade-off between embodied and operational energy. *Energy and Buildings*, *158*, 1189–1205. https://doi.org/10.1016/j.enbuild.2017.11.017

Shadram, F., & Mukkavaara, J. (2019). Exploring the effects of several energy efficiency measures on the embodied/operational energy trade-off: A case study of swedish residential buildings. *Energy and Buildings*, *183*, 283–296.

Shafigh, P., Asadi, I., & Mahyuddin, N. B. (2018). Concrete as a thermal mass material for building applications - A review. *Journal of Building Engineering*, *19*(April), 14–25. https://doi.org/10.1016/j.jobe.2018.04.021

Shah, S. N., Mo, K. H., Yap, S. P., & Radwan, M. K. H. (2021). Towards an energy efficient cement composite incorporating silica aerogel: A state of the art review. *Journal of Building Engineering*, *44*(August), 103227. https://doi.org/10.1016/j.jobe.2021.103227

Shah, S. N., Mo, K. H., Yap, S. P., Yang, J., & Ling, T. C. (2021). Lightweight foamed concrete as a promising avenue for incorporating waste materials: A review. *Resources, Conservation and Recycling*, *164*(August 2020), 105103. https://doi.org/10.1016/j.resconrec.2020.105103

Shakhnarovich, G., Darrell, T., & Indyk, P. (2006). *Nearest-neighbor methods in learning and vision: theory and practice (neural information processing)*. The MIT press.

Shaqadan, A. (2016). Prediction of concrete mix strength using random forest model. *International Journal of Applied Engineering Research*, *11*(22), 11024–11029.

Shariq, M., Prasad, J., & Masood, A. (2010). Effect of GGBFS on time dependent compressive strength of concrete. *Construction and Building Materials*, *24*(8), 1469–1478. https://doi.org/10.1016/j.conbuildmat.2010.01.007

She, W., Du, Y., Zhao, G., Feng, P., Zhang, Y., & Cao, X. (2018). Influence of coarse fly ash on the performance of foam concrete and its application in high-speed railway roadbeds. *Construction and Building Materials*, *170*, 153–166. https://doi.org/10.1016/j.conbuildmat.2018.02.207

Shen, Z., & Zhou, H. (2020). Predicting effective thermal and elastic properties of cementitious composites containing polydispersed hollow and core-shell micro-particles. *Cement and*

Concrete Composites, *105*(October 2019), 103439. https://doi.org/10.1016/j.cemconcomp.2019.103439

Shen, Z., Zhou, H., Brooks, A., & Hanna, D. (2021). Evolution of elastic and thermal properties of cementitious composites containing micro-size lightweight fillers after exposure to elevated temperature. *Cement and Concrete Composites*, *118*(December 2020), 103931. https://doi.org/10.1016/j.cemconcomp.2021.103931

Shi, J., Liu, B., He, Z., Liu, Y., Jiang, J., Xiong, T., & Shi, J. (2021). A green ultra-lightweight chemically foamed concrete for building exterior: A feasibility study. *Journal of Cleaner Production*, *288*, 125085. https://doi.org/10.1016/j.jclepro.2020.125085

Shon, C. S., Mukangali, I., Zhang, D., Ulykbanov, A., & Kim, J. (2021). Evaluation of non-autoclaved aerated concrete for energy behaviors of a residential house in Nur-Sultan, Kazakhstan. *Buildings*, *11*(12). https://doi.org/10.3390/buildings11120610

Short, C. A., Lomas, K. J., & Woods, A. (2004). Design strategy for low-energy ventilation and cooling within an urban heat island. *Building Research and Information*, *32*(3), 187–206. https://doi.org/10.1080/09613210410001679875

Siddique, R. (2010). Utilization of coal combustion by-products in sustainable construction materials. *Resources, Conservation and Recycling*, *54*(12), 1060–1066. https://doi.org/10.1016/j.resconrec.2010.06.011

Siddique, R., & Bennacer, R. (2012). Use of iron and steel industry by-product (GGBS) in cement paste and mortar. *Resources, Conservation and Recycling*, *69*, 29–34. https://doi.org/10.1016/j.resconrec.2012.09.002

Siddique, R., & Chahal, N. (2011). Use of silicon and ferrosilicon industry by-products (silica fume) in cement paste and mortar. *Resources, Conservation and Recycling*, *55*(8), 739–744. https://doi.org/10.1016/j.resconrec.2011.03.004

Sivakrishna, A., Adesina, A., Awoyera, P. O., & Kumar, K. R. (2020). Green concrete: A review of recent developments. *Materials Today: Proceedings*, *27*, 54–58. https://doi.org/10.1016/j.matpr.2019.08.202

Somna, R., Jaturapitakkul, C., Chalee, W., & Rattanachu, P. (2012). Effect of the Water to Binder Ratio and Ground Fly Ash on Properties of Recycled Aggregate Concrete. *Journal of Materials in Civil Engineering*, *24*(1), 16–22. https://doi.org/10.1061/(asce)mt.1943-5533.0000360

Sonawane, T. R., & Pimplikar, P. S. S. (2012). Use of Recycled Aggregate Concrete. *Journal of Mechanical and Civil Engineering (IOSR-JMCE)*, *1*(2), 52–59.

https://doi.org/10.5276/JSWTM.2016.137

Soudki, K. A., El-Salakawy, E. F., & Elkum, N. B. (2001). Full factorial optimization of concrete mix design for hot climates. *Journal of Materials in Civil Engineering*, *13*(6), 427–433.

Staszczuk, A., Wojciech, M., & Kuczyński, T. (2017). The effect of floor insulation on indoor air temperature and energy consumption of residential buildings in moderate climates. *Energy*, *138*, 139–146. https://doi.org/10.1016/j.energy.2017.07.060

Stránský, J., Vorel, J., Zeman, J., & Šejnoha, M. (2011). Mori-tanaka based estimates of effective thermal conductivity of various engineering materials. *Micromachines*, *2*(2), 129–149. https://doi.org/10.3390/mi2020129

Su, X., Tian, S., Shao, X., & Zhao, X. (2020). Embodied and operational energy and carbon emissions of passive building in HSCW zone in China: A case study. *Energy and Buildings*, *222*. https://doi.org/10.1016/j.enbuild.2020.110090

Sun, C., Zhu, Y., Guo, J., Zhang, Y., & Sun, G. (2018). Effects of foaming agent type on the workability, drying shrinkage, frost resistance and pore distribution of foamed concrete. *Construction and Building Materials*, *186*, 833–839. https://doi.org/10.1016/j.conbuildmat.2018.08.019

Suntharalingam, T., Gatheeshgar, P., Upasiri, I., Poologanathan, K., Nagaratnam, B., Rajanayagam, H., & Navaratnam, S. (2021). Numerical study of fire and energy performance of innovative light-weight 3d printed concrete wall configurations in modular building system. *Sustainability (Switzerland)*, *13*(4), 1–21. https://doi.org/10.3390/su13042314

Taffese, W. Z. (2018). Suitability Investigation of Recycled Concrete Aggregates for Concrete Production: An Experimental Case Study. *Advances in Civil Engineering*, *2018*. https://doi.org/10.1155/2018/8368351

Taher Ahmed, M., Zakaria, R., Majid, M. Z. A., & Mohd Affendi, I. (2012). Importance of sustainable concrete formwork system. *Advanced Materials Research*, *598*, 360–365.

Tam, C. T. (2021). The Past, Present and Future of Concrete Construction. *The Journal of The Institution of Engineers, Malaysia*, *82*(2).

Tam, V. W. Y., Butera, A., Le, K. N., & Li, W. (2020). Utilising CO2 technologies for recycled aggregate concrete: A critical review. *Construction and Building Materials*, *250*, 118903. https://doi.org/10.1016/j.conbuildmat.2020.118903

Tam, V. W. Y., Kotrayothar, D., & Xiao, J. (2015). Long-term deformation behaviour of recycled aggregate concrete. *Construction and Building Materials*, *100*, 262–272.

https://doi.org/10.1016/j.conbuildmat.2015.10.013

Tam, V. W. Y., Soomro, M., & Evangelista, A. C. J. (2018). A review of recycled aggregate in concrete applications (2000–2017). *Construction and Building Materials*, *172*, 272–292. https://doi.org/10.1016/j.conbuildmat.2018.03.240

Tan, Y., Peng, J., Curcija, D. C., Hart, R., Jonsson, J. C., & Selkowitz, S. (2020). Parametric study of the impact of window attachments on air conditioning energy consumption. *Solar Energy*, *202*(March), 136–143. https://doi.org/10.1016/j.solener.2020.03.096

Tao, C., Watts, B., Ferraro, C. C., & Masters, F. J. (2019). A Multivariate Computational Framework to Characterize and Rate Virtual Portland Cements. *Computer-Aided Civil and Infrastructure Engineering*, *34*(3), 266–278. https://doi.org/10.1111/mice.12413

Thomas, B. S., Yang, J., Mo, K. H., Abdalla, J. A., Hawileh, R. A., & Ariyachandra, E. (2021). Biomass ashes from agricultural wastes as supplementary cementitious materials or aggregate replacement in cement/geopolymer concrete: A comprehensive review. *Journal of Building Engineering*, *40*(July 2020). https://doi.org/10.1016/j.jobe.2021.102332

Thomas, C., Setién, J., Polanco, J. A., Alaejos, P., & Sánchez De Juan, M. (2013). Durability of recycled aggregate concrete. *Construction and Building Materials*, *40*, 1054–1065. https://doi.org/10.1016/j.conbuildmat.2012.11.106

Thomas, C., Setién, J., Polanco, J. A., Cimentada, A. I., & Medina, C. (2018). Influence of curing conditions on recycled aggregate concrete. *Construction and Building Materials*, *172*, 618–625. https://doi.org/10.1016/j.conbuildmat.2018.04.009

Thormark, C. (2002). A low energy building in a life cycle - Its embodied energy, energy need for operation and recycling potential. *Building and Environment*, *37*(4), 429–435. https://doi.org/10.1016/S0360-1323(01)00033-6

Tian, Y., Cheng, R., Zhang, X., Su, Y., & Jin, Y. (2018). A strengthened dominance relation considering convergence and diversity for evolutionary many-objective optimization. *IEEE Transactions on Evolutionary Computation*, *23*(2), 331–345.

Tijani, M. A., Ajagbe, W. O., & Agbede, O. A. (2022). Recycling sorghum husk and palm kernel shell wastes for pervious concrete production. *Journal of Cleaner Production*, *380*(P1), 134976. https://doi.org/10.1016/j.jclepro.2022.134976

Tinoco, M. P., de Mendonça, É. M., Fernandez, L. I. C., Caldas, L. R., Reales, O. A. M., & Toledo Filho, R. D. (2022). Life cycle assessment (LCA) and environmental sustainability of cementitious materials for 3D concrete printing: A systematic literature review. *Journal of Building Engineering*, *52*(March). https://doi.org/10.1016/j.jobe.2022.104456

Topc, B. (2008). *Prediction of mechanical properties of recycled aggregate concretes containing silica fume using artificial neural networks and fuzzy logic*. *42*, 74–82. https://doi.org/10.1016/j.commatsci.2007.06.011

Topçu, I. B., Karakurt, C., & Saridemir, M. (2008). Predicting the strength development of cements produced with different pozzolans by neural network and fuzzy logic. *Materials and Design*, *29*(10), 1986–1991. https://doi.org/10.1016/j.matdes.2008.04.005

Tošić, N., Marinković, S., Dašić, T., & Stanić, M. (2015). Multicriteria optimization of natural and recycled aggregate concrete for structural use. *Journal of Cleaner Production*, *87*(1), 766–776. https://doi.org/10.1016/j.jclepro.2014.10.070

Tran Le, A. D., Maalouf, C., Mai, T. H., Wurtz, E., & Collet, F. (2010). Transient hygrothermal behaviour of a hemp concrete building envelope. *Energy and Buildings*, *42*(10), 1797–1806. https://doi.org/10.1016/j.enbuild.2010.05.016

Tran, N. P., Nguyen, T. N., Ngo, T. D., Le, P. K., & Le, T. A. (2022). Strategic progress in foam stabilisation towards high-performance foam concrete for building sustainability: A state-of-the-art review. *Journal of Cleaner Production*, *375*(September), 133939. https://doi.org/10.1016/j.jclepro.2022.133939

Turner, L. K., & Collins, F. G. (2013). Carbon dioxide equivalent (CO2-e) emissions: A comparison between geopolymer and OPC cement concrete. *Construction and Building Materials*, *43*, 125–130. https://doi.org/10.1016/j.conbuildmat.2013.01.023

Tyagi, V. V., & Buddhi, D. (2007). PCM thermal storage in buildings: A state of art. *Renewable and Sustainable Energy Reviews*, *11*(6), 1146–1166. https://doi.org/10.1016/j.rser.2005.10.002

Tyagi, V. V., Kaushik, S. C., Tyagi, S. K., & Akiyama, T. (2011). Development of phase change materials based microencapsulated technology for buildings: A review. *Renewable and Sustainable Energy Reviews*, *15*(2), 1373–1391. https://doi.org/10.1016/j.rser.2010.10.006

Ürge-Vorsatz, D., Harvey, L. D. D., Mirasgedis, S., & Levine, M. D. (2007). Mitigating CO2 emissions from energy use in the world's buildings. *Building Research and Information*, *35*(4), 379–398. https://doi.org/10.1080/09613210701325883

Utama, A., & Gheewala, S. H. (2009). Indonesian residential high rise buildings: A life cycle energy assessment. *Energy and Buildings*, *41*(11), 1263–1268. https://doi.org/10.1016/j.enbuild.2009.07.025

Valente, M., Sambucci, M., Chougan, M., & Ghaffar, S. H. (2022). Reducing the emission of climate-altering substances in cementitious materials: A comparison between alkali-

activated materials and Portland cement-based composites incorporating recycled tire rubber. *Journal of Cleaner Production*, *333*(August 2021), 130013. https://doi.org/10.1016/j.jclepro.2021.130013

van Eck, N. J., & Waltman, L. (2010). Software survey: VOSviewer, a computer program for bibliometric mapping. *Scientometrics*, *84*(2), 523–538. https://doi.org/10.1007/s11192-009-0146-3

Van Eck, N. J., & Waltman, L. (2013). VOSviewer manual. *Leiden: Univeristeit Leiden*, *1*(1), 1–53.

Van Tran, M., & Chau, V. N. (2021). Mass Concrete Placement of the Offshore Wind Turbine Foundation: A Statistical Approach to Optimize the Use of Fly Ash and Silica Fume. *International Journal of Concrete Structures and Materials*, *15*(1). https://doi.org/10.1186/s40069-021-00491-8

Vangeem, M. G., Holm, T. A., & Ries, J. P. (2013). Optimal Thermal Mass and R-Value in Concrete. *First International Conference on Concrete Sustainability*, 411–418.

Vargas, J., & Halog, A. (2015). Effective carbon emission reductions from using upgraded fly ash in the cement industry. *Journal of Cleaner Production*, *103*, 948–959. https://doi.org/10.1016/j.jclepro.2015.04.136

Vejmelková, E., Keppert, M., Rovnaníková, P., Ondráček, M., Keršner, Z., & Černý, R. (2012). Properties of high performance concrete containing fine-ground ceramics as supplementary cementitious material. *Cement and Concrete Composites*, *34*(1), 55–61. https://doi.org/10.1016/j.cemconcomp.2011.09.018

Vejmelková, E., Pavl\'\iková, M., Keppert, M., Keršner, Z., Rovnanikova, P., Ondráček, M., Sedlmajer, M., & Čern\`y, R. (2009). Fly ash influence on the properties of high performance concrete. *Cement Wapno Beton*, *13*(75), 189–204.

Vellei, M., Herrera, M., Fosas, D., & Natarajan, S. (2017). The influence of relative humidity on adaptive thermal comfort. *Building and Environment*, *124*, 171–185. https://doi.org/10.1016/j.buildenv.2017.08.005

Venkatraj, V., & Dixit, M. K. (2021). Life cycle embodied energy analysis of higher education buildings: A comparison between different LCI methodologies. *Renewable and Sustainable Energy Reviews*, *144*(September 2020), 110957. https://doi.org/10.1016/j.rser.2021.110957

Vives, I., Varona, F. B., Tenza-Abril, A. J., & Pereiro-Barceló, J. (2021). A parametric study to assess lightweight aggregate concrete for future sustainable construction of reinforced concrete beams. *Sustainability (Switzerland)*, *13*(24). https://doi.org/10.3390/su132413893

Walsh, J. B. (1965). The effect of cracks on the compressibility of rock. *Journal of Geophysical Research*, *70*(2), 381–389.

Wang, B., Yan, L., Fu, Q., & Kasal, B. (2021). A Comprehensive Review on Recycled Aggregate and Recycled Aggregate Concrete. *Resources, Conservation and Recycling*, *171*(March), 105565. https://doi.org/10.1016/j.resconrec.2021.105565

Wang, E., Shen, Z., & Barryman, C. (2011). *A building LCA case study using Autodesk Ecotect and BIM model*.

Wang, H., Lu, W., Wu, Z., & Zhang, G. (2020). Parametric analysis of applying PCM wallboards for energy saving in high-rise lightweight buildings in Shanghai. *Renewable Energy*, *145*, 52–64. https://doi.org/10.1016/j.renene.2019.05.124

Wang, J. J., Wang, Y. F., Sun, Y. W., Tingley, D. D., & Zhang, Y. R. (2017). Life cycle sustainability assessment of fly ash concrete structures. *Renewable and Sustainable Energy Reviews*, *80*(May), 1162–1174. https://doi.org/10.1016/j.rser.2017.05.232

Wang, L., & Greenberg, S. (2015). Window operation and impacts on building energy consumption. *Energy and Buildings*, *92*, 313–321. https://doi.org/10.1016/j.enbuild.2015.01.060

Wang, L., Mathew, P., & Pang, X. (2012). Uncertainties in energy consumption introduced by building operations and weather for a medium-size office building. *Energy and Buildings*, *53*, 152–158. https://doi.org/10.1016/j.enbuild.2012.06.017

Wang, S., Abdulridha, A., Bravo, J., Naito, C., Quiel, S., Suleiman, M., Romero, C., Neti, S., & Oztekin, A. (2023). Thermal energy storage in concrete: Review, testing, and simulation of thermal properties at relevant ranges of elevated temperature. *Cement and Concrete Research*, *166*(December 2021), 107096. https://doi.org/10.1016/j.cemconres.2023.107096

Wang, Y., Liu, Z., Wang, Y., Wang, D., Yuan, C., & Liu, R. (2022). Effect of recycled aggregate and supplementary cementitious material on the chloride threshold for steel bar corrosion in concrete. *Construction and Building Materials*, *346*(February), 128418. https://doi.org/10.1016/j.conbuildmat.2022.128418

Wang, Y., & Witten, I. H. (1996). *Induction of model trees for predicting continuous classes*.

Wardeh, G., Ghorbel, E., & Gomart, H. (2015). Mix Design and Properties of Recycled Aggregate Concretes: Applicability of Eurocode 2. *International Journal of Concrete Structures and Materials*, *9*(1), 1–20. https://doi.org/10.1007/s40069-014-0087-y

Weger, D., Kim, H., Talke, D., Henke, K., Kränkel, T., & Gehlen, C. (2020). Lightweight concrete 3D printing by selective cement activation--investigation of thermal conductivity,

strength and water distribution. *Second RILEM International Conference on Concrete and Digital Fabrication: Digital Concrete 2020 2*, 162–171.

Wei, G., Wang, G., Xu, C., Ju, X., Xing, L., Du, X., & Yang, Y. (2018). Selection principles and thermophysical properties of high temperature phase change materials for thermal energy storage: A review. *Renewable and Sustainable Energy Reviews*, *81*(May 2017), 1771–1786. https://doi.org/10.1016/j.rser.2017.05.271

Williams Portal, N., Lundgren, K., Wallbaum, H., & Malaga, K. (2015). Sustainable Potential of Textile-Reinforced Concrete. *Journal of Materials in Civil Engineering*, *27*(7). https://doi.org/10.1061/(asce)mt.1943-5533.0001160

Witten, I. H., Frank, E., Hall, M. A., Pal, C. J., & DATA, M. (2005). Practical machine learning tools and techniques. *DATA MINING*, *2*, 4.

Wolfs, R. J. M., Bos, F. P., & Salet, T. A. M. (2018a). Early age mechanical behaviour of 3D printed concrete: Numerical modelling and experimental testing. *Cement and Concrete Research*, *106*(January), 103–116. https://doi.org/10.1016/j.cemconres.2018.02.001

Wolfs, R. J. M., Bos, F. P., & Salet, T. A. M. (2018b). Early age mechanical behaviour of 3D printed concrete: Numerical modelling and experimental testing. *Cement and Concrete Research*, *106*(May 2017), 103–116. https://doi.org/10.1016/j.cemconres.2018.02.001

Wu, H., Zuo, J., Zillante, G., Wang, J., & Yuan, H. (2019). Status quo and future directions of construction and demolition waste research : A critical review. *Journal of Cleaner Production*, *240*, 118163. https://doi.org/10.1016/j.jclepro.2019.118163

Wu, P., Xia, B., & Zhao, X. (2014). The importance of use and end-of-life phases to the life cycle greenhouse gas (GHG) emissions of concrete - A review. *Renewable and Sustainable Energy Reviews*, *37*, 360–369. https://doi.org/10.1016/j.rser.2014.04.070

Wu, Y., Wang, J. Y., Monteiro, P. J. M., & Zhang, M. H. (2015). Development of ultra-lightweight cement composites with low thermal conductivity and high specific strength for energy efficient buildings. *Construction and Building Materials*, *87*, 100–112. https://doi.org/10.1016/j.conbuildmat.2015.04.004

Xia, Y., Liu, C., Li, Y. Y., & Liu, N. (2017). A boosted decision tree approach using Bayesian hyper-parameter optimization for credit scoring. *Expert Systems with Applications*, *78*, 225–241. https://doi.org/10.1016/j.eswa.2017.02.017

Xiao, J., Wang, C., Ding, T., & Akbarnezhad, A. (2018). A recycled aggregate concrete high-rise building: Structural performance and embodied carbon footprint. *Journal of Cleaner Production*, *199*, 868–881. https://doi.org/10.1016/j.jclepro.2018.07.210

Xiao, J. Z., Song, Z. W., & Zhang, F. (2010). An experimental study on thermal conductivity of concrete. *Jianzhu Cailiao Xuebao/Journal of Building Materials*, *13*(1), 17–21. https://doi.org/10.3969/j.issn.1007-9629.2010.01.004

Xie, T., Yang, G., Zhao, X., Xu, J., & Fang, C. (2020). A uni fi ed model for predicting the compressive strength of recycled aggregate concrete containing supplementary cementitious materials. *Journal of Cleaner Production*, *251*, 119752. https://doi.org/10.1016/j.jclepro.2019.119752

Xie, X. S., Yan, D. J., & Zheng, Y. Z. (2011). Optimization design of high-performance concrete based on genetic algorithm toolbox of MATLAB. *Advanced Materials Research*, *250*, 2672–2677.

Xiong, C., Li, Q., Lan, T., Li, H., Long, W., & Xing, F. (2021). Sustainable use of recycled carbon fiber reinforced polymer and crumb rubber in concrete: mechanical properties and ecological evaluation. *Journal of Cleaner Production*, *279*, 123624. https://doi.org/10.1016/j.jclepro.2020.123624

Xu, X., Vignarooban, K., Xu, B., Hsu, K., & Kannan, A. M. (2016). Prospects and problems of concentrating solar power technologies for power generation in the desert regions. *Renewable and Sustainable Energy Reviews*, *53*, 1106–1131. https://doi.org/10.1016/j.rser.2015.09.015

Yan, D., Xia, J., Tang, W., Song, F., Zhang, X., & Jiang, Y. (2008). DeST — An integrated building simulation toolkit Part I: Fundamentals. *Building Simulation*, *1*(2), 95–110. https://doi.org/10.1007/s12273-008-8118-8

Yang, H., Liu, L., Yang, W., Liu, H., Ahmad, W., Ahmad, A., Aslam, F., & Joyklad, P. (2022). A comprehensive overview of geopolymer composites: A bibliometric analysis and literature review. *Case Studies in Construction Materials*, *16*(August 2021), e00830. https://doi.org/10.1016/j.cscm.2021.e00830

Yaphary, Y. L., Lam, R. H. W., & Lau, D. (2017). Chemical Technologies for Modern Concrete Production. *Procedia Engineering*, *172*, 1270–1277. https://doi.org/10.1016/j.proeng.2017.02.150

Yeo, D., & Gabbai, R. D. (2011). Sustainable design of reinforced concrete structures through embodied energy optimization. *Energy and Buildings*, *43*(8), 2028–2033. https://doi.org/10.1016/j.enbuild.2011.04.014

Yigit, S., & Ozorhon, B. (2018). A simulation-based optimization method for designing energy efficient buildings. *Energy and Buildings*, *178*, 216–227.

https://doi.org/10.1016/j.enbuild.2018.08.045

Yilmaz, Z. (2007). Evaluation of energy efficient design strategies for different climatic zones: Comparison of thermal performance of buildings in temperate-humid and hot-dry climate. *Energy and Buildings*, *39*(3), 306–316. https://doi.org/10.1016/j.enbuild.2006.08.004

Yuanliang, X., Baoliang, L., Chun, C., & Yamei, Z. (2021). Properties of foamed concrete with Ca(OH)2 as foam stabilizer. *Cement and Concrete Composites*, *118*(January), 103985. https://doi.org/10.1016/j.cemconcomp.2021.103985

Zandifaez, P., Asadi Shamsabadi, E., Akbar Nezhad, A., Zhou, H., & Dias-da-Costa, D. (2023). AI-Assisted optimisation of green concrete mixes incorporating recycled concrete aggregates. *Construction and Building Materials*, *391*(April), 131851. https://doi.org/10.1016/j.conbuildmat.2023.131851

Zeng, R., & Chini, A. (2017). A review of research on embodied energy of buildings using bibliometric analysis. *Energy and Buildings*, *155*, 172–184. https://doi.org/10.1016/j.enbuild.2017.09.025

Zhang, H., Xu, X., Liu, W., Zhao, B., & Wang, Q. (2022). Influence of the moisture states of aggregate recycled from waste concrete on the performance of the prepared recycled aggregate concrete (RAC) – A review. *Construction and Building Materials*, *326*(February), 126891. https://doi.org/10.1016/j.conbuildmat.2022.126891

Zhang, J., Huang, Y., Aslani, F., Ma, G., & Nener, B. (2020). A hybrid intelligent system for designing optimal proportions of recycled aggregate concrete. *Journal of Cleaner Production*, *273*, 122922. https://doi.org/10.1016/j.jclepro.2020.122922

Zhang, W., Min, H., Gu, X., Xi, Y., & Xing, Y. (2015). Mesoscale model for thermal conductivity of concrete. *Construction and Building Materials*, *98*, 8–16. https://doi.org/10.1016/j.conbuildmat.2015.08.106

Zhang, W., Wang, S., Zhao, P., Lu, L., & Cheng, X. (2019). Effect of the optimized triple mixing method on the ITZ microstructure and performance of recycled aggregate concrete. *Construction and Building Materials*, *203*, 601–607. https://doi.org/10.1016/j.conbuildmat.2019.01.071

Zhang, X., Yang, Q., Shi, Y., Zheng, G., Li, Q., Chen, H., & Cheng, X. (2020). Effects of different control methods on the mechanical and thermal properties of ultra-light foamed concrete. *Construction and Building Materials*, *262*, 120082. https://doi.org/10.1016/j.conbuildmat.2020.120082

Zhang, Y., Chen, Q., Zhang, Y., & Wang, X. (2013). Exploring buildings' secrets: The ideal

thermophysical properties of a building's wall for energy conservation. *International Journal of Heat and Mass Transfer*, *65*, 265–273. https://doi.org/10.1016/j.ijheatmasstransfer.2013.06.008

Zhang, Y., Luo, W., Wang, J., Wang, Y., Xu, Y., & Xiao, J. (2019). A review of life cycle assessment of recycled aggregate concrete. *Construction and Building Materials*, *209*, 115–125. https://doi.org/10.1016/j.conbuildmat.2019.03.078

Zhao, H., Liu, F., & Yang, H. (2018a). Thermal properties of coarse RCA concrete at elevated temperatures. *Applied Thermal Engineering*, *140*(November 2017), 180–189. https://doi.org/10.1016/j.applthermaleng.2018.05.032

Zhao, H., Liu, F., & Yang, H. (2018b). Thermal properties of coarse RCA concrete at elevated temperatures. *Applied Thermal Engineering*, *140*(November 2017), 180–189. https://doi.org/10.1016/j.applthermaleng.2018.05.032

Zhao, H. X., & Magoulès, F. (2012). A review on the prediction of building energy consumption. In *Renewable and Sustainable Energy Reviews* (Vol. 16, Issue 6, pp. 3586–3592). https://doi.org/10.1016/j.rser.2012.02.049

Zhao, M., Zhao, M., Chen, M., Li, J., & Law, D. (2018). An experimental study on strength and toughness of steel fiber reinforced expanded-shale lightweight concrete. *Construction and Building Materials*, *183*, 493–501. https://doi.org/10.1016/j.conbuildmat.2018.06.178

Zhao, X., Lim, S. K., Tan, C. S., Li, B., Ling, T. C., Huang, R., & Wang, Q. (2015). Properties of foamed mortar prepared with granulated blast-furnace slag. *Materials*, *8*(2), 462–473. https://doi.org/10.3390/ma8020462

Zhao, Y., Gao, J., Chen, F., Liu, C., & Chen, X. (2018). Utilization of waste clay bricks as coarse and fine aggregates for the preparation of lightweight aggregate concrete. *Journal of Cleaner Production*, *201*, 706–715. https://doi.org/10.1016/j.jclepro.2018.08.103

Zheng, C., Lou, C., Du, G., Li, X., Liu, Z., & Li, L. (2018). Mechanical properties of recycled concrete with demolished waste concrete aggregate and clay brick aggregate. *Results in Physics*, *9*(April), 1317–1322. https://doi.org/10.1016/j.rinp.2018.04.061

Zheng, L., Wu, H., Zhang, H., Duan, H., Wang, J., Jiang, W., Dong, B., Liu, G., Zuo, J., & Song, Q. (2017a). Characterizing the generation and flows of construction and demolition waste in China. *Construction and Building Materials*, *136*, 405–413. https://doi.org/10.1016/j.conbuildmat.2017.01.055

Zheng, L., Wu, H., Zhang, H., Duan, H., Wang, J., Jiang, W., Dong, B., Liu, G., Zuo, J., & Song, Q. (2017b). Characterizing the generation and flows of construction and demolition waste in

China. *Construction and Building Materials*, *136*, 405–413. https://doi.org/10.1016/j.conbuildmat.2017.01.055

Zhong, H., Wang, J., Jia, H., Mu, Y., & Lv, S. (2019). Vector field-based support vector regression for building energy consumption prediction. *Applied Energy*, *242*(February 2019), 403–414. https://doi.org/10.1016/j.apenergy.2019.03.078

Zhou, D., Zhao, C. Y., & Tian, Y. (2012). Review on thermal energy storage with phase change materials (PCMs) in building applications. *Applied Energy*, *92*, 593–605. https://doi.org/10.1016/j.apenergy.2011.08.025

Zhou, H., & Brooks, A. L. (2019). Thermal and mechanical properties of structural lightweight concrete containing lightweight aggregates and fly-ash cenospheres. *Construction and Building Materials*, *198*, 512–526. https://doi.org/10.1016/j.conbuildmat.2018.11.074

Zhou, Z., Hu, J., Li, F., Zhang, J., & Lei, M. (2022). Elastic Modulus Prediction Model of Foamed Concrete Based on the Walsh Formula. *Applied Sciences*, *12*(10). https://doi.org/10.3390/app12105142

Zhu, L., Dai, J., Bai, G., & Zhang, F. (2015). Study on thermal properties of recycled aggregate concrete and recycled concrete blocks. *Construction and Building Materials*, *94*, 620–628. https://doi.org/10.1016/j.conbuildmat.2015.07.058

Zhu, L., Hurt, R., Correia, D., & Boehm, R. (2009). Detailed energy saving performance analyses on thermal mass walls demonstrated in a zero energy house. *Energy and Buildings*, *41*(3), 303–310. https://doi.org/10.1016/j.enbuild.2008.10.003

Zimele, Z., Sinka, M., Korjakins, A., Bajare, D., & Sahmenko, G. (2019). Life Cycle Assessment of Foam Concrete Production in Latvia. *Environmental and Climate Technologies*, *23*(3), 70–84. https://doi.org/10.2478/rtuect-2019-0080

Zou, P. X. W., Wagle, D., & Alam, M. (2019). Strategies for minimizing building energy performance gaps between the design intend and the reality. *Energy and Buildings*, *191*, 31–41. https://doi.org/10.1016/j.enbuild.2019.03.013